THE ROLE OF THE THYMIC MEDULLA IN T CELL DEVELOPMENT AND TOLERANCE INDUCTION

By

JENNIFER ELIZABETH COWAN

A thesis submitted to the University of Birmingham

For the Degree of DOCTOR OF PHILOSOPHY

Department of Anatomy
School of Immunity and Infection
College of Medical and Dental Science
University of Birmingham

September 2013

ABSTRACT

The thymus is organised into functionally distinct microenvironments that facilitates development of a diverse and self-tolerant T cell repertoire. Following positive selection, thymocytes undergo chemotactic migration from the cortex to the medulla, a site that mediates negative selection of potentially autoreactive $CD4^+$ and $CD8^+$ single positive (SP) thymocytes. Importantly, current models suggest that the medulla also fosters the continued maturation of SP thymocytes, post-selection. However, the mechanisms of thymic medulla function remain unclear.

Using a novel approach based on chemokine receptor expression, we have mapped stages in the positive selection process, and developed a model to study αβT cell development in the absence of medullary thymic epithelial cells (mTEC), but in the presence of an otherwise intact immune system. We show that mTEC are dispensible for the continued development of newly selected $CD4^+CD69^+$ SP thymocytes, yet are essential for the generation of $FoxP3^+$ regulatory T cells and their $FoxP3^-CD25^+$ progenitors. In addition, although CCR4 represents a marker of early stage $CD4^+$ SP positive selection, it is dispensable for SP medullary accumulation and intrathymic development.

Collectively these findings highlight differences in the developmental requirements of conventional and regulatory $CD4^+$ T cells, and rule out a role for CCR4 in cortex to medulla migration.

ACKNOWLEDGMENTS

Firstly, I would like to thank Professor Graham Anderson for his fantastic supervision over the past 4 years. I am extremely grateful for all his guidance and support, which have been invaluable throughout my PhD. I feel very privileged to have had the opportunity to be Graham's student and will forever appreciate the patience and kindness he has always shown me.

I would also like to thank my second supervisor, Professor Eric Jenkinson, and all the members of the Anatomy group, past and present, for both their experimental help and for making the lab such an enjoyable place to work. I would particularly like to thank Sonia Parnell, Will Jenkinson, Andrea White and Kyoko Nakamura for their continuous help and support from the start, in addition to Song Baik, Amanda Holland, Nick McCarthy and Kieran James. Furthermore, I want to thank everyone on the 4th floor of the IBR who have made these past four years so much fun!

A special thank you to all my family and friends who have been such a huge help along the way. I would particularly like to thank my parents for their continual support throughout, and Yolando, who is the best friend a girl could ever ask for! I would finally like to thank Sio-Ban, 'my term time bestie', who has provided me with so many amazing memories during my time in B-Town.

TABLE OF CONTENTS

LIST OF FIGURES

CHAPTER 1

CHAPTER 2

CHAPTER 3

CHAPTER 4

CHAPTER 5

CHAPTER 6

LIST OF TABLES

ABBREVIATION LIST

-/-	deficient
2-dGuo	2-deoxyguanosine
AIRE	autoimmune regulator
APC	antigen presenting cell
APECED	Autoimmune polyendocrinopathy-candidiasis-ectodermal dystrophy
Bcl-2	B cell lymphoma 2
Bcl-xL	B cell lymphoma-extra large
BCR	B cell receptor
BM	Bone marrow
bTEC	bipotent thymic epithelial cell
BV	blood vessel
C	constant
CCL	chemokine ligand
CCR	CC chemokine receptor
CD	cluster of differentiation
cDC	conventional dendritic cell
cDNA	complementary DNA
CDR	complementarity-determining region
Cld	Claudin
CLP	common lymphoid progenitor
CMJ	corticomedullary junction
CMP	common myeloid progenitor
cTEC	cortical thymic epithelial cell
CTL	cytotoxic T lymphocyte
CTLA-4	cytotoxic T lymphocyte antigen 4
CXCL	CXC chemokine ligand
CXCR	CXC chemokine receptor
DAPI	4,6-diamidino-2-phenylindole
DAMP	danger associated molecular pattern
DC	dendritic cell
DMEM	Dulbecco's Modified Eagle's Medium
DN	double negative
DNA	deoxyribonucleic acid
DOCK	dedicator of cytokinesis
DP	double positive
EpCAM-1	epithelial cell adhesion molecule 1
ER	endoplasmic reticulum
ERK	extracellular signal-regulated kinases
FACS	fluorescence activated cell sorting
FCS	fetal calf serum
FoxN1	forkhead box N1

Foxo-1	factor forkhead box O -1
FoxP3	forkhead box P3
FTOC	fetal thymus organ culture
GFP	green fluorescent protein
HSA	heat stable antigen
HSC	haematopoietic stem cell
ICAM-1	intercellular adhesion molecule-1
IFN	interferon
iNKT	invariant natural killer T cells
ITAM	immunoreceptor tyrosine-based activation motive
IL	interleukin
IV	intravenous
J	junctional
JNK	Jun amino-terminal kinase
K	keratin
KLF 2	Kruppel-like factor 2
Lef-1	lymphocyte enhancer factor 1
Lin	lineage
LT	lymphotoxin
LTβR	lymphotoxin β receptor
LTi	lymphoid tissue inducer cell
MAPK	mitogen-activated protein kinases
MHC	major histocompatibility complex
MPP	multipotent progenitor
mRNA	messenger RNA
mTEC	medullary epithelial cell
NF-κB	nuclear factor kappa B
NFAT	nuclear factor of activated T cells
NK	natural killer
nTreg	natural T regulatory
ns	not significant
PAMP	pathogen associated molecular pattern
PBS	phosphate buffered saline
PCR	polymerase chain reaction
pDC	Plasmacytoid dendritic cell
pre-Tα	pre-TCR alpha chain
pre-TCR	pre-TCR complex
PRR	pattern recognition receptor
PSGL-1	P-selectin glycoprotein ligand 1
PTX	pertussis toxin
RAG	recombinase activating gene
RANK	receptor activator
RANKL	RANK ligand
RF10-H	RPMI-1640 Hepes

RNA	ribonucleic acid
RORγ	retinoic acid receptor-related orphan receptor γ
RT	reverse transcription
RTE	recent thymic emigrants
RTOC	reaggregate thymus organ culture
Runx	Runt-related transcription factor
SCZ	subcapsular zone
SP	single positive
S1P1	sphingosine-1-phosphate receptor-1
TCR	T cell receptor
TCf-1	The transcription factors T cell factor 1
TdT	terminal deoxyribonucleotidyl transferase
TEC	thymic epithelial cell
TGFβ	Transforming growth factor beta
Th1	T helper 1
Th2	T helper 2
Th7	T helper 17
TNF	tumour necrosis factor
TNFRSF	tumour necrosis factor receptor superfamily
TRA	tissue restricted antigen
TRAF6	TNF receptor associated factor 6
Treg	T regulatory
V	variable
WT	wildtype
ZAP-70	zeta chain associated protein kinase 70

CHAPTER ONE: GENERAL INTRODUCTION

1.1 AN OVERVIEW OF THE IMMUNE SYSTEM

1.1.1 The Role Of The Immune System

The fundamental role of the immune system is to protect its host against invading pathogens to prevent infectious disease. The immune system is comprised of an interactive network of diverse cell types, each with specialized roles in defending against infection. It has evolved to protect the host against infection through its ability to recognize foreign pathogens by self – non-self discrimination. The environment exposes the host to a vast array of pathogenic organisms that challenge the defense system using a broad spectrum of mechanisms. It is, therefore, pivotal the immune system operates an extensive range of protective strategies via a complexity of cellular interactions, to facilitate successful detection and elimination of pathogens, whilst avoiding destruction of its own tissues as a consequence (Chaplin, 2010).

The defense system operates at two levels; innate immunity and adaptive immunity, determined by the speed and specificity of the reaction. Innate immunity is an evolutionarily ancient defense system present to some degree within all multicellular organisms (Boehm, 2012). It provides a relatively non-specific, initial immune defense for immediate responsiveness to pathogenic exposure. In comparison, the adaptive immune system is more recent in its evolutionary status and is found only in vertebrates. Adaptive immunity is sophisticated, providing a delayed, but specific response to a target pathogen. Both branches of the immune response must function concurrently to effectively eradicate the threat and prevent the establishment of infection (Boehm, 2012; Janeway and Medzhitov, 2002; Turvey and Broide, 2010).

1.1.2 The Innate Immune Response

The innate immune system uses a broad range of recognition molecules for rapid detection of foreign pathogens to supply an initial defense against infection. The innate response lacks immunological memory, so will remain unchanged regardless of re-exposure to the same pathogen (Delves and Roitt, 2000a). The innate immune system has three principle components; mechanical, chemical and cellular. The mechanical elements of the innate system comprise of the host protective barriers. These barriers consist of cells from a non-hematopoietic origin such as the cellular components of the skin and the epithelial cell linings of the respiratory, gastrointestinal and genitourinary tracts (Basset et al., 2003; Turvey and Broide, 2010). If invading pathogens should successfully infiltrate the protective barriers of the host and inflict tissue damage, a series of danger signals are trigged. This results in secretion of many of the soluble components of the innate system, which include chemokines and cytokines (Kumar et al., 2009). Chemokines orchestrate cell migration and attract cells of both the innate and adaptive response to the site of infection. Cytokines regulate the function of neighboring cells and have both pro-inflammatory and anti-inflammatory properties to provide an appropriate response to enhance the clearance of pathogens (Basset et al., 2003; Chaplin, 2010). The cellular components involved in the innate defense system consist of cells from a hematopoietic origin including: mast cells, dendritic cells (DC), macrophages, neutrophils, eosinophils and natural killer (NK) cells (Janeway and Medzhitov, 2002).

The recognition strategy of the innate immune system is not to detect each foreign pathogen specifically, but to identify a small number of commonly expressed, highly conserved structures on entire classes of micro-organisms. These structures are known as pathogen-associated molecular patterns (PAMPs) and the innate immune system has evolved to

recognize them via pattern- recognition receptors (PRRs), expressed by many of the cellular components of the innate system (Medzhitov and Janeway, 1997). The specificities of these innate receptors are genetically predetermined, therefore variation is limited to the number of genes encoded within the host genome (Turvey and Broide, 2010). Each receptor has defined specificities to the most highly conserved structures expressed by infectious pathogens. They can be broadly categorized into three classes: secreted, transmembrane or cytosolic (Iwasaki and Medzhitov, 2010). Secreted PRRs can bind the invading pathogen cell surface and flag them for destruction, either via the compliment system or by phagocytosis by macrophages and neutrophils (Medzhitov and Janeway, 2002). Transmembrane bound PRRs are found on many of the cellular components of the innate system including DC, NK and marcrophages. This catorgy includes Toll-like receptors, scavenger receptors and complement receptors. Upon pathogen binding these transmembrane PRRs cells secrete high levels of cytokines and chemokines, which aids the recruitment of additional cells types to the site of infection (Basset et al., 2003; Dempsey et al., 2003). Several PRRs are expressed within the cytosol and detect intracellular pathogens. These receptor are particularly important during viral and bacterial infection (Janeway and Medzhitov, 2002). In addition to recognizing PAMPs, PRRs can also recognize self-molecules, released after cell death or damage, known as danger associated molecular patterns (DAMPs). These immunological danger signals are released as a consequence of infection or inflammation and are an additional surveillance mechanism utilized by the innate system to detect any possible invasions of the host system (Modlin, 2012).

Upon pathogen recognition through PRRs engagement, a series of intracellular signaling events occurs to activate the innate cell to perform its effector functions immediately

(Dempsey et al., 2003). Thus, facilitating short-lived effector cells to provide the characteristic rapid responses of the innate system (Basset et al., 2003; Medzhitov and Janeway, 2000). Such responses frequently succeed in removing the majority of pathogenic threats without the requirement of backup from the adaptive system. However, the innate immune response alone is not always sufficient and activation of adaptive immunity is necessary for additional aid to clear the infection (Janeway and Medzhitov, 2002).

As the adaptive immune system evolved in the presence of innate immunity the two do not operate in isolation. Many of the adaptive immune responses build on the foundations set by innate immunity (Dempsey et al., 2003). Various components of the innate system play a role in initiating and instructing the development of an adaptive immune response, which in turn can lead to recruitment and activation of additional innate cells to the site of infection. This synergy between the two arms of the immune system amplifies the responsiveness of both divisions and is essential to assure a fully efficient immune response (Chaplin, 2010; Dempsey et al., 2003; Medzhitov and Janeway, 1997).

1.1.3 The Adaptive Immune Response

In contrast to the limited number of pathogen recognition receptors of the innate response, the adaptive immune system possesses an exceptionally diverse and randomly generated receptor repertoire. The adaptive immune system uses antigen- specific receptors expressed by T and B lymphocytes to drive targeted responses against specific pathogens (Medzhitov and Janeway, 1997). Upon recognition of a specific pathogen, lymphocytes must undergo clonal expansion to greatly increase the numbers of antigen-specific cells to generate an efficient response. The antigen detection and expansion of cell numbers can take several days, during

which time the innate system has to work alone to control the invasion and prevent damage to the host (Delves and Roitt, 2000b). Once a specific response has been raised and the threat has been successfully eradicated, long-lived effector cells can persist in a dormant like state, ready to rapidly re-express their effector function if they ever should re-encounter the same antigen. This allows the adaptive response to have immunological memory and enables a rapid and enhanced response on re-exposure to the same pathogens, even decades after the primary encounter (Chaplin, 2010; Medzhitov and Janeway, 2000; Parkin and Cohen, 2001).

T and B lymphocytes represent essential cellular components of the adaptive immune system. Both cell types express unique T cell receptors (TCR) and B cell receptors (BCR) for recognition of a vast diversity of antigens, generated by somatic gene rearrangement (Hedrick et al., 1984). BCR can be secreted as immunoglobulin (Ig), which recognizes antigen in its native form, whilst membrane bound TCR require pathogens to be processed and presented via major histocompatibility complex (MHC) molecules (Parkin and Cohen, 2001). The major focus of this thesis is the developmental biology of T cells, therefore, an overview of T cell function is provided.

1.1.4 T lymphocytes

There are two functionally distinct subsets of T cells dependent upon their TCR, those that express a αβTCR and those that express a γδTCR. Both αβ and γδT cells develop from the same common progenitor within the thymus, yet what drives αβ versus γδ TCR commitment remains unresolved (Kreslavsky et al., 2010). The conventional αβT cells can be further classified into two populations, depending upon their surface expression of co-receptor molecules CD4 or CD8. Each subset binds antigen presented by a different class of MHC

molecule and upon activation each population differentiates into functionally distinct effector cells. $CD4^+$ T cells have a helper role, whilst $CD8^+$ T cells have cytotoxic functions. The co-receptors are not just phenotypic markers, but also have a functional role to stabilize the interactions between the TCR and the peptide-MHC complexes on the surface of antigen presenting cells (APC) (Chaplin, 2010; Parkin and Cohen, 2001). The lineage commitment of the αβT cell is decided during their multi-stage developmental program in the thymus. Thus on exit into the periphery T cells have committed to γδT cell fate, or a $CD4^+$ helper or $CD8^+$ cytotoxic αβT cell lineage (Allison and Havran, 1991).

γδT cell functions are less well characterized compared to their αβ T cell counterparts, constituting about 1-5% of the total lymphocyte population within the blood and peripheral organs (Carding and Egan, 2002). This specialized subset of lymphocytes possesses several innate-cell like features that enables their rapid activation upon stimulation by stress-induced ligands (Bonneville et al., 2010). The γδTCR recognize highly conserved antigens, which are released by stressed cells within the surrounding environment. Upon activation, γδT cells promptly produce cytokines to regulate pathogenic clearance and tissue homeostasis. This T cell subset is commonly homed to and resides within the epithelial layers of internal and external surfaces of the body, such as the skin, lung, tongue and intestinal epithelium(Allison and Havran, 1991). Within these areas this specialized lymphocyte cohort provides a first line of defense against invading pathogens (Bonneville et al., 2010; Xiong and Raulet, 2007).

All data and discussion of T cells and TCR from this point will refer to conventional αβT cells only, unless stated.

1.1.4.1 Cytotoxic $CD8^+$ T Cells

$CD8^+$ T lymphocytes recognize endogenous peptides generated from antigens that are synthesized from within the host cell and present within the groove of MHC Class I molecules. This T cell subset acts to kill viral infected cells, but also participates in the defense response against bacterial and protozal infections. On binding specific antigen on its target cell, $CD8^+$ T cells insert perforins into the infected cell membrane, which in turn results in DNA fragmentation and cell apoptosis. Cytotoxic $CD8^+$ T cells can also recognize death-inducing signals on the surface of infected host cells, known as Fas molecules. $CD8^+$ T cells express Fas ligands on their surface to detect these molecules, which upon binding induce cell apoptosis of the target cell (Harty et al., 2000).

1.1.4.2 Helper $CD4^+$ T Cells

$CD4^+$ T cells recognize exogenous antigens, which have been ingested, processed and presented by MHC class II molecules on the cell surface of APC. $CD4^+$ T cells have a helper function, regulating cellular and humoral immune responses (Chaplin, 2010). $CD4^+$ T cells are traditionally believed to differentiate into two additional subsets upon their activation. The effector function pathway chosen is dependent upon the specific signals received from the surrounding environment and the APC cell from which they were primed. Those naive $CD4^+$ T cells primed by APC that produce the cytokine interleukin (IL)-12 differentiate into effector cells that secrete high levels of IL-2 along with Interferon-γ (IFNγ) (Bottomly, 1988; Mosmann and Coffman, 1989; Parkin and Cohen, 2001). These cells are classified as T helper 1 (T_H1) cells and commonly help activate a cell-mediated inflammatory response to clear intracellular pathogens. IL-2 can stimulate T cell proliferation of most T cell lineages (Mosmann and Coffman, 1989), whilst IFNγ induces natural killer (NK) cells and activates

macrophages to kill intracellular pathogens, such as fungi and protozoa (Parkin and Cohen, 2001). Those naive $CD4^+$ T cells activated by IL-4 stimulated dendritic cells (DC) develop with a different effector function cell fate. These cells are known as T helper 2 (T_H2) cells and are generally important in the clearance of extracellular pathogens. Upon activation T_H2 cells produce cyokines: IL-4 IL-5, IL-9 and IL-13. These cytokines act to stimulate antibody production by B cells, whilst influencing the behavior of some cells of the innate response. (Bottomly, 1988; Chaplin, 2006; Mosmann and Coffman, 1989).

There are additional alternative developmental pathways induced during the activation of naive $CD4^+$ T cells. These different lineages include pro-inflammatory T helper 17 cells (T_H17) and anti-inflammatory T regulatory (Treg) effector cells (Zhou et al., 2009). Both effector lineages can be induced by the cytokine transforming growth factor- β (TGF-β), however, the effector fate of the differentiating naive T cells is dependent on the presence of IL-6, an acute phase protein released during inflammation (Bettelli et al., 2006; Kimura and Kishimoto, 2010). Activation in the presence of both TGF-β and IL-6 results in the differentiation of naive T lymphocytes into T_H17 cells and the suppression of TGF-β induced Treg generation (Bettelli et al., 2006). T_H17 are characterized by their IL-17 producing capabilities. The combination of IL-6 and TGF-β induces retinoid- related orphan receptor (ROR)γt and RORα, key transcription factors in the differentiation of the T_H17 lineage. T_H17 effector cells regulate defenses against extracellular pathogens and fungi, via their IL-17 secretions. However, cells of this lineage have also been identified to contribute considerably to the development of autoimmune conditions, due to their pro-inflammatory nature (Harrington et al., 2005; Kimura and Kishimoto, 2010).

Stimulation by TGF-β and IL-2, in the absence of IL-6, induces activated naive T cells to convert into T regulatory (Treg) effector cell (Bettelli et al., 2006; Curotto de Lafaille and Lafaille, 2009). This differentiation process is under the control of transcription factor forkhead box P3 (Foxp3), which is essential for the maintenance and function of this specialized $CD4^+$ T cell subset (Fontenot et al., 2003). These regulatory cells act to maintain immune homeostasis, prevent autoimmunity and modulate inflammatory responses to environmental and pathogenic insult (Sakaguchi et al., 1995). $Foxp3^+$ $CD4^+$ Treg achieve their objectives via several sophisticated suppressive mechanisms, targeted towards many cell types involved in immune response. The regulatory mechanisms used by this cell type include the secretion of inhibitory cytokines such as IL-10. IL-35 and TGF-β. In addition Treg can stimulate perforin dependent killing methods and cause metabolic disruptions to other effector T cell targets, including alterations to the maturation and function of DC (Vignali et al., 2008). Treg are not exclusively induced within the periphery, but can also be generated intrathymically during the $CD4^+$ T cell development program. Treg that develop within the thymus are known as natural (n)Treg and are believed to be generated through high avidity MHC Class II dependent TCR engagement (Bensinger et al., 2001; Jordan et al., 2001).

1.1.5 Antigen Processing And T Cell Presentation

MHC molecules are cell surface glycoproteins. MHC class I molecules display endogenous peptides synthesized within the host cell. MHC class I complexes are expressed on the cell surface of all nucleated cells and present peptide fragments that have been degraded from cellular proteins under the control of proteasomes (Neefjes et al., 2011). If cells are activated by IFNγ stimulation, proteasomes degrade antigens into peptide fragments for presentation on their surface. The generated peptides are translocated into the endoplasmic reticulum (ER)

where they are loaded into the class I protein-binding groove. This loading process is under the control of the ER protein tapasin, with the aid of various chaperone proteins (Hughes et al., 1997) The peptide loaded class I molecules are then transported via the golgi complex into exocytic vesicles and released onto the cell surface for detection by $CD8^+$ T cells or NK cells (Raposo et al., 1995). This system is well adapted for the presentation of viral peptides produced within virally infected cells (Van Bleek and Nathenson, 1990), but can also be used to display tumor specific proteins (Neefjes et al., 2011). This antigen presentation technique, therefore, provides both antiviral and antitumor immunity, by enabling infected host cells to identify themselves as targets to $CD8^+$ T cells. The $CD8^+$ T cells can then provided a highly targeted response and remove the threat by cytotoxic attack (Wong and Pamer, 2003). Peptides derived from extracellular proteins may also be loaded onto MHC class I molecules by a process of cross presentation. This method is used during some viral infections to overcome the ability of various viruses to suppress antigen presentation within the host and thus prevent the display of peptide via the typical MHC Class I endogenous route (Delamarre et al., 2003; Nopora et al., 2012).

MHC class II molecules are exclusively displayed on the cell surface of professional APC including DC, B cells and macrophages. This class of MHC complexes displays exogenous antigen to $CD4^+$ T cells, which upon activation affect the behavior of a wide range of cells within their surrounding environment. It is critical that T cell activation is tightly regulated. Thus, MHC class II molecules are only displayed on a small fraction of cells, in comparison to MHC class I complexes that are ubiquitously expressed (Neefjes et al., 2011). The exogenous antigens presented by MHC class II proteins are taken up by the environment and primarily consist of proteins from extracellular pathogens such as bacteria, parasites and

viruses (Delamarre et al., 2003). These antigens are ingested by APC though phagocytosis and processed into linear peptide fragments via proteolysis. The processed fragments then accumulate within the MHC class II loading compartments. MHC class II molecules are assembled within the ER before their transportation to the Class II loading areas, where they encounter the processed peptide fragments, which are loaded onto their peptide-binding groove. The antigen-MHC structures are then delivered to the cell surface for recognition by the TCRs of $CD4^+$ T cells (Landsverk et al., 2009).

1.1.6 TCR Structure And Generation

The αβTCR structure is comprised of two chains: the α chain and the β chain, held together by disulphide bonds to form a heterodimer. Each chain consists of a variable domain and a constant domain; with the variable regions determining the receptor antigen specificity. (Saito et al., 1984) The α and β variable domains encode for hypervariable complementarity-determining regions (CDRs) of the receptor, which are the binding sites to complimentary peptide-MHC complexes. The variable region of the β-chains is encoded by variable (V), diversity (D) and joining (J) gene segments, whilst only V and J gene fragments encode the variable region of the α-chain (Nikolich-Zugich et al., 2004; Parkin and Cohen, 2001).

Diversification of the TCR occurs through the random process of V(D)J recombination during the early developmental stages of intrathymic T cells generation. There is diversity in each V,D and J gene region and the recombination process joins only one gene segment per region to form a V(D)J complex consisting of randomly arranged fragments. This process involves nucleases to cut DNA fragments and ligases to bind gene fractions together, under the control of recombination activation genes (RAG-1) and RAG-2 (Mombaerts et al., 1992b; Shinkai et

al., 1992). The V(D)J gene segments are then joined to the constant gene regions, resulting in the formation of a final gene sequence from which proteins will be transcribed to generate either the α-chain or β-chain of the TCR. Using this system, each T lymphocyte has a different combination of gene segments to form a unique genetic code for antigen receptor synthesis. Diversity is further enhanced during the assembly of TCRs by imprecise splicing and frame shifts in base pairs, leading to synthesis of different amino acids (Delves and Roitt, 2000a; Nikolich-Zugich et al., 2004). The enzyme terminal deoxyribonucleotidyl transferase (TdT) can also act to additionally alter the gene sequence of the V domains via insertion of extra nucleotides, with disruption to its expression resulting in a reduction to TCR diversity (Gilfillan et al., 1993). On successful α and β segment generation, different α and β-chains are paired, in the last attempt to enhance variation in the final TCR structure (Nikolich-Zugich et al., 2004).

Although the production of a diverse TCR repertoire offers a huge benefit to the host in terms of defense against a vast range of invading pathogens, it also carries a great risk. The random nature of the generation of the repertoire bears the potential to generate lymphocytes with TCR specificity to self. Multiple complex tolerance mechanisms are in place to eliminate any potential self-reactive cells, which will be discussed in greater detail in Sections 1.2 and 1.3.

1.1.7 TCR Signaling

T cell receptors are associated with CD3 complexes on the surface that transmit activation signals into the cell upon T cell priming by antigen binding. The αβTCR subunits have short cytoplasmic tails, which makes it impossible for them to transduce down stream signals to the nucleus without the assistance of the accessory chains that make up the CD3 complex. The

CD3 complex comprises of transmembrane chains of CD3γ, CD3δ, CD3δε and CD3ζ. Each αβ TCR pair is non-covalently associated with a CD3γ heterodimer, a CD3ε heterodimer and a homodimer of two CD3ζ chains. All CD3 subunits contain immunoreceptor tyrosine-based activation motifs (ITAMs) within their cytoplasmic tails (van der Merwe and Dushek, 2011). TCR binding to peptide-MHC complexes results in biochemical changes to the CD3 complex. These changes include the phosphorylation of the tyrosines within the ITAMs by the receptor associate kinases: Lck and Fyn of the Src family. The phosphorylation of tyrosines within the cytoplasmic tails initiates ITAMs to interact with linker proteins; ζ-chain-associated protein kinase 70 (ZAP- 70), linker for activation of T cells (LAT) and SH2 domain containing leukocyte protein of 76kDa (SLP-76). Activation of these proteins leads to the stimulation of phospholipase C, G proteins Ras and Rac, along with protein tyrosine kinase (PTK) and mitogen-associated protein (MAP) kinase. Collectively the activation of these pathways results in down stream signaling cascades, which activate genes to control cell proliferation and differentiation (Smith-Garvin et al., 2009).

The interactions between peptide- MHC molecules and TCR/CD3 complexes only provide partial signals for T cell activation. Along with TCR antigen binding, T cells also need to receive a second signal mediated through co-stimulatory molecules. Co-stimulatory signals play an essential role in both positive and negative regulation of a variety of T cell effector functions (Yokosuka and Saito, 2009). The most well characterized example of a co-stimulatory molecule is CD28, expressed on the cell surface of T cells. CD28 can bind CD80/ CD86 complexes displayed on the surface of APC and particularly highly expressed on the cell surface of activated DC. Upon CD28 binding to CD80/86, in conjugtion with TCR antigen-MHC engagement, T cells become activated and induce their effector functions

(Sharpe and Freeman, 2002). Activated T cells can also express the co-stimulatory molecule cytotoxic T-lymphocyte antigen 4 (CTLA-4) on their surface, which additionally binds CD80/86. In contrast to CD28 activation signals via CD80/86 engagement, once bound CTLA-4 provides inhibitory signals to the T cells (Rudd and Schneider, 2003). The complicated costimulatory network for T cell activation enables the adaptive system to control signaling and ensure the most appropriate immune response is delivered for successful clearance of the immunological threat, without provoking unnecessary damaging to the host (Delves and Roitt, 2000b).

1.2 T CELL DEVELOPMENT

1.2.1 Structure And Function Of The Thymus

The thymus is a primary lymphoid organ that supports the differentiation of T cells. It is an evolutionary conserved organ that is a component of the adaptive immune response in all vertebrates (Boehm et al., 2012). The immunological role of the thymus was discovered over 50 years ago. It was observed that the thymectomy of mice in their immediate neonatal period of life resulted in an absence of the T cell population (Miller, 1961). It has since been well characterized for its ability to provide a specialized microenvironment to support the establishment and maintenance of a highly diverse, self-tolerant T cell repertoire (Rodewald, 2008). With increasing age, the thymus undergoes a gradual process of involution or atrophy, with the replacement of epithelial thymic tissue with a fibrofatty alternative. This disruption to the thymic architecture results in less efficient T cell development and the reduced emergence of naive T lymphocytes into the periphery. The role of the organ, therefore, is considered pivotal during early development, establishing and educating the T cell repertoire to protect the host from pathogenic threats for the remainder of its life (Lynch et al., 2009; Miller, 2002).

The thymic microenvironment is anatomically divided into two key regions, the outer cortex and the inner medulla. Each area is comprised of unique stromal cells, which provide the essential signals needed for the stringent T cell developmental program (Rodewald, 2008). The thymic stroma is organized into a three-dimensional cellular network, comprised of DC, macrophages, endothelium cells, fibroblasts and thymic epithelial cells (TEC). The most abundant cellular component of the stroma are the TEC populations, which can be sub-

divided into two distinct groups: cortical (cTEC) and medullary (mTEC), dependent upon their anatomical position within the two major thymic regions. These two thymic epithelium populations differ in their cellular morphology and their functional properties, but both are fundamental for successful T cell development. The cTEC subset has a vital role in the earlier stages of T cell development, in contrast to mTEC, which regulate later maturational periods of thymocyte differentiation. (Alves et al., 2009)

The key developmental stages of intrathymic T cell generation and the migratory pathway of differentiating cell through the thymic microenvironment are summarized within Figure 1.1 and 1.2.

1.2.2 Thymic Colonization And T Cell Precursors

T cell progenitors are derived from self-renewing multipotent hematopoietic stem cells (HSC) that have lineage potential to differentiate into all cellular components of the immune system. The site of development of HSC changes during ontogeny, with cells derived from the fetal liver during embryogensis and postnatally from the bone marrow. Fetal and postnatal T cell progenitors not only differ in their sites of development, but also in their methods of thymic colonization (Anderson et al., 2006). The initial colonization of a fetal thymus occurs approximately 11 days after gestation in mice (Owen and Ritter, 1969). At this stage in development the thymus lacks vascularization, resulting in precursors having to exit from adjacent blood vessels and migrate to the thymus through surrounding connective tissue. The immigration pathway to the fetal thymus occurs in a two step process. Firstly the T cell precursors must migrate to the mesenchymal layer, before travelling across an epithelial

Figure 1. 1 The Stages Of Intrathymic T Cell Development

The stages of the intrathymic T cell developmental program are defined by changes in surface expression patterns of co-receptors CD4 and CD8. Thymocyte differentiate from CD4- CD8- double negative (DN) to $CD4^+$ $CD8^+$ double positive (DP), before the final $CD4^+$ $CD8^-$ or $CD4^-$ $CD8^+$ single positive (SP) stage in development.

Alternative lineage potentials of populations are displayed in black boxes. The red arrows/text display essential checkpoints in the intrathymic T cell developmental program.

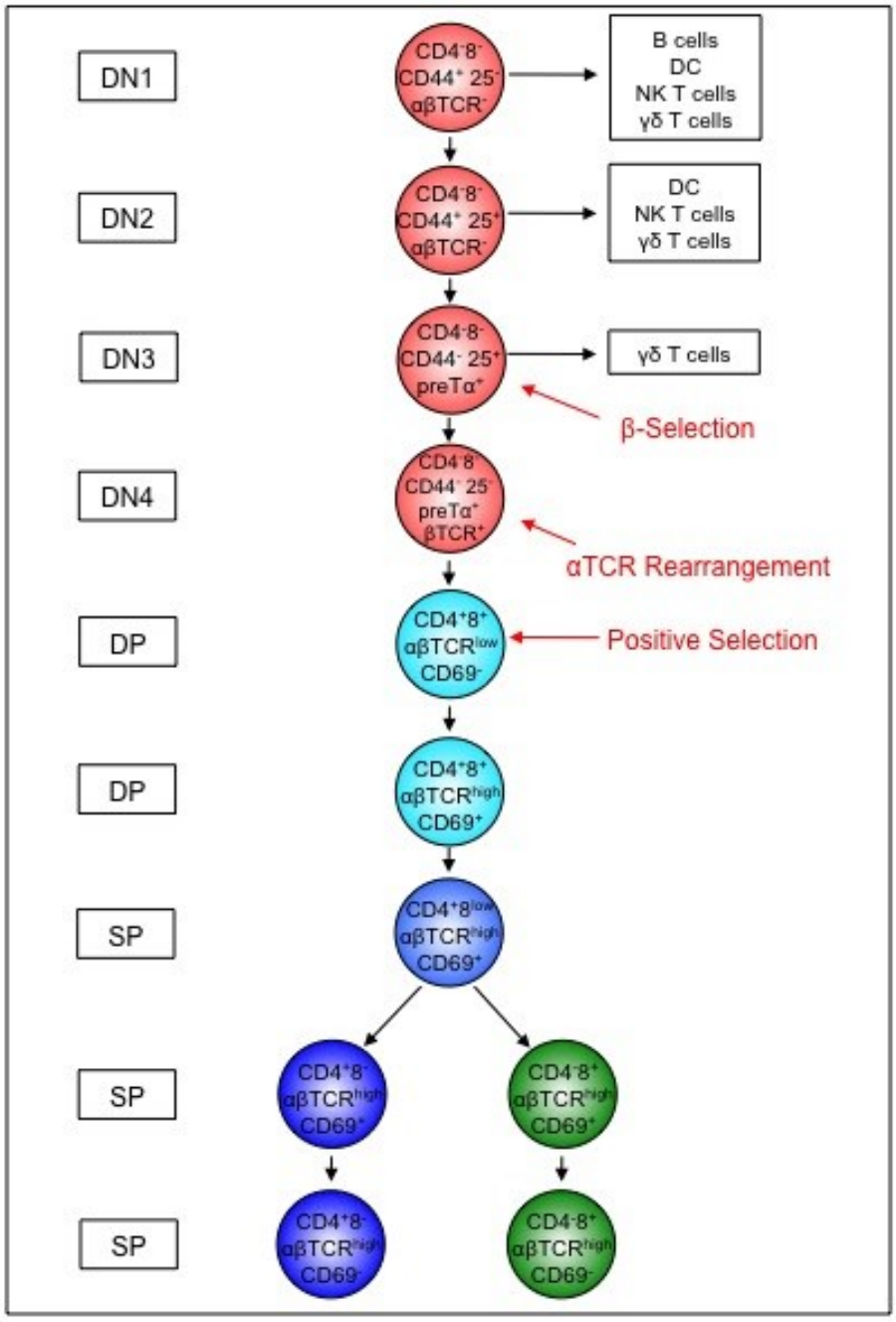
DN1
CD4-8-
CD44+ 25-
αβTCR-
B cells
DC
NK T cells
γδ T cells
DN2
CD4-8-
CD44+ 25+
αβTCR-
DC
NK T cells
γδ T cells
DN3
CD4-8-
CD44- 25+
preTα+
γδ T cells
β-Selection
DN4
CD4-8-
CD44- 25-
preTα+
βTCR+
αTCR Rearrangement
DP
CD4+8+
αβTCRlow
CD69-
Positive Selection
DP
CD4+8+
αβTCRhigh
CD69+
SP
CD4+8low
αβTCRhigh
CD69+
SP
CD4+8-
αβTCRhigh
CD69+
CD4-8+
αβTCRhigh
CD69+
SP
CD4+8-
αβTCRhigh
CD69-
CD4-8+
αβTCRhigh
CD69-

Figure 1. 2 The Migratory Pathway Of Developing Thymocytes

During T cell development thymocytes undergo directed migration through distinct regions of the thymic microenvironment, where they receive essential signals from specialised stromal cell populations. Arrows indicate the direction of migration. Early thymic progenitors (ETP) enter via blood vessels (BV) at the corticomedullary junction (CMJ), where they migrate out through the cortex as DN cells (DN1 to DN3) before accumulating at the subcapsular zone at the DN3 stage in development. Thymocytes then differentiate into DP cells and migrate back through the cortex in the direction of the medulla. DP cells that successfully undergo positive selection commitment to a $CD4^+$ SP or $CD8^+$ SP lineage fate and migrate across the CMJ into the medulla as a SP thymocyte.

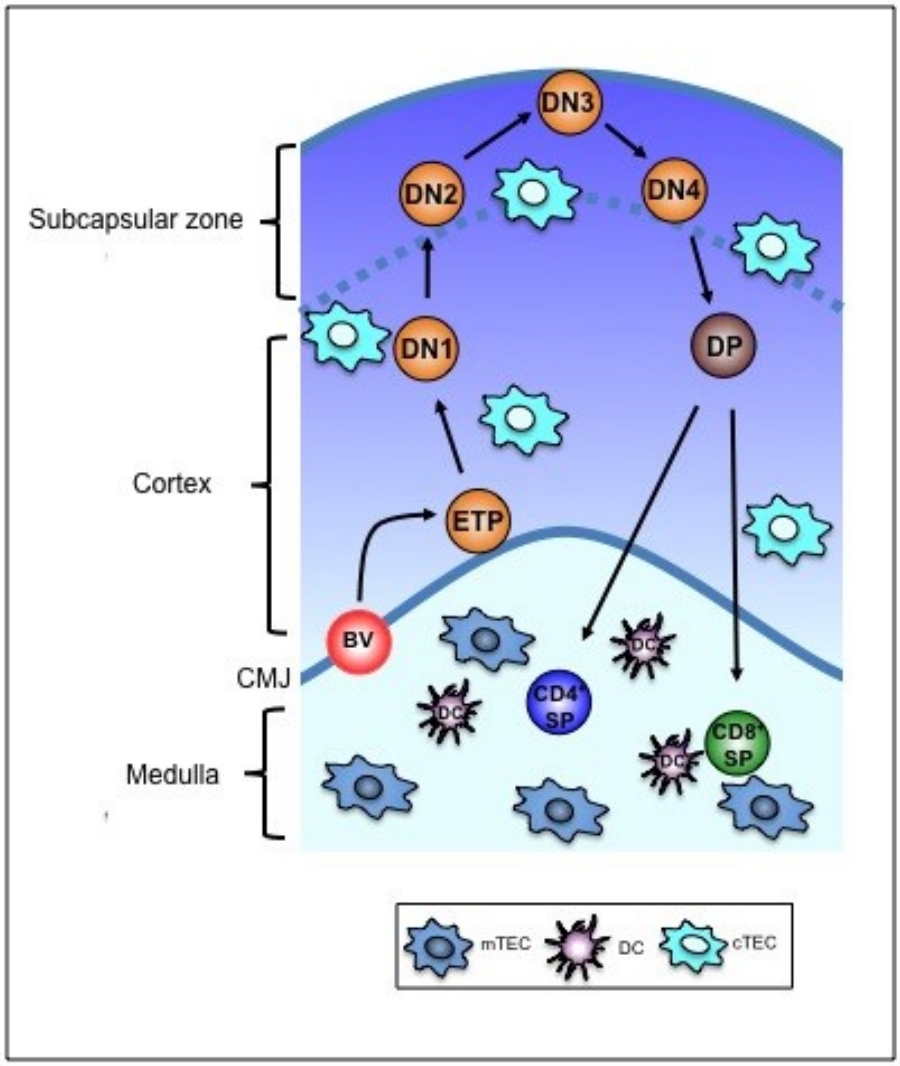
DN3
DN2
DN4
Subcapsular zone
DN1
DP
Cortex
ETP
BV
DC
CMJ
CD4+ SP
DC
CD8+ SP
DC
Medulla
mTEC
DC
cTEC

basement membrane to gain entry into the thymic environment (Itoi et al., 2001). In contrast, postnatal T cell precursors that reside within the bone marrow migrate out into the blood circulation system, from where they can directly enter the organ at the corticomedullary junction (CMJ) (Lind et al., 2001).

The differential pathway linking the multipotent HSC to the intrathymic T lineage committed cell is poorly understood. The developmental stages of T cell progenitors are commonly simplified into a multistep differentiation program. HSC within the bone marrow differentiate into short-lived, non-renewing multipotent progenitors (MPPs) (Morrison et al., 1997). These progenitors then undergo a series of irreversible lineage commitment events, resulting in the generation of downstream intermediate populations that are biased towards either a lymphoid lineage or a myeloid lineage. MPPs give rise to either common lymphoid progenitors (CLPs) that generate downstream precursors with T and B lineage potential, or common myeloid progenitor (CMP) that differentiate into cell types such as macrophages and granulocytes (Kondo, 2010). Some cell types cannot be clearly grouped into a CLP or CMP lineage, however, such as DC, which have the potential to arise from both progenitors (Manz et al., 2001).

It is unknown if thymic colonizing progenitors prethymically commit to a T cell fate or if lineage commitment can occur intrathymically (Bhandoola et al., 2007; Schlenner and Rodewald, 2010). Regardless of their lineage potential the earliest intrathymic progenitors have long been thought to have no self-renewing properties. Short-lived thymocytes are believed to have no long lasting thymic residency and therefore need steady recruitment from the bone marrow to the thymus throughout life to maintain constant T cell generation. This recruitment is not continuous, but an intermittent and gated event that occurs in episodic

waves into both fetal thymic tissue and the steady-state adult thymus (Foss et al., 2001; Petrie, 2003). Fetal thymic grafting experiments have demonstrated that under steady state conditions the thymocyte pool is replenished within a four week time period (Berzins et al., 1998). Thymic survival has more recently, however, been identified to be not only dependent on the short life span of thymocytes, but also reliant on competition between the incoming progenitors and the older residents. When placed under conditions of precursor deprivation thymocytes can persist and remain productive intrathymically for extended periods of time, demonstrating differential self-renewing capabilities. These findings suggest thymic turnover is not due to short-lived cell intrinsic programming, but instead is from the pressures of newly imported progenitors. This conflicts with the well accepted theory that a continuous progenitor input from the bone marrow is essential to sustain continuous T cell development (Martins et al., 2012; Peaudecerf et al., 2012)

Several key mechanisms are in operation to drive thymic progenitor entry into the thymus. Chemokine signaling has been implicated in mediating T cell progenitor recruitment and colonization in both the fetal and adult thymic environments. Chemokines are produced and secreted by the thymic microenvironment, creating chemoattractant gradients that attract T cells progenitors and coordinate their migration into the organ. Investigations indentified the specific involvement of chemokine receptors CCR7 and CCR9 in recruitment of T cells progenitors to both the prevascular neonatal thymus (Liu et al., 2006) and to the adulthood vascularized thymus (Zlotoff et al., 2010). Moreover, recent studies have identified a role for an additional chemokine receptor, CXCR4 in fetal thymic progenitor seeding. Absence of CCR9, CCR7 and CXCR4 results in a vast reduction of thymic homing, consequently leading to a reduction in thymocyte cell numbers. In contrast, the absence of only two of the receptors

in any combination (CCR9 x CCR7, CCR9 x CXCR4 or CCR7 x CXCR4), has much milder effects on the number of progenitors capable of migrating to the neonatal thymus (Calderon and Boehm, 2011).

Adhesions molecules have also been implicated in regulating the vasculature-dependent pathway of T cell progenitor entry into the adult thymus. Specificly, P-selectin and its ligand P-selectin glycoprotein ligand-1 (PSGL-1) have been identified to be critical in aiding thymic progenitor colonization. PSGL-1 expressed by T cell progenitors binds P-selectin on the thymic endothelium. The expression of P-selectin by the vasculature is thought to be quantitatively regulated by the number of empty thymic progenitor niches and thus, this adhesion molecule may modulate the waves of recruits into the postnatal thymus (Rossi et al., 2005).

1.2.3 Early Stages In T Cell Development

Following thymic colonization, the earliest $CD4^-$ $CD8^-$ double negative (DN) thymocytes undergo crucial events in thymocyte development including proliferation and pre-TCR gene rearrangement. The DN population represents 2-3% of total thymocytes and can be subdivided into four phenotypical and functional distinct subsets based on their differential expression of surface markers such as CD44 (phagocytic glycoprotein-1) and CD25 (IL-2 receptor α chain) (Godfrey et al., 1993). The populations are named DN1 through to DN4 and each is characterized to have several distinctive features, along with specific localizations within the thymus. The earliest of the four subsets, the DN1 fraction, express CD44 on their cell surface, whilst lacking CD25 expression. These early thymic settlers migrate out from the CMJ across the cortex where they upregulate CD25 expression and undergo the transition to a

DN2 phenotype ($CD25^+$ $CD44^+$), before down regulating CD44 to differentiate into a DN3 maturation status ($CD25^+$ $CD44^-$). The final stage in the DN developmental program involves down regulation of CD25 and the transition into the DN4 phase ($CD25^-$ CD44) (Godfrey et al., 1993; Zuniga-Pflucker and Lenardo, 1996). The earliest DN stage in development is the most proliferative stage in thymocyte development and each intrathymic progenitor is believed to expand approximately one million fold before reaching the DP stage in differentiation (Shortman et al., 1990).

The expression of CD25 is largely T cell specific, unlike CD44 that is widely expressed on many non-T cell lineages (Ponta et al., 2003; Porritt et al., 2004). It is, therefore, assumed the components of the $CD25^-$ $CD44^+$ DN1 population consists of earliest thymic progenitors that posses multi-lineage potential, although intrathymic T cell lineage commitment still remains unconfirmed. It is also thought that by $CD25^+$ DN2 and DN3 stages in development thymocytes have made the commitment to a T cell fate and lost their potential to differentiated into multi-lineages. Additional heterogeneity has been identified in the DN1 populations, with the classification of multiple subsets based on phenotypically distinct surface expression profile, including CD24 and CD117. All DN1 subsets are believed to have the potential to give rise to T cells, but present with different abilities to diverge into other cell types of a myeloid or B cell lineage (Porritt et al., 2004).

Thymocytes at the DN2 stage in development are found throughout the mid to outer cortical regions, whilst the most numerically abundant DN3 population are localized to the subcapsular zone, along with the most mature DN4 division (Lind et al., 2001). On transition to the DN2 stage in development, thymocytes shut down proliferation and initiate the process of TCR gene rearrangement to form the pre-TCR complex. The pre-TCR complex consists of

a TCR β chain paired to a glycosylated pre TCR α chain (gp33), in association with CD3 proteins (Saint-Ruf et al., 1994). Signaling through the complex involves the tyrosine kinase p56Lck. The β chain V(D)J gene recombination and expression precedes that of the TCR α chain and is initiated at the DN2 stage in development, but is not complete until the DN3 phase of differentiation (Dudley et al., 1994; Godfrey et al., 1993). It is during this developmental window that cells are believed to commit to a αβ or γδ lineage. (Dudley et al., 1994). The stage at which this lineage commitment occurs has been a topic of speculation, as evidence suggests progenitors can differentiate into cells of either lineage at the later stages of DN differentiation (Petrie et al., 1992). The successful arrangement of the pre-TCR complex acts as a key checkpoint in T cell development, with β selection driving survival, whilst unsuccessful generation results in apoptosis at the DN4 stage in development (Falk et al., 2001).

The generation of the pre-TCR enables the complex to induce signals to promote cell differentiation and clonal expansion, including the down regulation of CD25 for transition into the final DN4 developmental stage.(Dudley et al., 1994) Signaling through the pre-TCR complex also initiates α chain rearrangement. Thus, the α chain can bind the β chain to form a mature TCR, whilst initiating upregulation of CD4 and CD8 co-receptors for progression towards the $CD4^+$ $CD8^+$ double positive (DP) stage in development (Janas and Turner, 2010).

Introduction of a mutation into either the RAG-1 or RAG-2 genes that induce TCR gene re-arrangement results in a blockade of lymphocyte development with the absence of both T and B cells. T cell development arrests at the DN3 stage in both RAG-1 (Mombaerts et al., 1992b) or RAG-2 (Shinkai et al., 1992) mutant mice. These mutant mouse strains presents with considerable reductions to their thymocyte numbers, a total absence to DP or SP populations

and a failure of cells to express αβ or γδTCR on their cell surface (Mombaerts et al., 1992b; Shinkai et al., 1992). Mice deficient in TCR β genes have confirmed the particular importance of the TCR β gene rearrangement in the transition from DN to DP. The reintroduction of the TCR β gene into arrested DN cells from a RAG-1 (Mombaerts et al., 1992a) or RAG-2 deficient host (Shinkai et al., 1993) can completely rescue all stages in T cell differentiation. The β chain rearrangement has also specifically been identified in inducing CD3 surface expression (Shinkai et al., 1993). In contrast TCR α gene expression appears to be dispensable at this stage in development, during the transition from DN to DP maturation status (Mombaerts et al., 1992a).

The pre-TCR and Notch signaling pathways together are regarded as the minimal requirements needed for the survival and continued development of thymocytes beyond β selection (Ciofani and Zuniga-Pflucker, 2005). However, other receptors are believed to play a role in promoting survival via pre-TCR signaling, including IL-7 receptor and the tumor suppressor p53 (von Freeden-Jeffry et al., 1997). The chemokine receptor CXCR4 has additionally been identified to play a role at this early stage in thymocyte development. CXCR4 has been suggested to regulate thymocyte localization in the SCZ to promote optimal pre-TCR signaling (Trampont et al., 2010). In addition, it has been proposed the receptor can behave as a co-stimulator, along with pre-TCR, to promote survival and proliferation. Specifically CXCR4 is thought to induce upregulation of B-cell lymphoma 2 A (BCL-2A), belonging to the family of apoptotic regulators BCL-2. Thus, it is now accepted signals from the pre-TCR, Notch and CXCR4 collectively are required to support continuous thymocyte development (Janas et al., 2010; Trampont et al., 2010).

After successful rearrangement of the TCR β gene, cells undergo transition to the DN4 stage of intrathymic differentiation. Thymocytes within this phase of development are commonly referred to as pre-DP, as they express detectable levels of TCRβ, CD3, CD4 and CD8 on their cell surface and can rapidly differentiate into DP without any additional stimulation. Thus, this population of thymocytes is thought to represents a subset in transition and an immediate precursor to DP cells (Petrie et al., 1990). At this stage in development thymocytes begin their TCR α chain rearrangement, whilst reinitiating proliferation and expansion. This is temporally stopped between the DN2 to DN3 stage when cells are undergoing TCR β rearrangement (Penit et al., 1995; Tourigny et al., 1997). Differentiating thymocytes then reverse their migratory pathway inwards, towards the inner cortex, which is highly populated by DP cells (Petrie and Zuniga-Pflucker, 2007).

1.2.4 Positive Selection

DP thymocytes expressing functional αβTCRs are selected to continue their development program, via the process of positive selection. The selection of such thymocytes is based upon the abilities of their receptors to recognize self-peptide MHC complexes, present by cTEC (Laufer et al., 1996). Successful recognition and binding of the TCR to the self-peptide MHC complex induces TCR signaling, rescuing the developing thymocyte from programmed cell death. The generation of MHC recognizing TCRs from randomly paired α and β chains is thought to be moderately infrequent, with only a 3% successful selection rate. Around 90% of DP thymocytes are believed to die by neglect within the cortex, after a relatively short life span of on average 3-4 days, without successfully undergoing this key checkpoint in intrathymic T cell development (Hernandez-Munain et al., 1999; Starr et al., 2003).

The brief life span of cells at this stage in development is regulated by several factors that collectively control the expression of the anti-apoptotic protein B cell lymphoma-extra large (Bcl-xL). BcL-xL acts to prolong the life of DP cells, extending the period of which developing thymocytes can successfully undergo positive selection and progress to the $CD4^+$ $CD8^-$ or $CD4^-$ $CD8^+$ single positive (SP) stage in intrathymic T cell development (Guo et al., 2002). Such factors include the transcription factor RAR-related orphan receptor gamma (RORγ), which has been identified as essential in the survival of DP cells. Shut off RORγ expression causes attenuated Bcl-xL expression resulting in accelerated apoptosis and death by neglect (Sun et al., 2000). The transcription factors T cell factor 1 (TCF-1) and lymphocyte enhancer factor 1 (Lef-1), along with their co-activator β-catenin, have all additionally been highlighted as pivotal in T cell survival at the DP stage in development (Ioannidis et al., 2001; Verbeek et al., 1995). The transcription effects of TCF-1 and Lef-1 are regulated by Wnt glycoproteins. Wnt glycoproteins are produced and secreted by the thymic epithelial cells and bind to the frizzled (Fz) transmembrane receptors expressed by developing thymocytes (Pongracz et al., 2003). Signaling through Fz receptors, upon Wnt binding, stabilizes β-catenin and converts TCF-1 and Lef-1 into transcriptional activators. Both transcription factors act upstream of Bcl-xL to exert anti-apoptotic effects on DP thymocytes to prolong their life and increase their chances of undergoing successful positive selection (Ioannidis et al., 2001; Pongracz et al., 2003).

The strength of TCR signaling upon binding to self-peptide MHC is critical in determining the cells fate. The affinity-avidity model postulates that low affinity binding results in partial signaling, generating positively selected thymocytes, whilst high affinity binding drives negative selection to induce cell death and elimination of any potentially self-reactive cells.

Thus, the process of positive and negative selection is mediated by the signaling strength generated through the same receptors binding the same ligands, but triggering opposing cell fates of either differentiation or cell death (Alam et al., 1996; Starr et al., 2003).

There are several theories of how a TCR signaling threshold is established to drive positive selection, negative selection or peripheral activation, on exposure to foreign peptide. One strategy is that the kinetic threshold between positive and negative selection is based on the long avidity of the TCR self-peptide MHC complexes. Those complexes with weak interaction and short half-lives trigger positive selection, whilst those with longer half-lives induce the process of negative selection through the more complete signal received. Therefore, the cell fate of the developing thymocyte is determined primarily by the dissociation rate of the TCR (Williams et al., 1999). A second theory is that the signaling outcome is determined by TCR occupancy and ligand concentration. This model suggests the affinity of TCR engagement can be adjusted by the concentration of ligand present, with low occupancy resulting in positive selection and high occupancy resulting in negative selection. The process of positive selection, therefore, is driven by a lower affinity binding than those that undergo negative selection, yet very low affinity peptides can drive selection if present in large concentrations (Liu et al., 1998; Sebzda et al., 1994). Although it is not clear the exact mechanisms regulating differentiation down the two pathways of selection the threshold must involve a precise TCR affinity.

To maximize the chance of successful positive selection the rearrangement of the TCR α chain does not stop upon binding to the β chain, but continues and undergoes multiple cycles of secondary rearrangements within non-selected DP cells (Petrie et al., 1993). The Vα and Jα gene segment rearrangement can occur on both alleles simulations and precursors initiate α

locus recombination from the 5' prime end of the Jα locus to 3' prime end. Newly formed α chains compete with existing surface chains, enabling the substitution of any out of frame genes configurations or non-selected receptor combinations to generate TCRs with entirely new specificity. The multiple expression of the α chain in succession continues until the cell is selected on the basis of having a function αβTCR, or the cell dies by neglect via programmed cell death. (Davodeau et al., 2001; Petrie et al., 1995; Petrie et al., 1993). TCR engagement with self-peptide MHC complexes during positive selection results in the down-regulation of the expression of RAG genes, RAG-1 and RAG-2, to terminate further TCR α chain rearrangements (Brandle et al., 1992; Petrie et al., 1993).

1.2.4.1 Conventional Single Positive Lineage Commitment

Successful positive selection results in the commitment and differentiation of DP thymocytes into a CD4 or CD8 T cell lineage fate. During the transition from DP to the SP stage, developing thymocytes are required to commit to a CD4 or CD8 lineage, exclusively expressing only one of the two coreceptor glycoproteins and recognizing only one class of MHC molecules (Xiong and Bosselut, 2012). The defining mechanisms used by the DP cell to decide its lineage fate are relatively unclear and several models have been proposed. Two original lineage commitment models were proposed, stochastic and instructional, that aimed to explain how DP cells determine their co-receptor expression and MHC specificity (von Boehmer, 1996). The stochastic model suggests that early lineage commitment occurs independently of TCR specificity. With this model, only cells expressing a complimentry CD4 or CD8 co-receptor to the MHC Class I or Class II molecule bound upon TCR engagment continue their development (Robey et al., 1991). The instructive model proposes the recognition and co-engagement of a particular MHC by the TCR activates the specific

complimentary CD4 or CD8 differentiation program. Therefore, MHC Class I TCR recognition promotes the CD8 developmental program, including the switching off of CD4 signaling and vice versa for MHC Class II binding. It has also been suggested that the distinct instructional program within this model is delivered directly via the co-receptors (Hernandez-Hoyos et al., 2000; Robey et al., 1991; von Boehmer, 1996). More recent models have suggested a quantitative signaling model for lineage commitment. This is where the strength of the TCR signal received during positive selection instructs the developing DP precursor to commit to either the CD4 or CD8 lineage, with strong signals promoting $CD4^+$ SP differentiation, whilst weaker signals drive a $CD8^+$ SP cell fate (Hernandez-Hoyos et al., 2000; Matechak et al., 1996). Other studies suggest the duration of the TCR signal during positive selection, rather than the strength of the signal, directs a CD4 versus CD8 T cell lineage fate. Sustained TCR signaling is thought to support $CD4^+$ SP development, whereas transient receptor signaling promotes CD8 differentiation (Liu and Bosselut, 2004; Yasutomo et al., 2000). It has also been demonstrated that lineage commitment is additionally subject to temporal regulation, with the generation of the CD4 lineage occurring rapidly after positive selection, while the CD8 lineage has a more delayed emergence period of approximately 3 days (Saini et al., 2010).

Although it may be unclear what initial interactions are crucial in determining lineage commitment, various studies have identified a number of transcription factors with opposing repressive abilities that play a downstream role in promote lineage differentiation of DP thymocytes. Runt-related transcription factor (Runx) is a family of transcription factors involved in the differentiation of $CD8^+$ SP differentiation, by promoting CD8 gene transcription and lineage commitment. Specifically Runx3 has been identified in playing a

role at the DP stage of differentiation by binding and activating CD4 silencers, resulting in repression of CD4 gene transcription. In contrast, Thpok is the transcription factor thought to be required for the acquisition of the CD4 T cells helper effector function, whilst inhibiting the genetic programming towards the cytotoxic CD8 lineage (Wildt et al., 2007). On TCR MHC class II engagement, Thpok is activated via the reversal of the Thpok silencer activity. Thpok directly binds the CD4 gene silencer, antagonizing the repressive functions of Runx3 to activate the transcription of the CD4 gene. The upregulation and maintenance of the surface expression of CD4 facilitates the prolonged TCR engagement with MHC class II. This continues to antagonize the Thpok silencer and mediates further Thpok upregulation, overall inducing a feed back loop to inhibit cytotoxic lineage differentiation (Muroi et al., 2008). Loss of Thpok function can result in the redirection of MHC class II restricted thymocytes into a CD8 lineage, whilst transgenic over-expression of transcription factor can induce MHC class I restricted cells to differentiate into a CD4 T cell fate (He et al., 2005; Sun et al., 2005). In comparison, Runx3 over expression cannot reverse lineage commitment and induce differentiation of MHC class II restricted thymocytes into a CD8 cell fate, even though over expression during DP development can strongly reduce CD4 expression (Grueter et al., 2005). These findings demonstrate Thpok is a master regulator of lineage commitment on initiation of positive selection and dominates the effects of Runx3. Interestingly, regardless of final commitment to a CD4 or CD8 fate, all thymocytes undergo a transitional differentiation state between the DP and SP stages in maturation, where cells initially down regulate CD8 to give a common $CD4^{+}CD8^{low}$ phenotype. Those cells that have committed to a MHC class II restricted lineage then progress directly into $CD4^{+}$ SP cells, whilst those destined for a $CD8^{+}$SP cell fate must undergo two additional intermediate phases of development: $CD4^{low}$

$CD8^{low}$ followed by $CD4^{low}$ $CD8^{+}$, before finally maturing into a $CD8^{+}$ $CD4^{-}$ SP thymocyte (He et al., 2010; Lundberg et al., 1995).

1.2.4.2 Nonconventional Lineage Commitment

High affinity TCR binding does not always result in the negative selection, but can also trigger the differentiation of thymocytes down non-conventional developmental pathways, such as that of nTreg or invariant natural killer cells (iNKT). Some MHC Class II restricted thymocytes that receive stronger TCR stimulation high-affinity self-antigen binding, can be rescued from clonal deletion and differentiate into nTreg (Moran et al., 2011; Stritesky et al., 2012). The precise affinity threshold needed for Treg development, however, is still unknown. It has been suggested the affinity of binding is not equal to, but only slightly lower than the strength of TCR interactions required to drive clonal deletion, thus proposing the affinity threshold is unlikely to be a major cell fate determinant (Stritesky et al., 2013). The antigenic niches for this selection process are typically limited and nTreg precursors are believed to have to compete for interaction with these rare self-antigens (Bautista et al., 2009). It is also thought this multistep differentiation program involves cytokines, co-stimulatory molecules and a variety of antigen presenting cells. The availability of these environmental factors may also provide additional competition, limiting nTreg development (Lio and Hsieh, 2011). The process of intrathymic Treg induction is believed to occur in at least two sequential stages. TCR stimulation initially stimulates the upregulation of CD25 on the surface of those cells differentiation into nTreg, before the intracellular expression of FoxP3. This establishes a $Foxp3^{-}CD25^{+}$ nTreg precursor population, thought to not require additional TCR stimulation to complete their development into $Foxp3^{+}CD25^{+}$ nTreg (Lio and Hsieh, 2008). The precise requirements driving maturation down this non-conventional $CD4^{+}$ SP developmental route

remains poorly understood and a topic of great interest. Thus, one of the main focuses of Chapter 4 is to address what essential cellular components are needed to support the development of this non-conventional nTreg lineage fate.

1.2.4.3 Phenotypical Changes On Initiation Of Positive Selection

Although the initiation of positive selection is critically dependent upon TCR self-peptide MHC interactions, subsequent events during this multi-stage process can occur independently of ongoing MHC engagement. The MHC independent intermediate stage of positive selection is classified by the expression of the activation marker CD69, which is rapidly upregulated by T cells after TCR stimulation (Hare et al., 1999). This marker is detectable on a small fraction of DP cells along with a subset of newly generated, immature CD4 and CD8 SP thymocytes. This transient surface expression pattern of CD69, therefore, can be used in the identification of thymocytes that are undergoing or have recently undergone this critical selection process (Yamashita et al., 1993).

Additionally, induction of the positive selection process also drives thymocytes relocalization from the cortex into the medulla, where they undergo additional selection and differentiation. It is widely accepted this migratory pathway involves CCR7 (Kurobe et al., 2006; Kwan and Killeen, 2004; Nitta et al., 2009; Ueno et al., 2004). TCR engagement during positive selection elevates CCR7 surface expression on developing thymocytes (Davalos-Misslitz et al., 2007), which then migrate into the medulla via chemoattraction to CCR7 ligands: CCL19 and CCL21, produced within the medullary thymic environment (Ueno et al., 2002). If CCR7 signaling is disrupted it results in defective migration and consequently reduced negative selection (Nitta et al., 2009; Ueno et al., 2004). Following TCR stimulation, activated DP thymocytes are thought to also be strongly responsive to CCL25, expressed by cTEC, via

their surface expression of CCR9 at both the DP and the newly generated SP stages in maturation. Highly regulated expression of the protein PlexinD1 is thought to block the migrating of developing thymocytes down the CCL25 chemokine gradient, preventing their retention in the cortex. This inhibition facilitates newly selected thymocytes to migrate against the CCL25 chemokine gradient into the CCL19 and CCL21 enriched medullary thymic microenvironment, to continue their differentiation program (Choi et al., 2008). Although currently it is believed CCR7 and PlexinD1 exclusively orchestrate thymocyte trafficking, other chemokines have been speculated to play a role in this migratory pathway. Strong candidates that may contribute to the cortex-to-medulla migration include CCR4, reported to be upregulated on the thymocyte cell surface after the initiation of positive selection (Campbell et al., 1999). Its ligands, CCL17 and CCL22, are predominately expressed in the $CD80^{high}$ $AIRE^{+}$ mTEC population (Campbell et al., 1999; Laan et al., 2009). Specifically the most immature $CD4^{+}$ SP, classified as the SP1 population (see Section 1.2.6 for explanation of SP1 to SP4 classification system) demonstrate the highest *CCR4* mRNA levels, likely to represent the most recent subset of cells to undergo the positive selection process. *Ccr4 e*xpression is then down regulated by the SP2 stage in $CD4^{+}$ SP development (Teng et al., 2011). This tight window of CCR4 expression compliments the timing of when SP thymocytes are believed to undergo their re-localization to the medulla. However, the role of CCR4 in cortex to medulla migration needs additional investigation. We aim to explore the effects of the removal of this chemokine receptor in Chapter 5.

1.2.5 Negative Selection

The process of negative selection is a fundamental checkpoint in the establishment of central tolerance. The term central tolerance refers to the intrathymic mechanisms used to detect and

eliminate self-reactive T cells, before their export into the periphery, where they could potentially cause harm. Central tolerance mechanisms include clonal deletion of autoreactive cells via negative selection and clonal diversion of nTreg to suppress the activation of any self-reactive cells that escape into the periphery (Kyewski and Klein, 2006; Xing and Hogquist, 2012).

High affinity TCR recognition of self-peptide induces negative selection and activates apoptotic pathways. This pathway of cell death is mediated by the pro-apoptotic Bcl-2 family of BH-3 proteins. The cooperation of BH-3 proteins, Bim and Puma, specifically results in apoptotic deletion of autoreactive cells and the prevention of organ-specific autoimmunity (Gray et al., 2012). The intracellular mediators of negative selection are members of mitogen-activated protein kinases (MAPK) pathways, which included extracellular signal-regulated kinases (ERK) and Jun amino-terminal kinase (JNK). It has been suggested that no single MAPK pathway is exclusively associated with positive or negative selection, but rather the kinetics of MAPK activation mediates the differences in the positive and negative selecting signals. Both ERK and JNK are induced during positive and negative selection, however, high affinity binding induces rapid and robust activation of ERK to drive cell death, in contrast to low affinity binding which stimulates prolonged, lower intensity activation of the intracellular mediator (Daniels et al., 2006; Xing and Hogquist, 2012). The net result is the alteration to the activation patterns of these MAPK signaling intermediates determines the transcription factors that are triggered to control the cell fate, based upon the intensity of the ligands bound (Palmer, 2003).

Negative selection can occur at various stages throughout thymocyte development, from early stages in thymocyte maturation, when cells reside within the cortex, to the later stages in

intrathymic development when thymocytes inhabit the medulla (McCaughtry et al., 2008; Surh and Sprent, 1994). Evidence suggests thymocytes are susceptible to negative selection as early as the transitional phase from DN to DP, upon TCR antigen encounter within cortical regions (Takahama et al., 1992). It is therefore assumed negative selection is not a sequential event following positive selection, but the two selection processes occur independently of one another (Palmer, 2003). It has also been proposed that DP thymocytes within the cortex undergo 2-3 times higher negative selection rates compared to their SP mature counterparts residing within the medulla (Stritesky et al., 2013). Antigen presentation by the cTEC population alone is not believed to be efficient at inducing cell apoptosis, although they represent the major stromal cell population within the cortical compartment and can interact with developing thymocytes to trigger TCR activation during positive selection (Laufer et al., 1996). Instead, it is thought rare cortical DC populations mediate antigen specific clonal deletion within this region. (McCaughtry et al., 2008).

Although the rate of negative selection may be higher within the cortical region, the thymic medulla is considered to be a specialized site for optimal negative selection in the establishment of central tolerance. This is due to the medullary environment having a high prevalence of APC and the unique ability of the mTEC population to express a wide array of antigen to developing thymocytes (Gray et al., 2005). The mTEC populations can cross-present antigen to DC, in both their native and processed MHC-bound form. This facilitates both APC types to mediate deletion of potentially self-reactive T cells. This unidirectional transfer of self-antigen broadens the cellular base of self-tolerance and thus enhances it efficiency (Gallegos and Bevan, 2004; Koble and Kyewski, 2009). The specialized role of

mTEC and DC in the establishment of self-antigen mediated negative selection will be discussed in greater detail in Section 1.3.3.

In addition to TCR ligation, it has been suggested negative selection requires secondary signaling pathways provided by co-stimulatory molecules on APC. Although APC express a large variety of co-stimulatory molecules, it is not clear which are essential for successful negative selection. The co-stimulatory molecule CD28 has been implicated in driving cell apoptosis upon binding CD80/86, however the unaltered selection of CD28 deficient thymocytes demonstrates its role is nonessential, or alternatively, redundancy by other co-stimulatory molecules mask the effects of its removal. When CD28 deficient cells are placed in a competitive environment with their wild type (WT) counterparts, CD28 expressing thymocytes have a selective advantage, suggesting the CD28 co-stimulatory pathway increases the efficiency of this selection process (Walunas et al., 1996).

It is very difficult to accurately predict the number of potentially autoreactive thymocytes that undergo negative selection during their development within the thymus, with studies reporting a wide range of estimates. A recent report has predicted the rate of negative selection is far greater than the number of thymocytes undergoing positive selection. The estimated difference was reported to be as great as a 5-fold (Stritesky et al., 2013). This observation suggests the negative selection process must efficiently eliminate large numbers of intrathymically developing potentially self-reactive thymocytes.

1.2.6 Post-Selection Maturation

The medullary residency of newly generated SP thymocytes is commonly believed to be up to 2 weeks (Scollay and Godfrey, 1995), during which time cells undergo their final

differentiation steps before emigrating into the periphery as naive T cells (Egerton et al., 1990; Gabor et al., 1997a; Scollay and Godfrey, 1995). Transgenic mice for green florescent protein (GFP) driven by the RAG-2 promoter (RAG-2 GFP) can be used to identify recent thymic emigrants (RTE) within the periphery. The GFP levels can also act as a 'molecular timer', as the gradual loss of GFP expression on the termination of the RAG genes at the DP stage can define the 'age' of the differentiating thymocyte (Boursalian et al., 2004). On re-examination of developing thymocytes using this RAG-2 GFP transgenic mouse model, it has been proposed emigration of SP thymocytes into the circulation can occur after only a 4 to 5 day inhabitance within the medulla (McCaughtry et al., 2007).

During their occupancy within the medulla, SP thymocytes undergo a series of phenotypical and functionally distinct maturational stages. Newly generated SP thymocytes are characterized by a $CD69^{+}$, heat-stable antigen $(HSA)^{high}$, $Qa2^{-}$, $CD62L^{low}$ surface phenotype. SP thymocytes are estimated to express this surface phenotype for two thirds of their total residency time (Kelly and Scollay, 1990; Lucas et al., 1994; McCaughtry et al., 2007). SP cells then continue differentiating and the surface expression profile changes to $CD69^{-}$ HSA^{low} $Qa2^{high}$ $CD62L^{high}$. The mature thymocytes lose their susceptibility to apoptosis at this stage in development, but instead undergo proliferation upon antigen exposure (Gabor et al., 1997b; Kelly and Scollay, 1990; Kishimoto and Sprent, 1997; Lucas et al., 1994; McCaughtry et al., 2007; Weinreich and Hogquist, 2008). $CD4^{+}$ SP thymocytes have an additional sub-classification system for their maturation status, separated into four distinct subsets, SP1 ($CD69^{+}$ $6C10^{+}$ $Qa2^{-}$) SP2 ($CD69^{+}$ $6C10^{-}$ $Qa2^{-}$) SP3 ($CD69^{-}$ $6C10^{-}$ $Qa2^{-}$) and SP4 ($CD69^{-}$ $6C10^{-}$ $Qa2^{+}$). This differentiation of $CD4^{+}$ SP thymocytes within the medulla is believed to follow a linear and unidirectional developmental pathway (Jin et al., 2008). Interestingly,

transition of thymocytes from the SP3 to SP4 stage in development is believed to be dependent upon an intact medullary environment. Disruption of medullary microenvironments results in a block in development at the SP3 stage, resulting in the absence of the most mature $CD69^{-}$ $Qa2^{+}$ SP4 population (Li et al., 2007). The precise interactions provided by the medulla to support this important checkpoint in the conventional $CD4^{+}$SP maturation program are unknown and this will be explored in greater detail in Chapter 4.

Mature SP medullary residents undergo a wave of post-selection proliferation involving at least 6 rounds of cell divisions. This cellular expansion of SP thymocytes is evident at all development ages, but is more pronounced within the neonatal thymus, where it may aid the establishment of the neonatal peripheral T cell pool. The continued presence of thymic epithelial cells has been identified as both essential and sufficient to drive this proliferative wave. This stage in development can occur independently of ongoing TCR-MHC interactions, in the presence of MHC-deficient thymic stromal cells (Hare et al., 1999; Hare et al., 1998). It has instead been speculated that the essential role for mTEC is in its production of soluble factors, such as cytokines. Cytokine-mediated signaling has been implicated in the regulation of this late phase of intrathymic proliferation, specifically IL-7 and its receptor IL-7R. Successful TCR signaling during positive selection directly controls the upregulation of IL-7R on the thymocyte cell surface. Signaling through this receptor, upon IL-7 binding, is believed to be pivotal for thymocyte differentiation, as the lack of expression of the IL-7Rα complex results in a dramatic reduction in post-selection proliferation (Hare et al., 2000). The upregulation of this receptor is not believed to be a passive process of maturation, but rather an event dependent upon the quality of the TCR signaling received during positive selection.

Thus, the expression pattern of IL-7Rα can additionally control the selection of the T cell repertoire (Sinclair et al., 2011).

Mature thymocytes emigrate from the thymus via blood vessels at the cortical medullary junction. The process of thymic egress is regulated by the receptor sphingosine-1-phosphate receptor-1 ($S1P_1$). $S1P_1$ must be upregulated on the SP cell surface to aid migration towards the blood, where its ligand, S1P, is highly expressed (Allende et al., 2004). The absence of the receptor results in a complete lack of T cells within the periphery, due to a total block in thymic egress, whilst over-expression of $S1P_1$ results in premature release of thymocytes into the circulation (Allende et al., 2004; Matloubian et al., 2004; Zachariah and Cyster, 2010). The expression of $S1P_1$, therefore, plays a central role in regulating the number of peripheral T cells and its induction is directly dependent upon the transcription factor Kruppel-like factor (KLF) 2 (Carlson et al., 2006). The upregulation of both KLF-2 and $S1P_1$ increases with SP maturity, with the greatest expression of both molecules being in thymocytes displaying the most mature phenotype, based upon high CD62L/Qa2 and low RAG-2 GFP levels (McCaughtry et al., 2007). The mechanisms inducing KLF-2 expression, however, remains poorly understood. The transcription factor forkhead box O (Foxo) -1 has been implicated, at least in part, in the control of KLF-2 expression, but the exact process is unknown (Kerdiles et al., 2009).

Thymic export does not appear to be regulated by downstream alterations to the size of the peripheral T cell pool, as the complete deletion of total peripheral T cells has no influence on emigration rates of RTE (Gabor et al., 1997b). Instead emigration from the thymus is thought to occur via a ‘conveyor belt mechanism’. The oldest, most mature SP thymocytes exit into the periphery, once they have completed their maturation program and express the correct

‘exit’ phenotype, complementary to the profile expressed by recent thymic emigrant (RTE) within the circulation. This suggests that, the multi-step developmental program of SP thymocytes within the medullary is essential before cells can be exported into the periphery as naive T cells (Gabor et al., 1997a; McCaughtry et al., 2008).

1.3 THYMIC MICROENVIRONMENTS

1.3.1 The Ontogeny Of Thymic Epithelial Cells

1.3.1.1 Classification of cTEC and mTEC

TEC populations are commonly defined as CD45 negative cells that express the surface marker Epithelial Cell Adhesion Molecule 1 (EpCAM1) (Trzpis et al., 2007). In an adult mouse, cTEC and mTEC populations can be distinguished based on their expression of several phenotypical markers. The cortical epithelium is frequently characterized by the expression of a panel of markers including the intracellular expression of cytokeratin 8 (K8) and MTS44, in addition to the surface expression of Ly51. The cTEC population also acquires CD40 and high levels of MHC Class II. More recently cTEC specific proteosomal subunit β5T has been used as a tool for recognition of this distinct TEC population. This proteasomal subunit is expressed exclusively in cTEC and is responsible for the generation of a unique set of self-peptides presented by MHC Class I, key to the positive selection of $CD8^+$ SP (Anderson and Takahama, 2012; Gray et al., 2006; Murata et al., 2007). In contrast *Prss16* encodes thymus-specific serine protease (TSSP), which participates in self-peptide MHC class II presentation during the positive selection of $CD4^+$ SP thymocytes and is also specifically expressed by cTEC (Gommeaux et al., 2009). The endocytic receptor CD205 (also known as DEC-205) aids uptake and presentation of self-antigen and is an extra marker used in the identification of cTEC, but its expression is shared with thymic DC (Shrimpton et al., 2009).

In contrast to cTEC identification, the cell surface and cytoplasmic markers used for mTEC identification include cyokeratin5 (K5), CD80, AIRE, MTS10, the lectin UEA1 and claudin-

3/claudin-4. The mTEC population can be further subdivided into two main subsets, based upon the levels of expression of MHC class II and the co-stimulatory molecule CD80: $CD80^{high}$ MHC Class II^{high} mTEC (typically referred to as $mTEC^{high}$) and $CD80^{low}$ MHC Class II^{low} mTEC ($mTEC^{low}$) (Anderson and Takahama, 2012; Gray et al., 2006). These two mTEC subsets also display different levels of expression of promiscuous genes for tissue-restricted self-antigen (TRA) synthesis and autoimmune regulator (AIRE) protein (see Section 1.3.3.1). The $mTEC^{high}$ subset exhibit much greater levels of AIRE and present a greater range of TRAs compared to their $mTEC^{low}$ counterparts (Derbinski et al., 2005; Gray et al., 2007).

1.3.1.2 Differentiation Of cTEC And mTEC Lineages

At the early stages in thymic organogenesis, around E12, the thymic rudiment exists as a simple structure, consisting of a core of TEC progenitors. It has been observed that functionally detectable Foxn1-dependent progenitors at this stage in embryogenesis are bi-potent, giving rise to epithelial of both cortical and medullary lineages. (Bleul et al., 2006; Rossi et al., 2006). Clonal assays of single, individually selected, thymic epithelial progenitors at E12 demonstrated this bi-potent potential, with progenitors displaying the capacity to differentiate into both mTEC and cTEC phenotypes (Rossi et al., 2006). *In vivo* cell lineage assays further confirmed the existence of this common TEC progenitor, in addition to indicating its continued presence within the post-natal thymus, suggesting a possible role for the progenitor in cTEC and mTEC production later in life (Bleul et al., 2006). Although this common epithelial precursor has been identified, its phenotypical identity still remains relatively unclear. Initial studies into the phenotypical characteristics of thymic epithelial progenitor identified heterogeneity within the TEC precursor population, based upon the expression of the cell surface glycoprotein MTS24. It was demonstrated both

MTS24^{+} and MTS24^{-} populations had different progenitor potentials to reconstitute the complex thymus microenvironment, identifying this as a possible progenitor marker (Bennett et al., 2002; Gill et al., 2002). However, upon reassessment no discrimination was observed between the progenitor potential of MTS24^{+} and MTS24^{-} populations, with both demonstrating the capability to give rise to fully functional cortical and medullary thymic epithelium (Rossi et al., 2007a), highlighting the current lack of a cTEC/mTEC bi-potent precursor identification system.

The events occurring downstream of the bi-potent progenitors and the mechanisms that regulate the commitment and differentiation of distinct cortical and medullary areas are also poorly understood. Down stream of the bi-potent precursors, distinct lineage restricted progenitors are believed to initiate the emergence of cTEC or mTEC differentiated progeny (Rodewald et al., 2001). Further analysis of cTEC/mTEC lineage emergence has particular focus on the development of the specialized mTEC population, whilst the stages and mechanisms of cTEC differentiation remain more poorly understood. A correlation between lymphoid progenitor settling and the emergence of a cTEC population has been identified at E12, with the detection of EpCAM1^{+} TEC populations expressing cTEC lineage identifiers, including CD205 and β5T (Shakib et al., 2009). Nude mice, deficient in Foxn1 expression, demonstrate an absence of such cTEC define subsets, suggesting acquisition of such cTEC markers during the TEC development program is a FOXN1 dependent process at this early developmental stage. This Foxn1-dependepent cTEC population was also identified as a possible cTEC progenitor cell, due to its lack of expression of mature cTEC markers such a CD40 and MHC class II. This suggests this initial CD205^{+} CD40^{-} population would be positioned between the bi-potent cTEC/mTEC progenitor and the mature cTEC population,

before the occurrence of CD40 and MHC Class II upregulation. Although the emergence of the $CD205^+$ TEC population can occur in the absence of thymocyte-derived signals, their continued development to the mature $CD40^+$ MHC Class II^+ phenotype demonstrated a dependency on the presence of DN thymocytes, illustrating an essential requirement of thymic cross talk in the cTEC differentiation program (Shakib et al., 2009). A more recent investigation has identified that $CD205^+$ progenitors are capable of differentiating into both cortical and medullary microenvironments able to support thymocyte maturation, if purified and transplanted under the kidney capsule of a WT mouse. This population was detectable as early as E11 and was capable of simultaneously expressing hallmarks of both the cTEC and mTEC lineages, with the co-expression of the cTEC maker CD205 and the mTEC marker RANK. Collectively this data argues against the model that lineage restricted progenitors diverge simultaneously from a common bi-potent progenitor early in TEC development (Baik et al., 2013).

The idea of lineage-restricted mTEC progenitor pools was first founded on the discovery a single mTEC progenitor can give rise to individual medullary epithelial islets (Rodewald et al., 2001). Studies have also suggested a precursor-product relationship within the mTEC lineage, with the emergence of $CD80^+$ $Aire^+$ $mTEC^{high}$ cells from the immature $CD80^-$ $Aire^-$ $mTEC^{low}$ subset, establishing mTEC heterogeneity and suggesting AIRE expression is a late event in mTEC differentiation (Gray et al., 2007; Rossi et al., 2007b). The $AIRE^+$ $mTEC^{high}$ population demonstrates more rapid, steady state turner over rates compared to their more mature precursors, with an estimated turnover every 10-14 days. This suggests that AIRE not only drives TRA expression, but also promotes cellular changes to raise efficiency of cross-presentation, which may include down stream enhancement of cell death (Gray et al., 2007;

Gray et al., 2006). The initial emergence of mTEC committed progenitors occurs as early as E13, based on the expression of tight junction components claudin -3 and -4 (Cld3,4), along with more well known mTEC markers such as MTS10 and UEA1 (Hamazaki et al., 2007).

A simplified overall scheme of TEC lineage development is displayed within Figure 1.3.

1.3.2 The Regulation Of mTEC Development

Thymic crosstalk has been identified as being essential in mTEC development, with the requirement for αβTCR expression specifically for mTEC generation and maintenance (van Ewijk et al., 1994). The elimination of αβTCR expressing thymocytes, by disruption the *Tcr* α gene, results in a block in development at the DP stage (Philpott et al., 1992). Absence of the *Tcr* α gene consequently causes a dramatic reduction to the numbers of mTEC, suggesting mTEC development is dependent upon successful αβTCR interactions (Palmer et al., 1993). Additional lymphocyte deficient mouse models, such as RAG-1 or RAG-2 knock out mice, which have a halt in thymocyte development at the DN stage in differentiation, also present with similar reductions to mTEC cell numbers and obliteration of the medullary architecture (van Ewijk et al., 1994). Therefore, collectively this data highlights the dependency of interactions between haemopoietic cells and the mTEC population for the formation of intact medullary compartments, essential for the establishment of T cell tolerance.

The essential role of thymic crosstalk in TEC development has highlighted the importance of understanding the molecular basis of thymocyte-derived signals driving the successful development of the cTEC and mTEC compartments. Particular focus has been placed on the

Figure 1. 3 TEC Lineage Development From a Bipotent Progenitor

The Figure displays the developmental pathway of medullary thymic epithelal (mTEC) cells and cortical thymic epithelial cells (cTEC) from a common bipotent progenitor. $EpCAM^{+}$ progenitors can differentiate into either immature mTEC or immature cTEC, in a FOXN1 dependent manner (red arrow). The immature cTEC population has been demonstrated to give rise to immature mTEC (the alternative lineage potential is indicated as a curved dashed arrow). Both the immature cTEC and mTEC populations undergoing additional differentiation into a mature cTEC/mTEC phenotype based upon their surface expression and intracellular expression patterns of the stated markers

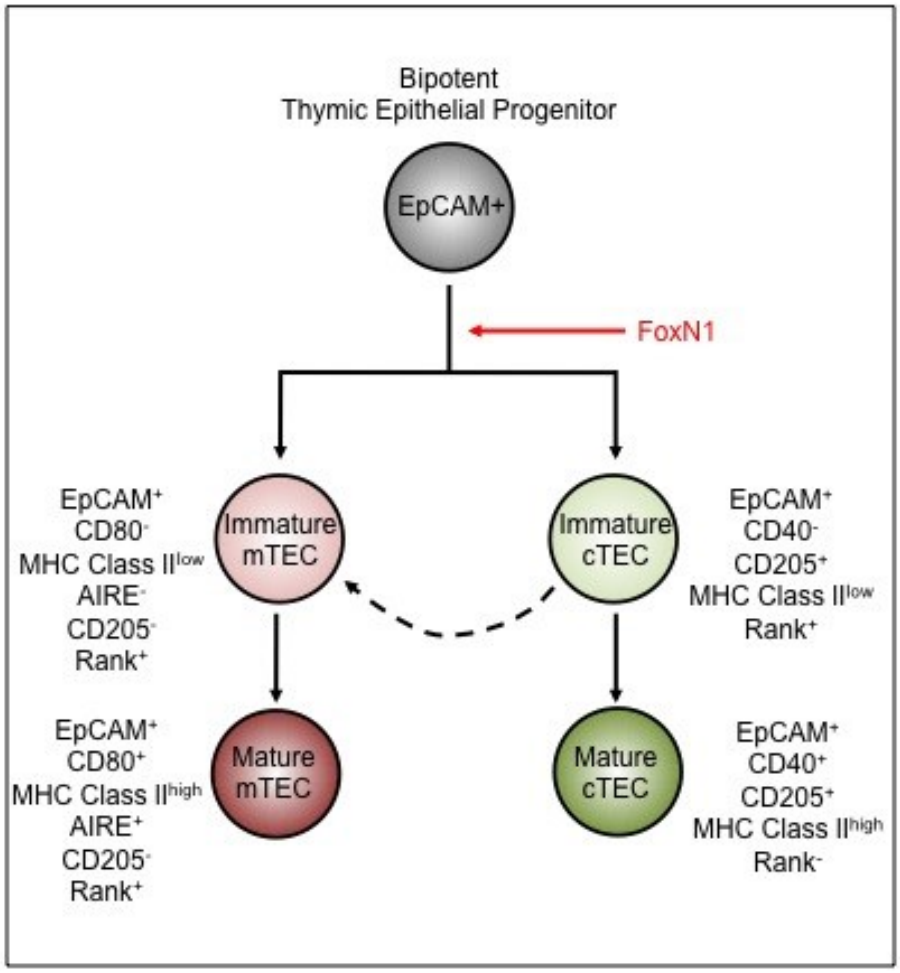
Bipotent
Thymic Epithelial Progenitor
EpCAM+
FoxN1
EpCAM+
CD80-
MHC Class IIlow
AIRE-
CD205-
Rank+
Immature
mTEC
Immature
cTEC
EpCAM+
CD40-
CD205+
MHC Class IIlow
Rank+
EpCAM+
CD80+
MHC Class IIhigh
AIRE+
CD205-
Rank+
Mature
mTEC
Mature
cTEC
EpCAM+
CD40+
CD205+
MHC Class IIhigh
Rank-

environmental cues underpinning the generation of an intact medullary compartment, specifically the involvement of members of the tumour necrosis factor receptor superfamily (TNFRSF). This large family of surface receptors mediate nuclear factor (NF)κB transcription factors and activates NFκB signaling pathways, which are important in peripheral lymphoid tissue development, along with organization of an intact medulla microenvironment (Anderson and Takahama, 2012). Mice deficient in RelB, a subunit of the NFκB complex, present with severe blocks in mTEC development and lack of medullary compartments, resulting in a breakdown of clonal deletion of autoreactive thymocytes and multi-organ autoimmunity (Burkly et al., 1995; Naspetti et al., 1997). TNFRSF expression is widespread in the mTEC population, but have a more restricted expression profile in cTEC. To date, four receptors of this family have been identified as playing a critical and distinct role in thymic organogenesis, specifically mTEC differentiation; receptor activator of nuclear factor κB (RANK), Osteoprotegerin (OPG) (a decoy receptor for RANK), CD40 and lymphotoxin β receptor (LTβR) (Anderson and Takahama, 2012).

Both CD40 and RANK have been identified as essential regulators of mTEC development, via signaling through the TNF receptor-associated factor (TRAF) 6. Mice deficient of TRAF6 have disorganized disruption of mTEC, with a particular absence of the $AIRE^{+}$ mature mTEC subset (Akiyama et al., 2005). Absence of RANK or RANK ligand (RANKL) results in the complete absence of $AIRE^{+}$ mTEC in the mouse embryonic thymus, whilst within the adult thymus the population is present, but at significantly reduced frequencies (Akiyama et al., 2008; Hikosaka et al., 2008). In contrast, the CD40 signaling pathway does not appear essential for development of the mTEC compartment, with CD40 or CD40 ligand (CD40L)

deficient adult mice presenting with no alterations to mTEC numbers, generation of $AIRE^+$ mTEC or medulla formation (Dunn et al., 1997; Hikosaka et al., 2008). Collectively, this data suggests RANK signaling is fundamental in the differentiation of $AIRE^+$ mTEC during embryogenesis and indicates the CD40 signaling pathway is redundant. It has been suggested, however, that cooperation between the two signaling pathways is crucial in postnatal mTEC development. After birth CD40-CD40L signals have been demonstrated to contribute to the development and maintenance of mTEC and this signaling pathway is thought to compensate for RANK-RANKL deficiency within the postnatal thymus (Akiyama et al., 2008; Desanti et al., 2012).

Further investigations into the essential role of RANK in mTEC differentiation identified intrathymic lymphoid tissue inducer (LTi) cells as the main provider of RANKL during embryogenesis. RANKL signals from the LTi population are thought to regulate the differentiation of $CD80^+$ $AIRE^+$ mTEC from their $CD80^-$ $AIRE^-$ progenitors. The transplantation of RANK deficient embryonic thymic lobes, with absent $AIRE^+$ mTEC compartments, into a T cell deficient nude host results in autoimmunity, identifying RANK as a prenatal key regulator of AIRE induction and central tolerance establishment (Rossi et al., 2007b). Specific subsets of γδ T cells, named $V\gamma5^+$ dendritic epidermal T cells, have also been implicated in providing RANKL for $AIRE^+$ mTEC induction in the embryonic thymus (Roberts et al., 2012). Within the adult thymus, SP thymocytes with an immature $CD69^+$ phenotype are thought to be the main intrathymic physiological source of RANKL and CD40L to the developing mTEC population. Interactions between the RANKL produced by positively selected thymocytes and RANK expressed on mTEC, drives positive-selection mediated medullary formation of $AIRE^+$ mTEC (Hikosaka et al., 2008). Additional

observations suggest positive selection of conventional $CD4^+$ SP T cells induces sequential acquisition of first, RANKL and then CD40L on their cell surface. Interestingly, however, $CD4^+$ SP that have committed to an nTreg cell fate provide RANKL, but lack CD40L expression, regardless of their maturation status. The expression of CD40 by the mTEC population is also dependent upon previous RANK signaling and occurs prior to the differentiation of mTEC into the $AIRE^+$ $CD80^{high}$ mature phenotype. Collectively this data suggests mTEC development in the adult setting is controlled by a sequence of thymic crosstalk events, initially involving RANK signaling, followed by CD40, which is influenced by distinct CD4 SP subsets (Desanti et al., 2012).

Deficiency of LTβR results in more of an overall disruption to medullary organization, compared to RANK and CD40, with no reduction in the $AIRE^+$ mTEC fraction. The absence of LTβR leads to a decrease in mTEC cell numbers and thymic retention of mature thymocytes, associated with inducing autoimmunity. This LTβR deficient phenotype suggests continuous signaling transduction through the receptor is required for the maintenance of the medullary architecture. Overall the suggests LTβR it is an additional member of the TNF receptor super-family involved in the crosstalk mechanisms controlling the development of mTEC, for the establishment of central tolerance (Boehm et al., 2003).

1.3.3 Specialization Of The Thymic Medulla In Tolerance Induction

The widely accepted role of the thymic medulla is in the establishment of immunological tolerance. This role is subdivided into the elimination of potentially self-reactive cells via clonal deletion and the generation of nTreg to suppress any escapee self-reactive T cells within the periphery (Li et al., 2007). The medulla is a complex three-dimensional structure

that has multiple mechanisms to ensure the successful production of a self-tolerant T cell pool. This involves the integration of signals from various stromal cellullar components, particularly mTEC and DC.

1.3.3.1 The Role Of mTEC In Central Tolerance

mTEC are a specialized type of stromal cell that supports clonal depletion by their ability to undergo promiscuous gene expression. This ectopic gene expression enables mTEC to express a vast range to TRA on their surface for either direct presentation to developing thymocytes or cross-presentation to DC. The TRA repertoire represents virtually all organ-specific antigens, mirroring peripheral self. This enables the pre-emptive encounter of potentially self-destructive T cells with peripheral self-antigens to purge them from the T cell repertoire, or drive their differentiation down the nTreg lineage. The intrathymic expression of TRA is a distinct characteristic of the mTEC cell type (Derbinski et al., 2001; Kyewski and Klein, 2006).

The precise mechanisms regulating the promiscuous gene expression of TRA by mTEC is currently poorly understood. However, the regulator protein, AIRE, has been identified as critical in promoting the ectopic expression of peripheral antigens. AIRE is a 545 amino acid protein localized to the nucleus, where it functions as a transcriptional factor to promote promiscuous gene expression of TRA (Anderson et al., 2002; Liston et al., 2003). Mutations to the AIRE gene in man results in a multi-organ autoimmune condition know as autoimmune polyendocrinopathy candidiasis ectodermal dystrophy syndrome (APECED) (Bjorses et al., 1998). AIRE deficiency in mice leads to a reduction in the expression of TRA by mTEC, but not a total absence, resulting in a similar multi-organ autoimmune phenotype to that observed in man (Anderson et al., 2002). Overall the consequence of AIRE removal in either mice or

man demonstrates its key role in regulating TRA expression and the establishment of tolerance to peripheral antigen. It has been reported, however, that the crucial role of AIRE becomes largely indispensible once a self-tolerant adult T cell pool has been established. At this stage in maturity regulatory mechanisms of peripheral tolerance are sufficient to control any self-reactive T cells that should arise from an AIRE deficient thymus (Guerau-de-Arellano et al., 2009).

AIRE has been implicated in mediating central tolerance by mechanisms independent of the regulation of TRA expression. This includes a role for AIRE in regulating the differentiation program of mTEC, therefore controlling the organization of the medullary thymic compartments. AIRE deficient mice, therefore, exhibit alterations to their medullary architecture (Gillard et al., 2007; Yano et al., 2008). AIRE expression by mTEC may also have additional functions in the regulation of chemotatic gradients within the medullary environment, controlling both the migratory pathway of newly selected SP thymocytes (Laan et al., 2009) and facilitating TRA cross-presentation from mTEC to DC, by bringing together these two APC types to enable this unidirectional antigen transfer (Hubert et al., 2011). AIRE has been identified as an essential regulator for the expression of several intrathymic chemokines. This includes the AIRE-dependent mTEC production of XCL-1, which is believed to mediate thymic DC accumulation (Lei et al., 2011), along with the mTEC expression of CCR4 and CCR7 ligands, which may be involved in DP to SP cortex to medulla migration (Laan et al., 2009).

1.3.3.2 The Specialized Role Of DC In Establishing Tolerance

The common functions ascribed to thymic resident DC are cross-presentation of TRA to developing thymocytes to mediate negative selection and the induction of nTreg generation

(Proietto et al., 2008b). The thymic DC population is comprised of heterogeneous subsets, classified into two distinct groups $CD11c^+$ $B220^+$ plasmacytoid DC (pDC) and $CD11c^+$ $B220^-$ conventional DC (cDC). The cDC can be further divided into two subsets, a majority $CD11b^-$ $CD8^+$ $Sirp\alpha^-$ DC population and a minority $CD11b^+$ $CD8^-$ $Sirp\alpha^+$ DC population (Wu and Shortman, 2005). The most common $CD11b^-$ $CD8^+$ $Sirp\alpha^-$ cDC are believed to be intrathymically generated from common lymphoid progenitor settlers at the DN stage in development, specifically before the DN3 maturational stage (Wu and Shortman, 2005; Yui et al., 2010) In contrast, the two additional subsets; the pDC and the less common $CD11b^+$ $CD8^-$ $Sirp\alpha^+$ cDC, are thought to be of extrathymic origin and continually migrate in from the blood to the thymus (Li et al., 2009).

Each DC subset is hypothesized to have individual functional capabilities to support the establishment of tolerance. Both divisions of cDC display the ability to cross-present antigen and induce T cell proliferation, superior to their splenic DC counterparts. The intrathymically generated $Sirp\alpha^-$ DC population, however, demonstrates a higher antigen presentation capacity in comparison to the more modest capabilities of the extrathymically produced $Sirp\alpha^+$ DC subset, suggesting the thymic derived $Sirp\alpha^-$ cDC subset may be more efficient in mediating the essential process of negative selection (Proietto et al., 2008a). In comparison, the $Sirp\alpha^+$ cDC subset migrating in from the periphery exhibit a greater efficiency for *in vitro* induction of functional nTreg generation, in contrast to the other thymic DC divisions (Proietto et al., 2008b). The $Sirp\alpha^+$ cDC display a phenotypically mature profile compared to the $Sirp\alpha^-$ cDC, expressing higher levels of MHC Class II, CD86, CD69 and the co-stimulatory molecules CD40 and CD80 (Proietto et al., 2008b). In addition the different DC

subsets display distinct chemokine expression profiles, which may also aid their functional abilities (Proietto et al., 2008a).

1.3.3.3 The Integrative Role Of mTEC And DC In Central Tolerance

Both the mTEC and DC populations within the medulla are believed to share the same common functions to support the establishment of central tolerance. The precise labor contribution of mTEC versus DC in both the process of negative selection and nTreg generation, however, remains unclear. It has been speculated that mTEC involvement in antigen presentation is limited and non-redundant, with the population merely serving as an antigen reservoir. Evidence has gone against this theory and demonstrated mTEC can mediate tolerance by directly presenting TSA to developing SP thymocytes. However, it is thought the indirect presentation of self-antigen by DC is optimal for APC mediated thymocyte deletion (Hubert et al., 2011; Klein et al., 2001). The mTEC population instead has been suggested to be the most likely cell type to foster nTreg cell generation. The contribution made by DC in driving nTreg induction, however is still unknown (Aschenbrenner et al., 2007). Interestingly in the absence of a MHC class II-expressing hemopoietic compartment the number of nTreg is only reduced by 30%, suggesting nTreg induction is not exclusively to MHC Class II mTEC and additional cell types must obtain the ability to facilitate induction of this specialist cell type (Proietto et al., 2008b). Additional studies have highlighted the possible plasticity of the thymic stroma for supporting the differentiation of this cell type, demonstrating that nTreg can promiscuously accept signals critical for their development from different cellular sources, delivered by either mTEC or DC (Spence and Green, 2008; Wirnsberger et al., 2009).

Regardless of the contributions of antigen presentation by these two APC subsets, the functional abilities of thymic DC are heavily dependent upon their interactions with mTEC,

particularly the AIRE^{+} division. The AIRE dependent, XCL1 mediated cross-presentation of TRA by mTEC to the DC subsets is essential for this specific APC to mediate antigen presentation (see Section 1.3.3.1). It is as of yet to be confirmed which specific thymic DC subsets express XCR1 and are dependent upon a XCL1 gradient for their medullary migration and positioning. The removal of XCL1 results in defective medullary accumulation of total DC, which consequently leads to a reduction in the generation of intrathymic nTreg (Lei et al., 2011). The reduction in the medullary thymic DC population and nTreg numbers observed within XCL-1 deficient microenvironments are also observed within AIRE deficient mice (Aschenbrenner et al., 2007; Lei et al., 2011), indicating that the XCL1-mediated medullary accumulation of thymic DC contributes to the differentiation of nTreg, which is indirectly regulated by AIRE expression by the mTEC population (Lei et al., 2011).

1.4 GENERAL AIMS

The complex thymic medullary microenvironment is home to SP thymocytes that have successfully undergone positive selection. During their medullary residency SP thymocytes undergoing a multiple- step developmental program and are screened for potential specificity to self. This SP medullary dwell time is evidently indispensible in the establishment of tolerance, at both the level of negative selection and nTreg generation. The precise multifaceted interactions between the various cellular components of this unique microenvironment facilitating these essential stages intrathymic T cell development, however, remain unidentified. We, therefore, aimed to explore the role of the thymic medulla in greater detail by addressing two key questions:

1) What is the role of the thymic medulla, in particular the mTEC population, in the post-positive selection maturation processes of conventional and Foxp3^{+} regulatory SP thymocytes?

2) What chemotactic signals control the cortical-to-medullary transition of developing SP thymocytes?

CHAPTER 2: MATERIALS AND METHODS

2.1 MICE

All mice used throughout this study were housed and maintained within the Biomedical Sciences Unit (BMSU), at the University of Birmingham, in accordance with Home Office regulations. Mice we obtained from the BMSU in-house stock, as a kind gift from research groups or from external commercial suppliers. Details of all mouse strains used throughout the study are listed in Table 2.1.

Wild type (WT) mice were used to characterize a normal, un-manipulated thymic microenvironment, whilst genetically manipulated mouse strains enabled precise investigations into the functions of specific genes and mechanisms involved in the T cell developmental process. All adult mice used through out this study were culled by cervical dislocation of the neck, in accordance with Home Office regulations. Mice were age and sex matched within each experimental condition and sacrificed between 6-12 weeks of age. WT mice were from the C57BL/6 colony, unless otherwise stated and all manipulated mice strains were on a C57BL/6 background. Timed matings were achieved by the housing of one male with two females overnight. Vaginal plug (VP) detection is then used to identify any successful timed matings, classified as day 0 of gestation (E0). The average gestation period for mice is between 18 and 21 days. This timed mating system made it possible to acquire embryonic tissue at specific developmental stages.

Table 2. 1 Wild Type And Genetically Modified Strains Used In This Study.

Mouse Stain	CD45 Isotype	Phenotype	Source
BALB/c	CD45.2	Wild type	BMSU or externally sourced from Harlan
C57BL/6	CD45.2	Wild type	BMSU
Boy J	CD45.1	Congenic C57BL/6 Wild type	BMSU
C57BL/6 x Boy J	CD45.1 x CD45.2	Wild type	BMSU
Ccr9$^{-/-}$	CD45.2	Deficiency in CCR9 results in a failure of thymocytes to display any chemotactic response to CCL25.	B.W. Agace, University of Lund, Sweden
Ccr7$^{-/-}$	CD45.2	Deficiency in CCR7 results in thymocytes displaying no chemotactic response to CCL19 or CCL21.	Antal Rot, University of Birmingham
Ccr4$^{-/-}$	CD45.2	Deficiency in CCR4 results in thymocytes displaying no chemotactic response to CCR4 ligands	The Jackson Laboratory
Ccr4$^{-/-}$ *x Ccr7*$^{-/-}$	CD45.2	Deficiency in CCR4 and CCR7 results in thymocytes displaying no chemotactic response to either CCR4 or CCR7 ligands	Cross *Ccr7*$^{-/-}$ and *Ccr4*$^{-/-}$ strains at the BMSU
Relb$^{-/-}$	CD45.2	Targeted mutation of the RelB gene results in a multi-organ inflammatory phenotype as a consequence of several immune disruptions, including severe disruptions to the thymic structure (Weih et al., 1995).	J. Caamano, University of Birmingham
RAG-2 GFP	CD45.2	Transgenic mice carrying bacterial artificial chromosomes (BACs) modified by homologous recombination to encode a green fluorescent protein (GFP) reporter within the *RAG-2* gene (Yu et al., 1999)	The Jackson Laboratory
Foxp3-GFP Knockin	CD45.2	Introduction of enhanced green fluorescent protein (EGFP) into the Foxp3 locus results in the ability to track Foxp3-expressing regulatory T cells (Bettelli et al., 2006)	T.Strom, Beth Israel Deaconess Medical Center, Boston
ZAP 70$^{-/-}$	CD45.2	Deletion of the entire gene segment encoding *Zap 70* results in a halt stage in T cell development at the positive selection stage resulting in a total absence of $CD4^+$ and $CD8^+$ single positive thymocytes, (Negishi et al., 1995).	B. Seddon, National Institute for Medical Research
C57BL/6 nude	CD45.2	Deficiency in the *FoxN1* gene results in abnormal thymic epithelial cell development. The thymic rudiment in not populated by lympoid precursors and consequently mice do not have T cells.	BMSU

2.2 MEDIUM AND TISSUE CULTURE REAGENTS

2.2.1 Medium

The short term handling of isolated tissues and cells was completed within a medium of RF10-H (preparation detailed in Table 2.2), whilst long term cultures were placed within a media of Dulbecco's Modified Eagle's Medium (DMEM) (Table 5.3 and Table 5:4). Aliquots of both mediums were prepared in advance and stored at 4^{o}C. All mediums and additives were purchased from Sigma, Poole, UK, unless otherwise stated.

2.2.2 Additives

To selectively eliminate all cells of a hematopoietic lineage from fetal thymic organ cultures (FTOC) (see Section 2.7) , 2- deoxyguanosine (2-dGuo) was added to the culture media of DMEM. Exposure to 2-dGuo results in a depletion of lymphoid cells, whilst thymic epithelial cells are undisrupted, resulting in the thymic lobes becoming 'empty', but maintaining their ability to support recolonisation by T cell progenitors. A final concentration of 1.35mM 2-dGuo was added to culture mediums of DMEM when desired. A stock solution of 9mM 2-dGuo was stored at -20°C until needed.

Table 2.2 Preparation Of RPMI-1640 Hepes (RF10-H)

Medium and Additives	Volume	Final Concentration
RPMI-1640 + 20mM Hepes, with L-glutamine, without bicarbonate	10mls	-
200nM L-glutamine	100µl	2mM
5000 IU/ml Penicillin and Streptomycin	200µl	100 IU/ml
Heat-inactivated fetal calf serum (FCS)	1ml	10%

Table 2.3 Preparation Of Dulbecco's Modified Eagle's Medium (DMEM)

Medium and Additives	Volume	Final Concentration
Dulbecco's Medium with 3.7g/l bicarbonate,without glutamine	20ml	-
100x non-essential amino acids (for component details see Table 2.4)	200ml	-
1M Hepes- Final conc.	200ml	10mM
$5x10^3$ M2 Mercaptoethanol	200ml	-
200mM L-Glutamine -Final conc.	400ml	4mM
5000 IU/ml Penicillin and Streptomycin	400ml	100 IU/ml
Heat-inactivated FCS	2ml	10%

Table 2. 4 Constituents Of 100x Non-Essential Amino Acids

Constituent	Concentration (mg/ml)
L-Alanine	8.9
L-Asparagine	15.0
L-Aspartic acid	13.0
Glycine	7.5
L-Glutamic acid	14.2
L-Proline	11.5
L-Serine	10.5

2.3 DISSECTION OF MOUSE TISSUE

Thymic lobes, spleen and lymph nodes (LN) were dissected from adult mice and placed into RF10-H. Tissues were then carefully cleaned to remove any unwanted excess material, such as fat or blood, using fine forceps under a dissection microscope. All handling of murine tissue was performed within a laminar flow hood to provide a sterile environment, using sterile surgical instruments and sterile medium. For the preparation of fetal material, embryos were removed from pregnant mice at the preferred day of gestation, separated from the womb and egg sac and washed in a solution of 1:1 Phosphate Buffered Saline (PBS) to RF10-H. Embryonic lobes were then dissected out from the thoracic tree, under a dissection microscope and transferred into a medium of RF10-H for short term handling, before being used as fresh material or prior to being placed into the FTOC system described in Section 2.7.

2.4 ISOLATION OF DISTINCT CELL TYPES

2.4.1 Isolation Of Thymocytes Or Peripheral T cells

To obtain a cell suspension of thymocytes, or peripheral lymphocytes, the thymus, LN and spleen were gently teased apart by glass slides to release the cells into a medium of RF10-H. All cell types were then filtered through a mesh-membrane filter to remove any cell clumps and centrifuged to form a pellet. The thymus/LN samples were then re-suspended in a known volume of RF10-H and placed on ice until needed. Alternatively splenocytes were re-suspended in 2mls red blood cell lysis buffer (Sigma-Aldrich) and left at room temperature for 5-10 minutes. An equal volume of RF10-H was then added the cell suspension to neutralize the buffer properties and centrifuged. Splenocytes were then re-suspended in a known volume of RF10-H and placed on ice until needed. Haemocytometer counts were acquired and absolute cell numbers calculated within each cell suspension. All cell counts and absolute numbers obtained throughout this study were via haemocytometer counts. The typical centrifugation settings used throughout the study were 4 minutes, at 4^{o}C, at a speed of 1200rpm, unless otherwise stated.

2.4.2 Isolation Of Stromal Cell Populations

To obtain a single cell suspension of thymic stromal cells, freshly dissected embryonic thymic lobes or thymic lobes placed into the FTOC system for 5-7 days, with or without 2-dGuo treatment (Section 2.7), underwent enzyme digestion. Thymic lobes were transferred to 1.5ml eppendorfs and washed three times with Ca^{2+}/Mg^{2+} free Phosphate Buffered Saline (PBS-). This removed any traces of serum that could possibly inactivate the enzyme function. The

lobes were then re-suspended in 600µl 1:10 trypsin dilution made up with 0.2% Ethylenediaminetetraacetic acid (EDTA) and incubated for 10-15 minutes at 37°C to disaggregate the structure and release the stromal cells into the suspension. The trypsin was then neutralized with an equal volume of RF10-H and centrifugation. The pellet was then re-suspended in 1ml RF10-H total volume and cell numbers were calculated from haemocytometer counts.

2.4.3 Immunomagnetic Separation Of Embryonic Stromal Cells

The isolated 2-dGuo treated FTOC thymic stromal cells described in Section 2.4.2 were subject to additional selection using the immunomagnetic separation technique to deplete any possible contaminating $CD45^+$ hematopoietic cells that may remain within the cell suspension. This immunomagnetic separation technique used Dynabeads® sheep anti-Rat IgG beads, coated with tissue culture derived anti-mouse CD45 supernatant. Beads in a stock concentration of 4×10^8 beads/ml were aliquoted into 500µl samples in 1.5ml eppendorfs and stored at 4^OC until needed. Aliquoted bead samples were prepared the day before needed by washing in RF10-H three times to remove sodium azide and then incubated at 4^0C overnight in the presence of 500µl neat anti-mouse CD45 supernatant. After overnight culture beads were washed three times with RF10-H to remove any excess antibody and re-suspended in 100µl RF10-H. A 10µl sample of beads was added per stromal cell suspensions, within a total volume of 200⌈l of RF10-H.

Samples were then centrifuged for 10 minutes at 1000 rpm, at 4°C in round bottomed sterile cryogenic vials (Cryovial, Quebec, Canada). The round bottomed vial ensures a large surface area for optimal cell to bead interactions. The cell/bead pellet was then gently re-suspended

and the centrifugation step repeated for a second time. The cell/bead pellet was again gently re-suspended and the suspension was checked for 'rosettes', clusters of cells bound to beads, visualized by light microscopy. This step ensured the beads had successfully bound any remaining $CD45^+$ cells, whilst confirming the beads were in excess of the stromal cells. Once positive binding was detected, unwanted $CD45^+$ cells bound to magnetic beads were separated from $CD45^-$ unbound cells using an Eppendorf (1.5ml) Dynal Magnetic Particle Concentrator (Dynal). Supernatant containing the $CD45^-$ population was removed and centrifuged, before re-suspension in 1ml RF10-H and a cell count was obtained. The beads and any $CD45^+$ bound cells were discarded.

2.4.4 Isolation Of Dendritic Cells

To obtain the most efficient isolation of DC subsets the adult thymus or thymic grafts were subject to enzyme digestion. The thymic samples were cut into small pieces within a 1 ml medium of RPMI + 2% FCS and transferred into polypropelene FACs tubes. A solution of 2.5mg/ml Collagenase Dispase (Roche) and a 1:20 dilution of DNase 1 (Sigma) were added to the 1ml RPMI + 2% FCS medium and incubated at 37^0C within a water bath for 45minutes. The supernatant was removed and transferred on ice into an equal volume of MACs buffer (PBS, 0.5% FCS and 2mM EDTA). The digestion step was repeated on any remaining tissue fragments for an additional 15 minutes and an equal volume of MACs buffer then added. The two cell suspensions were combined and a 5mM concentration of EDTA added. The medium was left on ice for 5 minute. The cell suspension was centrifuged and re-suspended in 1ml MACs buffer, before a cell count was obtained. Cells were handelled in the MACs buffer from this point.

2.5 IMMUNOLABELLING AND FLOW CYTOMETRY

2.5.1 Antibodies

All primary antibodies used for flow cytometry during this study are listed within Table 2.5 and secondary antibodies are listed within Table 2.6. The antibodies used were either directly conjugated to a fluorochrome or biotinylated and thus, required a secondary fluorochrome conjugated antibody for their detection. For surface staining of CCR7, cells were first labeled with recombinant CCL-19 fusion protein, followed by a biotinylated antibody (Table 2.5), which was then detected by a tertiary fluorochrome conjugated antibody (Table 2.6). Prior to usage, all antibodies we titrated to optimize working concentrations.

2.5.2 Immunolabelling For Flow Cytometric Analysis

After the isolation and preparation of the desired cell populations for staining, approximately 1 x 10^6 or 3 x 10^6 cells (dependent upon the frequency of cell population of interest) were aliquot into 1.5ml eppendorfs and centrifuged to form a pellet. After the removal of the supernatant, cells pellets were re-suspended in 50µl (1 x 10^6) or 100µl (3 x 10^6) of the desired primary, secondary or tertiary antibodies. All antibody suspensions were made up in Fluorescence-activated cell sorting (FACS) medium, consisting of PSB- with 3% FCS. The samples were then indicated on ice for 30 minutes. A single colour sample for each individual fluorochrome was prepared to set compensation parameters. A control sample for each biotinylated antibody was prepared to measure non-specific binding and set a negative peak of florescence. This was achieved by having an additional sample to which 50µl FACS medium was added at the primary antibody stage in substitution for the biotinylated antibody.

Once the incubation period was completed the samples were washed with 1ml FACS medium and centrifuged. Each wash step was repeated twice. At this point, if required the relevant secondary or tertiary antibodies were added, in an identical manner to the primary and incubated on ice for an additional 30 minutes, before repeating the to times washing step. After the final wash, samples were re-suspended in 200µl FACS buffer and transferred in 12.5ml polystyrene FACS tubes (Becton) in preparation of FACS acquisition.

2.5.3 Intracellular Immunolabelling For Flow Cytometric Analysis

For the intracellular staining of Foxp3, cells were first surface stained as described in Section 2.5.2. After the final washing step the surface stain was fixed and the cells were permeabilized using the Foxp3/Transcription Factor Staining Buffer Set (eBioscience) according to the manufacturer's protocol. Each sample was re-suspended in 200µl Fixation/Permeabilization solution made up of 1 part concentrate to 3 parts diluent. Cells were then stored at 4°C for 30 minutes. Cells were washed two times in 1ml 10% permeabilization buffer, made up with distilled water. After the permeabilization step was completed cells were stained with a directly conjugated Foxp3 antibody (see Table 2.5), in the same manner as surface stain technique stated in Section 2.5.2, however, the FACS buffer was substituted with the permeabilization buffer for any handelling or wash steps.

To analysis intracellular IFNγ cytokine production cells were stimulated on plates coated with 5µg/ml anti-CD3 antibody and 0.5µg/ml of soluble anti-CD28 antibody, (BD) in the presence of GoliStop (BD), in vitro for 4 hrs at 37^{o}C. Plates were coated approximately 12hrs in advance and left at 4^{0}C until needed. After stimulation, cells were transferred to Eppendorf tubes and the plate was washed two times with 1ml RF10-H. Cell suspensions were then

centrifuged and re-suspended in 1ml RF10-H, before a cell count was obtained. Cells were then surface stained as described in Section 2.5.2. After the final washing step the cells were fixed and permeabilization with Cytofix/Cytoperm Plus (BD) in accordance to the manufactures instructions. The permeabilized cells were then stained with a directly conjugated IFNγ antibody (see Table 2.5).

2.5.4 Flow Cytometric Analysis

The acquisition of all samples was performed on a BD LSR Fortessa flow cytometer using BD FACS diva software. Subsequent analysis was performed using FlowJo software. Prior to the acquisition of the experimental samples, single colour controls were obtained to adjust the compensatory levels between various fluorochrome detection channels, whilst examination of the negative samples enable the negative peaks of expression levels to be set for specific antibodies. The number of events recorded during analysis was dependent upon both the cell numbers prior to immunolabelling and the frequency of the cell population of interest. On average 500,000 events were recorded per experimental sample, with a minimal event rate of approximately 100,000. The forward and side scatter gates were set to exclude any non-viable cells.

Table 2. 5 Primary Antibodies Used For Flow Cytometric Immunolabelling

Specificity (Clone)	Fluorochrome	Working Dilution	Supplier
Anti-CD4 Clone GK1.5	PECy7 Alexa Fluor 700 PE	1:1500 1: 200 1:800	eBioscience eBioscience eBioscience
Anti-CD4 Clone RM4-5	PerCP-Cy5.5 APC eFluor 780 APC V500 eFluor 450	1:400 1:100 1:400 1:200 1:100	eBioscience eBioscience eBioscience BD Bioscience eBioscience
Anti-CD8 Clone 53-6.7	eFluor 450 FITC V500 PE	1: 200 1: 800 1:200 1:200	eBioscience eBioscience BD Bioscience eBioscience
Anti-TCRβ Clone H57-597	APC eFluor 780	1:100	eBioscience
Anti-CD69 Clone H1.2F3	FITC APC PerCP-Cy5.5	1:200 1:200 1:200	eBioscience eBioscience eBioscience
Anti-CD62L Clone MEL-14,	APC	1:3000	BioLegend
Anti- CD44 Clone IM7,	FITC Alexa Fluor 700	1:200 1:100	eBioscience eBioscience
Anti-CD3 Clone 145-2C11	PE	1:200	eBioscience
Anti-mouse HSA/CD24 Clone M1/69	APC eFluor 780 PE	1:500 1:500	eBioscience BD Bioscience
Anti-Qa2 Clone 695H1-9.9	Biotinylated FITC	1:200 1: 50	BioLegend eBioscience
Anti-CD45.1 Clone A20	eFluor 780 eFluor 450	1:200 1:200	eBioscience eBioscience
Anti-CD45.2 Clone 104	PE Alexa Fluor 700	1:200 1:200	eBioscience
Anti-CCR9 Clone eBio CW-1.2	PE	1:200	eBioscience
Anti-CD25 Clone PC61/PC61.5	APC PE	1:500	BioLegend eBioscience
CCR7 staining 1: Recombinant CCL19-Ig 2: Goat anti–human Ig	- Biotinylated	1:500 1:500	eBioscience eBioscience
Anti–IFNγ Clone XMG1.2	APC	1:100	BD Bioscience
Anti-Foxp3 Clone FJK-16s	PE	1:100	eBioscience
Anti-CCR4 Clone 2G12	APC Biotinylated	1:200 1:200	BioLegend BioLegend
Anti-CXCR4 Clone 2B11	APC	1:50	eBioscience
Rat 1gG2b isotype Clone eB149/10HS	APC	1:50	eBioscience
Anti-Sirpα^{+} Clone P84	Biotinylated	1:200	eBioscience
Anti-B220 Clone RA3-6B2	FITC	1:200	eBioscience

Specificity (Clone)	Fluorochrome	Working Dilution	Supplier
Anti-CD205 (DEC205) Clone NLDC145	Biotinylated	1:50	AbCAM
Anti- EpCAM-1 Clone G8.8	APC	1:800	eBioscience
Anti-CD40 Clone 3/23	PE	1:100	BD Bioscience
Anti-CD80 (B7.1) Clone 16-10A1	FITC	1:100	eBioscience
Anti-CD45 Clone 30-F11	APCCy7	1:800	eBioscience
Anti-CD11c Clone N418	PE	1:200	eBioscience

Table 2.5 Primmary Antibodies continued…..

Table 2. 6 Secondary Reagents Used For Flow Cytometric Immunolabelling

Specificity (Clone)	Fluorochrome	Working Dilution	Supplier
Streptavidin	PECy7	1:1500	eBioscience

2.6 PREPARATION OF CELLS FOR HIGH SPEED SORTING

Cells populations were immunolabelled in preparation for high speed sorting by the same technique as used for flow cytometry. The total cell number labeled, however, was greatly increased for cell sorting, with each experimental sample containing a maximum of 30 x 10^6 cells, re-suspended in a total volume of 350µl antibody solution. Following immunolabelling, samples were re-suspended in 500µl RF10-H and pooled together if required. The cell suspensions were then filtered to remove any adherent cell clumps through a 30 mm mesh-membrane filter unit (Miltenyi Biotech). The samples were transferred to polypropylene

FACS tubes (Becton Dickinson) in preparation of sorting. Purified populations were sorted using a MoFlo XDP sorted (Beckman Coulter). Isolated cell populations were collected into FACS tubes containing 500µl RF10-H and then centrifuged before re-suspension in 1ml RF10-H. The cell numbers were then calculated and a small fraction of cells were extracted for FACS re-analysis on the BD LSR Fortessa flow cytometer to determine purification rates. The gates used for the isolation of specific cell populations were set in accordance to negative and positive peaks generated from the control samples.

2.7 FETAL THYMUS ORGAN CULTURE (FTOC)

The well established FTOC systems supports the full program of T cell development *in vitro,* whilst maintaining the integrity of the complex three-dimensional architecture of the thymic stroma. The unaltered structure of the fetal lobes promotes efficient interactions between the developing thymocytes and stromal cells, thus, mimicking a typical thymic microenvironment *in vivo* (Jenkinson and Anderson, 1994).

Thymic lobes were dissected from embryos at the desired E15 stage of gestation. The lobes were placed onto 0.8µm sterile nuclepore filters (purchased from Millipore), which lay on top of a sterile artiwrap sponge support, approximately 1cm^2 in size (purchased from Medipost Ltd) within a DMEM medium (Figure 2.1). Lobes were transported to the surface of the nuclepore filters using a finely drawn, mouth-controlled sterile glass pipette. All WT fetal lobes were set up in 90 mm petri dishes (sterilin) containing a 4ml DMEM volume. Up to six individual lobes were cultured on one sponge-filter complex and two complexes were added per dish. In the case of heterogeneous matings of genetically modified mouse strains, when the genotype of each embryo was unknown, lobes were handled separately and set up in

Figure 2. 1 Fetal Thymic Organ Culture

Thymus lobes were dissected from mouse embryos day 15 of gestation. The thoracic cavity was exposed to allow the thymus lobes to become visible (contained within yellow based box), positioned above the heart (labeled H) (A). Lobes were isolated (B) and placed within the organ culture system (C).

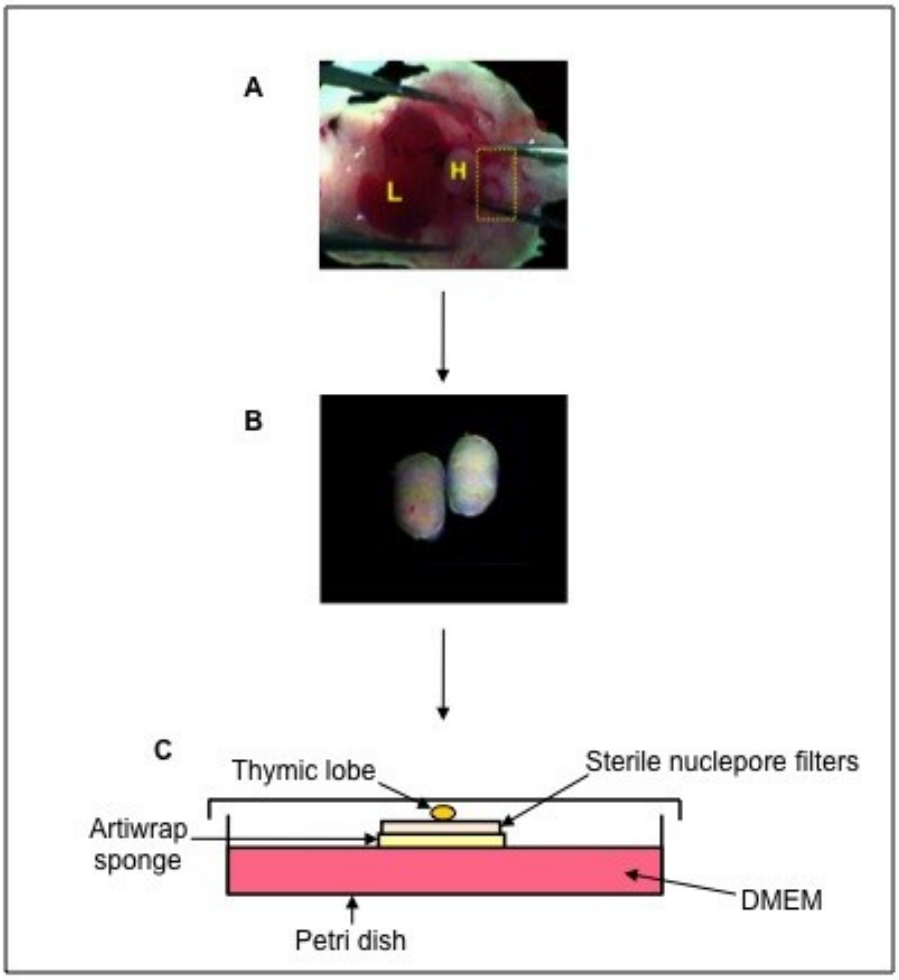
A
L
H
B
C
Thymic lobe
Sterile nuclepore filters
Artiwrap
sponge
DMEM
Petri dish

individual 35mm petri dishes (sterilin) containing a 2ml DMEM volume. When desired, 2-dGuo was added to the DMEM medium, with 600μm added to a 4ml DMEM medium volume within a 90 mm petri dishes and 300μm added to the 2ml DMEM medium volume in a 35mm petri dishes. Petrie dishes were then placed in sterile humidified chambers and gassed with 10% CO_2 for approximately 10 minutes, to achieve a desired pH of 7.2-7.4. The chambers were then sealed to keep the environment sterile and placed into a 37°C incubator for approximately 5- 7 days (Anderson and Jenkinson, 2007).

2.8 REAGGREGATE THYMIC ORGAN CULTURE (RTOC)

The formation of reaggregate thymus organ cultures (RTOCs) enables the investigation of the differentiation of a single thymocyte cohort, at a specific intra-thymic developmental window, within an i*n vitro* 3D thymic microenvironment (Hare et al., 1999; Jenkinson et al., 1992). Desired thymocytes subsets were isolated from adult mice by MoFlo cell sorting, as stated in Section 2.6. The isolated thymocyte populations were mixed with a cell suspension of E15 dGuo treated FTOC cultured 5-7 days, that had be subject to both enzyme digestion (Section 2.4.2) and $CD45^+$ depletion (Section 2.4.3). The input number of thymocytes varied, dependent upon the desired population and the disparity between sorts, whilst commonly 2.5 x 10^5 stromal cells were added per RTOC. The combined stromal and thymocytes cell suspension were centrifuged at 1000rpm for 10 minutes at 4^oC. The supernatant was carefully removed and the cell pellet vortexed to produce a suspension of cells within an approximate 2-3μl volume. Using a mouth pipette, the cell suspension was transferred into a finely drawn pipette and onto the centre of a 0.8μm sterile Whatman filter, under a dissection microscope. Filters were placed on top of a sterile anti-wrap sponge support in a culture system, in an

identical manner to the FTOC system described in Section 2.7 (see Figure 2.1). Each filter was limited to a singular reaggregate and cultured for a desired period of time, before the gentle disaggregation of the structure to explore thymocyte development, via flow cytometric analysis.

2.9 IMMUNOHISTOLOGY TECHNIQUES

2.9.1 Sectioning And Fixation Of Frozen Tissues

After the dissection and isolation of the adult tissued desired for immunohistology (Section 2.3) the material was frozen as soon as possible. Tissues were frozen on dry ice, on top of tin foil sections. Thymic grafts were frozen within Optimal Cutting Temperature (OCT) compound on the tin foil, due to their small size, whilst larger adult thymic lobes were frozen alone. All thymic tissue was frozen at a defined orientation and mounted onto a microtome within additional OCT compound. 7μm thick section were cut and mounted onto 4 spot glass slides (Hendley- Essex). All slides were left to dry at room temperature for an hour, followed by fixation in acetone (Baker) for 20 minutes at 4°C. Sections were then air dried for 10 minutes and stored within polythene grip seal bags at -20°C until wanted for immunolabelling.

2.9.2 Immunolabelling Of Frozen Tissue Sections

Sections were removed from storage at -20°C and left at room temperature to dry for approximately 30 minutes prior to immunolabelling. Tissue sections were rehydrated in a PSB (Sigma) bath for 10-15 minutes. The tissue sections were stained with fluorochrome conjugated anti-mouse antibodies. The details of all primary antibodies used for confocal

analysis through out this study are listed with Table 2.7 and all secondary/tertiary antibodies are within Table 2.8. Antibody solutions were made up in PBS containing 1% bovine serum albumin (BSA). A 75µl volume of antibody mixed was applied directly to each section and incubated for 45 minutes, in a dark humidified chamber at room temperature. Sections were then washed within a PBS bath for 5-10 minutes. Once all staining steps were complete, if required section were fully emerged in a DAPI (4',6-diamidino-2-phenylindole) solution for a maximum of 30 seconds and then washed four times with PBS. DAPI is a strong nuclear stain that facilitates the visitation of all nucleated cellular components of the whole tissue section. A small drop of DABCO (1,4 diazabicyclooctane), in glycerol at pH 7, was added to each tissue section, to preserve the flurochromes. The slide was mounted with a cover slip (Sigma) and sealed with a thin layer of clear nail varnish. Slides were stored at -20°C until needed for confocal analysis.

2.9.3 Confocal Analysis

Confocal images were obtained using a LSM 780 microscope at an x 25 magnification (unless otherwise stated) and analyzed using LSM software (Carl Zeiss). The digital images were recorded in four channels and each was scanned separately, with no overlap in the detection of emissions from individual fluorochromes. TRITC and Alexa 555/594 conjugated antibodies were excited with a 561nm helium laser, FITC/Alexa 488 conjugated antibodies were excited with a 488nm argon laser, Alexa 647 conjugated antibodies were excited with the 633nm helium laser and DAPI were exited by the 405nm diode laser.

Table 2.7 Details Of Primary Antibodies Used For Immunohistology

Specificity (Clone)	Host/Isotype	Working Dilution	Supplier
Purified anti-mouse CD4 (Monoclonal GK 1.5) conjugated to Alexa 647 by D. Withers, University of Birmingham	Rat IgG1	1:100	eBioscience
Anti-mouse CD8β Biotinylated Monoclonal Clone YTS156.7.7	Rat IgG2b	1:200	BioLegend
ERTR5 mTEC marker		1:2000	W.van Ewijk, Riken Yokohama Institute, Kanagaw, Japan.
Anti-mouse β5T cTEC marker Polyclonal	Rabbit	1:100	MBL
Anti-mouse CD45.1 Biotinylated Monoclonal Clone A20	Mouse IgG2a	1:100	eBioscience
Anti-mouse CD45.2 FITC Monoclonal Clone 104	Mouse IgG2a	1:100	eBioscience
Anti-mouse CD11c FITC Monoclonal Clone N418	Armenian Hamster IgG	1:300	eBioscience
Anti-mouse IgG FITC	Goat	1:100	SouthernBiotech

Table 2. 8 Details Of Secondary And Tertiary Reagents Used For Immunohistology

Specificity (Clone)	Host/Isotype	Working Dilution	Supplier
Anti FITC Polyclonal	Rabbit	1:200	Invitrogen
Anti-Rabbit IgG Alexa Fluor 488 Monoclonal	Goat	1:200	Invitrogen
Anti-rat IgM Alexa Fluor 594 Monoclonal	Goat	1:300	Invitrogen
Streptavidin Alexa Fluor 647 Monoclonal		1:200	Invitrogen
Streptavidin Alexa Fluor 488 Monoclonal		1:200	Invitrogen
Streptavidin Alexa Fluor 405 Monoclonal		1:50	Invitrogen

2.9.4 Confocal Quantification

To explore if cortex to medulla migration was effected by the absence of CCR4 or CCR7 expression, individually or combined, we counted the number of $CD4^+$ SP and $CD8^+$ SP cells within a given medullary area of WT and deficient thymic sections (*Ccr4*$^{-/-}$, *Ccr7*$^{-/-}$ and *Ccr4*$^{-/-}$ *x Ccr7*$^{-/-}$). Numerical quantitation of the number of $CD4^+$ SP and $CD8^+$ SP was achieved by adopting a previously published technique (Ueno et al., 2004). Adult thymic lobes were frozen and serial sections cut as described in Section 2.9.1. Sections were then immunolabeled for confocal analysis (Section 2.9.2 and 2.9.3). The sections were stained for CD4 and CD8, in conjunction with cortical (β5T) and medullary markers (ERTR5), to aid the identification of the two distinct microenvironments and establish the positioning of the CMJ. Pictures were taken containing both cortical and medullary regions at an x 25 objective. Using LSM software (Carl Zeiss) 100μm x 100μm square areas were arbitrarily set within the medullary region, at least 100μm inside the CMJ. The number of $CD4^+$ SP and $CD8^+$ SP cells within this selected medullary area was quantified using the LSM software. This strategy was adopted for all sections and the numbers of $CD4^+$ SP and $CD8^+$ SP populations within each medullary area was recorded within the Prism 4 file to enable the average numbers of both SP populations to be complied, per adult mouse, from serial sections. For confocal quantification of thymus sections of mixed bone marrow chimeras, the same strategy was applied, but the numbers of $CD45.2^+$ cells were calculated within a 100μm x 100μm area of both medullary and cortical regions. The areas were arbitrarily set at least 100μm inside the CMJ for both the cortical and medullary regions.

2.10 THYMIC KIDNEY CAPSULE TRANSFER

To compare intrathymic T cell development within a WT and *Relb*$^{-/-}$ deficient microenvironment, E15 *Relb*$^{-/-}$ or WT (litter mate) 2-dGuo FTOC were transferred under the kidney capsule of WT or nude hosts (experimental design described in Figure 4.1). Mice undergoing surgery were between 5-6 weeks in age and were weighed prior to surgery to calculate the correct dose of analgesia to administer. Mice were initially anaesthetized within a chamber containing 4% isoflurane (May and Barker, Dagenham, UK) carried within oxygen. Once mice lost consciousness and displayed deep, slow breathing patterns, they were transferred onto a heat pad and the anesthesia was administered through a facemask, at a 2% isoflurane rate. At this point 2mg per kg pre-operative Buprenorphine (Tamgesic, AnimalCare, UK) was administered subcutaneously, in the back of the neck, using a 25-gauge needle. The loss of the pedal withdrawal reflex was confirmed before surgery commenced, to ensure a sufficient depth of anesthesia.

Mice were positioned on their front and fur surrounding the site of incision, above the left lumbar region, was removed using an electrical shaver. The area was then cleaned using 70% alcohol. A small cut was first made to the skin, using blunt ended scissors, in a region slightly below the assumed position of the left kidney. The incision was then increased to approximately 0.5 to 1 cm in length, dependent upon the size of the host. A space was created between the skin and the peritoneum using a closed pair of blunt ended scissors. A similar cut was then made in the peritoneum, approximately 0.5cm in size. The kidney was gently drawn out of the body cavity by grasping the fat attached at the lower end of the organ with blunt

ended forceps. Once the kidney was externalized, it was held in position by the skin layer and kept rehydrated with sterile PBS soaked gauze.

A small cut was made in the fibrous kidney capsule with fine forceps, under a dissection microscope. Extreme care was needed at this point to ensure no damage to the kidney parenchyma. The embryonic material for transplantation was transferred under the kidney capsule, via the edge of forceps. Up to three E15 thymic lobes were grafted under the capsule of one kidney. The kidney was gently drawn back into the body cavity by the elevation the edge of the peritoneum. The peritoneum layer was sutured (Vicryl, 16mm round bodied sutures) and the skin sealed by a surgical staple. The mice were removed from the anesthesia facemask and placed within a warm box, until consciousness was regained. The recovery of the mice was closely monitored at regular intervals by BMSU staff post-operation, until sacrificed between 6 to 12 weeks later.

2.11 ANALYSIS OF AUTOIMMUNITY

The assessment of autoimmunity was performed on nude hosts, scarified 6 weeks after receiving either WT or *Relb*$^{-/-}$ grafts. The LN of nude hosts were harvest for intracellular staining of IFNγ cytokine production within the peripheral T cells subset, as described in Section 2.5.3. In addition, the blood serum of the each host was investigated for the presence of autoantibodies. The peripheral blood sample was obtained via cardiac punctures of the host, under anesthesia, in accordance to the Home Office regulations. The samples acquired were left at room temperature for up to 4hrs to aid blood cell coagulation. The samples were centrifuged and the serum supernatant removed carefully and transferred into Eppendorfs tubes, for storage at -4^{0}C until needed.

We detected autoantibody in blood serum of the hosts as previously described (Gaspal et al., 2011). The serum samples were loaded onto slides of composite tissue blocks containing rat liver/kidney/stomach (INOVA Diagnostics). The tissue slides were stored at -4^{0}C prior to usage and thus, were left at room temperature for approximately 30 minutes before serum loading. Before the addition of serum samples, slides were blocked with 10% anti-goat serum, made up in PBS and incubated for 20 minutes in a dark humidified chamber at room temperature. Excess goat serum was tapped off slides and a 50µl sample of blood serum added directly to each section, at a 1:40 concentration, made up in PBS. The sections were incubated for 20 minutes and then washed within a PBS bath for 5-10 minutes. Autoantibodies were then detected with goat anti-mouse IgG FITC (Table 2.7), with a 50µl sample added to each section at a 1:100 concentration. Slides had an additional 20 minutes incubation period, followed by a wash step. The slides were then fully emerged in a DAPI solution and mounted with a cover slip, as described in Section 2.9.2, however the mounting medium was substituted with Polyvinyl alcohol mounting medium (Sigma). Confocal images were taken of the slides using the method described in Sections 2.9.3.

As an additional sign of autoimmunity, liver sections from the nude hosts were analyzed for the presence of lymphocytic infiltrates. Liver sections were isolated from the nude hosts and fixed and stored within Formalin solution, neutral buffered, 10% (Sigma). Tissues were then paraffin-embedded and sections cut and stained with Hematoxylin & Eosin (H & E) as previously described (Rossi et al., 2007b). The pathology department at the University of Birmingham performed all H & E stains. The images of the section were acquired using the DM6000 Leica microscope, at an x20 objective.

2.12 INTRAVENOUS (IV) CELL TRANSFER

Desired thymocyte populations for IV cell transfer were isolated via high-speed cell sorting (as described in Section 2.6) from adult WT or Foxp3-GFP 'knockin' donors. The purity level of each sort was determined and a cell count obtained. The desired cell numbers for transfer was extracted from the total volume into Eppendorf tubes and the populations undergoing co-transfer were combined. The freshly purified cells samples were centrifuged and re-suspended in a 300µl of sterile PBS, (without calcium and magnesium) (Sigma). The 300µl cell suspensions were transferred into 25 gauge needles, attached to a 1ml syringes and all air bubbles were removed. Total cell suspensions were then transferred into the WT host, intravenous, via the tail vein.

The transferred cell numbers varied between specific populations and the efficiency of the sort. On average 2.5 x 10^5 thymocytes of the DP, immature $CCR7^-CCR9^+CD69^-$ $CD4^+$ SP or mature $CCR7^+CCR9^-CD69^-$ $CD4^+$ SP subsets were transferred into a WT host. In comparison, the numbers obtained from the purity of $Foxp3^-CD25^+$ $CD69^+$nTreg precursors was considerably lower and thus, commonly bellow 5 x 10^4 cells were transferred per host.

2.13 COMPETITIVE BONE MARROW CHIMERAS

To explore if *Ccr4*$^{-/-}$ thymocytes displayed deficiency in their ability to undergo cortex to medulla migration or SP maturation within a competitive environment with their WT counterparts, mixed bone marrow chimeras were generated (experimental design detailed in Figure 5.10). Bone marrow (BM) was obtained from the femur and tibia bones of the WT or *Ccr4*$^{-/-}$ donors. BM was flushed from the bones into a medium of RF10-H using a syringe

attached to a 27 gauge needle. The extracted BM was passed through the needle to break up any clumps. The cell suspensions were then filtered through a 30 mm mesh-membrane filter unit (Miltenyi Biotech). Samples were centrifuged and re-suspended in red blood cell lysis buffer (Sigma-Aldrich) (1ml buffer per donor mouse sacrificed) and left at room temperature for 3-5 minutes. An equal volume of RF10-H was added to each cell suspension to neutralize the buffer properties and centrifuged. The BM samples were re-suspended in PBS (without calcium and magnesium) and cell counts obtained.

At this point BM samples undergoing T cell depletion were immunolabelled as described in Section 2.5.2 for CD4, CD8 and CD3, all directly conjugated to PE (see Table 2.5). T cell depletion of samples removes the possibility of mature T cells within the BM recirculating into the thymus. Cells were surface stained within MACs Buffer (PBS, 0.5% FCS and 2mM EDTA). After the final wash step of immunolabelling cells were resuspended within a 1:10 dilution of Anti-PE microbeads (miltenyi Biotec). 10µl of beads were added per 1 x 10^7 cells, diluted in MACs buffer. BM cells were incubated at 4^oC for 15 minutes and tapped every 5 minutes to resuspend the medium, increasing the possibility of cell-bead interaction. Cells were then washed x 2 with MACs buffer. On the final wash step the BM samples were resuspended in 500µl MACs buffer and added to MACs separation 25 LS columns (miltenyi biotec), previously primed with 3ml MACs buffer, on a QuadroMACs separator magnets. All PE labeled cells with the medium bind the magnets, enabling the collection of non-PE ($CD4^-$ $CD8^-$ $CD3^-$) BM cells. Columns were washed x 3 with 3mls MACs buffer. Samples were then centrifuged and resuspended in 5mls RF10-H, before a cell count was obtained.

The desired cell numbers were extracted from each sample (non- T cell depleted or T cell depleted) and mixed with their corresponding WT or *Ccr4*$^{-/-}$ counterparts. Each host received

5 x 10^6 bone marrow cells per condition (WT or *Ccr4*$^{-/-}$), resulting in a 1x10^7 total cell transfer. The mixed bone marrow donor samples were then centrifuged and each re-suspended in 300µl PBS (without calcium and magnesium), in preparation of their transfer into irradiated hosts.

The WT hosts receiving the BM transfers received baytril antibiotic drinking water for one week prior to irradiation. On the 7th day of treatment hosts were irradiated using a CIS IBL 437 Cs-137 irradiator (CIS BIO International, Cedex, France). Mice were irradiated with two times 450 Rad (900 Rad total), with a 3-hour gap between the two administrations. The bone marrow transfer was performed the following day, into irradiated hosts. The fresh 300µl BM suspensions were transferred into each host using a 25 gauge needle, attached to a 1ml syringe, intravenous via the tail vein. BMSU staff monitored recipient mice closely after transfer to ensure successful reconstitution and the baytril antibiotic drinking water was continued for an additional week, post I.V. The chimera mice were harvest 5 weeks post BM transfer and the post-selection localization and maturation of WT or *Ccr4*$^{-/-}$ thymocytes was explored by flow cytometry and confocal analysis.

2.14 PREPARATION OF SAMPLES FOR GENE EXPRESSION ANALYSIS

All gene expression analysis was carried in collaboration with S. Parnell, University of Birmingham.

2.14.1 Snap Freezing Of Cell Populations

Isolated cell populations obtained by MoFlo sorting for gene expression analysis were transferred into 1.5ml RNase-free Eppendorf tubes (Camlab) and centrifuged at 1000rpm, at

4^0C, for 10 minutes. The supernatants were removed to leave a dry pellet and immersed in liquid nitrogen, before storage at -80°C until needed

2.14.2 mRNA Extraction And cDNA Synthesis

mRNA was extracted directly from the isolated MoFlo cell sorted populations using a μMACSTM one-step mRNA Isolation and reverse transcription kit (Miltenyi Biotec). All lysis/binding and wash buffers were left at room temperature to equilibrate prior to use. Snap frozen cell pellets were re-suspended within approximately 1ml lysis/binding buffer. Cells were vigorously vortexed for 3 to 5 minutes, or passed through a 21gauge needle, to ensure their complete lysis. Cell lysates were then centrifuged at 13,000g for 3 minutes in LysateClear columns. A 50μl sample of μMACS oligo deoxy-thymidine (dT) microbeads was added to each lysate sample and gently mixed to facilitate the polyA tails of any present mRNA to hybridise to the oligo microbeads. The mixtures were then loaded into MACSm columns, which had been previously primed with 100ml Lysis/Binding buffer and placed within a magnetic field of the MACS^{TM} Separator. As the samples passed through the columns any magnetically labeled mRNA present within the samples bound to the columns. The columns were then washed twice with 200ml of lysis/binding buffer to remove any protein or DNA, followed by an additional rinse with 100μl wash buffer, four times, to remove ribosomal RNA and DNA. cDNA was then synthesis directly from the retained mRNA, within the same separation columns. 100ml equilibration/wash buffer was added twice to each column matrix and allowed to run through. The lyophilised reverse transcription mastermix was dissolved in 20ml re-suspension buffer and then added to columns, followed by the addition of 1ml sealing solution, to prevent sample evaporation. The columns were

incubated at 42°C for 1 hour on a thermo block, for reverse transcription to occur. Following this incubation period columns were washed twice with 100ml of equilibration/wash buffer. To release the cDNA, 20ml of release solution was applied to each sample, which were incubated at 42°C for an additional 30 minutes. The cDNA was then eluted from the columns by the addition of 50ml of cDNA elution buffer and collected in eppendorfs. The cDNA was stored at 20°C until needed.

2.14.3 Real Time Quantitative PCR

Real Time quantitative PCR was performed on the RotorGene RG-3000 (Corbett Research) using SYBR green with primers specific for the variety of genes of interest. The details of all primers used through out this study are summarized within Table 2.9. Prior to the amplification of target genes of interest, β-actin was selected as the housekeeping gene for sample normalization. Oligonucleotides were synthesized by Sigma-Genosys. PCR reactions were performed in either triplicates or duplicates within a 15µl reaction buffer. This buffer comprised of 7.5µl qPCR mastermix at a 2 x concentration (Bioline Sensimix NoRox SybrGreen), 0.15µl (20µM stock concentration) forward and reverse primers (final concentration of 0.2µM), 6.2µl DNAse-free/RNAse-free PCR grade water (Sigma) and 1µl cDNA template. The master mix contained heat activated Taq polymerase, dNTPs, MgCl2 and reaction buffer. In order to avoid any pseudogenes within the endogenous reference gene, β-actin primers were designed and synthesized by QIAGEN (QuantiTect Mm Actb 1SG Primer Assay: QIAGEN QT00095242) and used at a 1 x concentration. The amplification program included an initial 'hot start' at 95°C for 10 minutes, followed by cycling at 95°C for 15 seconds, 58 to 62°C (dependent upon the specific primer pair) for 20 seconds and 72°C for 15 seconds. This cycling stage was repeated for 39 cycles. At the end of each cycle the

fluorescent signal produced from the amplicon was obtained and at the final amplification a dissociation curve was generated (72-99°C, hold 30 seconds on the first step, then 5 seconds on subsequent steps), per primer pair, to verify the specificity of the amplicon. The reaction amplification efficiency and Ct values were acquired from Rotor Gene 6.0 software (Corbett Research, Sydney Australia) using standard curves predominantly generated from mouse universal cDNA (Biochain). The Pfaffl model was adopted to calculate the relative expression values of each sample, normalized to β-actin. The Pfaffl model was selected as it takes into account gene dependent efficiencies within the amplification process.

Table 2.9 Details Of Primers Used for qPCR

Primer	Forward 5' end primer sequence	Reverse 3' end primer sequence
CCR4	AACAGAGCAGTGCGCATGAT	CGTTGTACGGCGTCCAGAA
CCR7	CTAGCTGGAGAGAGACAAGA	TATCCGTCATGGTCTTGAGC
CCR9	ACCATGATGCCCACA- GAACT	GGGAAGAGTGGCAAGAAAGA
Foxo1	TGTCAGGCTAAGAGTTAGTGAGCA	GGGTGAAGGGCATCTTTG
S1pr1	AAATGCCCCAACGGAGACT	CTGATTTGCTGCGGCTAAATTC
Klf2	CTCA- GCGAGCCTATCTTGCC	CACGTTGTTTAGGT- CCTCATCC
Plxnd1	AGGACTCACCCACCAACAAG	GCCACCACCTGTTCAAACTT
RANKL	CACACCTCACCATCAATGCTG	GAAGGGTTGGACACCTGAATGC
CD40L	CCTTGCTGAACTGTGAGGAGA	CTTCGCTTACAACGTGTGCT
Foxp3	CCCAGGAAAGACAGCAACCTT	TTCTCACAACCAGGCCACTTG
CCL22	CTGATGCAGGTCCCTATGGT	GGAGTAGCTTCTTCACCCAG
CCL17	AGTGGAGTGTTCCAGGGATG	CCAATCTGATGGCCTTCTTC

2.15 GRAPHS AND STATISTICAL ANLAYSIS

All graphs presented within this study were created using Prism 4 software. All statistical analysis of data was also performed using this program. An unpaired student two-tailed T test was performed for all statistical analysis and any P values obtained below 0.05 were considered significant.

CHAPTER 3: DYNAMIC CHANGES IN CHEMOKINE RECEPTOR EXPRESSION PATTERNS REVEAL MULTIPLE CHECKPOINTS DURING THYMOCYTE POSITIVE SELECTION.

3.1 INTRODUCTION

The process of positive selection is an essential checkpoint in intrathymic T cell development. Thymocytes that successfully rearrange and express functional αβTCRs are positively selected via TCR engagement with self-peptide MHC complexes, expressed on the cell surface of cTEC (Laufer et al., 1996). Positively selected cells escape apoptosis and continue on with their developmental program, committing to either a CD4 or CD8 SP lineage fate. The transition from DP to SP on the initiation of selection is accompanied with thymic relocalization from cortical to medullary regions (Takahama, 2006).

Positive selection is a multistep process involving a transitional phase through an intermediate $CD69^{+}CD4^{+}CD8^{+}$ DP phenotype (Hare et al., 1998). Newly generated SP thymocytes undergo subsequent post-selection maturation stages, before their export out into the periphery to become naive T cells. The multiple developmental steps of SP thymocytes are defined by changes in expression levels of several surface markers. These include the progressive down regulation of HSA and CD69 and the upregulation of CD62L and Qa2 (Figure 3.1) (Gabor et al., 1997a; Kelly and Scollay, 1990; Lucas et al., 1994). The differentiation program of CD4 SP thymocytes has been further characterized with the aid of additional markers such as 6C10 (Jin et al., 2008). The functional relevance of the majority of surface markers used in the classification system of SP thymocytes, however, remains relatively unknown.

Chemokine receptors are thought to play a major role in the relocation of thymocytes from the cortex to the medulla, during the positive selection process. CCR7 specifically has been

Figure 3. 1 A Current Model Of The Phenotypic Changes Associated With The Multistep Positive Selection Process

On the initiation of positive selection $CD4^+CD8^+$ DP thymocytes rapidly upregulate CD69 on their cell surface, and differentiate into either CD4 or CD8 SP thymocytes. Newly generated $CD4^+$ and $CD8^+$ SP thymocytes are defined by a surface expression pattern displaying high levels of CD69 and HSA. With increased maturity both CD4 and CD8 SP thymocytes downregulate CD69 and HSA, whilst upregulating CD62L and Qa2 to exhibit a mature surface profile of $CD69^-$ HSA^- $CD62L^+$ $Qa2^+$ before their exit into the periphery to develop as naive T cells.

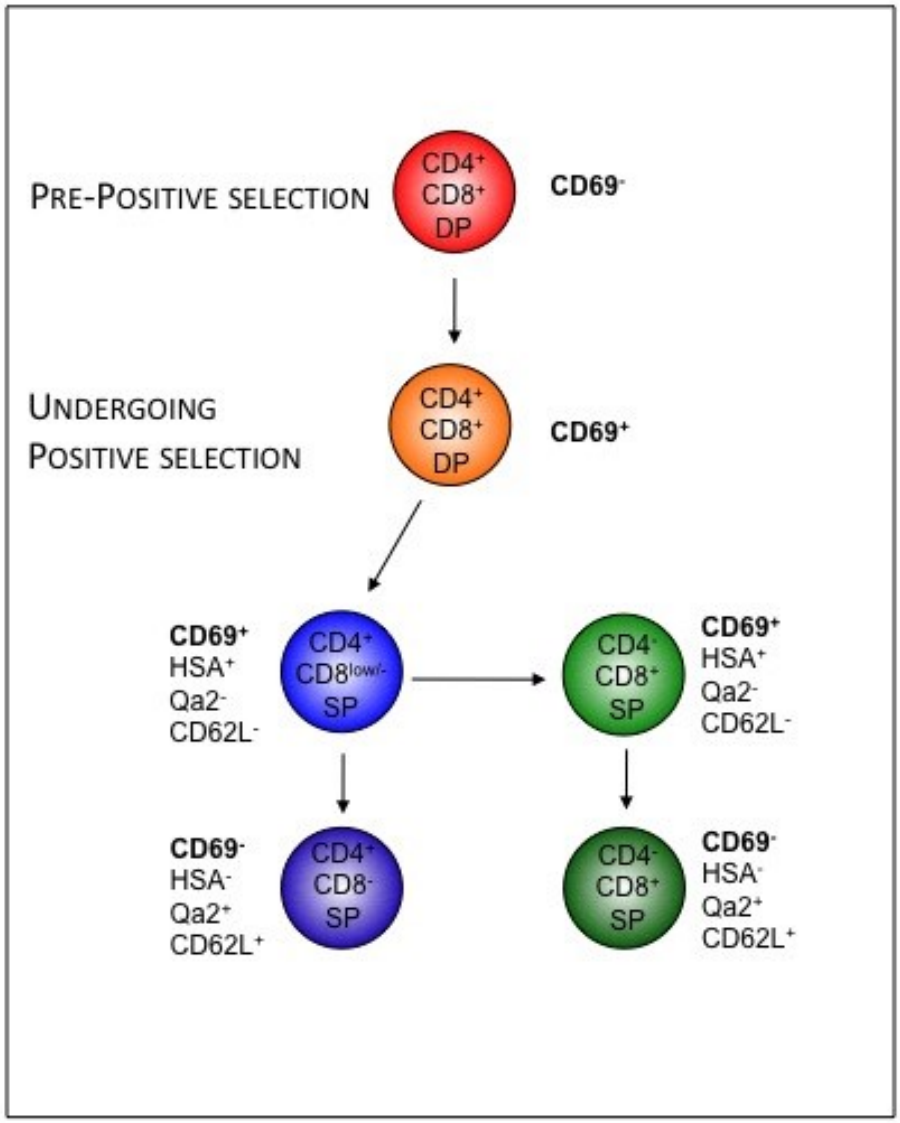
PRE-POSITIVE SELECTION
CD4+ CD8+ DP
CD69-
UNDERGOING POSITIVE SELECTION
CD4+ CD8+ DP
CD69+
CD69+ HSA+ Qa2- CD62L-
CD4+ CD8low/- SP
CD4- CD8+ SP
CD69+ HSA+ Qa2- CD62L-
CD69- HSA- Qa2+ CD62L+
CD4+ CD8- SP
CD4- CD8+ SP
CD69- HSA- Qa2+ CD62L+

identified in playing a major role in this process, which involves migration towards CCL19 and CCL21 gradients within medullary areas (Kwan and Killeen, 2004; Ueno et al., 2004). Whether CCR7 is solely responsible for this thymic relocalization, however, remains unclear. The blockade of all chemokine-mediated migration by Pertussis Toxin treatment resulted in the inability of SP cells to cross the corticomedulla junction, leading to their retention within cortical regions and medullary areas devoid of SP thymocytes (Ehrlich et al., 2009; Suzuki et al., 1999). Deficiency in CCR7 or its ligands, however, has less severe consequences, which include the formation of small medullary areas that still contain SP4 and SP8 thymocytes, albeit at reduced numbers (Ueno et al., 2004). Thus, absence of CCR7 signaling does not result in a total arrest in thymocyte migration to the medulla. Additional investigations have questioned the importance of CCR7 in guiding cortex to medulla migration of positively selected thymocytes, speculating the removal of CCR7 signaling has only a minor influence on CD4 SP migration and the defect on migration is exclusive to the CD8 SP population (Davalos-Misslitz et al., 2007). Moreover, on initiation of positive selection, CCR7 expression is reportedly upregulated on only a small fraction of $CD69^{+}$ DP thymocytes, complimenting data that suggests this population migrates poorly towards CCR7 ligands *in vivo* (Campbell et al., 1999; Davalos-Misslitz et al., 2007). Collectively this implies CCR7 may not exclusively control cortex to medulla relocalization of developing thymocytes and suggests possible redundancy by other chemokines receptor in orchestrating thymocyte trafficking at this key developmental checkpoint.

The goal of this chapter is to investigate chemokine receptor surface expression patterns at different maturational stages of the multistep positive selection process. The exploration of the chemokine receptor profile of cells undergoing the selection process, along with post

selection maturation of CD4 and CD8 SP thymocytes, will aid the classification of the differentiation stages of thymocyte maturation using molecules with known function, as an alternative to the markers widely used of unknown function. By attempting to define multiple checkpoints in the development of positively selected thymocytes, we also aim to reveal other possible chemokine receptor candidates, in addition to CCR7, that may be involved in directing cortex to medulla migration of positively selected thymocytes.

3.2 RESULTS

3.2.1 Changes In Chemokine Receptor Expression Patterns During The Initiation Of Positive Selection

To determine the changes in chemokine receptor expression during positive selection, the chemokine receptor profile of thymocytes at a pre-positive selection stage was first established by flow cytometric analysis of adult thymocytes from *Zap70*$^{-/-}$ mice, in which absence of TCR signaling results in an arrest in thymocyte development at the pre-selection DP stage (Negishi et al., 1995). Surface staining of co-receptors CD4 and CD8 with CD69 on WT and *Zap70*$^{-/-}$ thymocytes revealed all DP *Zap70*$^{-/-}$ thymocytes were CD69^{-}, with a total absence of CD69^{+} DP cells, readily detectable in WT mice (Figure 3.2 A and C). Analysis of the expression of additional chemokine receptors was then performed, chosen on the basis of two criteria. Firstly, the availability of relevant reagents for reliable flow cytometric analysis as assessed. Secondly, 'The Immunological Genome Project' (http://www.immgen.org) was used to identify expression of those chemokine receptor genes showing an induction of expression during thymocyte positive selection. From this process, we focused analysis on CCR7, CCR4, CXCR4 and CCR9. Gating on the pre-selection total DP *Zap70*$^{-/-}$ thymocyte population for chemokine receptor expression identified that all cells during this developmental window expressed high levels of CCR9 and CXCR4, but lacked surface expression of CCR7 or CCR4 (Figure 3.2 B). To establish whether the initiation of positive selection altered the expression of chemokine receptors, the profile of adult WT CD69^{+} DP

Figure 3. 2 Changes In Chemokine Receptor Expression Patterns During The Initiation Of Positive Selection

Thymocytes from adult *Zap70*$^{-/-}$ (A and B) or WT C57BL/6 (C to F) were isolated and stained for flow cytometry analysis.

The CD4^{+}CD8^{+} DP fraction of *Zap70*$^{-/-}$ (A) or WT (C) thymocytes were gated using a CD4 vs CD8 contour plot and their expression of CD69 displayed as a histogram. The CD69^{-} DP population of *Zap70*$^{-/-}$ thymoytes (B) or the CD69^{+} DP subsets of WT C57BL/6 thymocytes (D) were analyzed for expression of CCR9, CCR7, CCR4 and CXCR4. Grey shaded histograms represent negative controls of CD69^{-} or CD69^{+} DP thymocytes from the equivalent: *Ccr9*$^{-/-}$, *Ccr7*$^{-/-}$ or *Ccr4*$^{-/-}$ adult mice, or a CXCR4 isotype control. The numbers displayed on the histograms and contour plots represent the percentage of cells within the gates.

(E) The percentages of CD69^{+} (white bar) and CD69^{-} (grey bar) WT DP cells positive for each receptor: CCR9, CCR7, CCR4 and CXCR4 are displayed in mean bar graphs. The bar graph represents 7 independent experiments with the exception of CXCR4 staining, where data is representative of 3 experimental replicates. The standard error bars indicate the SEM.

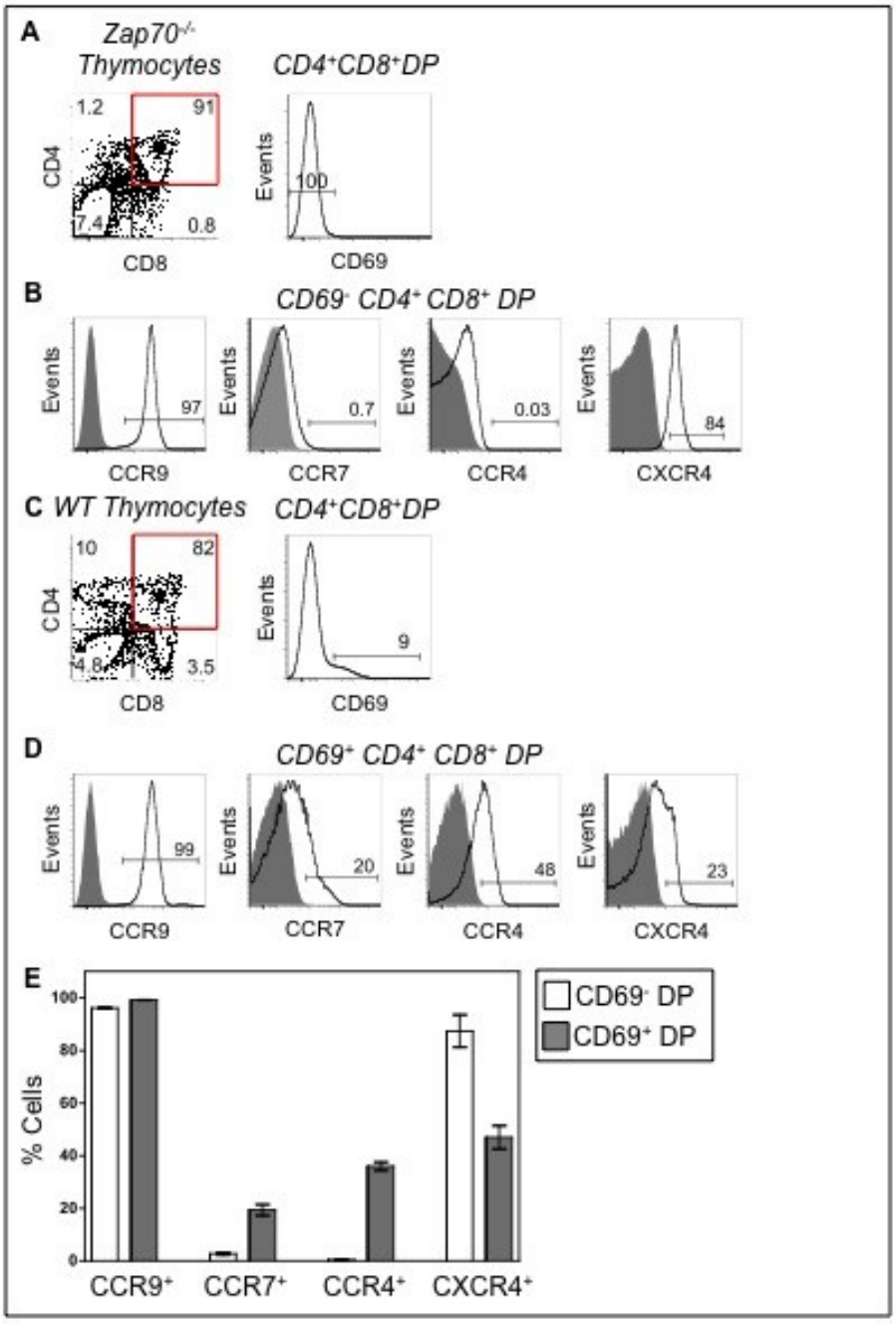
A
Zap70-/-
Thymocytes
CD4+CD8+DP
1.2
91
7.4
0.8
CD4
CD8
Events
100
CD69
B
CD69- CD4+ CD8+ DP
Events
97
CCR9
0.7
CCR7
0.03
CCR4
84
CXCR4
C WT Thymocytes
CD4+CD8+DP
10
82
4.8
3.5
9
D
CD69+ CD4+ CD8+ DP
99
20
48
23
E
% Cells
100
80
60
40
20
0
CD69- DP
CD69+ DP
CCR9+
CCR7+
CCR4+
CXCR4+

thymocytes were analyzed. Flow cytometry analysis revealed that at this stage in intrathymic development thymocytes maintained high levels of CCR9 on their cell surface, but showed evidence of downregulation of CXCR4 expression, with less than 40% of $CD69^+$ DP cells displaying high levels of CXCR4 on their cell surface, in comparison to over 80% of the population at the pre-selection stage (Figure 3.2. D and F). In addition the initiation of the selection process resulted in the induction of both CCR4 and CCR7 expression, with approximately 20% of $CD69^+$ DP thymocytes acquiring CCR7 and just fewer than 50% upregulating CCR4.

Collectively the chemokine receptor profile of DP thymocytes pre-selection, in comparison to $CD69^+$DP thymocytes undergoing the selection process, suggests that the initiation of positive selection results in downregulation of CXCR4 and upregulation of CCR4 and CCR7. In contrast, the initiation of positive selection does not alter the surface expression of CCR9, detectable at high levels on the cell surface at both DP $CD69^-$ and DP $CD69^+$ stages.

3.2.2 Newly Generated $CD69^+$ And Late Stage $CD69^-$ SP4 Thymocyte Subsets Have Distinct Chemokine Receptor Profiles

Having characterized the changes in chemokine receptor expression on the initiation of positive selection we went on to classify changes in chemokine receptor expression during later stages of this process, including the different maturational stages of SP4 thymocyte development (Figure 3.3). The immature $CD69^+$ and mature $CD69^-$ subsets of $TCR\beta^{high}$ SP4 thymocytes were explored for their surface expression of CCR9, CCR7, CCR4 and CXCR4. A large fraction of newly generated immature $CD69^+$ SP4 thymocytes maintained high levels

Figure 3. 3 The Chemokine Receptor Expression Profile Of Positively Selected $CD4^+$ SP Thymocytes

(A) Thymocytes obtained from adult WT C57BL/6 mice were analysed for expression of CD4, CD8, CD69 and TCRb.

(B) The $TCR\beta^{high}$ SP4 population was subdivided based on their $CD69^+$ or $CD69^-$ status and gated for their expression of chemokine receptors CCR9, CCR7, CCR4 and CXCR4. The shaded grey area on each histogram represents a negative control of $CD69^+$ or $CD69^-$ $TCR\beta^{high}$ $CD4^+$ SP thymocytes from the equivalent: *Ccr9*$^{-/-}$, *Ccr7*$^{-/-}$ or *Ccr4*$^{-/-}$ adult mice, or a CXCR4 isotype control.

(C) The percentage of positive cells for each chemokine receptor from the $CD69^+$ $TCR\beta^{high}$ SP4 population (white box), the $CD69^-$ $TCR\beta^{high}$ SP4 subset (gray bar) and $TCR\beta^{high}$ $CD4^+$ splenocytes (striped bars) are displayed as a mean bar graph from 7 independent experimental repeats, with the stand error bars representing the SEM.

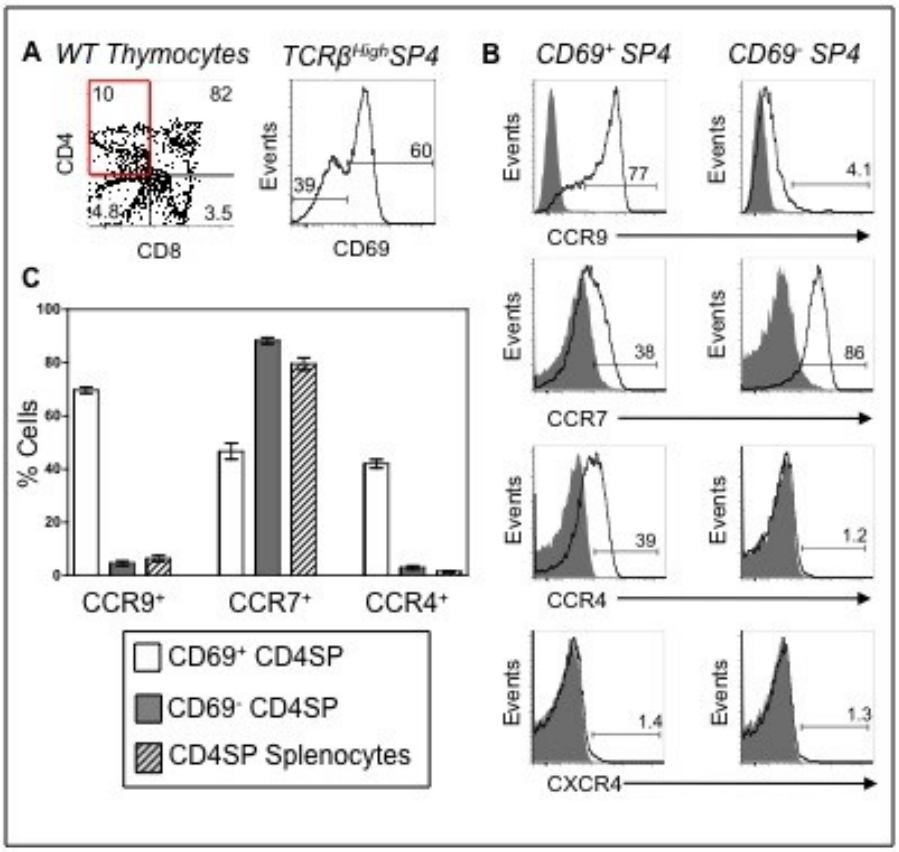
A
WT Thymocytes
TCRβ^High SP4
10
82
4.8
3.5
CD4
CD8
Events
39
60
CD69
B
CD69+ SP4
CD69- SP4
Events
77
4.1
CCR9
38
86
CCR7
39
1.2
CCR4
1.4
1.3
CXCR4
C
% Cells
CCR9+
CCR7+
CCR4+
CD69+ CD4SP
CD69- CD4SP
CD4SP Splenocytes

of CCR9 on their cell surface, while approximately 40% of the population also expressed CCR4 and CCR7 (Figure 3B and C). However, from this staining analysis it is not clear if these receptors are co-expressed by the same thymocyte cohort or by two distinct populations. In contrast to the positive staining acquired for CCR9, CCR4 and CCR7, at the $CD69^+$ SP4 stage in development, CXCR4 was absent from the cell surface. Moreover, CXCR4 was also absent on the mature $CD69^-$ SP4 subset (Figure 3.3B and C). This would suggest CXCR4 undergoes rapid downregulation upon the initiation of positive selection, which is completed before the transition into SP4 thymocytes and remains absent from the surface of cells committed to this lineage during the rest of their thymic residency.

The more mature $CD69^-$ fraction of SP4 thymocytes displayed a distinct chemokine receptor phenotype, compared to their immature $CD69^+$ counterparts. At this advanced developmental stage SP4 thymocytes lack surface expression of both CCR9 and CCR4, while approximately 90% express CCR7 (Figure 3.3B and C). Collectively, this suggests that with increasing maturity, during the transition from a $CD69^+$ to $CD69^-$ phenotype, SP4 thymocytes downregulate CCR9 and CCR4, whilst upregulating CCR7. The chemokine receptor profile of $TCR\beta^{high}CD4$ T cells within the spleen of WT adult mice closely mirrors that of mature $CD69^-$ SP4 thymic residents (Figure 3.3C), with the large majority of the spleen-resident $CD4^+$ T cells expressing high levels of CCR7, whilst lacking CCR9 and CCR4.

3.2.3 Simultaneous Analysis Of Chemokine Receptor Expression Patterns Reveals Distinct Subsets Of SP4 Thymocytes

After establishing the chemokine receptor profile of SP4 thymocytes at both their immature $CD69^+$ and mature $CD69^-$ stages in development, we were interested to continue to explore

SP4 thymocyte development using analysis of simultaneous expression of a panel of chemokine receptors. As CXCR4 did not have detectable levels of expression during any phase of SP4 differentiation, we focused our investigations on the relationship between the expression patterns of CCR7, CCR4 and CCR9 during the maturation of WT adult SP4 thymocytes (Figure 3.4 A). On examination of the relationship between CCR9 and CCR7 expression within the immature $CD69^+$ and mature $CD69^-$ cohorts of SP4 cells, we identified distinct heterogeneity within the $CD69^+$ fraction. Simultaneous flow cytometry analysis of CCR9 and CCR7 expression of the $CD69^+$ immature SP4 population revealed thymocytes do not co-express both chemokine receptors during this maturational stage. Rather, the majority of $CD69^+$ SP4 thymocytes expressed high levels of CCR9, whist expressing low levels of CCR7, with a small fraction of the population displaying the reverse expression pattern. In contrast, analysis of CCR9 versus CCR4 expression within the $CD69^+$ SP4 population revealed that approximately 35% of cells co-expressed both chemokine receptors, suggesting that downregulation of these chemokine receptors during development occurs in unison, perhaps with CCR9 undergoing downregulation slightly later than CCR4. The expression pattern of CCR4 against CCR7 within the immature $CD69^+$ SP4 subset displayed heterogeneity that essentially reflected the relationship of expression between CCR9 and CCR7, offering additional confirmation of co-expression of CCR4 and CCR9.

With the identification of heterogeneity within the immature fraction of SP4 thymocytes, we were interested to explore the maturation status of the different populations identified on the basis of their chemokine receptor profiles. To achieve this we analysed different SP4 thymocyte populations from RAG-2 GFP adult mice. We used RAG-2 GFP levels as an age defining marker of thymocyte differentiation, as decreasing levels of GFP expression is

Figure 3. 4 The Dynamic Changes In Chemokine Receptor Expression Patterns Reveals Distinct Subsets Of SP4 Thymocytes

(A) $CD69^+$ and $CD69^-$ $TCR\beta^{high}$ SP4 thymocytes subsets from adult RAG-2 GFP mice were analysed for expression of CCR7, CCR9 and CCR4 (B) The levels of HSA, Qa2, CD62L and RAG-2 GFP are displayed in the following subsets, as overlays on a histogram:

$CCR7^-CCR9^+CD69^+TCR\beta^{high}$ SP4 (red line)

$CCR7^+CCR9^-CD69^+TCR\beta^{high}$ SP4 (blue line)

$CCR7^+CCR9^-CD69^-TCR\beta^{high}$ SP4 (green line)

The black line on the RAG-2 GFP histogram displays the expression levels on total $CD4^+$ $CD8^+$ DP thymocytes. All data is representative of at least 3 experimental replicates.

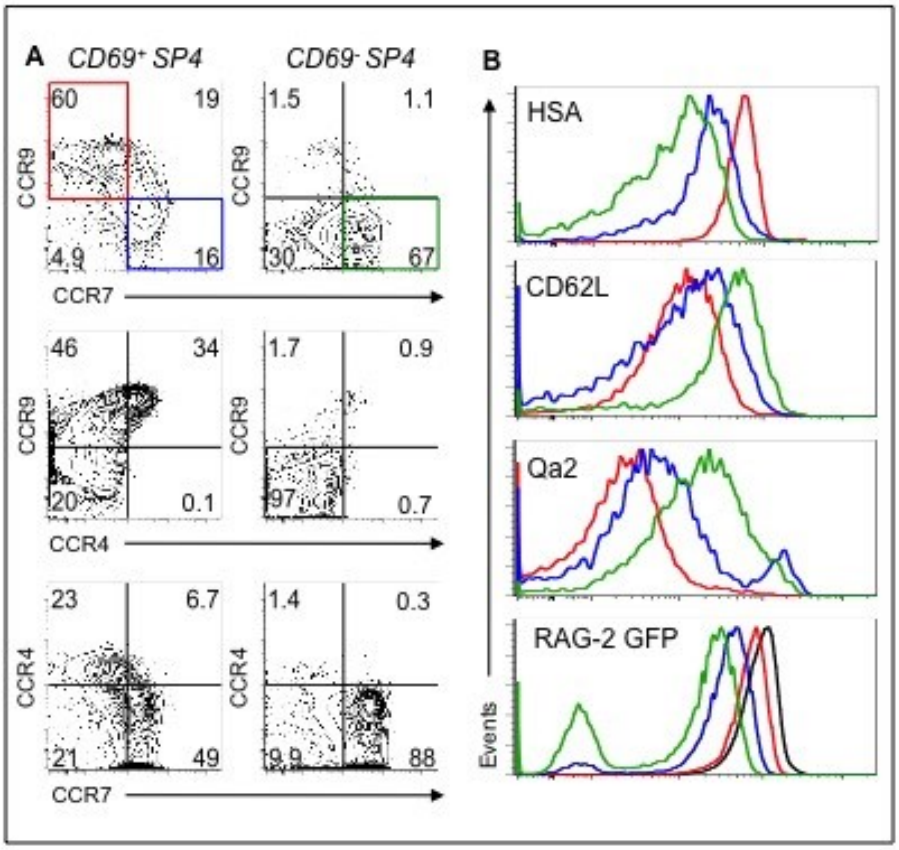
A
CD69+ SP4
CD69- SP4
60
19
4.9
16
1.5
1.1
30
67
CCR9
CCR7
46
34
20
0.1
1.7
0.9
97
0.7
CCR4
23
6.7
21
49
1.4
0.3
9.9
88
B
HSA
CD62L
Qa2
RAG-2 GFP
Events

directly linked to increasing maturity (Boursalian et al., 2004). We compared the RAG-2 GFP levels of expression between each SP4 population, along with a control DP thymocyte cohort, displaying the brightest RAG-2 GFP signal. We also used additional, well-established markers of maturation status; HSA Qa2 and CD62L to define the maturity of the different SP4 populations (Figure 3.4 B). We explored the expression levels of all four age defining markers in the newly define three independent SP4 TCRβ^{high} populations: CCR7^{-} CCR9^{+}CD69^{+}, CCR7^{+}CCR9^{-}CD69^{+} and CCR7^{+}CCR9^{-}CD69^{-}. Although we did not include the CCR4 staining profile in our gating strategy, data obtained (Figure 3.4A) suggested CCR4 expression mimics that of CCR9, due to their closely related surface expression profiles and therefore, the CCR7CCR9^{+}CD69^{+} TCRβ^{high}SP4 cells were assumed to also include the CCR4^{+} CD69^{+}SP4 population. Figure 3.4B shows that the most immature SP4 cells had a surface expression profile of CCR7^{-}CCR9^{+}CD69^{+}, based upon their high levels of HSA and RAG-2 GFP expression and their low expression levels of Qa2 and CD62L, in comparison to the additional two SP4 thymocyte subsets. The expression levels of this collection of markers also showed that the CCR7^{+}CCR9^{-}CD69^{+}TCRβ^{high}SP4 fraction of thymocytes had an intermediate maturational status, as cells displaying this specific chemokine receptor profile demonstrated intermediate levels of expression for all four differentiation markers; HSA, RAG-2 GFP, Qa2 and CD62L. As anticipated from their CD69^{-} status, the CCR7^{+}CCR9^{-} CD69^{-}TCRβ^{high}SP4 population displayed the most mature phenotype, exhibiting the lowest levels of HSA and Rag-2 GFP of all three populations, whilst displaying the highest levels of Qa2 and CD62L. Collectively, from this data we propose the following sequence of TCRβ^{high}SP4 development: CCR7^{-}CCR9^{+}CD69^{+} cells develop into CCR7^{+}CCR9^{-}CD69^{+}SP4, which differentiate into CCR7^{+}CCR9^{-}CD69^{-} SP4 thymocytes.

3.2.4 The Chemokine Receptor Expression Patterns Of Positively Selected SP8 Thymocytes

As with our SP4 thymocyte analysis, we next investigated the surface expression profile of SP8 thymocytes for an identical chemokine receptor panel and used CD69 levels to distinguish between the immature and mature fractions (Figure. 3.5). The proportions of immature versus mature cells within the SP8 population differs to that of SP4 cells, with the largest percentage of the population expressing a mature $CD69^-$ SP8 phenotype, as opposed to SP4 cells, where the majority of thymocytes display a immature $CD69^+$ profile.

The separation of immature $CD69^+$ and mature $CD69^-$ SP8 populations revealed little phenotypical changes to the chemokine receptor profile with increasing maturity (Figure 3.5 B and C). In general, at both the $CD69^+$ and $CD69^-$ developmental stages of SP8 differentiation cells displayed high levels of CCR9 and CCR7 on their cell surface. Interestingly, however within the $CD69^+$SP8 subset a small fraction of cells express lower levels of surface CCR7, with only approximately 80% of the population displaying a high frequency of the receptor. Furthermore, both $CD69^+$ and $CD69^-$ fractions of thymocytes lacked surface expression of CCR4 and CXCR4, suggesting neither of these receptors are expressed by SP8 at any stage of their maturational program (Figure 3.5 B) The total lack of CXCR4 throughout SP8 differentiation mirrors the absence of this receptor on all SP4 thymocytes. The absence of CCR4 on both SP8 populations, however, differs greatly to the newly generated SP4 subset that displays this chemokine receptor on their cell surface.

Figure 3. 5 The Chemokine Receptor Expression Patterns Of Positively Selected $CD8^+$ SP Thymocytes

Thymocytes obtained from WT C57BL/6 mice were stained for FACS analysis. (A) $CD4^-CD8^+$ SP cells were identified via a CD4 vs CD8 contour plot, and the $TCR\beta^{high}$ population was gated from a histogram and CD69 expression explored.

(B) The $TCR\beta^{high}$ SP8 population was subdivided based on their $CD69^+$ or $CD69^-$ status and gated for their expression of chemokine receptors CCR9, CCR7, CCR4 and CXCR4. The shaded grey area on each histogram represents a negative control of $CD69^+$ or $CD69^-$ $TCR\beta^{high}$ $CD8^+$ SP thymocytes from the equivalent population of *Ccr9*$^{-/-}$, *Ccr7*$^{-/-}$ or *Ccr4*$^{-/-}$ thymocytes, or a CXCR4 isotype control.

(C) The percentage of positive cells for each chemokine receptor from the $CD69^+$ $TCR\beta^{high}$ SP8 population (white box) $CD69^-$ $TCR\beta^{high}$ SP8 subset (gray bar) and $TCR\beta^{high}$ $CD8^+$ splenocytes (striped bars) are displayed as a mean bar graph from 7 independent experimental repeats, with the stand error bars representing the SEM.

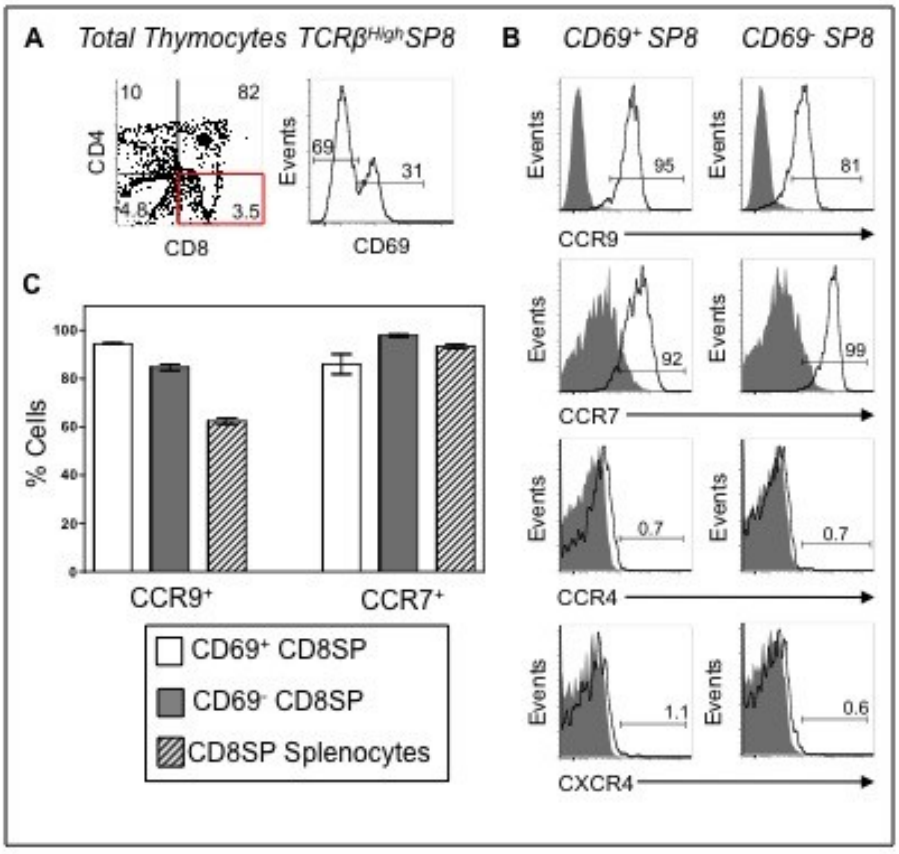
A
Total Thymocytes TCRβ^High SP8
10
82
4.8
3.5
CD4
CD8
Events
69
31
CD69
B
CD69+ SP8
CD69- SP8
Events
95
81
CCR9
92
99
CCR7
0.7
0.7
CCR4
1.1
0.6
CXCR4
C
% Cells
100
80
60
40
20
0
CCR9+
CCR7+
CD69+ CD8SP
CD69- CD8SP
CD8SP Splenocytes

Comparison of mature SP8 thymocytes and $CD8^+$ T cells residing with the spleen identified a similar chemokine receptor expression profile between the two populations in regards to CCR7, while a smaller proportion of CD8 T cells within the spleen expressed CCR9 (Figure 3.5C).

3.2.5 Simultaneous Analysis Of Chemokine Receptor Expression Patterns During SP8 Thymocyte Development

As CCR4 and CXCR4 did not have detectable levels of expression during either phase of SP8 differentiation, we next explored possible further heterogeneity within the SP8 thymocyte subsets by performing simultaneous analysis of CCR7 and CCR9 expression (Figure 3.6). By analyzing the relationship between CCR9 and CCR7 expression using an identical gating strategy to that applied to the SP4 subsets, we observed potential heterogeneity in the population based upon their expression of CCR7. Although the populations we not as distinct as those detected within the SP4 subset, a small fraction of the $CD69^+$ SP8 population expressed lower levels of CCR7 on their cell surface (as identified in Figure 3.5 B), whilst expressing high levels of CCR9. This resulted in a tail of CCR7 expression and the possible distinction of two SP8 populations; $CCR9^+CCR7^{low}CD69^+$ and $CCR9^+CCR7^+CD69^+$ (Figure 3.6A). Overall, however, the staining confirmed that the vast majority of SP8 cells co-express high levels of CCR9 and CCR7 through out their maturation.

We explore further the possible heterogeneity within the SP8 population by investigating the maturational status of the newly identified TCR^{high} SP8 subsets ($CCR9^+CCR7^{low}CD69^+$, $CCR9^+CCR7^+CD69^+$ and $CCR9^+CCR7^+CD69$). We classified the 'age' of each population

Figure 3. 6 Changes In Chemokine Receptor Expression During The Maturation Of SP8 Thymocytes, Post Positive Selection

(A) $CD69^+$ and $CD69^-$ $TCR\beta^{high}$ SP8 thymocytes subsets from adult RAG-2 GFP mice were analysed for expression of CCR7, CCR9.

(B) The levels of HSA, Qa2, CD62L and RAG-2 GFP are displayed as overlays on a histogram for the following:

$CCR7^{low}CCR9^+CD69^+TCR\beta^{high}$ SP8 (red line)

$CCR7^+CCR9^+CD69^+TCR\beta^{high}$ SP8 (blue line)

$CCR7^+CCR9^+CD69^-TCR\beta^{high}$ SP8 (green line)

The black line on the RAG-2 GFP histogram displays the expression levels of total $CD4^+$ $CD8^+$ DP thymocytes. All data is representative of at least 3 experimental replicas.

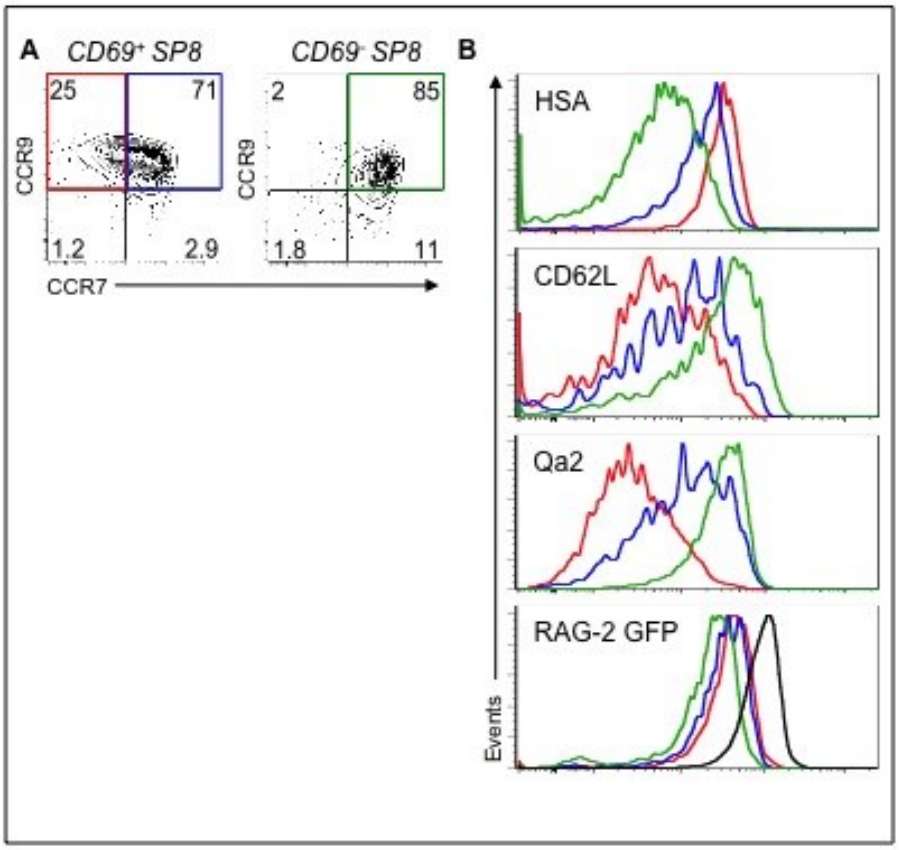
A
CD69+ SP8
CD69- SP8
25
71
1,2
2.9
2
85
1.8
11
CCR9
CCR7
B
HSA
CD62L
Qa2
RAG-2 GFP
Events

based upon their expression of RAG-2 GFP, HSA, Qa2 and CD62L (Figure 3.6B). By using these age defining markers we identified the $CCR9^{+}CCR7^{low}CD69^{+}$ $TCR^{high}SP8$ cohort to be the most immature phenotype, exhibiting the highest level of HSA and the lowest levels of CD62L and Qa2. Interestingly, RAG-2 GFP levels between the $CCR9^{+}CCR7^{low}CD69^{+}$ and $CCR9^{+}CCR7^{+}CD69^{+}$ cohorts, was indistinguishable and therefore this was not a suitable marker to distinguish the maturation statuses of these two subsets. The $CCR9^{+}CCR7^{+}CD69^{+}$ $TCR^{high}SP8$ subset displayed an intermediate maturational phenotype, based upon its expression levels of HSA, Qa2 and CD62L, which resided in-between of the other two SP8 populations. The pattern of expression for all four age defining markers clearly identified the $CCR9^{+}CCR7^{+}CD69^{-}TCR^{high}SP8$ subset as the most mature, in comparison to the additional two SP8 fractions. This population displayed the lowest expression levels of RAG-2 GFP and HSA, whilst exhibiting the highest levels of CD62L and Qa2.

3.2.6 Gene Expression Patterns Of Distinct SP4 Thymocyte Subsets

Having identified heterogeneity within the SP4 population, based upon their expression patterns of CCR9 and CCR7, it was of interest to gain more insight into the maturational state of these three distinct populations. The three populations of $TCR\beta^{high}SP4$ thymocytes classified in Figure 3.4 ($CCR7^{-}CCR9^{+}CD69^{+}$, $CCR7^{+}CCR9^{-}CD69^{+}$ and $CCR7^{+}CCR9^{-}CD69^{-}$) along with $CD4^{+}CD8^{+}$ DP cells, were isolated via cell sorting from adult WT thymocyte samples. These populations were then analysed by quantitative PCR for their mRNA expression levels of a panel of genes linked to thymocyte development (Figure 3.7).

Initially, expression of *Ccr4*, *Ccr9* and *Ccr7* was analyzed to confirm if mRNA levels corresponded to the surface protein expression profiles of these chemokine receptors

Figure 3. 7 Gene Expression Patterns Of Distinct SP4 Thymocyte Subsets

Quantitative real time PCR was performed on the indicated thymocyte populations, cell sorted from BALB/c WT adult mice:

$CD4^{+}CD8^{+}$ DP (white bars)

$CCR7^{-}CCR9^{+}CD69^{+}TCR\beta^{high}$ SP4 (right horizontal strip bars)

$CCR7^{+}CCR9^{-}CD69^{+}TCR\beta^{high}$ SP4 (grey bars)

$CCR7^{+}CCR9^{-}CD69^{-}TCR\beta^{high}$ SP4 (left horizontal strip bars)

Error bars indicate the SEM and mRNA levels were normalized to house keeping gene β-actin. Data is from at least two independently sorted biological samples, with each gene analyzed a minimum of two times and each PCR ran in triplicates to obtain a SEM.

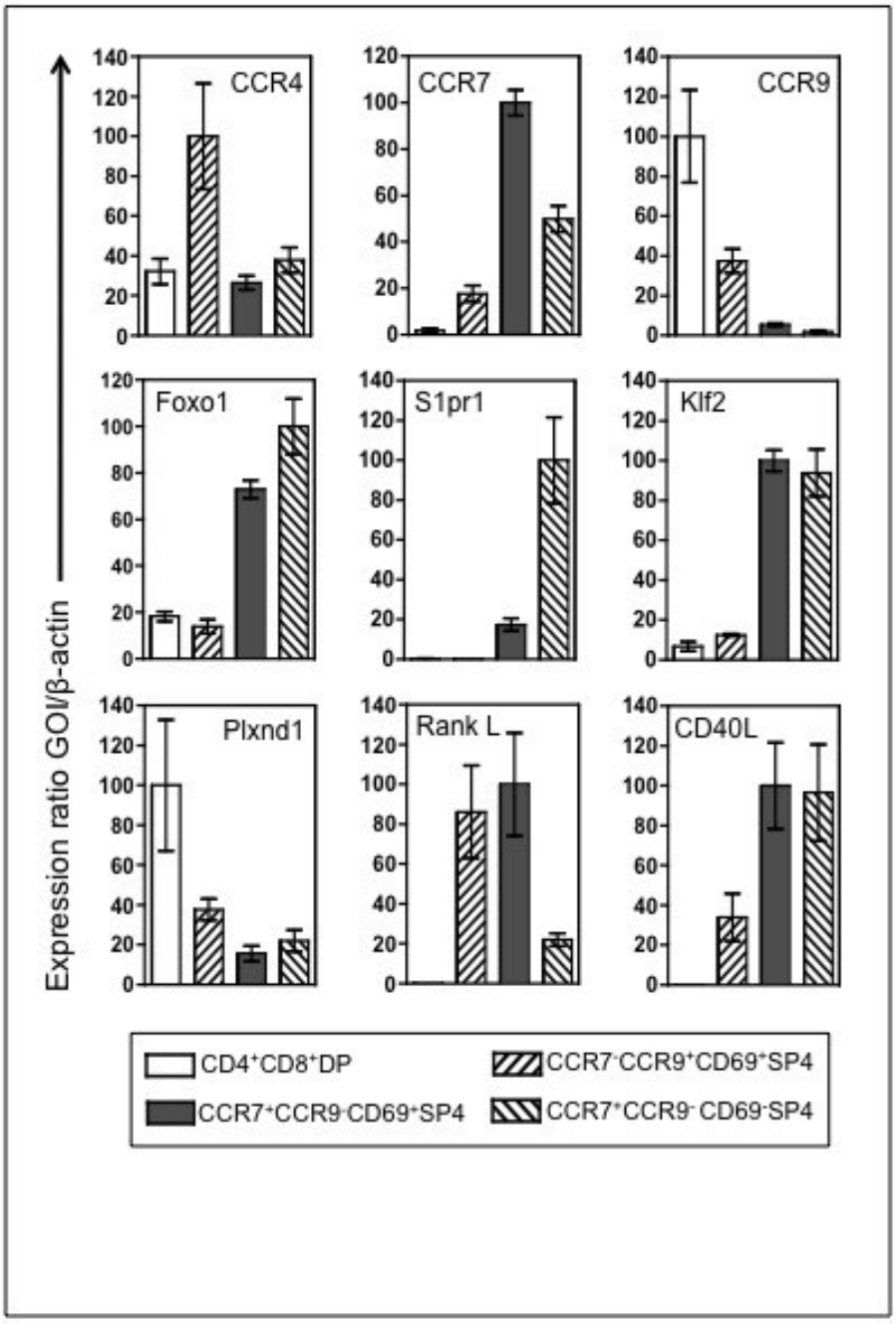
Expression ratio GOI/β-actin
CCR4
CCR7
CCR9
Foxo1
S1pr1
Klf2
Plxnd1
Rank L
CD40L
CD4+CD8+DP
CCR7-CCR9+CD69+SP4
CCR7+CCR9-CD69+SP4
CCR7+CCR9-CD69-SP4

demonstrated within Figures 3.3 and 3.4. *Ccr4* mRNA levels were greatest within the immature, newly generated $CCR7^{-}CCR9^{+}CD69^{+}TCR\beta^{high}$ SP4 population, when the majority of cells are expressing this receptor on their surface. *Ccr7* mRNA was highest within the intermediate $CCR7^{+}CCR9^{-}CD69^{+}$ $TCR\beta^{high}$ SP4 fraction, while, *Ccr9* gene expression was highest within the DP fraction of thymocytes, when it is highly expressed on the thymocyte cell surface. Interestingly, however, *Ccr9* mRNA levels were substantially reduced during the transition from DP to the immature $CCR7^{-}CCR9^{+}CD69^{+}$ $TCR\beta^{high}$ SP4 stage, although high levels of surface protein expression of CCR9 is maintained at both developmental phases, suggesting a delay between the cessation of *Ccr9* gene expression and the downregulation of the receptor on the cell surface. A similarly surprising result was observed with the decrease in *Ccr7* mRNA expression levels between the intermediate $CCR7^{+}CCR9^{-}CD69^{+}$ $TCR\beta^{high}$ SP4 and the late stage $CCR7^{+}CCR9^{-}CD69^{-}TCR\beta^{high}$ SP4 populations, which does not fully correspond to the maintained levels of surface expression of this chemokine receptor during this transition. The DP population of thymocytes demonstrated very low levels of *Ccr4* mRNA expression and an almost absent level of *Ccr7* mRNA. These findings fit well with the surface expression of these two chemokine receptors on this thymocyte subset, as they are both induced on the surface of only a fraction of $CD69^{+}$DP cells undergoing the positive selection process, which represents less than 10% of the total DP population (Figure 3.2).

Isolated thymocyte populations were also explored for their expression patterns of genes associated with late stage intrathymic T cell development, including *Foxo1*, Kruppel-like factor 2 (*Klf2*) and Sphingosine-1-phosphate receptor-1 (*S1pr1*). Foxo1 and Klf2 are both transcription factors known to regulate thymic emigration, along with recirculation to peripheral lymphoid organs (Carlson et al., 2006; Gubbels Bupp et al., 2009). High levels of

Foxo1 and *Klf2* mRNA expression were detected within the $CCR7^{+}CCR9^{-}CD69^{+}$ and $CCR7^{+}CCR9^{-}CD69^{-}$ TCRβhighSP4 populations (Figure 3.7). In contrast, mRNA encoding S1pr1, an additional regulator of thymic egress (Matloubian et al., 2004), was limited to only the most mature $CCR7^{+}CCR9^{-}CD69^{-}TCR\beta^{high}$ SP4 population. Collectively the gene expression patterns of these three late stage thymocyte regulators offers additional support to the proposed sequence of development for SP4 thymocyte subsets in which immature $CCR7^{-}CCR9^{+}CD69^{+}$ cells develop into a $CCR7^{+}CCR9^{-}CD69^{+}$ phenotype, before maturing into $CCR7^{+}CCR9^{-}CD69^{-}$ thymocytes. In addition the gene expression patterns of *Klf2* and *Foxo1* would suggest that both $CCR7^{+}CCR9^{-}CD69^{+}$ and $CCR7^{+}CCR9^{-}CD69^{-}$ populations represent SP4 cells of an advance developmental state and thus, proposes CCR7 acquisition occurs as a relatively late stage maturational event in SP4 thymocyte positive selection.

The expression of additional genes was also explored within the four thymocyte populations, including plexinD1 (*Plxnd1*), which has been suggested to control the migration of positively selected thymocytes into the medulla, via the repression of CCR9 signaling (Choi et al., 2008). Complementary to this proposed function, DP thymocytes express high levels of mRNA for *Plnxd1*, which is reduced within the most immature $CCR7^{-}CCR9^{+}CD69^{+}$ $TCR\beta^{high}$SP4 subset and further still within the additional two SP4 populations. The levels of *Rankl* and *Cd40lg* mRNA within the different thymocyte populations were also examined and both were readily detectable in the intermediate $CCR7^{+}CCR9^{-}CD69^{+}$ population. While *RankL* mRNA was also present within the $CCR7^{-}CCR9^{+}CD69^{+}$ SP4 fraction, *Cd40lg* expression was detectable in the $CCR7^{+}CCR9^{-}CD69^{-}$ SP4 subset (Figure 3.7).

3.2.7 Determining Precursor-Product Relationships Within Heterogonous CD4 SP Thymocyte Subsets

To directly confirm the maturation sequence of the three distinct SP4 thymocyte populations defined above, we used the reaggregate thymus organ culture (RTOC) system to follow the development of a single cohort of $CCR7^{-}CCR9^{+}CD69^{+}$ SP4 thymocytes. Cells were isolated via high speed cell sorting from total adult WT thymocytes and reaggregated with WT stromal cells from disaggregated 2-dGuo treated FTOC. As a comparison, the $CCR7^{+}CCR9^{-}CD69^{-}$ SP4 thymocyte subset was also isolated and placed into the RTOC system. Each input population is displayed in Figure 3.8 A and B. The RTOC were harvested after 5 days in culture and analyzed to explore the maturation status of the input populations (Figure 3.8).

Analysis of the $CCR7^{-}CCR9^{+}CD69^{+}$ SP4 input population after culture revealed the presence of both SP4 and SP8 thymocyte lineages (Figure 3.8 A, C and D). This finding is compatible with the notion that these cells represent an SP4 thymocyte subset at an immature stage, prior to commitment to a particular SP4 or SP8 lineage. Closer investigations into the SP4 thymocyte subset demonstrated that cells had down regulated CD69 and CCR9, whilst upregulating CCR7, to reach the mature SP4 surface phenotype of $CCR7^{+}CCR9^{-}CD69^{-}$ (Figure 3.8 A and C) In comparison, the $CCR7^{+}CCR9^{-}$SP4 input population remained committed to a SP4 lineage, had downregulated CD69 and maintained a $CCR7^{+}CCR9^{-}$ surface profile after 5 days in culture (Figure 3.8 B, C and D). Collectively, data obtained from RTOC analysis of thymocyte developmental potential enabled the direct confirmation of a precursor-product relationship within newly defined SP4 thymocyte subsets, providing evidence for a maturation sequence in which $CCR7^{-}CCR9^{+}CD69^{+}$ SP4 cells, representative of

Figure 3. 8 Determining Precursor-Product Relationships Within Heterogeneous SP4 Thymocyte Subsets

$CCR7^{-}CCR9^{+}$ SP4 and $CCR7^{+}CCR9^{-}$ CD4 SP populations were isolated from adult BALB/C WT thymocyte sample and incorporated into RTOC system with 2dGuo treated E15 WT FTOC (Input populations A and B- top FACS plots).

RTOC were cultured for 5 days and outputs stained for FACS analysis of CD4, CD8, CD69, CCR7 and CCR9 expression (Output populations A and B- bottom FACS plots).

(C and D) The percentages of cells recovered from $CCR7^{-}CCR9^{+}$ SP4 input RTOCs (white bars) and $CCR7^{+}CCR9^{-}$ CD4 SP input RTOC (gray bars) are displayed as mean bar graphs. The percentages of total CD4 SP cells (C-left graph), $CCR7^{-}$ $CCR9^{+}$ $CD69^{-}$ SP4 thymocytes (C- right graph) and total $CD8^{+}$ SP cells (D) recovered from the RTOC system are displayed, and graphs represent at least 4 independent experiments per condition. Error bars indicate SEM.

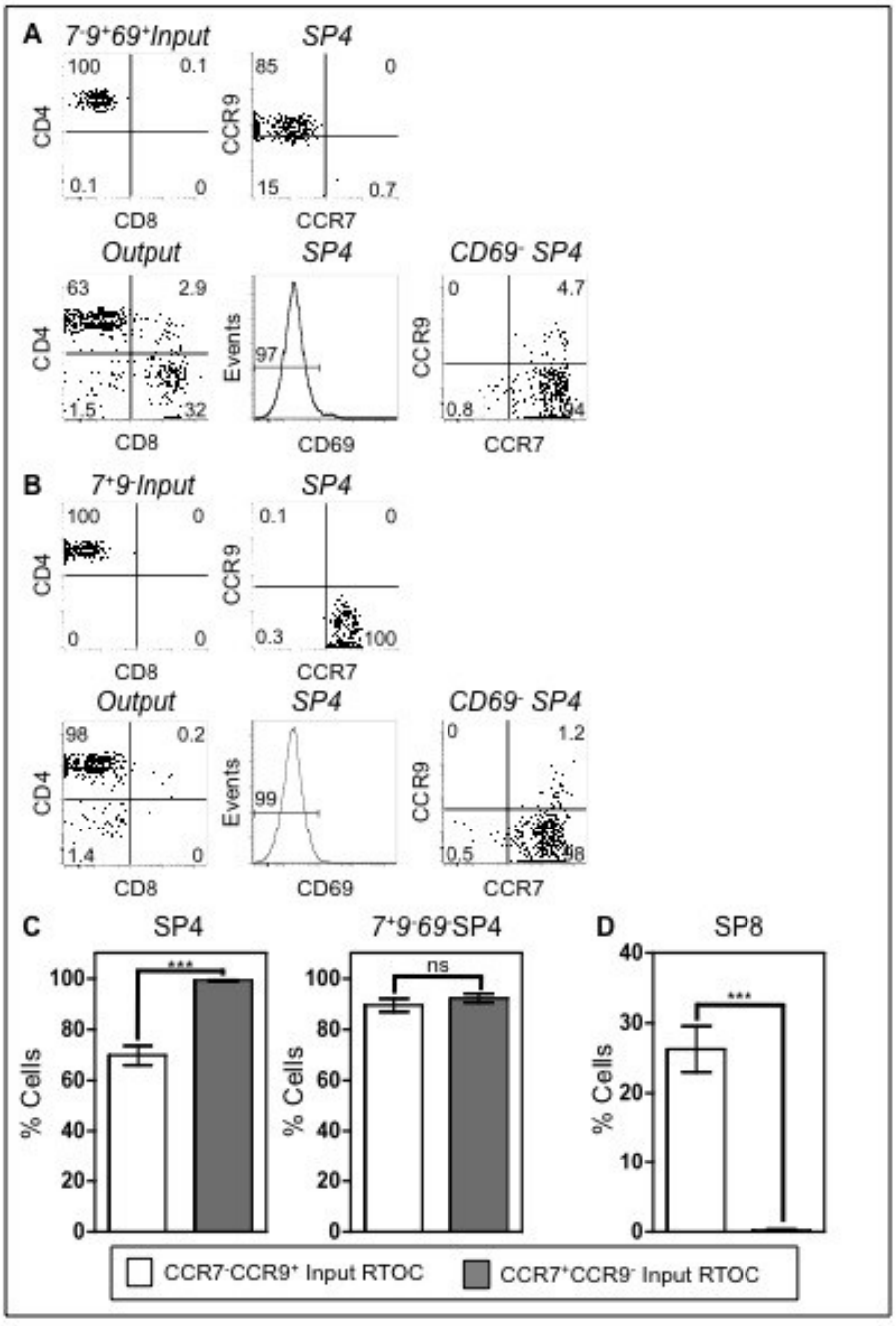
A
7-9+69+Input
SP4
100
0.1
0.1
0
CD4
CD8
85
0
15
0.7
CCR9
CCR7
Output
SP4
CD69- SP4
63
2.9
1.5
32
CD4
CD8
Events
97
CD69
0
4.7
0.8
94
CCR9
CCR7
B
7+9-Input
SP4
100
0
0
0
CD4
CD8
0.1
0
0.3
100
CCR9
CCR7
Output
SP4
CD69- SP4
98
0.2
1.4
0
CD4
CD8
Events
99
CD69
0
1.2
0.5
98
CCR9
CCR7
C
SP4
7+9-69-SP4
***
ns
% Cells
100
80
60
40
20
0
D
SP8
40
30
20
10
0
***
% Cells
CCR7-CCR9+ Input RTOC
CCR7+CCR9- Input RTOC

newly generated SP4 thymocytes after positive selection, give rise to $CCR7^{+}CCR9^{-}CD69^{+}$ thymocytes, which then give rise to the mature $CCR7^{+}CCR9^{-}CD69^{-}$ SP4 stage.

3.2.8 The Developmental Emergence Of $Foxp3^{+}$ T Regulatory CD4 SP Thymocytes

During their maturation, SP4 thymocytes can differentiate into non-conventional developmental pathways, including the $Foxp3^{+}$ natural T-regulatory cell (nTreg) lineage. The process of intrathymic nTreg induction is believed to occur in a series of sequential stages; the initial upregulation of CD25 on the cell surface, followed by intracellular expression of the transcription factor Foxp3. Therefore, the $Foxp3^{-}CD25^{+}$ SP4 population represents an nTreg precursor population to their $Foxp3^{+}CD25^{+}$ nTreg progeny (Lio and Hsieh, 2008). We aimed to explore at which stage in development nTreg SP4 thymocytes and their precursors emerge, in relation to the newly defined SP4 thymocyte subsets. We therefore examined the presence of $Foxp3^{+}CD25^{+}$ SP4 nTreg and $Foxp3^{-}CD25^{+}$ SP4 nTreg precursor populations within the $CCR7^{-}CCR9^{+}CD69^{+}$, $CCR7^{+}CCR9^{-}CD69^{+}$ and $CCR7^{+}CCR9^{-}CD69^{-}$ subsets of WT adult $TCR\beta^{high}$SP4 thymocytes, via flow cytometric analysis.

Data shown in Figure 3.9 A and B shows that the immature, newly generated $CCR7^{-}CCR9^{+}CD69^{+}$ SP4 population did not include any $Foxp3^{+}CD25^{+}$ nTreg and contained a barely detectable population of $Foxp3^{-}CD25^{+}$ SP4 nTreg precursors. In contrast, both populations were readily detectable at the intermediate $CCR7^{+}CCR9^{-}CD69^{+}$ stage in SP4 development, suggesting it is during this developmental window when SP4 thymocytes initiate differentiation down this non-conventional T cell lineage. The most mature $CCR7^{+}CCR9^{-}CD69^{-}$ SP4 cohort included the largest proportion of nTreg, but no nTreg

Figure 3. 9 The Developmental Emergence Of Foxp3$^+$ T Regulatory CD4 SP Thymocytes

Thymocytes were isolated from Foxp3-GFP 'knockin' adults.

(A) The surface expression of CD25 and intracellular expression of Foxp3 was identified on three developmental subsets of TCRβ^{high} SP4 population; CCR7$^-$ CCR9$^+$CD69$^+$, CCR7$^+$CCR9$^-$CD69$^+$ and CCD7$^+$CCR9$^-$CD69$^-$.

(B) The frequency of CD25$^+$Foxp3$^-$ and CD25$^+$Foxp3$^+$ cells from each SP4 subset are displayed as mean bar graph, representative of three individual experimental repeats. Stand error bars display the SEM.

(C) Quantitative real time PCR of *Foxp3* mRNA expression was performed on indicated cell populations, isolated from BALB/c WT adults:

CD4$^+$CD8$^+$ DP (white bars)

CCR7$^-$CCR9$^+$CD69$^+$TCRβ^{high} SP4 (right horizontal striped bars)

CCR7$^+$CCR9$^-$CD69$^+$TCRβ^{high} SP4 (grey bars)

CCR7$^+$CCR9$^-$CD69$^-$TCRβ^{high} SP4 (left horizontal striped bars)

Error bars indicate the SEM and mRNA levels were normalized to house keeping gene β-actin. Data is from two independently sorted biological samples, with each gene analyzed two times.

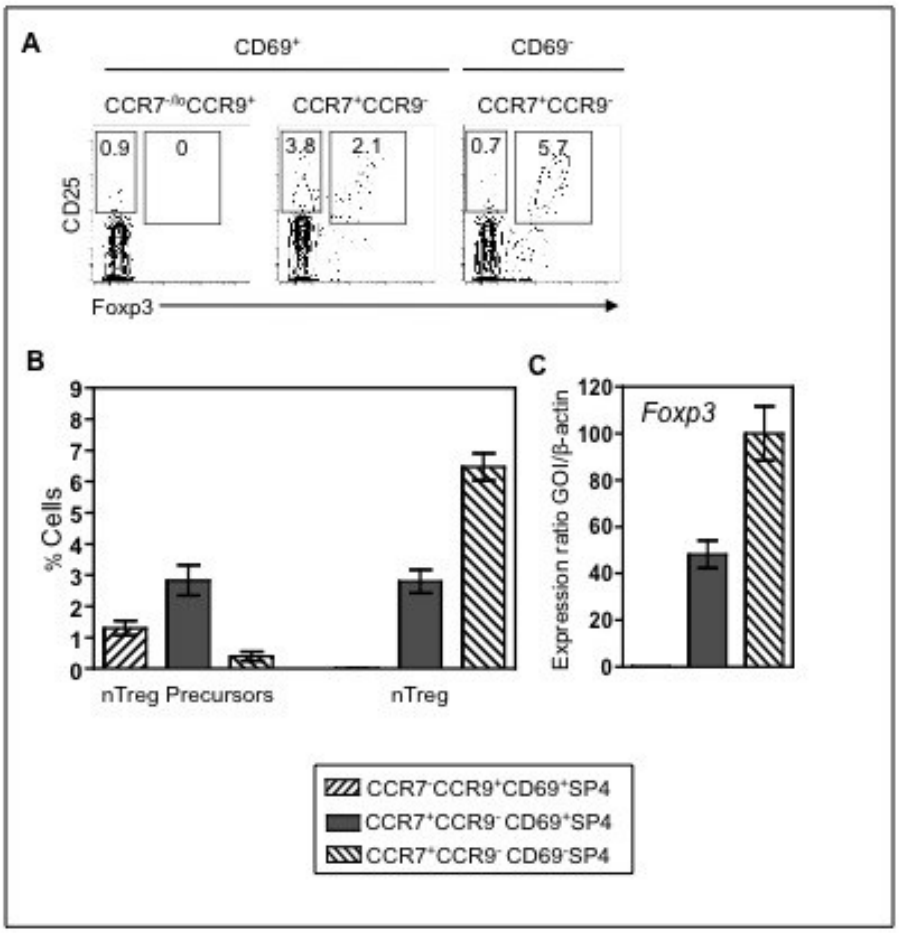
A
CD69+
CD69-
CCR7-/loCCR9+
CCR7+CCR9-
CCR7+CCR9-
0.9
0
3.8
2.1
0.7
5.7
CD25
Foxp3
B
% Cells
nTreg Precursors
nTreg
C
Foxp3
Expression ratio GOI/β-actin
CCR7-CCR9+CD69+SP4
CCR7+CCR9-CD69+SP4
CCR7+CCR9-CD69-SP4

precursors were detectable. Consistent with the data obtained by flow cytometry analysis, the most immature $CCR7^{-}CCR9^{+}CD69^{+}$ SP4 population did not display detectable levels of *Foxp3* mRNA (Figure 3.9 C), while it was readily detectable in both $CCR7^{+}CCR9^{-}CD69^{+}$ and $CCR7^{+}CCR9^{-}CD69^{-}$ SP4 subsets. Collectively these results indicate that $Foxp3^{+}$ nTreg development is evident at the $CD69^{+}$ stage in SP4 development, after CCR7 induction and loss of CCR9 expression, with the appearance of both nTreg and nTreg precursors populations first occurring during this maturational period.

3.3 DISCUSSION

Positive selection is an essential checkpoint in intrathymic T cell development where DP thymocytes are induced to differentiate into mature SP thymocytes, committing to a CD4 or CD8 T cell fate. This multistep developmental process includes the relocalization of positively selected thymocytes from the cortex into the thymic medulla, a process thought to be essential for the establishment of central tolerance (Kurobe et al., 2006). Chemokines and their receptors have been implicated in cortex to medulla migration of positively selected thymocytes, as inhibition of the receptors results in the complete halt in SP migration into medullary regions (Ehrlich et al., 2009; Suzuki et al., 1999). CCR7 specifically has been identified as a major regulator in this relocalization process (Kwan and Killeen, 2004; Ueno et al., 2004), although it's essential involvement in this migratory pathway is under some dispute (Davalos-Misslitz et al., 2007). Post-positive selection, SP thymocytes continue on with their development program, undergoing several phenotypical changes, classified by alterations to the surface expression profiles of several age defining markers, many of which have unknown functions, before their exit into the periphery as naive T cells (Jin et al., 2008). The studies within this chapter aimed to explore the chemokine receptor profile of thymocytes throughout the multiple stages of the positive selection process. We hoped this would offer greater insight into the receptors that may be driving this essential relocalisation step, whilst trying to use these functional molecules as phenotypical markers in the identification of different stages of SP development.

3.3.1 Classification Of Distinct SP Populations Based On Their Chemokine Receptor Expression Profiles

The surface receptor expression patterns of CCR9, CCR7, CCR4 and CXCR4 were mapped throughout intrathymic T cell development, on pre-positive selection DP thymocytes, DP cells undergoing selection and post-selection CD4 and CD8 SP subsets. This analysis identified distinct stages of CD4 SP and CD8 SP thymocyte development, as well as nTreg, based upon their chemokine receptor expression profiles. A model for the developmental sequence of these newly classified SP populations is shown in Figure 3.10. This chemokine receptor classification system, therefore, enabled the substitution of commonly used age defining markers such as HSA and Qa2, with markers of known function within the intrathymic T cell development process.

Within the conventional SP4 population, examination of the relationships between different chemokine receptors revealed three distinct subsets: $CCR7^{-}CCR9^{+}CD69^{+}TCR\beta^{high}SP4$, $CCR7^{+}CCR9^{-}CD69^{+}TCR\beta^{high}SP4$ and $CCR7^{+}CCR9^{-}CD69^{-}TCR\beta^{high}SP4$. The proposed developmental sequence of the three individual cohorts was established via comparison of their expression levels of HSA, Qa2, CD62L and RAG-2 GFP. This model suggests the most immature, newly generated SP4 thymocytes that have recently undergone selection display a $CCR7^{-}CCR9^{+}CD69^{+}$ phenotype. With increased maturity cells downregulate CCR9 and upregulate CCR7 to reach an intermediate $CCR7^{+}CCR9^{-}CD69^{+}$ stage, before down regulating CD69 and undergoing the transition into the most mature SP4 population, exhibiting a surface phenotype of $CCR7^{+}CCR9^{-}CD69^{-}TCR\beta^{high}SP4$. The maturational sequence of the three individual SP4 subsets was confirmed via the use of RTOC systems. Interestingly, this

Figure 3. 10 A Model Of The Developmental Sequence Of Conventional And Foxp3$^+$ nTreg SP Thymocytes

DP thymocytes pre-positive selection express high levels of CCR9 on their cell surface. On the initiation of selection, DP thymocytes rapidly upregulate CD69 whilst CCR7 and CCR4 expression is induced within a fraction of cells at this developmental stage.

Newly generated SP4 thymocytes express high levels of CD69, CCR9 and CCR4 but express only low CCR7 surface expression. At this phase of maturation SP4 thymocytes maintain the ability to differentiate into the SP8 lineage. Those cells that commit to a SP4 lineage down regulate both CCR9 and CCR4 and upregulate CCR7, before the downregulation CD69 to reach their most mature intrathymic phenotype of CCR7$^+$CCR9$^-$CCR4$^-$CD69$^-$TCRβ^{high}.

At the intermediate CCR7$^+$CCR9$^-$CCR4$^-$CD69$^+$ stage of SP4 differentiation T-regulatory precursors emerge, displaying a surface expression profile of CD25$^+$Foxp3$^-$ CCR7$^+$CD69$^+$. These cells continue with their maturation to become CD25$^+$Foxp3$^+$CCR7$^+$CD69$^+$ before the down regulation of CD69 to reach their most mature nTreg phenotype of CD25$^+$Foxp3$^+$CCR7$^+$CD69$^-$.

Those SP4 thymocytes still capable of differentiating into SP8 thymocytes have an immature phenotype expressing low levels of CCR7. With increasing maturity SP8 increase their surface expression of CCR7 before downregulating CD69 to become mature SP8 thymocytes expressing high levels of both CCR9 and CCR7.

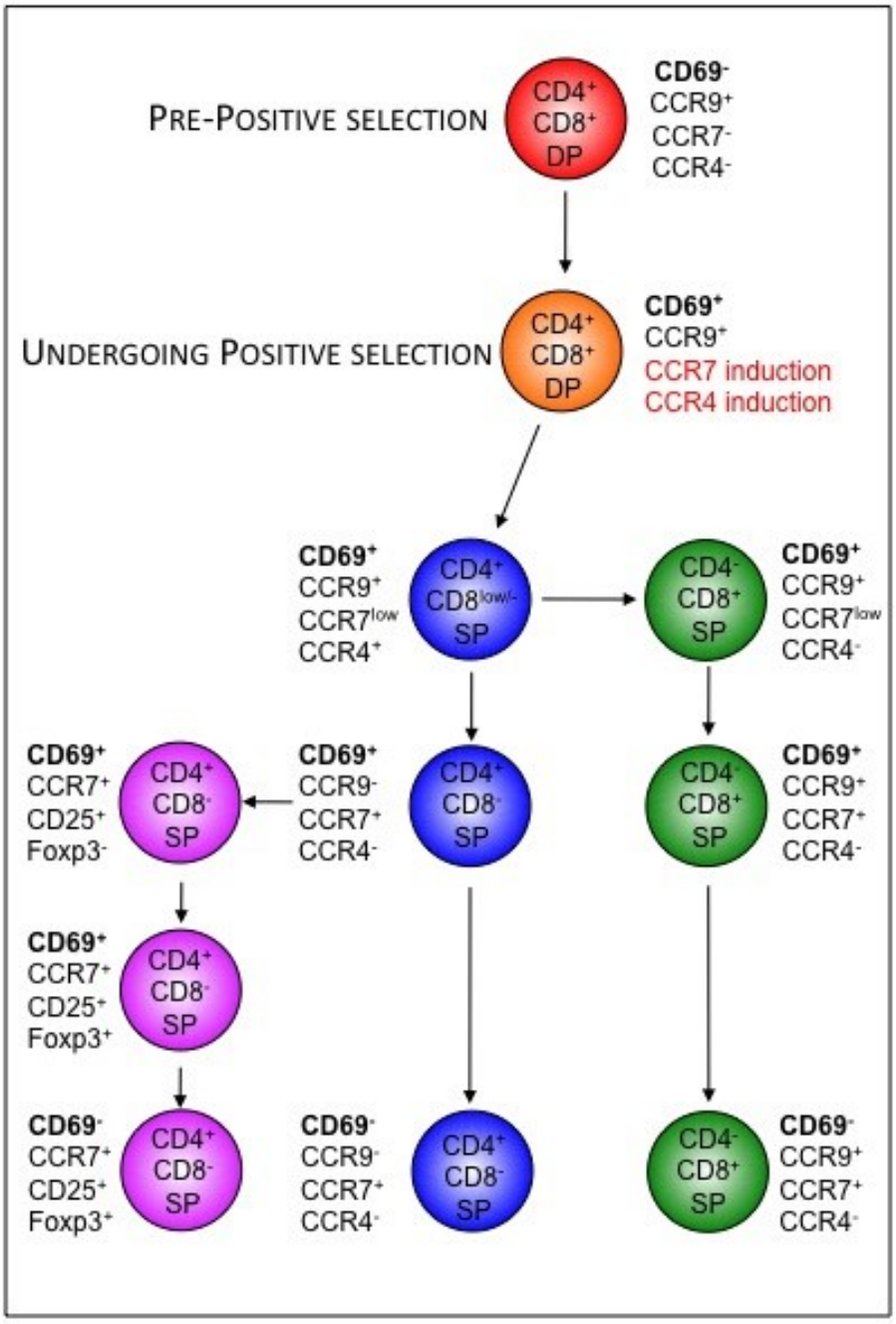
PRE-POSITIVE SELECTION
CD4+ CD8+ DP
CD69-
CCR9+
CCR7-
CCR4-
UNDERGOING POSITIVE SELECTION
CD4+ CD8+ DP
CD69+
CCR9+
CCR7 induction
CCR4 induction
CD69+
CCR9+
CCR7low
CCR4+
CD4+ CD8low/- SP
CD4- CD8+ SP
CD69+
CCR9+
CCR7low
CCR4-
CD69+
CCR7+
CD25+
Foxp3-
CD4+ CD8- SP
CD69+
CCR9-
CCR7+
CCR4-
CD4+ CD8- SP
CD4- CD8+ SP
CD69+
CCR9+
CCR7+
CCR4-
CD69+
CCR7+
CD25+
Foxp3+
CD4+ CD8- SP
CD69-
CCR7+
CD25+
Foxp3+
CD4+ CD8- SP
CD69-
CCR9-
CCR7+
CCR4-
CD4+ CD8- SP
CD4- CD8+ SP
CD69-
CCR9+
CCR7+
CCR4-

in vitro system also revealed the ability of the most immature $CCR7^{-}CCR9^{+}CD69^{+}$SP4 to differentiate into both CD4 and CD8 SP lineages, a characteristic not shared by the more mature $CCR7^{+}CCR9^{-}$SP4 population. Thus, at the most immature SP4 stages in development, newly selected SP thymocytes have yet to commit to a specific SP lineage, which is fitting with lineage commitment models that suggest regardless of MHC class restriction, most thymocytes will initially downregulate CD8 to achieve a $CD4^{+}CD8^{low}$ transitional phenotype, before maturing into either a $CD4^{+}CD8^{-}$ or $CD4^{-}CD8^{+}$ SP thymocytes (He et al., 2010). Differences in the gene expression patterns of the three distinct SP4 populations offered additional confirmation to the phenotypical distinctions of the subsets. Considerable differences were detected between the mRNA expression levels of *Rankl* and *Cd40lg*, where both genes were highly expressed within the intermediate $CCR7^{+}CCR9^{-}CD69^{+}$SP4 population, but showed differences within the additional two populations. *Rankl* mRNA was highly expressed in the immature $CCR7^{-}CCR9^{+}CD69^{+}$ SP4 population, whilst demonstrating low expression in the mature $CCR7^{+}CCR9^{-}CD69^{-}$SP4 subset, in contrast to *Cd40lg* that displayed the opposite expression pattern. This mRNA expression pattern matched the surface expression difference of these ligands that had previously been detected by flow cytomotery (Desanti et al., 2012).

With regard to the SP4 nTreg lineage, we identified the initial detection of both $Foxp3^{-}CD25^{+}$ nTreg precursors and their $Foxp3^{+}CD25^{+}$ nTreg progeny within the intermediate $CCR7^{+}CCR9^{-}CD69^{+}$SP4 population. The most mature $CCR7^{+}CCR9^{-}CD69^{-}$SP4 subset, however, displayed a large number of nTreg, but no nTreg precursors were detectable at this late developmental stage. This was confirmed via intracellular staining of Foxp3 via flow cytometry analysis and *Foxp3* mRNA levels within the different populations. Collectively,

this data suggest that branching point for nTreg differentiation from selected conventional SP4 thymocytes occurs at an intermediate stage in maturity, when cells have downregulated CCR9, but are expressing high levels of CCR7 and have fully committed to a CD4 SP lineage.

The analysis of CCR7 and CCR9 expression patterns of the SP8 population also suggested heterogeneity within this thymocyte lineage. Although SP8 subsets were not as distinct as those identified in the SP4 lineage, a 'tail' for CCR7 expression could be detected with in the immature $CD69^+$ SP8 fraction. The maturational status of the three identified $CCR9^+CCR7^{low}CD69^+$, $CCR9^+CCR7^+CD69^+$ and $CCR9^+CCR7^+$CD69- SP8 populations was explored via flow cytometry analysis of HSA, Qa2, CD62L and RAG-2 GFP. The results suggested newly generated SP8 thymocytes express only low levels of CCR7 on their cell surface, which they upregulated during their early maturation, resulting in a $CCR9^+CCR7^+$ profile, which they maintain throughout their remaining intrathymic differentiation program. The use of RAG-2 GFP transgenic mice has been an extremely beneficial tool in the identification of the maturational status of SP thymocytes. Interestingly, while identifying SP thymocyte subsets expressing progressively lower levels of RAG-2 GFP, analysis also indentified a subset of SP4 cells, particularly within the $CD69^-CCR7^+CCR9^-$ subset, that entirely lacked RAG-2 GFP expression. At this stage it is not clear whether these cells represent peripheral T cells that have recirculated back to the thymus, or SP thymocytes that have persisted intrathymically and hence lost detectable RAG-2 GFP expression levels (McCaughtry et al., 2007).

3.3.2 The Role Of Chemokine Receptors In Positive Selection And Cortex To Medulla Migration

The examination of chemokine receptors changes during multiple stages of intrathymic T cell development raises the possibility that cortex-to-medulla migration involves multiple chemokine/chemokine receptors. The comparison of chemokine receptor expression patterns pre-positive selection and cells undergoing the selection process revealed the initiation of the selection stimulates CCR4 and CCR7 induction, whilst initiating CXCR4 downregulation. CCR4 induction occurs within just under half the thymocyte population undergoing this selection process, whilst upregulation of CCR7 is estimated to be limited to only 20% of this subset. Complimentary to the flow cytometry data, *Ccr7* mRNA levels within the DP population are at almost undetectable rates and considerably reduced in comparison to the C*cr4* mRNA levels within the same population. As CCR7 is the main chemokine thought to mediate the relocation of thymocytes into the thymic medulla on the initiation of positive selection, it is surprisingly that only a small fraction of the cells undergoing the selection process express this chemokine receptor on their cell surface. This finding is consistent with previous data (Davalos-Misslitz et al., 2007) and questions the dominant role of CCR7 in mediating cortex to medulla migration, following the initiation of positive selection. The rapid down regulation of CXCR4 on initiation of selection and its total absence on the cell surface of both SP4 and SP8 throughout their developmental suggests this receptor could have a possible role in cortex retention, maintaining DP thymocytes positioning within cortical regions pre-selection. Interestingly, CXCR4 and its ligand CXCL12 have been identified to play a role in retention of immature DP human thymocytes within cortical regions, adding

additional support to our suggested role for this receptor within the mouse thymic microenvironment (Halkias et al., 2013).

The chemokine receptor profile of SP4 thymocytes offers additional doubt to the role of CCR7 in the migration of positively selected cells. The suggested sequence of development of SP4 thymocytes implies the most immature SP4 thymocytes, recently to have undergone positive selection, express CCR9 and CCR4, but importantly lack CCR7, which is not acquired until later stages in SP4 development. The gene expression profiles of known regulators of late stage intrathymic T cell development within these three distinct SP4 population further verified CCR7 upregulation is a later stage event of SP4 development. Both the intermediate $CCR7^{+}CCR9^{-}CD69^{+}$SP4 and the most mature $CCR7^{+}CCR9^{-}CD69^{-}$SP4 subsets display a mature developmental phenotype based upon their high levels of mRNA for *Foxo1* and *Klf2* expression, compared to very low mRNA levels within the immature $CCR7^{-}CCR9^{+}CD69^{+}$ SP4 fraction. Interestingly, the expression pattern of CCR7 on SP8 thymocytes differs to that of SP4 thymocytes. Although we predict the newly generated SP8 cells express lower levels of CCR7, the receptor is not totally absent on the cell surface and only a very small fraction of $CD69^{+}$ SP8 cells display this low level CCR7 phenotype. Thus, we would predict the increase in expression of CCR7 occurs at a very early SP8 maturational stage. We, therefore, cannot speculate CCR7 is not involved in cortex to medulla migration of SP8 thymocytes based on its surface expression pattern of cells committed to this lineage. Interestingly, CCR7 upregulation has been linked to CD8 lineage commitment. It has been reported that MHC Class I mediated positive selection leads to CCR7 upregulation on DP thymocytes and the enforced over expression of CCR7 has been demonstrated to increase CD8 SP development (Yin et al., 2007). Therefore it is a possibility the small fraction of

$CCR7^{+}CD69^{+}$DP are destined for a CD8 SP cell fate and migrate from the cortex to the medulla under the control of this receptor, down a gradient of CCR7 ligands. This would offer an explanation as to why deficiencies in CCR7 signaling results in more severe defects in SP8 medullary numbers in comparison to SP4 thymocytes (Davalos-Misslitz et al., 2007; Nitta et al., 2009).

Regardless of the role of CCR7 in directing SP8 migration, the low induction level of CCR7 on the initiation of positive selection and the absence of the receptor on newly generated SP4 thymocytes raises the possibility that other chemokine receptors are also involved in the cortex to medulla migration of MHC class II restricted cells. This offers an explanation to the phenotypical effects observed within CCR7 deficient hosts, with reduced, but not absent SP thymocytes within thymic medullary areas (Nitta et al., 2009; Ueno et al., 2004). The data also compliments previously published data that suggests no significant reductions are detectable in SP4 cell numbers as a consequence of CCR7 deficiency, but alternatively suggest this chemokine receptor is involved in negative selection of SP thymocytes (Davalos-Misslitz et al., 2007).

A very attractive alternative chemokine receptor to be involved in cortex to medulla migration of positively selected thymocytes, highlighted through our investigations, is CCR4. Although CCR4 is not upregulated on the surface of all $CD69^{+}$ DP thymocytes undergoing the selection process, the rapid induction of CCR4 on the initiation of positive selection within close to half the population and the detectable levels of *Ccr4* mRNA within the DP thymocytes population, would highlight this receptor as a strong candidate. CCR4 surface expression, post-positive selection, is restricted to thymocytes committed to a CD4 SP lineage, sustained on only immature CD4 SP and downregulated with increased maturity. Moreover, CCR4 ligands

including CCL17 demonstrate high gene expression patterns within both the mTEC populations (Griffith et al., 2009) and the thymic DC cell subsets (Lieberam and Forster, 1999). Currently, the intrathymic role of CCR4 is not well understood. It has been demonstrated that on initiation of positive selection $CD69^+$ DP thymocytes become responsive to CCL22, which is maintained with the most immature CD4 SP population ($CD69^+$ $CD62L^-$), but disappears, however, at the latest stages of CD4 SP development ($CD69^-$ $CD62L^+$) (Campbell et al., 1999). Complementary to this data, *Ccr4* mRNA levels have also been identified to be upregulated with $CD69^+$DP and immature $CD69^+$ CD4 SP thymocytes subsets (Campbell et al., 1999; Suzuki et al., 1999), strengthening the hypothesis CCR4 and its ligands are involved in the repositioning of positively selected thymocytes into medullary areas. While CCR4 deficient mice have been generated, analysis has specifically focused on the role of CCR4 in the context of peripheral Th2 CD4 T cells (Chvatchko et al., 2000). The consequence of the removal of CCR4 signaling on intrathymic T cell development remains to be confirmed. In view of this the major aim of Chapter 5 is to analysis the potential involvement of CCR4 in cortex to medulla migration of positively selected cells.

CHAPTER 4: THE THYMIC MEDULLA IS REQUIRED FOR FOXP3^{+} REGULATORY, BUT NOT CONVENTIONAL SP4 OR SP8 THYMOCYTE DEVELOPMENT.

4.1 INTRODUCTION

Within both primary and secondary lymphoid tissues, anatomical compartmentalization provides functionally distinct microenvironments that support the generation, selection and function of T cells expressing the ⟨®T cell receptor. In the thymus, the cortex supports the generation of immature $CD4^+8^+$ thymocytes expressing a diverse repertoire of αβTCR specificities. Interactions with cortical thymic epithelial cells (cTEC) trigger the positive selection of those thymocytes capable of recognizing self-peptide/MHC at low avidity/affinity (Laufer et al., 1996), a process characterized by upregulation of the αβTCR and CD69 (Hare et al., 1999; Yamashita et al., 1993). Importantly, positive selection also induces changes in thymocyte chemokine receptor expression, which enables the accumulation of newly selected $CD4^+8^-$ and $CD4^-8^+$ ⟨®TCR^{high} cells in the thymic medulla (Campbell et al., 1999). Tolerance induction occurs within thymic medullary regions, a process involving both DC and mTEC, including the subset defined by Aire expression. While negative selection of potentially autoreactive thymocytes occurring through the induction of programmed cell death represents a key function of the thymus medulla (Xing and Hogquist, 2012), this site has also long been thought to be important in supporting further maturation of SP4 and SP8 thymocytes following initial positive selection in the cortex. Indeed, many studies have highlighted how maturation markers such as Qa2, HSA, CD62L are acquired and lost during SP thymocyte maturation (Gabor et al., 1997a; Kelly and Scollay, 1990; Lucas et al., 1994), while our own data in Chapter 3 has shown how changes in chemokine receptor expression can be used to monitor the maturational state of SP thymocytes.

The length of time that SP thymocytes spend within the thymic medulla is not fully clear. Initial estimates suggested that medullary dwell time could be as long as 14 days (Scollay and Godfrey, 1995), consistent with the notion that prolonged interactions with medullary stromal cells are important during SP thymocyte maturation. In agreement with this, the progression of SP4 cells through distinct intrathymic developmental stages defined by downregulation of CD24/CD69 and acquisition of CD62L/Qa2 is altered in the absence of normal development of the thymic medulla (Li et al., 2007). However, using RAG-2 GFP mice it has been suggested that following positive selection, SP4 and SP8 thymocyte medullary residency may be much shorter than previously thought, with cells having an average dwell of 4-5 days, which results in an ordered 'conveyor belt' style emigration process (McCaughtry et al., 2007).

In addition to conventional αβTCR^{high} SP4 thymocytes, medullary regions of the thymus contain SP4 thymocytes expressing the transcription factor Foxp3. These Foxp3^{+} natural regulatory T cells (nTreg) have important regulatory roles and aid in the control of unwanted T cell autoreactivity (Sakaguchi et al., 1995). However, the developmental requirements of this specific SP4 subset remain unclear, in particular the involvement of the thymic medulla. While some studies have suggested a specific role for mTEC in the intrathymic generation of Foxp3^{+} nTreg (Aschenbrenner et al., 2007; Hinterberger et al., 2010), other studies demonstrate a role for thymic dendritic cells (Proietto et al., 2008b; Spence and Green, 2008; Watanabe et al., 2005a; Wirnsberger et al., 2009). Recently, it has also been reported that nTreg development in the thymus is a multi-stage process (Lio and Hsieh, 2011; Wirnsberger et al., 2011) in which signaling mediated via TCR-MHC (Lio and Hsieh, 2008) and CD28-CD80/86 (Hinterberger et al., 2011; Lio et al., 2010; Vang et al., 2010) interactions results in

the generation of Foxp3$^-$CD25$^+$ nTreg precursors. This precursor population gives rise to Foxp3$^+$CD25$^+$ nTreg in a process that is independent of further TCR-mediated interactions, but instead requires continued IL-2, IL-7 or IL-15 cytokine signaling (Burchill et al., 2008; Lio and Hsieh, 2008). However, the potential for mTEC involvement during the generation of Foxp3$^-$CD25$^+$ nTreg precursors is unestablished.

Given the heterogeneity within SP4 and SP8 thymocytes post-positive selection, the finding that SP thymocytes spend upwards of 4 days within the thymic medulla and the known links between nTreg and mTEC, the main aim of this chapter is to map the requirements for medullary thymic epithelial cell microenvironments during the continued development of both conventional and nTreg SP4 cells following positive selection. To study this, we exploited the well-known and severe mTEC defect that occurs in *Relb*$^{-/-}$ mice and combined this with thymus transplantation into WT adult mice, to study the consequences of mTEC deficiency in the presence of an otherwise intact immune system.

4.2 RESULTS

4.2.1 An *in vivo* Model To Study T Cell Development In The Selective Absence Of mTEC

Recent studies have suggested a correlation between defective thymic medullary compartments and the generation of the most mature $CD69^{-}Qa2^{+}$ SP4 thymocyte subset (Li et al., 2007). This relationship has been explored within $Relb^{-/-}$ mice, which present with an absence of medullary areas, caused by a severe blockade in development of their mTEC compartment (Burkly et al., 1995; Weih et al., 1995) and interestingly a lack of late stage SP4 thymocytes (Li et al., 2007)(also confirmed in Figure 4.3A). This multistep SP4 developmental program was reportedly critically dependent not only on mTEC, but also expression of Aire, as $Aire^{-/-}$ mice were found to have the same severe block in the transition from immature $CD69^{+}Qa2^{-}$ to mature $CD69^{-}Qa2^{+}$ SP4 thymocytes (Li et al., 2007). The effects of RelB deficiency, however, are not exclusive to mTEC development and $Relb^{-/-}$ mice present with dramatic multi-organ autoimmunity as a consequence of numerous severe defects, including reduced frequencies of thymic DC and failed lymph nodes organogenesis (Burkly et al., 1995; Weih et al., 1995; Wu et al., 1998). Therefore, although the absence of the mature SP4 subset within the adult $Relb^{-/-}$ mouse suggests that the completion of SP4 thymocyte development requires signals from mature mTEC, detailed analysis of the possible role of mTEC during SP thymocyte development in $Relb^{-/-}$ mice is confounded by the complex phenotype of these mice.

In order to isolate and define the potential role of mTEC in the maturation of SP4 thymocytes, we transplanted alymphoid 2-dGuo treated FTOC from either E15 $Relb^{-/-}$ or WT (litter mate

control) embryos, under the kidney capsule of background matched un-manipulated C57BL/6 mice (Rossi et al., 2007b) (model illustrated in Figure 4.1). The confocal analysis of WT and *Relb*$^{-/-}$ TEC grafts (Figure 4.2 A) confirmed a severe defect within the mTEC compartment within the latter, with a total absence of ERTR5^{+} areas compared to their WT counterparts (Figure 4.2A). This data is consistent with a cell autonomous role for RelB in mTEC development and its role in the alternative NF-kB signaling pathway activated by the TNFRSF members RANK, CD40 and LTβR, all of which are linked to mTEC development (Mouri et al., 2011). Importantly, as described previously (Zhang et al., 2007), the transplantation of *Relb*$^{-/-}$ 2dGuo thymic grafts into T-lymphopaenic nude hosts presented with symptoms of autoimmunity (Figure 4.2). Interestingly, in marked contrast, *Relb*$^{-/-}$ TEC transplantation into a WT host did not induce detectable autoimmunity, with host mice displaying no signs of disease in accordance to home office regulations, including no recorded weight lost (Figure 4.2 B), up to 12 weeks post surgery. Moreover, nude hosts receiving *Relb*$^{-/-}$ 2dGuo grafts had to be culled due to sickness 5 to 8 weeks post transplantation. Nude hosts presented with significant weight loss (Figure 4.2 B), detectable autoantibodies within blood serum samples and tissue infiltrates within liver sections (Figure 4.2 C). Analysis of peripheral CD4 T cells also revealed an increased percentage of CD44^{+} CD62L^{-} effector memory cells recovered from nude host receiving *Relb*$^{-/-}$ TEC grafts compared to their WT counterparts and increased IFNγ production by these peripheral CD4 T cells (Figure 4.2 D). Collectively Figure 4.2 demonstrates that *Relb*$^{-/-}$ TEC grafts display major disruption to the development of medullary epithelial cell compartment, which triggers a severe autoimmunity

Figure 4. 1 A Schematic View Of The Model Used To Explore The Impact Of mTEC Deficiency In The Absence Of Autoimmunity

(A) *Relb*$^{-/-}$ adult mice display an mTEC deficient thymic mircoenvironments. RelB deficiency also, however, results in additional severe phenotypical defects such as a reduced population of thymic dendritic cells, lack of lymph node formation and consequently multi-organ autoimmunity.

(B) We developed a model system where we grafted E15 2-dGuo treated *Relb*$^{-/-}$ FTOC under the kidney of a un-manipulated WT C57BL/6 host, 6 to 8 weeks in age. We sacrificed the host and harvested the grafts 6-12 weeks post transplantation and explored T cell development within the RelB-dependent mTEC deficient thymic microenvironment, via flow cytometry analysis or confocal microscopy.

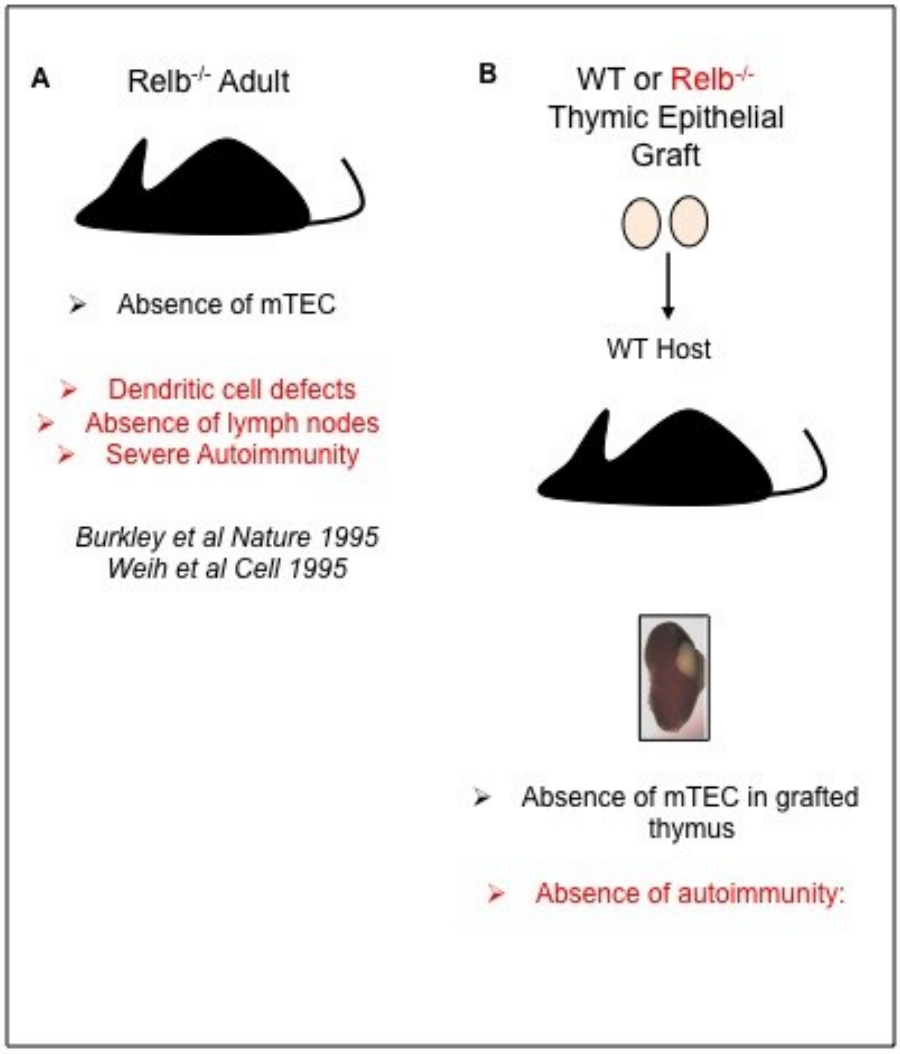
A
Relb-/- Adult
Absence of mTEC
Dendritic cell defects
Absence of lymph nodes
Severe Autoimmunity
Burkley et al Nature 1995
Weih et al Cell 1995
B
WT or Relb-/-
Thymic Epithelial
Graft
WT Host
Absence of mTEC in grafted
thymus
Absence of autoimmunity:

Figure 4. 2 The Grafting Of A RelB Dependent mTEC Deficient Thymic Microenvironment Into An Athymic Host Induces Autoimmunity

E15 *Relb*$^{-/-}$ or WT (littermate controls) 2-dGuo treated FTOC were grafted under the kidney capsule of a WT C57BL/6 adult host (A and B) or a nude adult host (B, C and D) 6- 8 weeks in age. The grafts were then harvest 6-12 weeks post surgery for confocal and FACS analysis. (A) WT (left) and *Relb*$^{-/-}$ (right) grafts were frozen for immunoflorescence staining. 7μm sections were cut and stained for β5t and ERTR5. C denotes cortex, and M denotes medulla. The bars per condition (WT or *Relb*$^{-/-}$) on the left represent 200μm and on the right represent 100μm.

(B) Weight (g) per mouse of each host before grafting (white bars) and on day of sacrifice (gray bars) for WT or *Relb*$^{-/-}$ grafts into either WT hosts (left) or nude hosts (right). Data is displayed as mean bar graphs, where error bars represent the SEM.

Assessment of autoimmunity was performed in nude hosts receiving WT or *Relb*$^{-/-}$ grafts (C and D). (C top) The presence of autoantibodies in blood serum from nude mice (top) receiving WT (left) or *Relb*$^{-/-}$ (right) TEC grafts was analyzed on sections of composite tissue blocks containing stomach and liver, and detected with goat anti–mouse IgG FITC, and counterstained with DAPI. (C bottom) Lymphocytic infiltrates (black arrows) were detected by histological analysis of Haematoxylin & Eosin stained paraffin wax liver sections from the same mice. Bars represent 100μm. (D) Lymph node CD4 T cells were recovered from the nude host receiving WT (top) or *Relb*$^{-/-}$ TEC grafts (bottom) and antibody labeled for flow cytometric analysis. LN cells were gated on CD3^{+} CD4 T cells and analyzed for CD44 versus CD62L expression (left), along with intracellular IFNγ.

All data is typical of at least three experimental replicates.

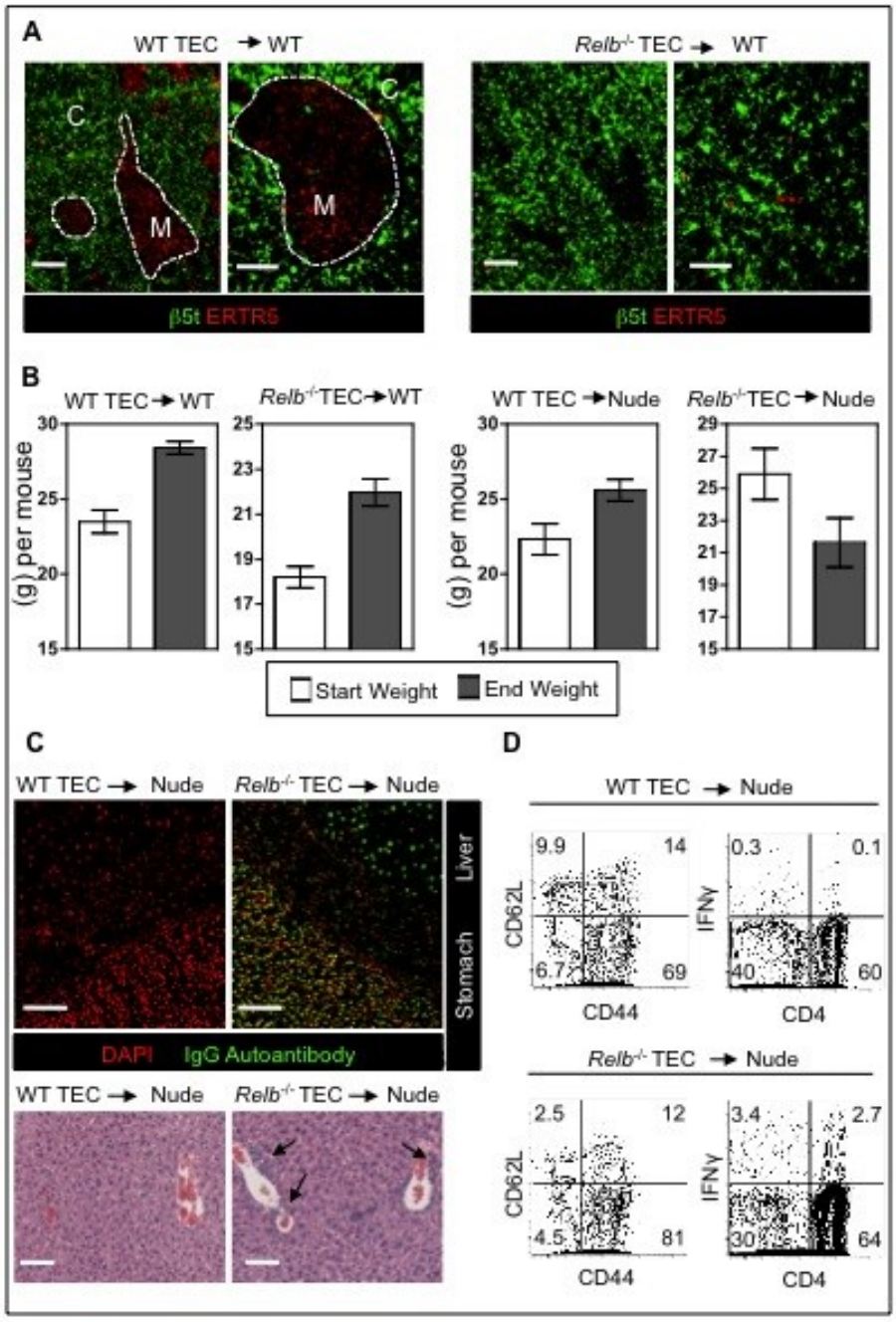
A
WT TEC → WT
Relb-/- TEC → WT
C
M
β5t ERTR5
B
WT TEC → WT
Relb-/- TEC → WT
WT TEC → Nude
Relb-/- TEC → Nude
(g) per mouse
Start Weight
End Weight
C
WT TEC → Nude
Relb-/- TEC → Nude
Liver
Stomach
DAPI IgG Autoantibody
D
WT TEC → Nude
Relb-/- TEC → Nude
CD62L
CD44
IFNγ
CD4
9.9
14
6.7
69
0.3
0.1
40
60
2.5
12
4.5
81
3.4
2.7
30
64

phenotype when grafted into a T-lymphopaenic nude hosts, but has no detected effects when placed under the kidney of a WT host. Therefore grafting un-manipulated WT host with grafts harboring this cell intrinsic RelB-dependent mTEC deficiency provides a model to investigate the role of mTEC during T cell development in the absence of other compounding factors, such as autoimmunity.

4.2.2 Conventional SP4 And SP8 Thymocytes Can Develop Independently Of Medullary Epithelial Cell Support

Analysis of conventional SP4 development within the *Relb*$^{-/-}$ TEC grafts within a WT host revealed the presence of both immature CD69^{+}Qa2^{-} and mature CD69^{-} Qa2^{+} TCRβ^{high} SP4 fractions, at similar proportions to those present within a WT grafts (Figure 4.3 B). The block in SP4 maturation at this development stage observed within the *Relb*$^{-/-}$ adult (Figure 4.3 A), therefore, has been restored within mTEC deficient thymus grafts. Both the percentages and absolute numbers of the thymocytes recovered from either WT TEC grafts or *Relb*$^{-/-}$ TEC grafts displayed comparable rates within the total SP4 population, immature CD69^{+} Qa2^{-} TCRβ^{high} SP4 fractions and mature CD69^{-} Qa2^{+} TCRβ^{high} SP4 subsets, with no significant alterations observed within any of these three populations (Figure 4.3 C). Therefore conventional SP4 thymocyte development can occur independently of mTEC interactions within a *Relb*$^{-/-}$ mTEC deficient microenvironment, in the absence of other compounding factors that may be present within a *Relb*$^{-/-}$ adult that could effect SP4 maturation.

The development of conventional SP8 thymocytes was also explored within the same *Relb*$^{-/-}$ or WT TEC grafts transferred into a WT host (Figure 4.4). *Relb*$^{-/-}$ adult mice displayed disrupted development of CD69^{-} Qa2^{+} TCRβ^{high} SP8 thymocytes, in comparison to the WT

Figure 4. 3 Grafting Of An mTEC Deficient Thymic Microenvironment Into A WT Host Restores Conventional SP4 T Cell Development

(A) Thymocytes from adult *Relb*$^{-/-}$ (bottom) or WT C57BL/6 (top), 5 weeks in age were isolated and stained for flow cytometry analysis. The Qa2 and CD69 expression was explored within the TCRβ^{high} SP4 fraction of cells and represented as contour FACS plots. (B) The same expression patterns for Qa2 and CD69 were explored within the TCRβ^{high} SP4 fraction of thymocytes recovered from WT (top panel) and *Relb*$^{-/-}$ (bottom panel) TEC grafts into WT hosts.

(C) The percentages (top) and absolute numbers (AN) (bottom) of three thymocyte subsets: total SP4 thymocytes, CD69^{+} Qa2^{-} TCRβ^{high} SP4 and CD69^{-} Qa2^{+} TCRβ^{high} SP4, were calculated and displayed as bar graphs. Each bar graph represents the mean percentage or AN of thymocyte subsets recovered from either WT TEC grafts (white bars) or *Relb*$^{-/-}$ TEC grafts (gray bars) into WT host from a minimum of 5 individual grafts per conditions. The standard error bars display the SEM, and a student's two tailed unpaired T test was performed on all results, where ns denoted a non-significant difference as $P > 0.05$.

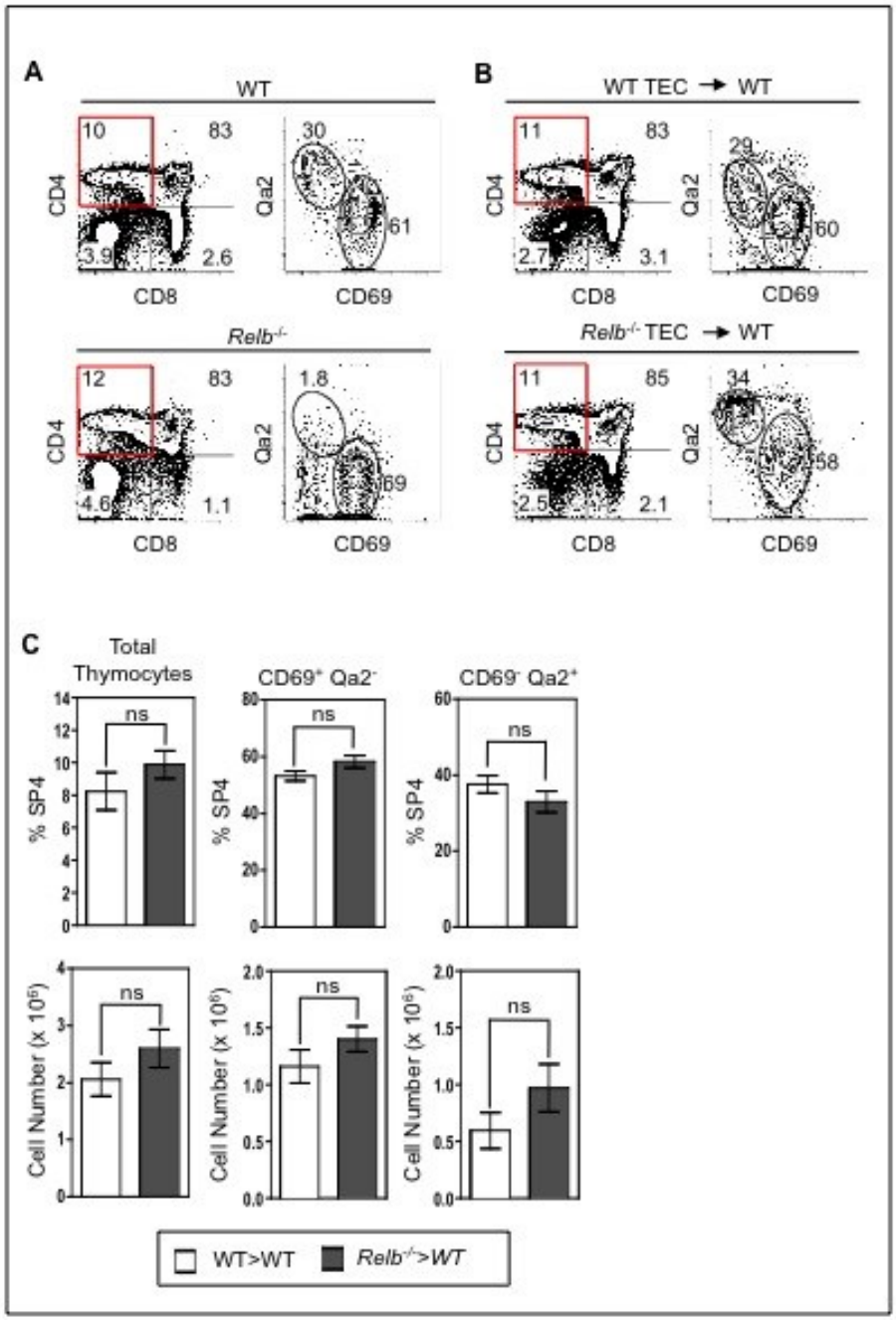
A
WT
10
83
3.9
2.6
CD4
CD8
30
61
Qa2
CD69
Relb-/-
12
83
4.6
1.1
1.8
69
B
WT TEC → WT
11
83
2.7
3.1
29
60
Relb-/- TEC → WT
11
85
2.5
2.1
34
68
C
Total Thymocytes
CD69+ Qa2-
CD69- Qa2+
% SP4
Cell Number (x 10^6)
ns
WT>WT
Relb-/->WT

controls. This mature SP8 population was not as severely disrupted as the conventional CD69^{-} Qa2^{+} TCRβ^{high} SP4 fraction of cells detected within this deficient adult thymic microenvironment (Figure 4.4 A). The disrupted development of mature CD69^{-} Qa2^{+} TCRβ^{high} SP8 thymocytes was restored, however, within the *Relb*$^{-/-}$ TEC graft transplanted into a WT host. The percentages of both the immature CD69^{+} Qa2^{-} TCRβ^{high} SP8 and mature CD69^{-} Qa2^{+} TCRβ^{high} SP8 were at equal levels within both the WT and *Relb*$^{-/-}$ grafts (Figure 4.4 B and C). Interestingly, however, both the percentages and absolute numbers of the total SP8 population was reduced within the *Relb*$^{-/-}$ grafts, in comparison to the SP8 population recovered from WT grafts. This significant reduction to total SP8 numbers consequently resulted in a significant reduction to the absolute numbers of both the immature CD69^{+} Qa2^{-} TCRβ^{high} SP8 and mature CD69^{-} Qa2^{+} TCRβ^{high} SP8 fractions, in comparison to WT control grafts, even though the percentages of these two cohorts were comparable between the two conditions (Figure 4.4C). Collectively, Figure 4.4 suggests that conventional SP8 thymocytes can progress to the mature CD69^{-} Qa2^{+} TCRβ^{high} stage of development within an mTEC deficient thymus microenvironment. However, these results also imply the maintenance, or perhaps efficacy of development, of thymocytes restricted to SP8 lineage is influenced by mTEC, as deficiency in RelB-dependent mTEC results in overall reductions to the numbers of MHC class I restricted thymocytes.

Importantly, we wanted to confirm those mature CD69^{-} Qa2^{+} SP4 and SP8 cells recovered from the *Relb*$^{-/-}$ grafts were intrathymically generated from within the grafted microenvironment and did not represent host peripheral CD4 or CD8 T cells circulating into the mTEC deficient thymic compartments. We therefore explored the surface expression patterns of CD44, Qa2 and HSA, as the reported phenotype of peripheral T cells homing back

Figure 4. 4 Grafting Of An mTEC Deficient Thymic Microenvironment Into An WT Host Restores Conventional SP8 T Cell Development

(A) Thymocytes from adult *Relb*$^{-/-}$ (bottom) or WT C57BL/6 (top), 5 weeks in age were isolated and stained for flow cytometry analysis. The Qa2 and CD69 expression was explored within the TCRβ^{high} SP8 fraction of cells and represented as contour FACS plots. (B) The same expression patterns for Qa2 and CD69 were explored within the TCRβ^{high} SP8 fraction of thymocytes recovered from WT (top) and *Relb*$^{-/-}$ (bottom) TEC grafts into WT hosts.

(C) The percentages (top) and AN (bottom) of three thymocyte subsets: total SP8 thymocytes, CD69^{+} Qa2^{-} TCRβ^{high} SP8 and CD69^{-} Qa2^{+} TCRβ^{high} SP8, were calculated and displayed as bar graphs. Each bar graph represents the mean percentage or AN of thymocyte subsets recovered from either WT TEC grafts (white bars) or *Relb*$^{-/-}$ TEC grafts (gray bars) into WT hosts, from a minimum of 5 individual grafts per condition. The standard error bars display the SEM, and an student's two tailed unpaired T test was performed on all results, where ns denoted a non-significant difference as $P > 0.05$ and * or ** indicate a significant difference (* = $P < 0.05$ and ** = $P < 0.01$).

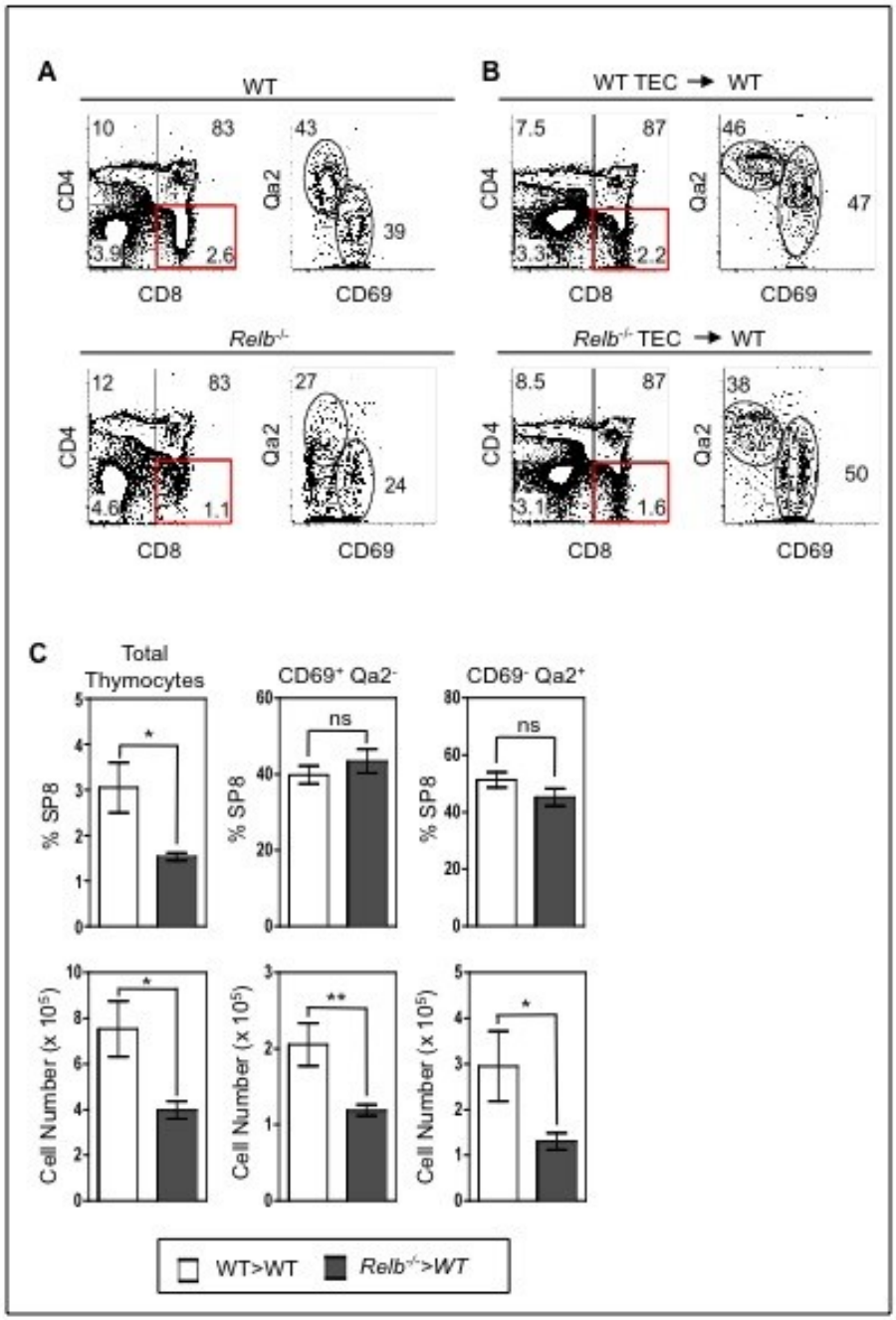
A
WT
10
83
3.9
2.6
CD4
CD8
43
39
Qa2
CD69
Relb-/-
12
83
4.6
1.1
27
24
B
WT TEC → WT
7.5
87
3.3
2.2
46
47
Relb-/- TEC → WT
8.5
87
3.1
1.6
38
50
C
Total Thymocytes
CD69+ Qa2-
CD69- Qa2+
% SP8
ns
*
**
Cell Number (x 10^5)
WT>WT
Relb-/->WT

to thymus has been shown to be HSA^{-} Qa2^{hi} CD44^{+} SP cells (Hale and Fink, 2009). In contrast to this recirculating T cell phenotype, the vast majority of both the TCRβ^{high} SP4 and SP8 subsets obtained from both WT and TEC *Relb*$^{-/-}$ grafts were CD44^{low} (Figure 4.5 A, B and 4.6 A, B). In fact, *Relb*$^{-/-}$ TEC grafts contained fewer Qa2^{hi} CD44^{+} and HSA^{-} CD44^{+} thymocytes, compared to WT grafts. This reduction was significant between both the percentage and absolute number of SP4 and SP8 resident populations of the *Relb*$^{-/-}$ grafts compared to WT controls (Figure 4.5 B and 4.6 B). Therefore this data would imply those mature CD69^{-} Qa2^{+} TCRβ^{high} SP4 and SP8 thymocytes detected within the RelB-dependent mTEC deficient grafts are intrathymically generated within the grafted thymic microenvironment and have not migrated in from the hosts periphery.

To obtain further support for this conclusion, we also grafted *Relb*$^{-/-}$ and WT 2-dGuo FTOC under the kidney capsule of RAG-2 GFP reporter mice and explored the GFP levels of SP4 and SP8 present within the grafted thymic microenvironment. Although it is yet to be confirmed if the RAG-2 GFP^{-} proportions of SP thymocytes detected within the thymus of these report mice represent recirculating peripheral T cells or thymocytes retained with the thymus for long periods (Hale and Fink, 2009; McCaughtry et al., 2007), we were interested to explored the GFP$^{-/low}$ populations of SP cells detected within the WT and *Relb*$^{-/-}$ TEC grafts. Most of the SP4 (Figure 4.5C) and SP8 (Figure 4.6C) thymocyte cohorts recovered from the *Relb*$^{-/-}$ TEC grafts were RAG-2 GFP^{+} and displayed close to equal levels of GFP expression in comparison to those SP thymocytes obtained from WT grafts, providing further evidence that these cells are intrathymically produced and not recirculating RAG-2 GFP^{-} peripheral T cells. Within the SP4 population, the fraction of GFP^{+} cells within the *Relb*$^{-/-}$ grafts were actually higher than those observed within WT grafts. The mean fluorescence intensities (MFI) of Qa2

Figure 4. 5 Mature CD69$^-$ Qa2$^+$ SP4 Thymocytes Present Within mTEC Deficient Grafts Are Not Recirculating Host Peripheral T Lymphocytes

(A) Thymocytes recovered from WT (top) and *Relb*$^{-/-}$ (bottom) TEC grafts into WT hosts were isolated and stained for flow cytometric analysis. CD44 expression against HSA (left) or Qa2 (right) was determined within the TCRβ^{high} SP4 fraction of cells and represented as contour FACS plots.

(B) The percentages and AN of both TCRβ^{high} SP4 populations: CD44$^+$ HSA$^-$ and Qa2$^+$ CD44$^+$ subsets, were calculated from WT TEC grafts (white bars) and *Relb*$^{-/-}$ TEC grafts (gray bars) into WT hosts and displayed as mean bar graphs, representing at least 5 separate grafts per condition. The standard error bars indicate the SEM, and a student's two tailed unpaired T test was performed on all results, where *** denoted a highly significant difference, as $P < 0.001$.

(C) The RAG-2 GFP levels of expression was analyzed within the TCRβ^{high} SP4 subset of thymocytes obtained from either WT TEC grafts (top) and *Relb*$^{-/-}$ TEC grafts (bottom), transplanted into RAG-2 GFP adult hosts. CD4 versus CD8 profiles are displayed as contour plots whilst RAG-2 GFP expression levels are represented as a histogram. The data is typical of two independent experiments repeats per condition.

(D) The mean fluorescence intensity (MFI) of Qa2 expression in CD69$^-$ TCRβ^{high} SP4 thymocyte population recovered from WT TEC grafts (white bars) or *Relb*$^{-/-}$ TEC grafts (grey bars) into WT hosts are presented along side WT CD4$^+$ splenocytes (striped bars). Data is displayed as mean bars graphs, representative of at least 5 individual grafts per condition. The standard error bars denote the SEM and a student's two tailed unpaired T test was performed on the results, where ns denoted a non-significant difference ($P > 0.05$) and *** denoted a highly significant difference ($P < 0.001$).

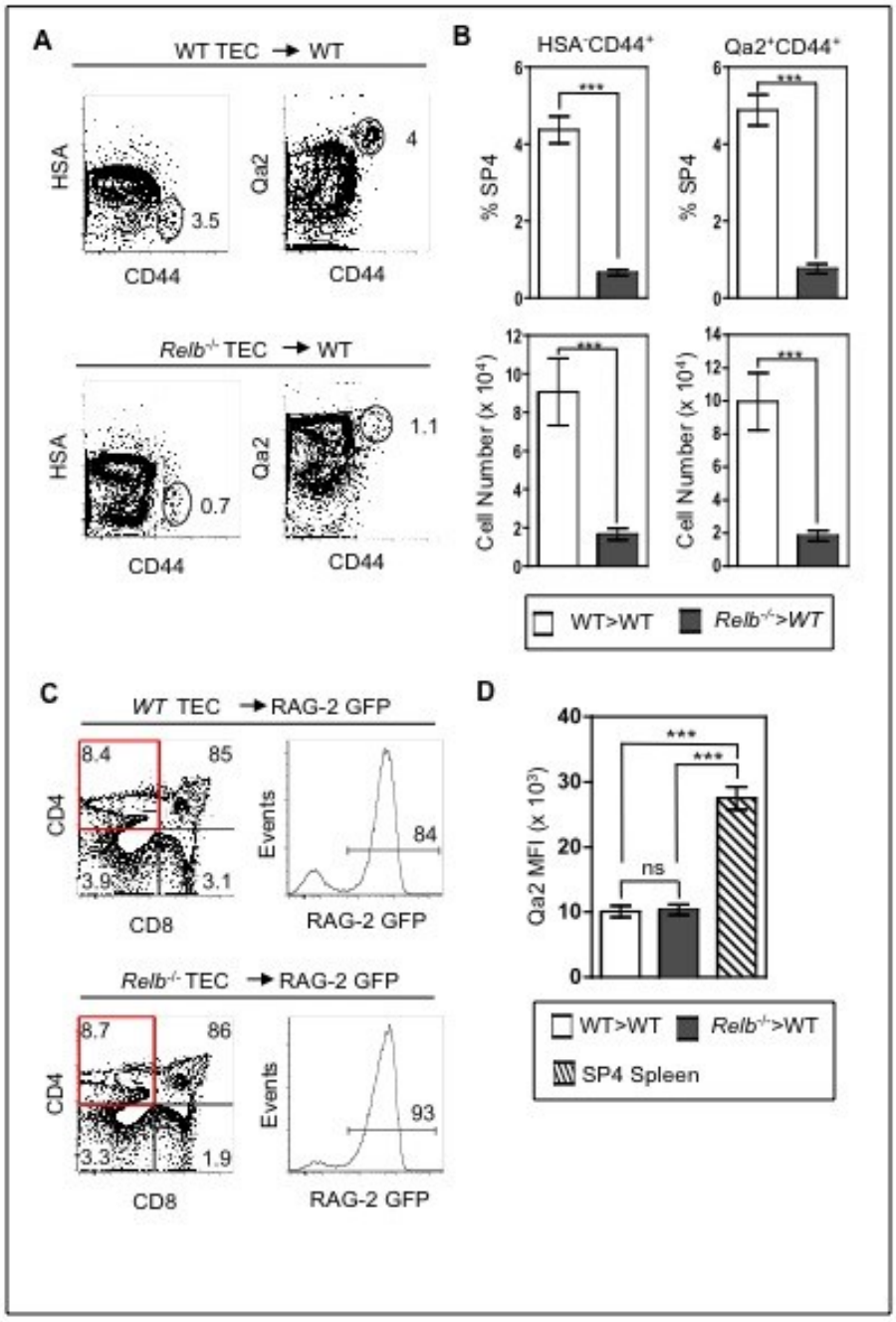
A
WT TEC → WT
HSA
3.5
CD44
Qa2
4
CD44
Relb-/- TEC → WT
HSA
0.7
CD44
Qa2
1.1
CD44
B
HSA-CD44+
Qa2+CD44+
% SP4
Cell Number (x 10⁴)
***
WT>WT
Relb-/->WT
C
WT TEC → RAG-2 GFP
CD4
8.4
85
3.9
3.1
CD8
Events
84
RAG-2 GFP
Relb-/- TEC → RAG-2 GFP
CD4
8.7
86
3.3
1.9
CD8
Events
93
RAG-2 GFP
D
Qa2 MFI (x 10³)
***
***
ns
WT>WT
Relb-/->WT
SP4 Spleen

Figure 4. 6 Mature CD69^{-} Qa2^{+} SP8 Thymocytes Present Within mTEC Deficient Grafts Are Not Recirculating Host Peripheral T Lymphocytes

(A) Thymocytes recovered from WT (top) and *Relb*$^{-/-}$ (bottom) TEC grafts into WT hosts were isolated and stained for flow cytometry analysis. CD44 expression against HSA (left) or Qa2 (right) was explored within the TCRβ^{high} SP8 fraction of cells and represented as contour FACS plots.

(B) The percentages and AN of both TCRβ^{high} SP8 populations: CD44^{+} HSA^{-} and Qa2^{+} CD44^{+} subsets, were calculated from WT TEC grafts (white bars) and *Relb*$^{-/-}$ TEC grafts (gray bars) into WT hosts and displayed as a mean bar graph, representing at least 5 individual grafts per condition. The standard error bars indicate the SEM, and a student's two tailed unpaired T test was performed on all results, where * or ** indicate a significant difference (* = $P < 0.05$ and ** = $P < 0.01$).

(C) GFP levels of expression was explored within the TCRβ^{high} SP8 subsets of thymocytes obtained from WT TEC grafts (top) and *Relb*$^{-/-}$ TEC grafts (bottom), transplanted into RAG-2 GFP adult hosts. CD4 versus CD8 profiles are displayed as contour plots whilst RAG-2 GFP expression levels are represented as a histogram. The data is typical of two independent experiments repeats per condition.

(D) The mean fluorescence intensity (MFI) of Qa2 expression within the CD69^{-} TCRβ^{high} SP8 thymocyte population recovered from WT TEC grafts (white bars) or *Relb*$^{-/-}$ TEC grafts (grey bars) into WT hosts are presented alongside WT CD8^{+} splenocytes (striped bars). Data is displayed as mean bars graphs, representative of at least 5 individual grafts per condition. The standard error bars denote the SEM and a student's two tailed unpaired T test was performed on the results, where ns denoted a non-significant difference ($P > 0.05$) and ** denotes a significant difference ($P < 0.01$).

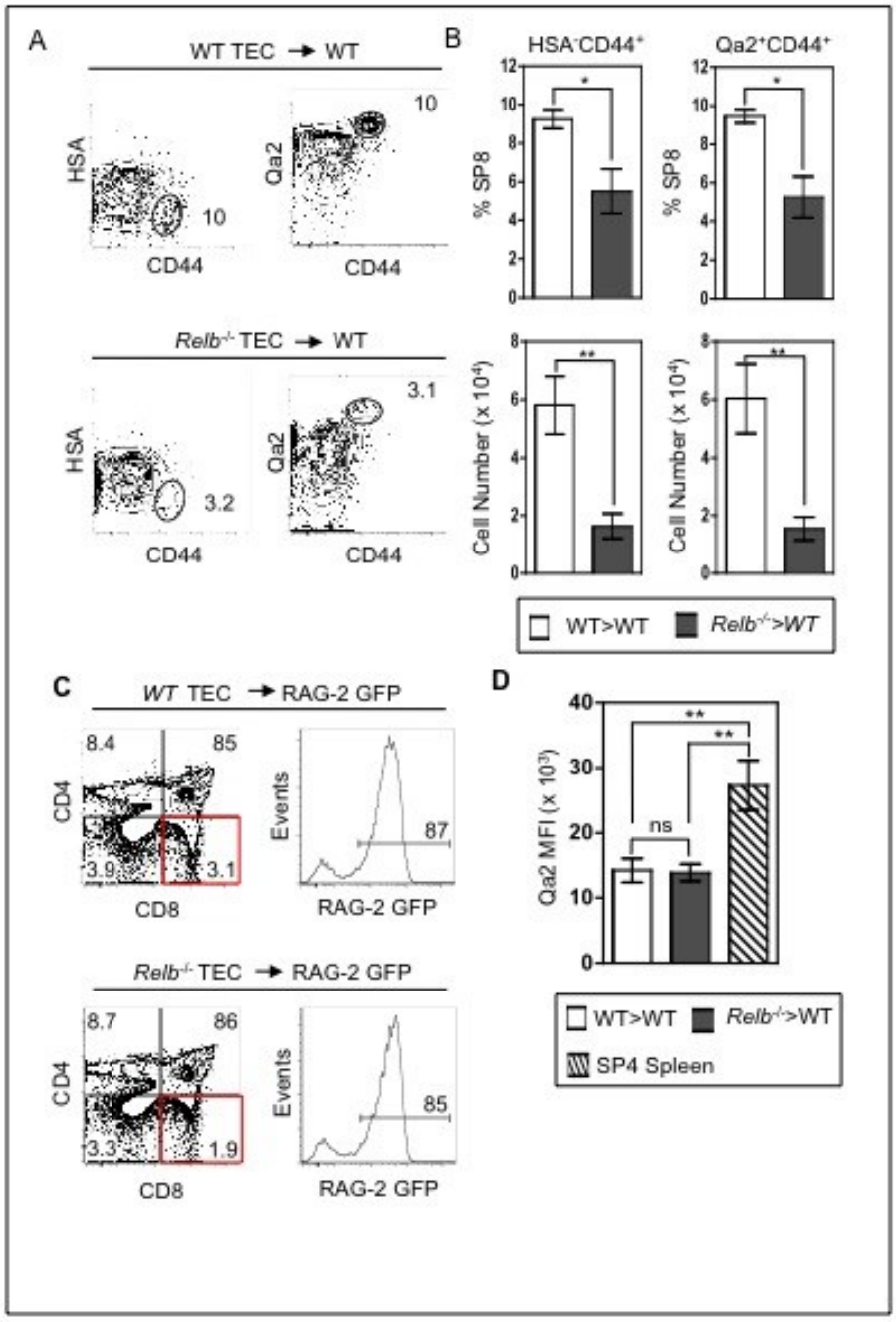
A
WT TEC → WT
HSA
CD44
10
Qa2
10
CD44
Relb-/- TEC → WT
HSA
3.2
CD44
Qa2
3.1
CD44
B
HSA-CD44+
Qa2+CD44+
% SP8
Cell Number (x 10-4)
WT>WT
Relb-/->WT
C
WT TEC → RAG-2 GFP
8.4
85
CD4
3.9
3.1
CD8
Events
87
RAG-2 GFP
Relb-/- TEC → RAG-2 GFP
8.7
86
CD4
3.3
1.9
CD8
Events
85
RAG-2 GFP
D
Qa2 MFI (x 10³)
ns
WT>WT
Relb-/->WT
SP4 Spleen

within the CD69^{-} fraction of TCRβ^{high} SP4 (Figure 4.5 D) and TCRβ^{high} SP8 subsets (Figure 4.6 D) obtained from WT and *Relb*$^{-/-}$ grafts were also investigated, as peripheral T cells demonstrate increased Qa2 levels in comparison to mature CD69^{-} Qa2^{+} TCRβ^{high} SP thymocytes (Boursalian et al., 2004). Consistent with the data described above, the CD69^{-} TCRβ^{high} SP4 and SP8 thymocytes recovered from the *Relb*$^{-/-}$ grafts displayed equal Qa2 MFI levels to the equivalent thymocyte population obtained from WT grafts, whilst mature CD69^{-} TCRβ^{high} SP4 and SP8 thymocytes from both WT and *Relb*$^{-/-}$ TEC grafts had significantly lower Qa2 MFI levels in comparison to peripheral CD4 and CD8 T cells.

Collectively, Figures 4.5 and 4.6 summaries three independent experimental approaches to demonstrate that the mature SP4 and SP8 populations detected within the RelB-dependent mTEC deficient microenvironment have been generated intrathymically within the grafted microenvironment and do not represent a cohort of recirculating T cells migrating in from the periphery of the host.

4.2.3 Conventional CD4 SP Thymocytes Can Develop Extrathymically, From The Time They First Emerge As Immature CCR9^{+}CCR7^{-}CD69^{+} Cells

To further explore the dependence of newly selected SP4 cells on medullary support for their continued maturation we investigated the ability of these cells to survive and mature extrathymically. Whilst recent thymic emigrants (RTE) have been shown to complete their maturation extrathymically (Boursalian et al., 2004) it is not known how far back in development this window of thymic independence extends, particularly in relation to the post-positive selection stages of SP differentiation. To investigate this, we explored the extrathymic development of the least mature CD4 SP thymocytes, based on the criteria

defined in Chapter 3, ie. cells of a $CCR7^{-}CCR9^{+}CD69^{+}$ immature $TCR\beta^{high}$ SP4 surface phenotype. Using the experimental approach described in Figure 4.7 A, $CCR9^{+}CCR7^{-}CD69^{+}$ SP4 thymocytes, which also express a $HSA^{high}CD62L^{low}Qa2^{-}CD69^{+}$ phenotype (Figure 4.8 B 'input population') were isolated from adult $CD45.2^{+}$ C57BL/6 mice and intravenously injected into congenic $CD45.1^{+}$ C57BL/6 hosts. Analysis of lymph node and splenic lymphocyte preparations from mice sacrificed 7 days later showed that injected donor $CD45.2^{+}$ cells had remained as SP4 cells within the host peripheral lymphoid tissue (Figure 4.8 A). Closer examination of the maturational status of this persisting SP4 thymocyte population recovered from the host LN and spleen revealed the input population had undergone extrathymic maturation (Figure 4.8 B). Thus, when compared to the surface phenotype of $CD45.1^{+}$ host peripheral CD4 T cells (black line), the donor $CD45.2^{+}$ populations (red line) had acquired a corresponding $HSA^{low}CD62L^{high}Qa2^{high}$ $CD69L^{low}$ phenotype. Thus, the data obtained confirms conventional CD4 SP development can occur independently of thymic support from the time these cells first emerge as $CCR9^{+}CCR7^{-}$ $CD69^{+}$ $TCR\beta^{high}$ SP4 thymocytes. Therefore, these results identify a window of thymic independence within the T cell developmental process, which extends as far back as the earliest stages of SP4 thymocyte development following positive selection.

Additionally, we were interested in providing a comparative analysis of extrathymic maturation of $CCR9^{+}CCR7^{-}CD69^{+}TCR\beta^{high}$ SP4 thymocytes in relation to other thymocyte subsets; either the less mature $CD4^{+}$ $CD8^{+}$ DP cell fraction or the more mature $CCR9^{-}$ $CCR7^{+}CD69^{-}TCR\beta high$ SP4 fraction. By using the experimental techniques described in Figure 4.7 B and C, immature $CCR9^{+}CCR7^{-}CD69^{+}TCR\beta^{high}$ SP4 cells were isolated from $CD45.1^{+}$ WT donors and co-injected into $CD45.1^{+}$ x $CD45.2^{+}$ WT hosts at a 1:1 ratio with

Figure 4. 7 Experimental Approaches To Explore Extrathymic Maturation Of Conventional SP4 Thymoyctes

(A) $CCR7^{-}CCR9^{+}CD69^{+}TCR\beta^{high}$ SP4 thymocytes were isolated via high speed cell sorting from a $CD45.2^{+}$ WT adult donor and intravenously (IV) transferred into a $CD45.1^{+}$ WT adult host. Purity checks were performed on isolated cell populations and are displayed as FACS contour plots (left), displaying the CD4 versus CD8 profile then the CD4 SP population for the expression of CCR9 versus CD69. 7 days post IV transfer, $CD45.1^{+}$ hosts were sacrificed and total LN or spleen analyzed separately by flow cytometry for the presence and maturation status of $CD45.2^{+}$ donor cells.

(B and C) An identical $CCR7^{-}CCR9^{+}CD69^{+}TCR\beta^{high}$ SP4 thymocyte subset was isolated via high speed cell sorting from a $CD45.1^{+}$ donor and mixed at a one to one ratio with either $CCR7^{+}CCR9^{-}CD69^{-}TCR\beta^{high}$ SP4 cells (B) or DP thymocytes (C) isolated from a WT adult $CD45.2^{+}$ donor. The cells were then co-injected IV into a $CD45.1^{+}$ x $CD45.2^{+}$ host. The sort purities of each input population per cell cocktail are displayed on the left of each box. 7 days post IV the $CD45.1^{+}$ x $CD45.2^{+}$ hosts were sacrificed and the total LN or spleen analyzed separately by flow cytometry for the presence of both $CD45.1^{+}CD45.2^{-}$ and the $CD45.2^{+}CD45.1^{-}$ donor cells.

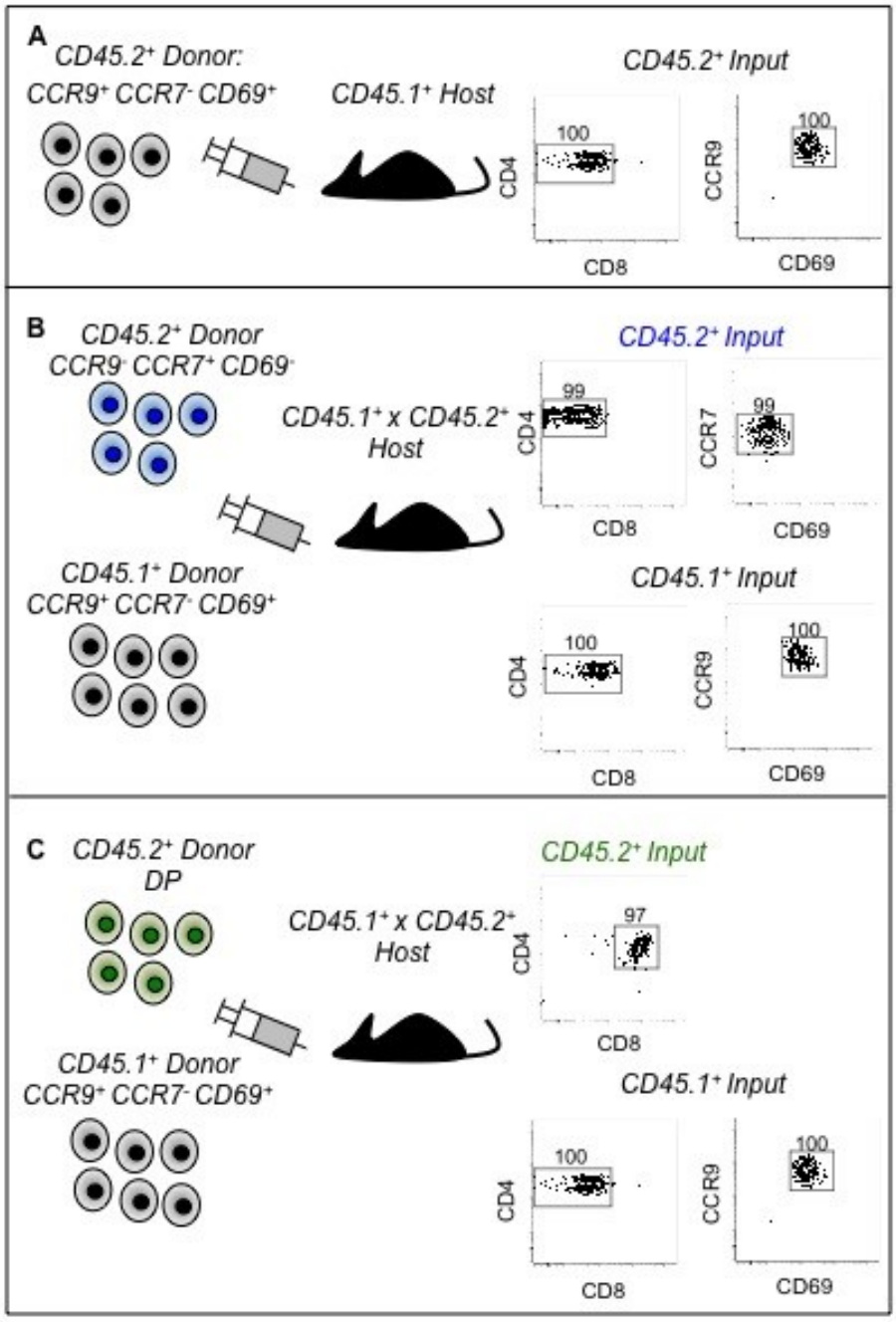
A
CD45.2+ Donor:
CCR9+ CCR7- CD69+
CD45.1+ Host
CD45.2+ Input
CD4
CD8
CCR9
CD69
100
B
CD45.2+ Donor
CCR9- CCR7+ CD69-
CD45.1+ x CD45.2+
Host
CD45.2+ Input
CD45.1+ Donor
CCR9+ CCR7- CD69+
CD45.1+ Input
CCR7
99
C
CD45.2+ Donor
DP
CD45.1+ x CD45.2+
Host
CD45.2+ Input
97
CD45.1+ Donor
CCR9+ CCR7- CD69+
CD45.1+ Input

Figure 4. 8 Extrathymic Maturation Of Conventional SP4 Thymocytes Within The Periphery Of A WT Host

Using the experimental approach described in Figure 4.8 A $CCR7^{-}$ $CCR9^{+}CD69^{+}TCR\beta^{high}$ SP4 thymocytes from a WT adult $CD45.2^{+}$ donor were IV transferred into a WT adult $CD45.1^{+}$ host. 7 days post IV $CD45.1^{+}$ hosts were sacrificed and total LN analyzed by flow cytometry for the presence and maturational status of $CD45.2^{+}$ donor cells.

(A) The output populations of CD45.1 versus CD45.2 cells from the LN of a $CD45.1^{+}CD45.2^{-}$ host are displayed as dot plot. Both the $CD45.1^{+}$ and $CD45.2^{+}$ populations were then gated for their CD4 versus CD8 profiles.

(B) The left histograms display the expression levels for HSA, CD62L, Qa2 and CD69 of the input $CCR7^{-}$ $CCR9^{+}$ $CD69^{+}$ $TCR\beta^{high}$ SP4 $CD45.2^{+}$ donor population. The histograms on the right display overlays of the expression levels of HSA, CD62L, Qa2 and CD69 within either the detected donor $CD45.2^{+}$ $TCR\beta^{high}$ SP4 output cell populations (red line) or $TCR\beta^{high}$ CD4 T cells obtained from the $CD45.1^{+}$ host LN (black line).

All data in this figure is representative of at least 3 independent experiments.

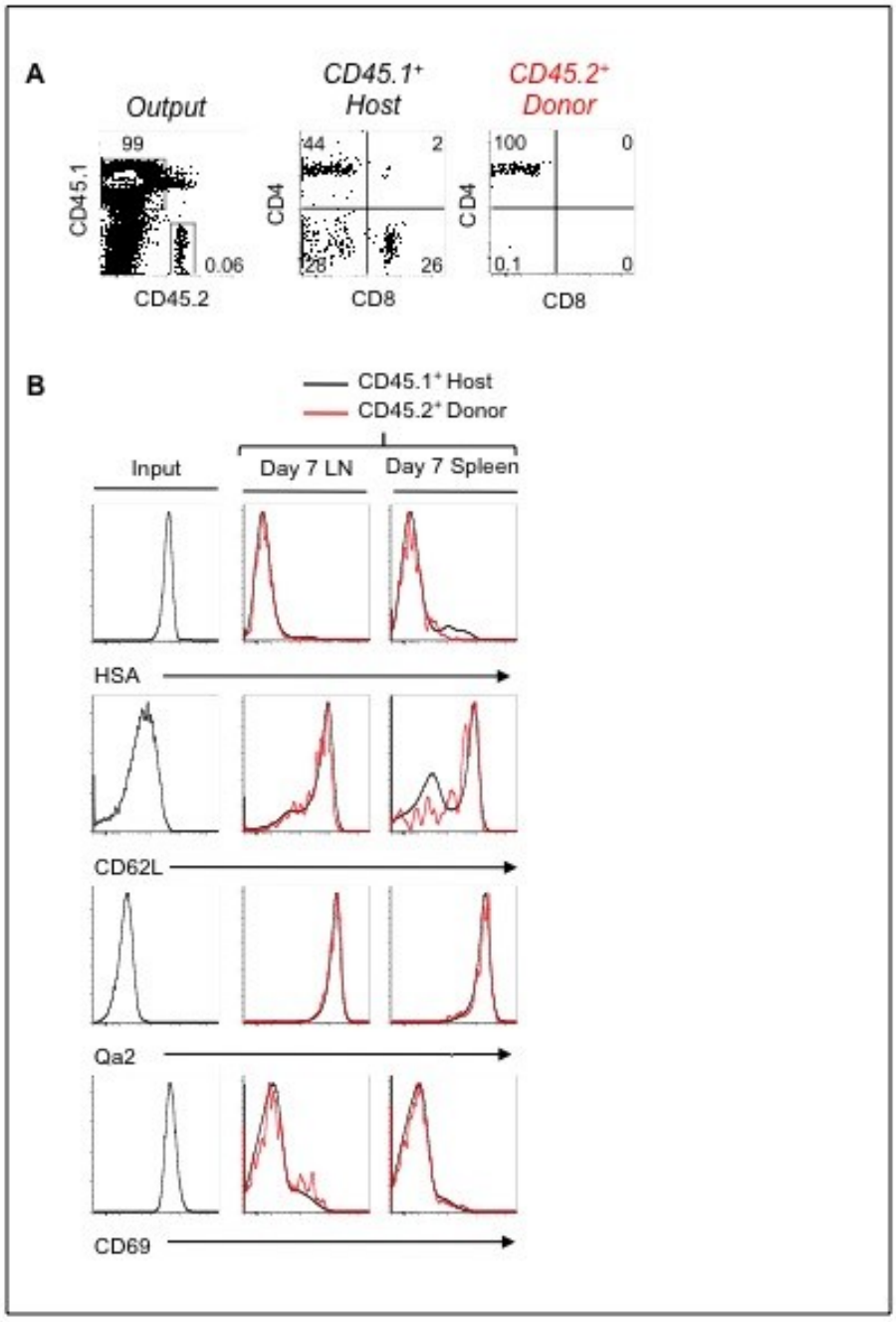
A
Output
CD45.1+
Host
CD45.2+
Donor
99
0.06
CD45.1
CD45.2
44
2
26
26
CD4
CD8
100
0
0.1
0
CD4
CD8
B
CD45.1+ Host
CD45.2+ Donor
Input
Day 7 LN
Day 7 Spleen
HSA
CD62L
Qa2
CD69

either DP or mature $CCR9^{-}CCR7^{+}CD69^{-}TCR\beta^{high}$ SP4 thymocyte subsets, obtained from $CD45.2^{+}$ WT adult donor mice. This co-injection system enabled the development and survival of thymocytes at different stages of their maturation program to be compared directly, within the same host peripheral environment. The survival rates of each input thymocyte population recovered from the $CD45.1^{+}$ x $CD45.2^{+}$ WT hosts 7 days post IV transfer revealed a ratio of 10:1 after co-injection of $CCR9^{+}CCR7^{-}CD69^{+}TCR\beta^{high}$ SP4 and less mature DP thymocytes (Figure 4.9 D), whilst a 0.2:1 ratio was obtained after co-injection of $CCR9^{+}CCR7^{-}CD69^{+}TCR\beta^{high}$ SP4 and more mature $CCR9^{-}CCR7^{+}CD69^{-}TCR\beta^{high}$ SP4 thymocytes (Figure 4.9 B). Both the immature and mature SP4 fractions of cells maintained a $CD4^{+}CD8^{-}$ phenotype (Figure 4.9 A), whilst the small DP population that persisted within host peripheral tissues differentiated into cells of both CD4 and CD8 lineages (Figure 4.9 C). Collectively, the data obtained via this co-injection experimental technique indicate that immature, newly selected $CCR9^{+}CCR7^{-}CD69^{+}TCR\beta^{high}$ SP4 thymocytes display a reduced capacity for extrathymic development compared to their mature $CCR9^{-}CCR7^{+}CD69^{-}TCR\beta^{high}$ SP4 counterparts, whilst demonstrating a greater rate of extrathymic development compared to their more immature DP thymocyte populations.

4.2.4 Differentiation of $Foxp3^{+}CD25^{+}$ nTreg Precursors is dependent on medullary epithelial cell support

The medullary thymic microenvironment has an essential role, not just in the harboring of conventional SP4 and SP8 thymocyte subsets, but also in the generation of thymocytes of non conventional lineages, such as nTreg within the SP4 cohort, defined by their expression of the transcription factor Foxp3. Differentiation down this specialized SP4 thymocyte fate is

Figure 4. 9 Comparison Of The Persistence Of Immature Conventional CCR7$^-$ CCR9$^+$CD69$^+$ SP4 Thymocytes Within The Periphery Of A WT Host

Using the experimental approaches described in Figure 4.8 B and C, CCR7$^-$ CCR9$^+$CD69$^+$ TCRβ^{high} SP4 from a CD45.1$^+$ donor were co-injected with either CCR7$^+$CCR9$^-$CD69$^-$ SP4 CD45.2$^+$ donor cells (A) or DP CD45.2$^+$ donor cells (C) at a one to one ratio and IV transferred into a CD45.1$^+$ x CD45.2$^+$ host. 7 days post IV the CD45.1$^+$ x CD45.2$^+$ hosts were sacrificed and total LN analyzed by flow cytometry for the presence of both the CD45.2$^+$ CD45.1$^-$ and CD45.1$^+$ CD45.2$^-$ donor populations. The output populations from each subset are displayed as a FACS dot plot with the numbers displayed denoting the percentages of each cohort detected. The CD4 versus CD8 profile of each population is also displayed as contour plots (A and C).

The ratios of the percentages recovered from the CCR7$^-$CCR9$^+$CD69$^+$ and CCR7$^+$CCR9$^-$CD69$^-$ SP4 co-injection (B) or the CCR7$^-$ CCR9$^+$ CD69$^+$ and DP (D) co-injection from the total host LN cell population are displayed as bar graphs, with the error bars representing the SEM. Data displayed is typical of four individual grafts per condition.

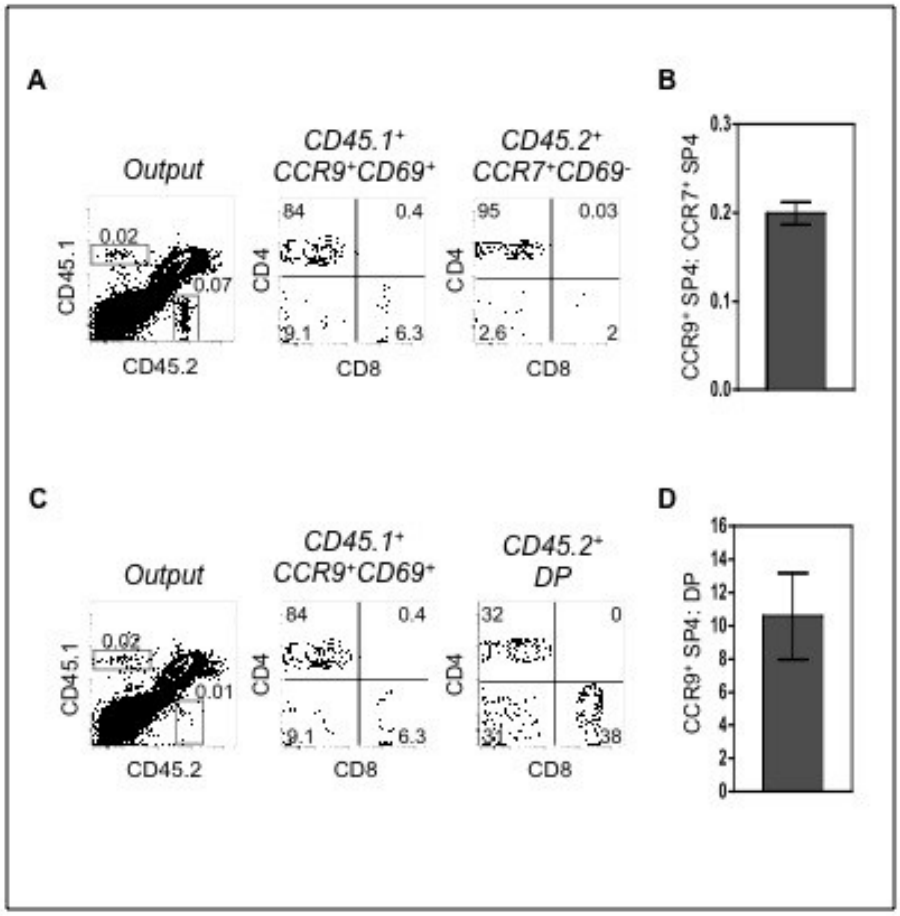
A
Output
CD45.1+ CCR9+CD69+
CD45.2+ CCR7+CD69-
CD45.1
CD45.2
0.02
0.07
CD4
CD8
84
0.4
9.1
6.3
95
0.03
2.6
2
B
CCR9+ SP4; CCR7+ SP4
0.3
0.2
0.1
0.0
C
Output
CD45.1+ CCR9+CD69+
CD45.2+ DP
0.02
0.01
84
0.4
9.1
6.3
32
0
38
D
CCR9+ SP4; DP
16
14
12
10
8
6
4
2
0

thought to involve a series of developmental stages, including the initial generation of a Foxp3$^-$CD25$^+$ nTreg precursor population, which undergo differentiation into Foxp3$^+$CD25$^+$ nTreg progeny (Lio and Hsieh, 2008). The transition from Foxp3$^-$CD25$^+$nTreg precursor to Foxp3$^+$CD25$^+$ nTreg is believed to be independent of TCR-mediated interactions (Burchill et al., 2008; Lio and Hsieh, 2008). However, we were interested to explore this further using our RelB-dependent mTEC deficient model and investigate the requirement of mTEC in the generation of Foxp3$^-$CD25$^+$ nTreg precursors, which to date remains unknown.

The analysis of WT and *Relb*$^{-/-}$ TEC grafts for the presence of Foxp3$^+$CD25$^+$ nTreg and their Foxp3$^-$CD25$^+$ precursors revealed reduced percentages and numbers of both populations in *Relb*$^{-/-}$ TEC grafts, in comparison to their WT counterparts (Figure 4.10A and B). Thus, indicating the generation of Foxp3$^-$CD25$^+$ nTreg precursors, previously identified to occur at the intermediate CCR7$^+$CCR9$^-$CD69$^+$ stage of SP4 development (Chapter 3, Figure 3.9), is a process dependent on a normal medullary compartment. Therefore, the selective absence of a normal mTEC compartment impacts heavily upon intrathymic Foxp3$^+$ CD25$^+$ nTreg development at an early stage, through their control of the generation of Foxp3$^-$CD25$^+$ nTreg precursors.

To further define the stages of nTreg development in relation to dependency upon thymic medullary support we investigated nTreg generation following intravenous transfer of defined populations. In agreement with an earlier study (Lio and Hsieh, 2008), we found that Foxp3$^-$ CD25$^+$ nTreg precursors, predominantly within the intermediate CCR9$^-$CCR7$^+$CD69$^+$ TCRβ^{high} SP4 population (Figure 3.9), differentiated into Foxp3$^+$CD25$^+$ nTreg following intravenous transfer into the periphery of a WT host, 7 days post transfer (Figure 4.11A

Figure 4. 10 The Generation Of Foxp3^{+} CD25^{+} nTreg And CD25^{+} Foxp3^{-} nTreg Precursors Is An mTEC Dependent Process

(A) Thymocytes recovered from WT (top) and *Relb*$^{-/-}$ (bottom) TEC grafts into WT hosts were isolated and analyzed for intracellular staining of Foxp3 within the TCRβ^{high} SP4 population. The Foxp3^{-} fraction of the TCRβ^{high} SP4 thymocytes was also explored for their surface expression levels of CD25.

(B) The percentages (top) and AN (bottom) of the Foxp3^{+} TCRβ^{high} SP4 nTreg subset (left) and Foxp3^{-} CD25^{+} TCRβ^{high} SP4 nTreg precursors (right) were calculated from WT TEC grafts (white bars) and *Relb*$^{-/-}$ TEC grafts (gray bars) into WT hosts and displayed as a mean bar graph, representing at least 5 individual grafts per condition. The standard error bars indicate the SEM, and a student's two tailed unpaired T test was performed on all results, where *** denoted a significant difference ($P < 0.001$) and ** denotes a significant difference ($P < 0.01$).

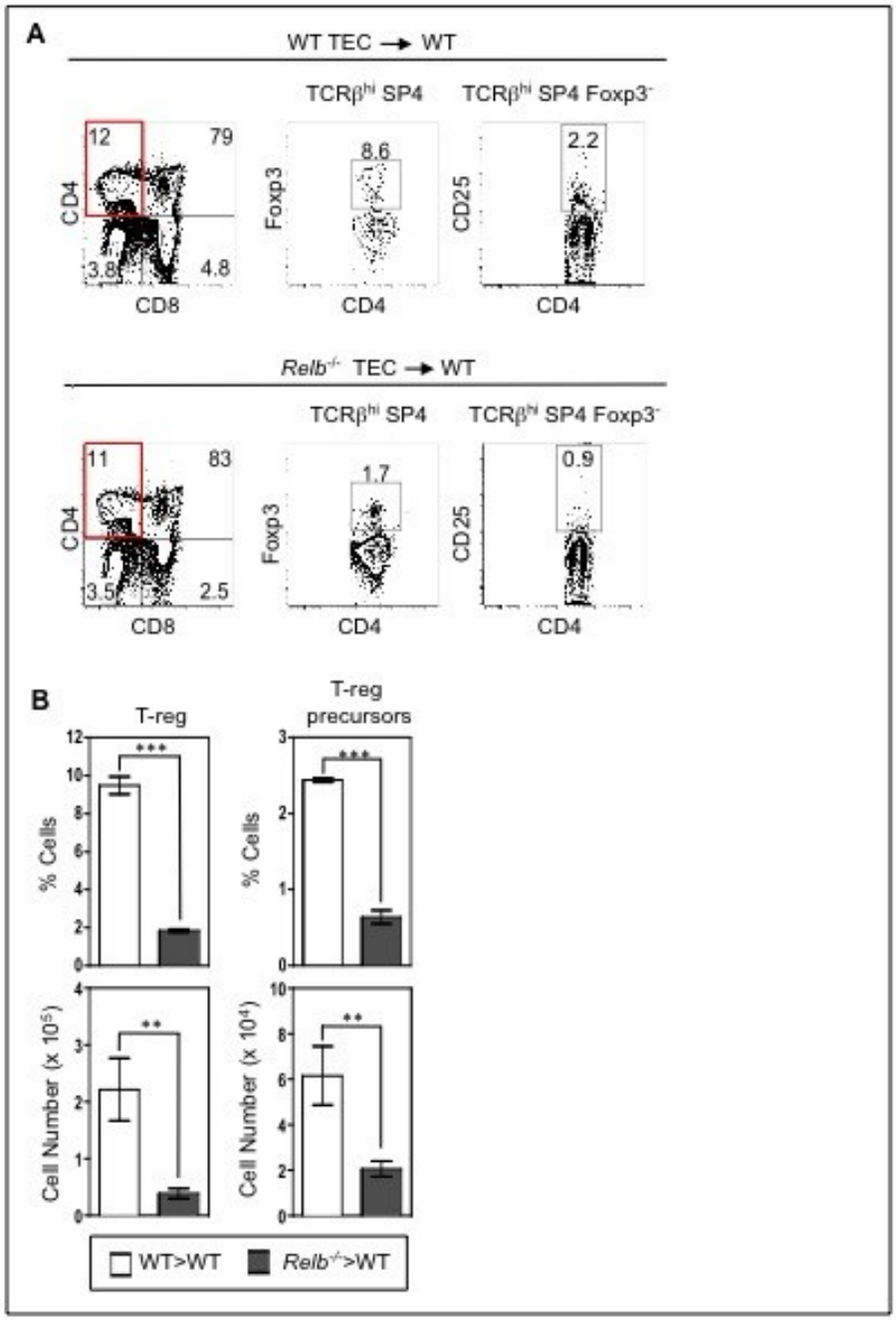
A
WT TEC → WT
TCRβhi SP4
TCRβhi SP4 Foxp3-
12
79
3.8
4.8
CD4
CD8
8.6
Foxp3
CD4
2.2
CD25
CD4
Relb-/- TEC → WT
TCRβhi SP4
TCRβhi SP4 Foxp3-
11
83
3.5
2.5
CD4
CD8
1.7
Foxp3
CD4
0.9
CD25
CD4
B
T-reg
T-reg precursors
% Cells
% Cells
Cell Number (x 10^5)
Cell Number (x 10^4)
***
***
**
**
WT>WT
Relb-/->WT

middle panel). This isolated Foxp3^{-}CD25^{+} nTreg precursor population also generated nTreg *in vitro*, within the RTOC system (Figure 4.11 A bottom panel). Collectively Figure 4.11A indicates that Foxp3^{-}CD25^{+} nTreg precursors can undergo the transition into Foxp3^{+}CD25^{+} nTreg, with or without the presence of mTEC. In marked contrast, we found the less mature CD69^{+}CCR7^{-}CCR9^{+} TCRβ^{high} SP4 thymocyte cohort was unable to give rise to Foxp3^{+}CD25^{+} nTreg extrathymically, (Figure 4.11B top panel), in marked contrast to this cohort's capacity to generate conventional CD4 T cells within the periphery (Figure 4.8). This isolated immature SP4 population demonstrated the capability to differentiate into both Foxp3^{-}CD25^{+} nTreg precursors and their Foxp3^{+}CD25^{+} nTreg progeny *in vitro,* within the RTOC system (Figure 4.11 B bottom panel), suggesting that mTEC interactions alone may be sufficient to drive the differentiation of Foxp3^{+}CD25^{+} nTreg from the CCD9^{+}CCR7^{-} CD69^{+}SP4 stage.

4.2.5 The Generation And Homing Of Distinct DC Subsets Within The Thymic Microenvironment Is Dependent On Medullary Epithelial Cell Support

The ability of immature SP4 thymocytes to continue their maturation into conventional mature cells, independent of mTEC interaction, caused us to consider other cell types that may be present within both the *Relb*$^{-/-}$ grafts and the peripheral lymphoid tissue of WT hosts that may facilitate this continued differentiation program. DC are a strong candidate, as this cell type would be present with the peripheral lymphoid tissue of a WT host to assist extrathymic conventional SP4 development, whilst this population may also be within the *Relb*$^{-/-}$ grafts. Analysis of the presence of total CD11c^{+} DC populations, via confocal

Figure 4. 11 $CCR7^{-}CCR9^{+}CD69^{+}TCR\beta^{high}$ SP4 Thymocytes Do Not Generate $Foxp3^{+}$ nTreg Extrathymically

Using the experimental approach described in Figure 4.8 $CCR7^{-}CCR9^{+}CD69^{+}TCR\beta^{high}$ SP4 (B) or $CD25^{+}Foxp3^{-}$ $TCR\beta^{high}$ SP4 nTreg precursors (A) from a $CD45.2^{+}$ host were isolated using a high speed cell sorter and either: IV injected into a $CD45.1^{+}$ host, or reaggregated with TEC preparations from E15 C57BL/6 WT 2-dGuo FTOCs within the RTOC system.

(A) The cell purity of the isolated $CD25^{+}Foxp3^{-}CD69^{+}$ SP4 input population is displayed in the top panel. The output populations were then analyzed by flow cytometry, 7 days post IV injection (middle), or 7 days after RTOC culture (bottom). The recovered $CD45.2^{+}$ thymocytes were identified and stained CD4 versus CD8 expression. The $TCR\beta^{high}$ SP4 population was explored for surface expression of CD25 against the intracellular staining of Foxp3.

(B) The $CCR7^{-}CCR9^{+}CD69^{+}$ $TCR\beta^{high}$ SP4 input population was analysed by flow cytometry 7 days post IV injection (top) or 7 days after RTOC culture (bottom). The recovered $CD45.2^{+}$ thymocytes were identified and stained for CD4 versus CD8 expression and the $TCR\beta^{high}$ SP4 population was analyzed for surface expression of CD25 against the intracellular staining of Foxp3.

All data within this figure is representative of at least 2 experimental repeats.

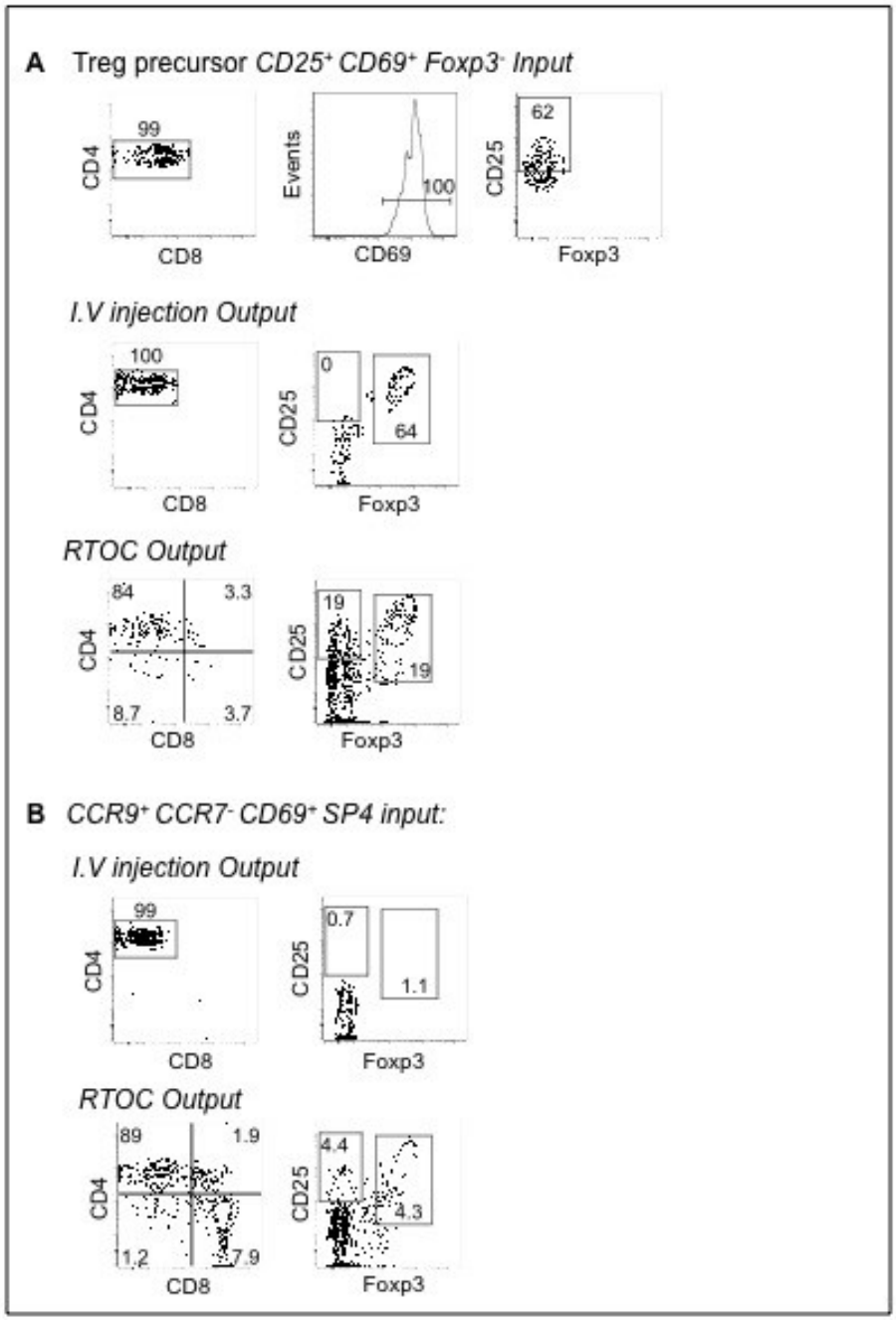
A Treg precursor CD25+ CD69+ Foxp3- Input
99
CD4
CD8
Events
100
CD69
62
CD25
Foxp3
I.V injection Output
100
CD4
CD8
0
64
CD25
Foxp3
RTOC Output
84
3.3
8.7
3.7
CD4
CD8
19
19
CD25
Foxp3
B CCR9+ CCR7- CD69+ SP4 input:
I.V injection Output
99
CD4
CD8
0.7
1.1
CD25
Foxp3
RTOC Output
89
1.9
1.2
7.9
CD4
CD8
4.4
4.3
CD25
Foxp3

microscopy analysis, revealed $CD11c^+$ DC within both WT and *Relb*$^{-/-}$ TEC grafts (Figure 4.12 A). Within the WT grafts these $CD11c^+$ cells were localized to $ERTR5^+$ medullary areas. However, as described earlier (Figure 4.2 A), all $ERTR5^+$ medullary regions were absent within the *Relb*$^{-/-}$ grafts, yet clustering of $CD11c^+$ DC was still observed. Thus, this simple confocal analysis confirms the presence of DC within the RelB-dependent mTEC deficient thymic environments and offers support to our proposal that this cell type may be driving conventional SP4 development within this grafting environment. In addition, this data also suggests that the defect in nTreg production observed within the Relb$^{-/-}$ grafts is not due to the absence of DC.

To investigate further the potential role of DC in supporting conventional SP4 development, we explored the presence of different DC subsets within the *Relb*$^{-/-}$ thymic microenvironments (Figure 4.12 B and C). Thymic DC can be divided into two distinct subsets $CD11c^+B220^+$ plasmacytoid DC (pDC) and $CD11c^+$ $B220^-$ conventional DC (cDC). cDC can be further subdivided into two subsets: $CD11b^-$ $CD8^+$ $Sirp\alpha^-$ DC and $CD11b^+$ $CD8^-$ $Sirp\alpha^+$ DC (Wu and Shortman, 2005). The $CD11b^-$ $CD8^+$ $Sirp\alpha^-$ cDC subset is thought to be intrathymic generated (Wu and Shortman, 2005; Yui et al., 2010), while the additional $CD11b^+CD8^-Sirp\alpha^+$ cDC and pDC populations migrate into thymus from periphery (Li et al., 2009).

The proportions of the different DC subsets recovered from WT grafts closely resembled those obtained for WT adult thymus samples (Figure 4.12 B), with similar percentages of pDC and cDC subsets and approximately the same fractions of $CD11b^-CD8^+Sirp\alpha^-$ versus $CD11b^+CD8^-Sirp\alpha^+$ cDC subsets. In contrast, however, the *Relb*$^{-/-}$ grafts displayed striking differences to the proportions of these three distinct DC subsets (Figure 4.12B and C). In

Figure 4. 12 Homing Of Distinct Dendritic Cells Subsets To mTEC Deficient Thymic Microenvironments Within A WT Host

(A) WT (top panel) or *Relb*$^{-/-}$ (bottom panel) TEC grafts into WT hosts were harvest 6-12 weeks post transplantation and frozen for confocal analysis. 7μm sections were cut and stained for CD11c and ERTR5. Bars represent 100 μm.

(B) WT (middle) or *Relb*$^{-/-}$ TEC (bottom) grafts into WT host were analyzed by FACS analysis, along side adult WT C57BL/6 thymocytes (top), for the presence of different DC subsets. Thymocytes were stained for CD11c versus B220 (left) and both the CD11c^{+}B220^{-} conventional DC and B220^{+}CD11c^{+} plasmacytoid DC subsets identified. The

CD11c^{+}B220^{-} cDC population was then gated and analyzed for Sirpα and CD8 expression (right). The numbers displayed within each FACS plot gate represent the percentages of each distinct DC subset.

(C) The percentages (top) and AN (bottom) of pDC versus cDC subsets (left) and Sirpα^{+}CD8^{-} versus Sirpα^{-}CD8^{+} cDC subsets (right) obtained from WT TEC grafts (white bars) or *Relb*$^{-/-}$ TEC grafts (grey bars) are displayed as mean bar graphs, representative of at least 5 individual grafts per condition. The error bars represent the SEM and a student's two tailed unpaired T test was performed on all results, where ns denoted a non-significant difference ($P > 0.05$), and *, ** or *** indicates a significant difference (* = $P < 0.05$, ** = $P < 0.01$, ***= $P < 0.001$).

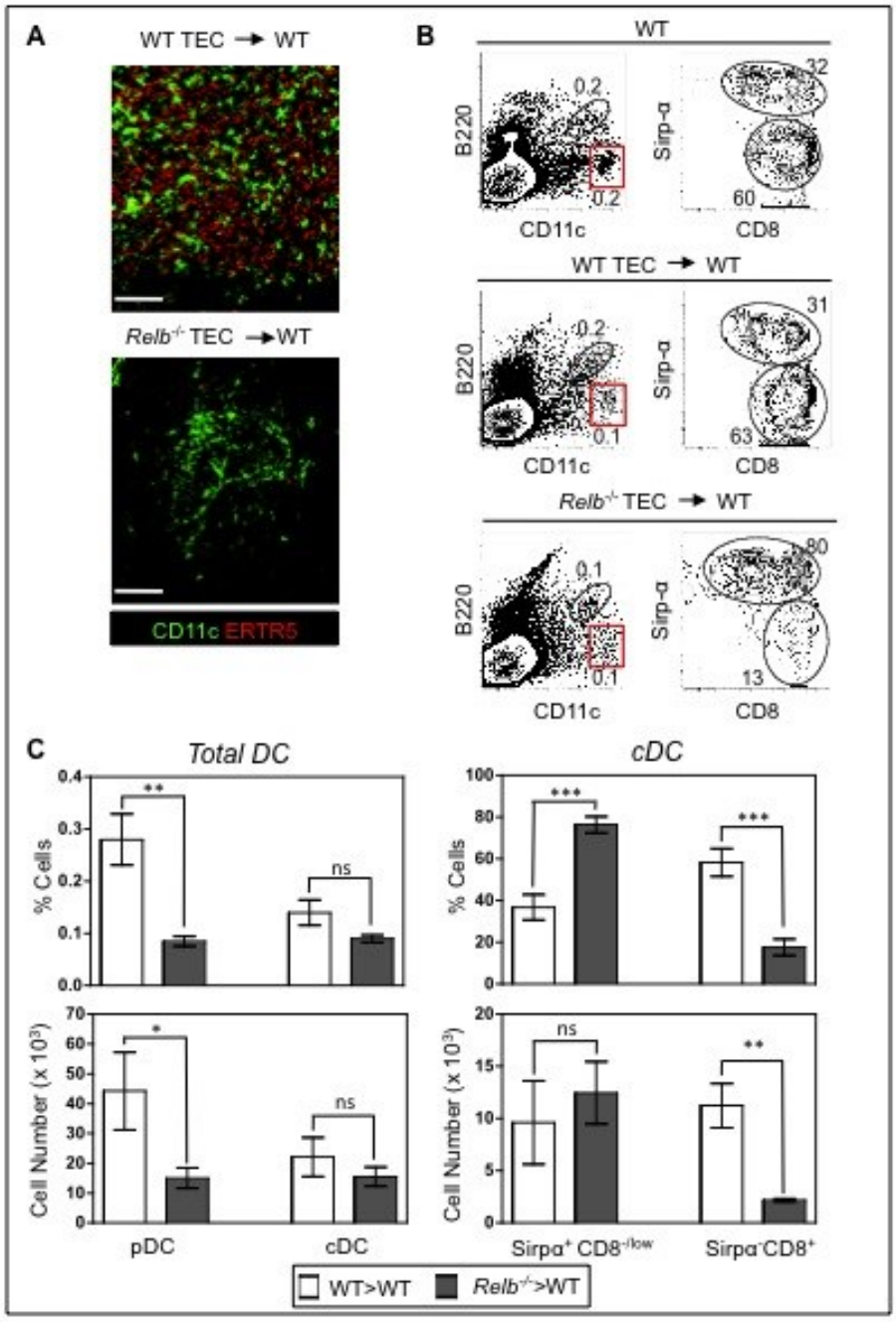
A
WT TEC → WT
Relb-/- TEC →WT
CD11c ERTR5
B
WT
B220
Sirp-α
CD11c
CD8
0.2
0.2
32
60
WT TEC → WT
0.2
0.1
31
63
Relb-/- TEC → WT
0.1
0.1
80
13
C
Total DC
cDC
% Cells
Cell Number (x 10³)
**
ns
*
***
pDC
cDC
Sirpα+ CD8-/low
Sirpα-CD8+
WT>WT
Relb-/->WT

comparison to WT grafts, *Relb*$^{-/-}$ grafts exhibited significant reductions in both the percentages and absolute numbers of the pDC subset, extrathymically generated and home to thymus from the periphery. In contrast, no differences in the overall percentages and absolute numbers of cDC were seen between WT and *Relb*$^{-/-}$ grafts (Figure 4.12C), however, disruptions to the proptions of CD11b^{-} CD8^{+} Sirpα^{-} DC versus CD11b^{+} CD8^{-} Sirpα^{+} cDC were observed within the *Relb*$^{-/-}$ grafts. Unlike the approximate proportions of 60% CD8^{+}Sirpα^{-} to 40% CD8^{-}Sirpα^{+} cDC subsets displayed within the WT grafts, *Relb*$^{-/-}$ grafts displayed 20% CD8^{+}Sirpα^{-} to 80% CD8^{-}Sirpα^{+} cDC. This change in the cDC distribution resulted in a highly significant reduction in the absolute numbers of CD8^{+}Sirpα^{-} cDC recovered from the *Relb*$^{-/-}$ grafts compared to the WT controls. In contrast, the percentage increase in the CD8^{-}Sirpα^{+} cDC population from *Relb*$^{-/-}$ grafts did not translate into a significant difference in terms of absolute numbers.

Overall, exploration into the different DC subsets within the *Relb*$^{-/-}$ TEC grafts suggests the absence of a structured mTEC compartment results in a reduction to both the intrathymically generated CD8^{+}Sirpα^{-} cDC subset and the extrathymically generated pDC populations that migrate into the thymus from the periphery. Therefore, this data suggests a possible requirement for the thymic medulla in both the homing of pDC to the thymic microenvironment and perhaps in the intrathymic generation of CD8^{+} Sirpα^{-} cDC. Additionally, the results identified peripherally induced CD8^{-}Sirpα^{+} cDC as a potential candidate in the involvement of conventional SP4 generation within the *Relb*$^{-/-}$ grafts, due to their presence been unaffected by the absence of RelB-dependent mTEC compartments. This data also does not rule out the possibility that the defect in nTreg production observed within

the RelB-dependent mTEC deficient thymic microenvironment is not a consequence, at least in part, of the reduction in both the pDC and the $CD8^{-}Sirp\alpha^{+}$ cDC subsets.

4.3 DISCUSSION

Following positive selection in the cortex, SP4 and SP8 thymocytes migrate into specialized medullary thymic microenvironments, where they reside between 5 to 14 days, although the precise medullary dwell time remains controversial(McCaughtry et al., 2007; Scollay and Godfrey, 1995). During this residency, developing SP thymocytes interact with medullary thymic epithelial cells and DC, which is known to be essential for establishing T cell tolerance, via the deletion of thymocytes displaying αβTCRs with potential specificity to self (Anderson and Takahama, 2012). However, the involvement of the thymus medulla in other aspects of αβT cell development remains unclear, including its role in the generation and selection of $Foxp3^+$ nTreg and the continued maturation of the multistep conventional SP developmental program. Investigations into the effect of medullary defects on conventional SP development have suggested intact mTEC compartments are critical in the differentiation program of SP4 development (Li et al., 2007), while additional studies have proposed a specific role for mTEC in the intrathymic generation of $Foxp3^+$ nTreg (Aschenbrenner et al., 2007; Hinterberger et al., 2010).

The data obtained through exploring T cell development *in vivo* within either the RelB-dependent mTEC deficient grafting models or extrathymically, is in both accordance and disagreement with these proposed roles of the mTEC population. Our findings do not support the suggestion mTEC provide essential support for SP4 differentiation, but rather that conventional CD4 SP thymocyte development can occur independently of the thymic medulla. Data showed that SP4 thymocytes are capable of undergoing their maturation program extrathymically, with complete thymic independence occurring from the newly selected

$CCR7^{-}CCR9^{+}CD69^{+}$ stages of development, immediately following positive selection. In marked contrast, however, experiments showed that mTEC are crucial for the intrathymic generation of $Foxp3^{+}$ nTreg. Investigations suggest $Foxp3^{+}$ nTreg development is dependent upon an intact thymic medulla, with a specific requirement for mTEC mapping to early stages in nTreg development to foster the generation of $Foxp3^{-}CD25^{+}$ nTreg precursors. Collectively, these results demonstrate a differential requirement for the thymus medulla in relation to $Foxp3^{+}$nTreg versus conventional SP4 thymocyte development.

Given that the generation of $Foxp3^{-}CD25^{+}$ nTreg precursors is thought to be dependent upon CD28-CD80/CD86 interactions (Hinterberger et al., 2011; Lio et al., 2010; Vang et al., 2010), as well as TCR-MHC binding (Lio and Hsieh, 2008), our findings fit well with the expression of both these co-stimulatory molecules and MHC class I and class ll by the mTEC population (Derbinski et al., 2005; Gray et al., 2007). Thus, the ability of mTEC to provide these fundamental molecules may be the basis of why $Foxp3^{-}CD25^{+}$ nTreg precursors generation is dependent upon an intact medulla. This suggestion that mTEC provide peptide/MHC ligands for nTreg development fits well with reports documenting the generation of antigen-specific TCR transgenic nTreg following the targeting of model antigens to mTEC (Aschenbrenner et al., 2007; Hinterberger et al., 2010) and the normal numbers of Treg are generated in bone marrow chimaeras, where the haemopoietic compartment is MHC class II deficient (Aschenbrenner et al., 2007; Liston et al., 2008). Although these experimental models revealed an essential role of mTEC in $Foxp3^{-}CD25^{+}$ nTreg precursors development, they did not identify the cell types responsible for driving continued SP4 T cell development down this nonconventional lineage. Additional investigations are needed to confirm the precise interactions between mTEC and developing SP4 thymocytes, essential to drive nTreg

precursor development, be it cell-cell mediated interactions, or perhaps indirect mTEC effects of nTreg selection through their manipulation of the thymic microenvironment and the behavior of other cell types. It has been demonstrated mTEC can influence DC mediated selection of nTreg via their cytokine production (Hanabuchi et al., 2010), whilst XCL1-mediated medullary accumulation of thymic DC, produced by $Aire^{+}$ mTEC, is thought to critically contribute to the development of nTreg (Lei et al., 2011). Thus, further investigation of the dual role of mTEC and DC in nTreg development is required.

A further limitation to our investigation is whether mTEC interactions alone are sufficient to direct the generation of $Foxp3^{-}CD25^{+}$ nTreg precursors, or if interactions with additional cell types, particularly thymic DC, are required to drive differentiation of nTreg. Although preliminary data acquired from the reaggregation of immature $CCR9^{+}CCR7^{-}CD69^{+}$SP4 thymocytes with WT TEC populations *in vitro* demonstrated that both $Foxp3^{-}CD25^{+}$ nTreg precursors and their $Foxp3^{+}CD25^{+}$ nTreg progeny can develop in the presence of mTEC, additional studies are needed to explore the potential impact of other cell types in the development of this specialized SP4 lineage. Extensive studies have suggested that DC mediate central tolerance via their ability to select nTreg, (Proietto et al., 2008b; Spence and Green, 2008; Watanabe et al., 2005a; Wirnsberger et al., 2009). However, how DC are involved in the process of nTreg differentiation, be it exclusively, or in cooperation with mTEC (Watanabe et al., 2005b), still remains relatively unclear.

The examination of DC within the RelB-dependent medullary deficient thymic microenvironments identified dramatic alterations to both the anatomical positioning of this cell type and the proportions of their distinct cohorts. DC predominantly accumulate within the medullary region of the thymus (Barclay, 1981), which was confirmed within the WT

TEC grafting environments, where $CD11c^+$ DC clustering was detected within the $ERTR5^+$ medullary areas. Interestingly, however, even though $ERTR5^+$ regions were absent within the RelB-dependent mTEC deficient grafts, $CD11c^+$ DC still clustered within particular areas. The nature of these areas is currently unclear and we are presently investigating whether they represent cortical regions, or areas rich in vasculature that could represent sites of cell entry in the graft. On closer inspection of the DC populations within this environment, significant reductions were detected within both the intrathymic generated $Sirp\alpha^-CD8^+$ cDC population and the pDC subset, that is extrathymically generated and homed to the thymus. These striking results highlight a potential role for mTEC in DC recruitment and/or generation and extend previous observations that mTEC mediated chemokine production controls the intrathymic positioning of DC (Lei et al., 2011). These results also raise the possibility that the considerable reduction in the numbers of these two specific DC populations within the *Relb*$^{-/-}$ thymic microenvironment is consequently causing the decrease in the nTreg precursors and thus, their nTreg progeny. Clearly, further, more extensive investigations are required to dissect the division of labor between mTEC and DC populations in the generation of this specialized non-conventional SP4 lineage.

Furthermore, in addition to the role the DC population may be playing in nTreg generation, our experimental approaches do not address whether thymic DC are involved in continued conventional SP4 and SP8 development. The finding that conventional CD4 SP thymocyte development can occur independently of the thymus medulla from the earliest $CD69^+CCR7^-CCR9^+$ stages in their differentiation program raises the possibility that thymic DC may be involved in this developmental process. It is possible that the mislocalized DC clusters present within the RelB-dependent mTEC deficient microenvironment may support the continued

maturation of the SP4 and SP8 thymocytes observed within these grafts. This proposal is aided by the strong assumption DC populations would also be present within the secondary lymphoid tissue of WT hosts, to drive conventional SP4 extrathymic maturation. As the *Relb*$^{-/-}$ grafts display significant reduction to both their pDC and SirpαCD8^{+} cDC populations, perhaps the unaltered Sirpα^{+}CD8^{-} subset is exclusively capable of driving this conventional maturational program.

The further effects of mTEC deficiency observed within the *Relb*$^{-/-}$ grafted microenvironment on thymocyte development suggest possible supplementary roles for this specialized stromal population in the later stages of intrathymic T cell development. Although RelB-dependent mTEC deficiency displayed no effect on the ability of conventional SP8 thymocytes to mature to the Qa2^{+}CD69^{-} stage in differentiation, the overall reduction to the number of SP8 cells within *Relb*$^{-/-}$ grafts imply that maintenance, or perhaps efficacy of development, of MHC class I restricted thymocytes is influenced by mTEC. It has been reported that SP8 thymocytes have higher rates of proliferation in comparison to their SP4 counterparts (Boursalian et al., 2004; McCaughtry et al., 2007). The mTEC deficient microenvironment may, therefore, limit their proliferation ability and thus, result in the overall reduction to the cell numbers of this population. However, the significant reduction to the CD44^{high}Qa2^{+}HSA^{low} recirculating, or perhaps long term thymic residents, within the SP8 populations may be accountable, in part, for this reduction in total SP8 cell numbers.

This decrease in recirculating SP4 and SP8 populations may also suggest an involvement of mTEC in homing of peripheral T cells back to the medulla. It has been reported peripheral T cells that return to the thymus enter at the corticomedullary junction and persist in the medulla. It has also been reported that the thymic architecture is affected by the presence of this

recirculating population, with the mature T cells causing mTEC regeneration (Hale and Fink, 2009; Surh et al., 1992). Therefore intact mTEC environments may be essential for recruitment of peripheral T cells back to the thymus. Interestingly, with the use of RAG-2 GFP reporter mice, it has been suggested up to 50% of GFP^- thymic residents are Treg (McCaughtry et al., 2007; Weinreich and Hogquist, 2008). Therefore, regardless of whether this population represents immigrating mature peripheral T cells or long term thymic residents, the reduction in the $CD44^{high}Qa2^+HSA^{low}$ SP4 subsets, along with the reduced GFP^- SP4 cells obtained from *Relb*$^{-/-}$ grafts into a RAG-2 GFP host may contribute to the reduced numbers of nTreg observed within the same environment.

In conclusion these results not only highlight differences in the maturational requirements for conventional SP thymocytes and nTreg, they warrant a rethinking of the role of the thymus medulla in T cell development. Thus, rather than representing a specialised microenvironment that is required to foster the completion of late stage αβT cell development *per se*, the primary role of the thymic medulla appears to be the generation of self tolerance via both negative selection and the generation of $Foxp3^-CD25^+$ nTreg precursors and their $Foxp3^+CD25^+$ T cells progeny.

CHAPTER 5: THE ROLE OF CCR4 IN T CELL DEVELOPMENT AND CORTEX TO MEDULLA MIGRATION OF POSITIVELY SELECTED THYMOCYTES.

5.1 INTRODUCTION

One of the dramatic migratory changes in intrathymic T cell development is the re-localisation of positively selected CD4 or CD8 SP thymocytes from the cortex into the medulla. An early study using Pertussis Toxin treatment to inhibit G-protein coupled chemokine receptors resulted in a profound block in cortex to medulla migration of SP thymocytes, implicating chemokines in this migratory process (Ehrlich et al., 2009; Suzuki et al., 1999). Of the large family of chemokine receptors, CCR7 has been identified to play a key role in driving the cortex to medulla migration of newly generated CD4 and CD8 SP thymocytes (Kwan and Killeen, 2004; Ueno et al., 2004). CCR7 ligands, CCL21 and CCL19, are predominantly produced by mTEC and are distributed within the medulla (Ueno et al., 2002), whilst a fraction of cortical DP thymocytes receive TCR-mediated positive selection survival signals upregulate CCR7 on their cell surface (Davalos-Misslitz et al., 2007). Interestingly, it has also been reported that MHC Class I mediated positive selection leads to an enhanced upregulation of CCR7 expression on DP thymocytes compared to selection via MHC class II. In line with this, the enforced over expression of CCR7 has been demonstrated to increase CD8 SP development (Yin et al., 2007), suggesting that CCR7 may be more important in the specific migration of CD8 SP thymocytes into medullary regions and that other unidentified chemokine receptors may be involved in the migration of CD4 SP cells.

Data in Chapter 3 showing that CCR4 is rapidly upregulated on the initiation of positive selection at the DP stage of development identifies this chemokine receptor as possible additional regulator of thymocyte entry to the medulla. In addition, CCR4 ligands, CCL17 and CCL21, are highly expressed within the medullary microenvironment, produced primarily

by mTEC (Griffith et al., 2009) and thymic DC (Lieberam and Forster, 1999). It has been demonstrated that on initiation of positive selection $CD69^+$ DP thymocytes become responsive to CCL22, which is maintained with the most immature CD4 SP population (Campbell et al., 1999). Complementary to this data, *Ccr4* mRNA levels have also been shown to be upregulated within the same CCL22 responsive $CD69^+$ DP and immature CD4 SP thymocytes subsets (Campbell et al., 1999; Suzuki et al., 1999), suggesting a potential role for CCL22 in migration of positively selected thymocytes from the cortex to the medulla. However, the possible role of CCR4 in the thymus is not well understood. Using $Ccr4^{-/-}$ mice (Chvatchko et al., 2000), the aim of this chapter was to explore the potential involvement of CCR4 in cortex to medulla thymocyte migration and post-positive selection maturation of both conventional and $Foxp3^+$ T regulatory lineages.

5.2 RESULTS

5.2.1 CCR7 Mediates Medullary Accumulation Of SP4 And SP8 Thymocytes, But Is Dispensable For Their Development

In initial experiments aimed at defing the role of chemokine receptors on medullary migration, we analysed the thymus of *Ccr7*$^{-/-}$ mice, known to have defective cortex-to-medulla transition (Ueno et al., 2004), in order to provide comparison with subsequent analysis of *Ccr4*$^{-/-}$ mice. The analysis of thymocyte development in adult *Ccr7*$^{-/-}$ mice revealed no gross abnormalities to T cell development (Figure 5.1). No significant alterations to thymocyte cellularity were observed as a consequence of CCR7 deficiency (Figure 5.1 A). The absolute numbers of cells at all four main stages of thymocytes development; DN, DP, SP4 and SP8, also displayed no difference in CCR7 deficient mice compared to their WT controls (Figure 5.1 A and C). In addition, DP thymocytes from adult *Ccr7*$^{-/-}$ mice revealed no disruption to the frequencies of pre-positive selection CD69^{-}DP cells compared to CD69^{+} DP cells undergoing the selection process (Figure 5.1 D). The percentages and absolute numbers of the immature CD69^{+} Qa2^{-} fraction of thymocytes versus the mature CD69^{-} Qa2^{+} cell population within both the SP4 (Figure 5.2 A and B) and SP8 (Figure 5.2 C and D) subsets showed no alterations between the *Ccr7*$^{-/-}$ mice and their WT counterparts. Collectively, this data suggest the absence of CCR7 does not perturb conventional αβT cell development. In contrast, while analysis of the CD25^{+} FoxP3^{+} nTreg lineage revealed an increase to both the percentage and absolute number in *Ccr7*$^{-/-}$ mice compared to their WT controls (Figure 5.3), no detectable differences were observed in the percentage or absolute number of CD25^{+} FoxP3^{-} nTreg precursors.

Figure 5. 1 Grossly Normal T Cell Development In CCR7 Deficient Mice

Adult *Ccr7*$^{-/-}$ or WT thymocyte cell suspensions were isolated and cell numbers obtained, before staining for flow cytometry analysis.

The absolute numbers (AN) of each distinct population was calculated per mouse from the total thymocte cell count and the percentage of each population acquired via flow cytometry analysis. The AN of each distinct population was displayed as a mean bar graph from WT (white bars) or *Ccr7*$^{-/-}$(grey bars) samples, with data representing x5 independent mice per condition and the error bars denoting the SEM. A student's two tailed unpaired T test was performed on all results, where ns denoted a non-significant difference, as $P > 0.05$.

(A) The absolute cell count of total WT or *Ccr7*$^{-/-}$ thymus samples.
(B) WT (top) and *Ccr7*$^{-/-}$ (bottom) total cell samples were explored for CD4 versus CD8 surface expression, displayed as a contour plot, or TCRβ and CD69 expression levels, displayed as histograms. The numbers depict the frequency of cells within each gate.
(C) The AN of $CD4^{-}CD8^{-}$ DN, $CD4^{+}$ $CD8^{+}$ DP, $TCR\beta^{high}$ $CD4^{+}CD8^{-}$ SP and $TCR\beta^{high}$ $CD8^{+}CD4^{-}$ SP thymocyte cohorts from WT or *Ccr7*$^{-/-}$ samples.
(D) The $CD4^{+}$ $CD8^{+}$ DP population was separated on the basis of their CD69 expression and the AN of $CD69^{-}$ versus $CD69^{+}$ DP subsets calculated and displayed from WT or *Ccr7*$^{-/-}$cell suspensions.

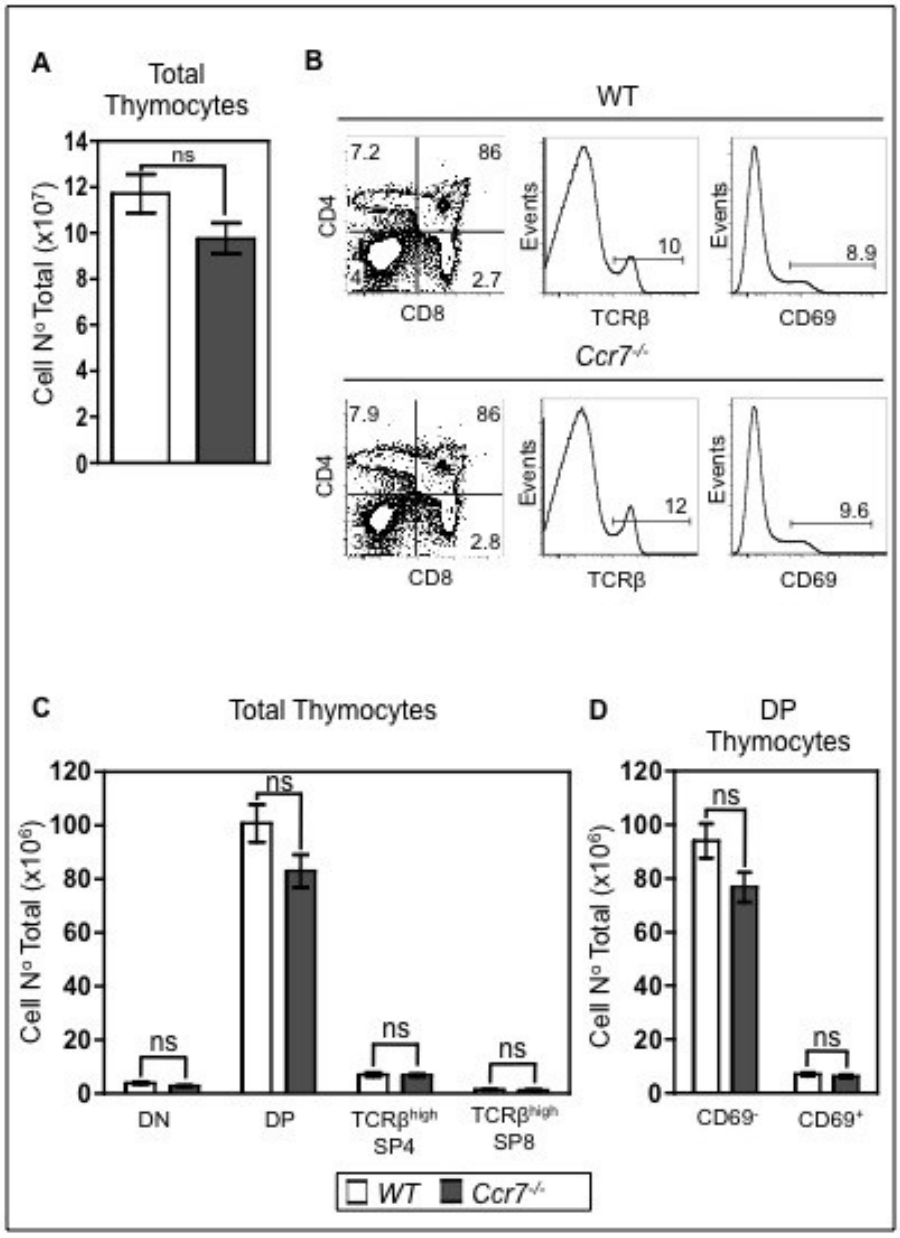
A
Total Thymocytes
Cell N° Total (x10⁷)
ns
B
WT
7.2
86
4
2.7
CD4
CD8
Events
10
TCRβ
8.9
CD69
Ccr7-/-
7.9
86
3
2.8
12
9.6
C
Total Thymocytes
Cell N° Total (x10⁶)
ns
DN
DP
TCRβhigh SP4
TCRβhigh SP8
WT
Ccr7-/-
D
DP Thymocytes
CD69-
CD69+

Figure 5. 2 Conventional SP4 and SP8 T Cell Development Is Not Disrupted In CCR7 Deficient Mice

Thymocytes from adult WT (top) or *Ccr7*$^{-/-}$ (bottom) mice were isolated and stained for flow cytometry analysis. The Qa2 and CD69 expression was explored within the (A) TCRβ^{high} SP4 population or (C) TCRβ^{high} SP8 subset and represented as contour FACS plots.

The percentages (top) and AN (bottom) of (B) SP4 populations: CD69^{+} Qa2^{-} TCRβ^{high} SP4 (left) and CD69^{-} Qa2^{+} TCRβ^{high} SP4 (right), or (D) SP8 populations: CD69^{+} Qa2^{-} TCRβ^{high} SP8 (left) and CD69^{-} Qa2^{+} TCRβ^{high} SP8 (right), were calculated per mouse and displayed as bar graphs. Each bar graph represents the mean percentages or AN of thymocyte subsets recovered from x5 individual WT (white bars) or *Ccr7*$^{-/-}$ (gray bars) mice. The standard error bars display the SEM, and a student's two tailed unpaired T test was performed on all results, where ns denoted a non-significant difference, as $P > 0.05$.

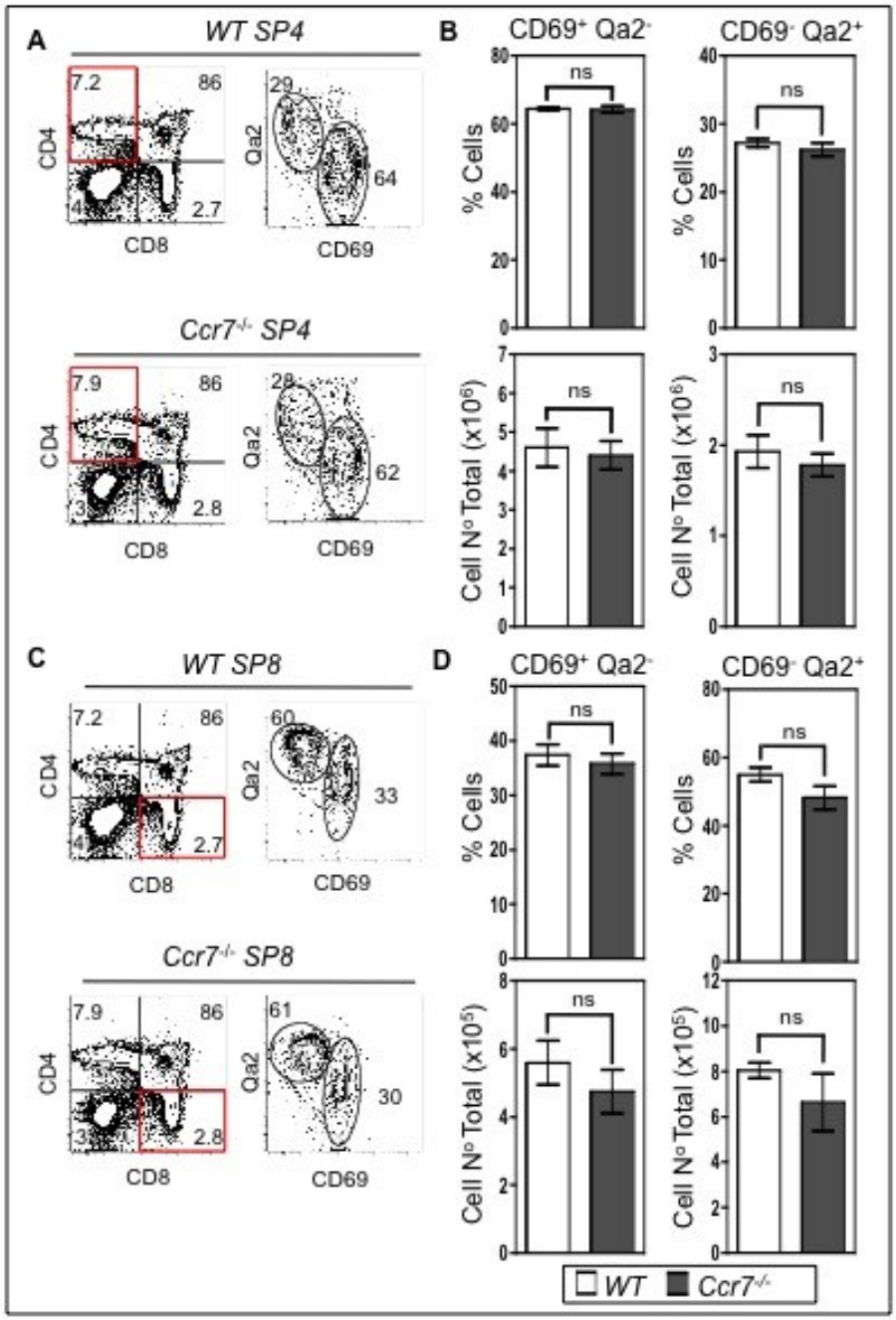
A
WT SP4
7.2
86
2.7
CD4
CD8
29
64
Qa2
CD69
Ccr7-/- SP4
7.9
86
2.8
CD4
CD8
28
62
Qa2
CD69
B
CD69+ Qa2-
CD69- Qa2+
% Cells
Cell Nº Total (x10⁶)
ns
C
WT SP8
7.2
86
2.7
CD4
CD8
60
33
Qa2
CD69
Ccr7-/- SP8
7.9
86
2.8
CD4
CD8
61
30
Qa2
CD69
D
CD69+ Qa2-
CD69- Qa2+
% Cells
Cell Nº Total (x10⁵)
ns
WT
Ccr7-/-

Figure 5. 3 CCR7 Deficient Mice Have Increased Frequencies Of Foxp3^{+} CD25^{+} Treg Whilst The Generation Of CD25^{+} Foxp3^{-} Treg Precursors Is Unaffected

(A) Thymocytes recovered from adult WT (top) or *Ccr7*$^{-/-}$ (bottom) mice were isolated and analysed for intracellular staining of Foxp3 within the TCRβ^{high} SP4 population. The Foxp3^{-} fraction of the TCRβ^{high} SP4 thymocytes was also explored for their surface expression levels of CD25.

(B) The percentages (top) and AN (bottom) of the Foxp3^{+} TCRβ^{high} SP4 Treg subset (left) and Foxp3^{-} CD25^{+} TCRβ^{high} SP4 Treg precursors (right) were calculated from WT (white bars) and *Ccr7*$^{-/-}$ (gray bars) hosts and displayed as mean bar graphs, representing x5 individual mice per condition. The standard error bars indicate the SEM, and a student's two tailed unpaired T test was performed on all results, where ns denoted a non-significant difference ($P > 0.05$), and ** or *** indicate a significant difference (** = $P < 0.01$ and ***= $P < 0.001$).

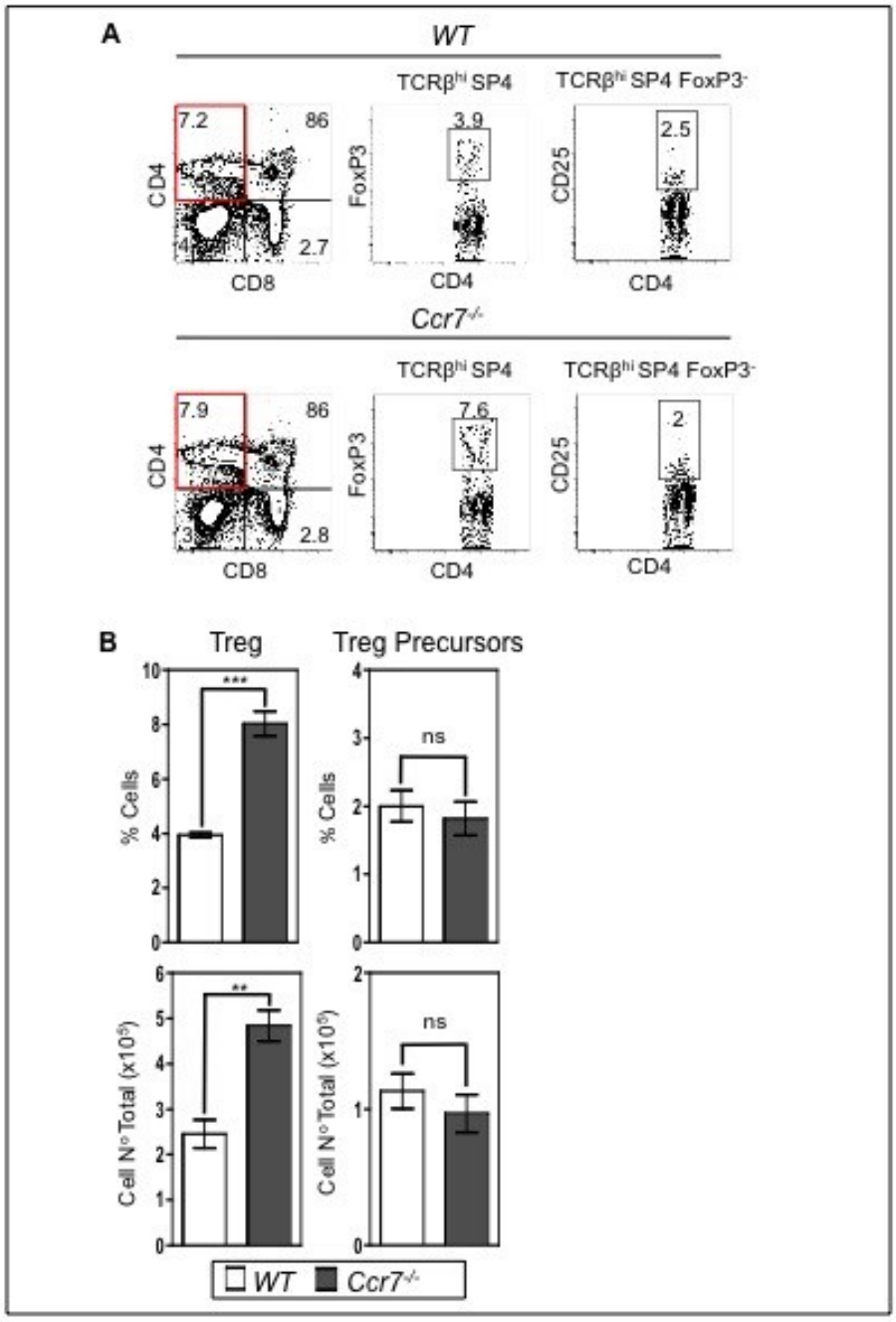
A
WT
TCRβhi SP4
TCRβhi SP4 FoxP3-
7.2
86
2.7
3.9
2.5
CD4
CD8
FoxP3
CD25
CD4
CD4
Ccr7-/-
TCRβhi SP4
TCRβhi SP4 FoxP3-
7.9
86
2.8
7.6
2
CD4
CD8
FoxP3
CD25
CD4
CD4
B
Treg
Treg Precursors
% Cells
***
ns
Cell N° Total (x10⁵)
**
ns
WT
Ccr7-/-

Low resolution (Figure 5.4) images of whole thymic sections confirmed previously published findings that *Ccr7*$^{-/-}$ adult thymic environments display abnormal medullary structures compared to WT controls (Figure 5.4A) (Ueno et al., 2004). *Ccr7*$^{-/-}$ mice had small, sparsely distributed medullas, in comparison to the larger WT medullary areas. Higher resolution images of thymic medullary areas of adult *Ccr7*$^{-/-}$ or WT mice were taken to assess the distribution of SP4 and SP8 thymocytes as described in the Section 5.2, which confirmed the previously reported findings that absence of CCR7 results in a reduction in SP4 and SP8 thymocyte numbers in the thymic medulla (Figure 5.4 C) (Nitta et al., 2009; Ueno et al., 2004). In line with earlier reports (Davalos-Misslitz et al., 2007; Nitta et al., 2009), the greatest reduction in medullary accumulation was observed within the SP8 population (5 fold reduction). However, the reduction in medullary SP4 numbers (2 fold reduction in *Ccr7*$^{-/-}$ compared to WT), contrast with reports that have disputed the effects of CCR7 deficiency on SP4 medullary accumulation (Davalos-Misslitz et al., 2007). Overall, this data supports the idea that absence of CCR7 reduces medullary retention of both SP4 and SP8 thymocytes in the adult thymus.

5.2.2 CCR4 Is Not Essential For Normal T Cell Development Or Medullary Positioning Of Post-Positive Selection SP Thymocytes

To study the involvement of CCR4 in thymocyte development and cortex to medulla reclocalisation, we first explored thymic expression of CCL22 and CCL17 via quantitative PCR (Figure 5.5). TEC and DC populations were isolated from digested thymus samples acquired from either E15 WT FTOC or adult WT mice and the mRNA levels of CCL17 and CCL22 determined within each individual subset. Examination of CCL21 and CCL17 mRNA

Figure 5. 4 CCR7 Deficiency Results In Reduced Numbers Of SP4 And SP8 Thymocytes Within Thymic Medullary Regions

WT and *Ccr7*$^{-/-}$ adult thymi were frozen for confocal analysis. 7μm thymus sections were cut and stained for immunofluorescence confocal analysis.

(A) Tile scans of a series of low resolution images are shown for whole thymus sections from WT (left) and *Ccr7*$^{-/-}$ (right) hosts, stained for ERTR5 and β5T. Bars represent a scale of 1mm

(B) Higher resolution images of smaller thymic areas stained for CD4 and CD8. The white dashed line denotes the corticomedullary junction, C=cortex and M=medulla. Bars represent a scale of 100 μm

(C) The number of SP4 (left graph) or SP8 (right graph) cells within a 100μm x 100μm square medullary area were counted within x3 regions per section, on x4 serial section images per host. The numbers acquired from x3 WT (white bars) and x3 *Ccr7*$^{-/-}$ (grey bars) hosts are displayed as mean bar graphs. The standard error bars indicate the SEM and a student's two tailed unpaired T test was performed on all results, where *** denotes highly significant difference, as $P < 0.001$.

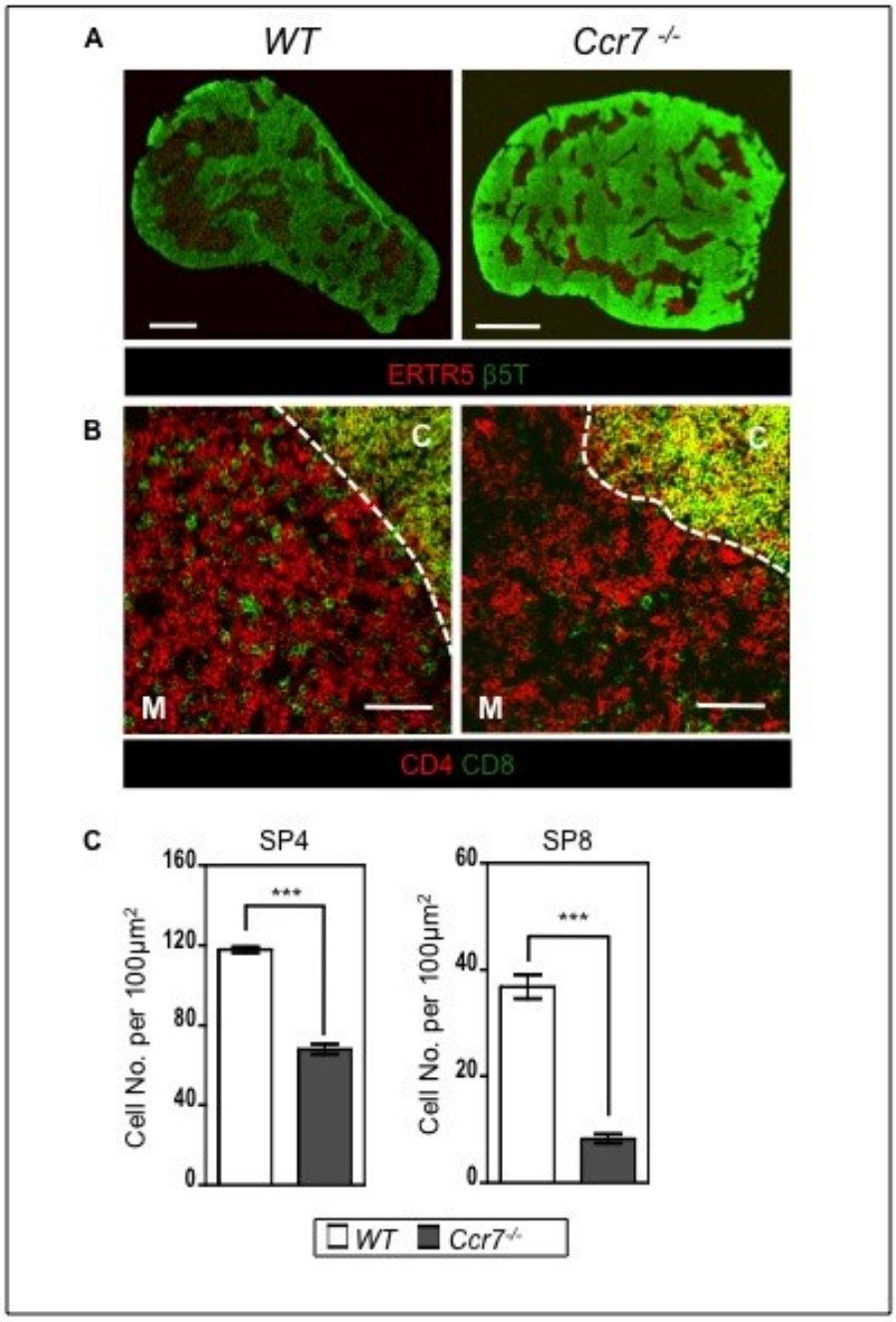
A
WT
Ccr7 -/-
ERTR5 β5T
B
C
M
CD4 CD8
C
SP4
SP8
Cell No. per 100μm²
160
120
80
40
0
60
40
20
0
***
WT
Ccr7-/-

Figure 5. 5 Gene Expression Patterns Of CCR4 Ligands CCL22 and CCL17 In Distinct TEC And DC Populations

Quantitative real time PCR was performed for gene expression analysis of CCL17 (left) or CCL22 (right) on the indicated populations:

(A) TEC populations were isolated from WT BALB/c E15 FTOC samples, cultured 5 to 7 days, via high speed cell sorting:

$CD45^{-}EpCAM^{+}CD40^{+}DEC205^{+}$Mature cTEC (white bars)

$CD45^{-}EpCAM^{+}CD40^{+}DEC205^{-}CD80^{-}$Immature mTEC (right horizontal strip bars)

$CD45^{-}EpCAM^{+}CD40^{+}DEC205^{-}CD80^{+}$Mature mTEC (large square lined bars)

Total FTOC (grey bars)

Total 2-dGuo treated FTOC (checkered bars)

Or isolated from fresh WT BALB/c E15 thymic lobes:

$CD45^{-}$ $EpCAM^{+}CD40^{-}DEC205^{+}$Immature cTEC (left horizontal strips bars)

(B) DC populations were isolated from BALB/c WT adult thymus samples via high speed cell sorting:

$B220^{+}$ $CD11c^{+}$plasmacytoid DC (pDC) (right horizontal strip bars)

$B220^{-}$ $CD11c^{+}$ $Sirp\alpha^{+}$ conventional DC (cDC) (grey bars)

$B220^{-}$ $CD11c^{+}Sirp\alpha^{-}$ cDC (right horizontal strip bars)

Mature mTEC (white bars) were isolated as described in (A)

Error bars indicate the standard error of the mean (SEM) and mRNA levels were normalized to house keeping gene β-actin. Data is from at least two independently sorted biological samples, with each gene analyzed a minimum of two times, with each PCR ran in triplicates to obtain a SEM.

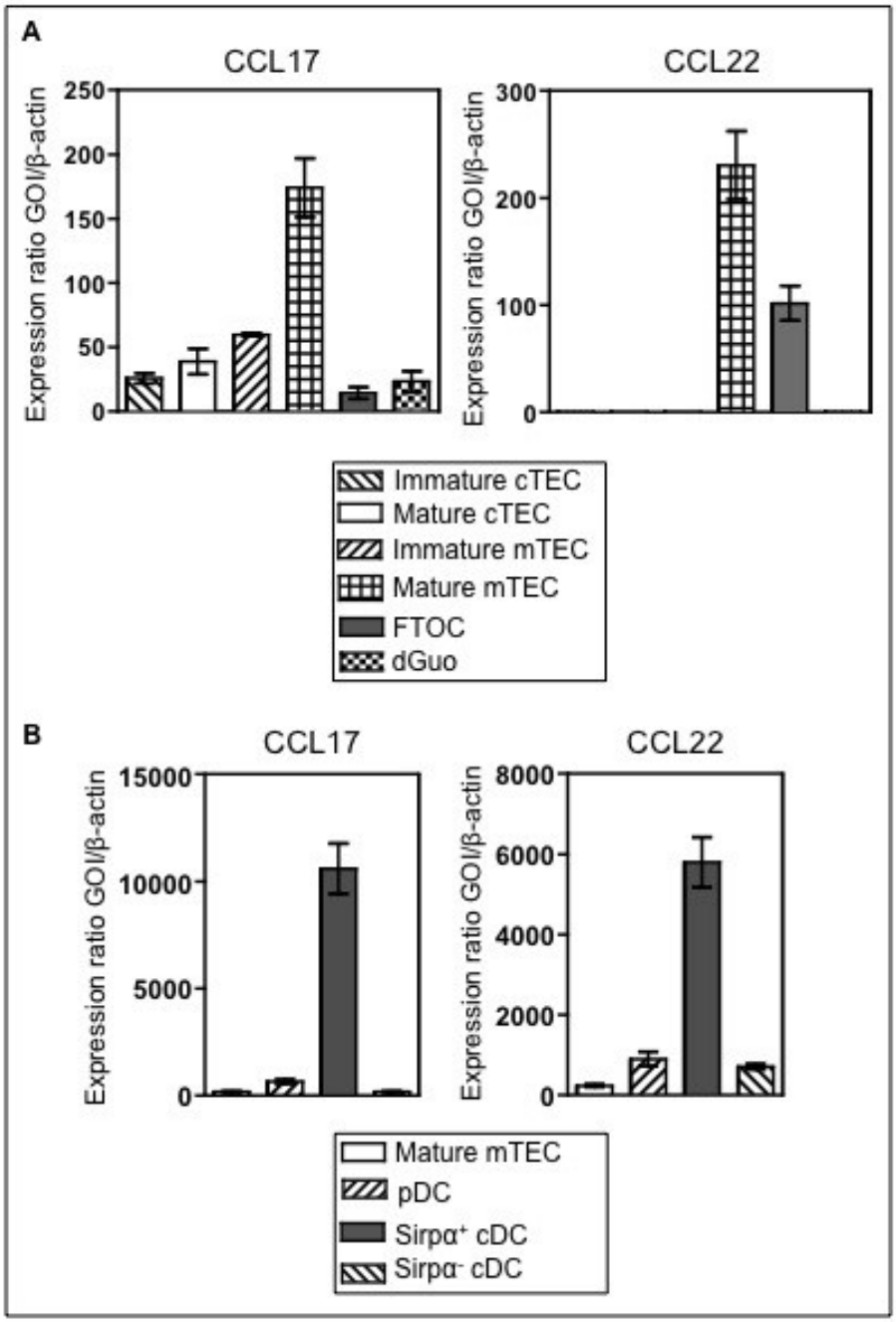
A
CCL17
CCL22
Expression ratio GOI/β-actin
250
200
150
100
50
0
300
200
100
0
Immature cTEC
Mature cTEC
Immature mTEC
Mature mTEC
FTOC
dGuo
B
CCL17
CCL22
Expression ratio GOI/β-actin
15000
10000
5000
0
8000
6000
4000
2000
0
Mature mTEC
pDC
Sirpα+ cDC
Sirpα- cDC

levels within the four distinct TEC populations revealed that both ligands were higher in mature mTEC (Figure 5.5 A). Although CCL22 mRNA was not detectable within any of the additional three TEC subsets, CCL17 mRNA was present in all TEC subsets, although at a considerably lower level than that of the mature mTEC fraction. Examination of CCL17 and CCL22 expression within the three distinct thymic DC subsets: pDC, Sirpα^{+} cDC and Sirpα^{-} cDC, identified striking differences. Both CCL17 and CCL22 mRNA levels were greater in Sirpα^{+} cDC compared to the other two DC populations. In addition, CCL17 and CCL22 mRNA levels were significantly greater within Sirpα^{+} cDC compared to mature mTEC. Collectively this data suggests that while mature mTEC displayed the highest levels of CCL17 and CCL22 mRNA expression amongst TEC populations, Sirpα^{+} cDC expressed the highest CCL17 and CCL22 mRNA levels compared to all thymic populations tested.

To explore the effects of the absence of CCR4 expression on both thymocyte development and the intrathymic distribution of SP4 and SP8 lineages, we analysed *Ccr4*$^{-/-}$ mice (Chvatchko et al., 2000), using an identical experimental strategy to that used for *Ccr7*$^{-/-}$ mice. Collectively, Figures 5.6 to 5.9 display detailed analysis of T cell development and intrathymic thymocyte positioning in the thymus of adult *Ccr4*$^{-/-}$ mice, compared to their WT counterparts. No discernable differences were seen between WT and *Ccr4*$^{-/-}$ mice, including the generation of mature CD69^{-} Qa2^{+} SP4 and SP8 cohorts (Figure 5.7), along with the differentiation of CD25^{+} FoxP3^{-} nTreg precursors and their CD25^{+} FoxP3^{+} nTreg progeny (Figure 5.8), indicating that CCR4 is not essential during intrathymic T cell development. In addition, no significant reductions to medullary size or perturbed SP4 or SP8 thymocyte positioning were observed within *Ccr4*$^{-/-}$ mice (Figure 5.9), ruling out an essential role for this chemokine receptor in cortex-to-medulla migration.

Figure 5. 6 Grossly Normal T cell Development In CCR4 Deficient Mice

Adult *Ccr4*$^{-/-}$ or WT thymocyte cell suspensions were isolated and absolute cell numbers obtained, before staining for flow cytometry analysis.

The absolute numbers (AN) of each distinct population was calculated per mouse from the total thymocte cell count and the percentage of each population acquired via flow cytometry analysis. The AN of each distinct population was displayed as a mean bar graph from WT (white bars) or *Ccr4*$^{-/-}$(grey bars) samples, with data representing x6 independent mice per condition and the error bars denoting the SEM. A student's two tailed unpaired T test was performed on all results, where ns denoted a non-significant difference, as $P > 0.05$.

(A) The absolute cell count of total WT or *Ccr4*$^{-/-}$ total thymus samples.
(B) WT (top) and *Ccr4*$^{-/-}$ (bottom) total cell samples were explored for CD4 versus CD8 surface expression, displayed as a contour plot, or TCRβ and CD69 expression levels, displayed as histograms. The numbers depict the frequency of cells within each gate.
(C) The AN of $CD4^{-}CD8^{-}$ DN, $CD4^{+}$ $CD8^{+}$ DP, $TCR\beta^{high}$ $CD4^{+}CD8^{-}$ SP and $TCR\beta^{high}$ $CD8^{+}CD4^{-}$ SP thymocyte cohorts from WT or *Ccr4*$^{-/-}$samples.
(D) The $CD4^{+}$ $CD8^{+}$ DP population was separated on the basis of their CD69 expression and the AN of $CD69^{-}$ versus $CD69^{+}$ DP subsets calculated and displayed from WT or *Ccr4*$^{-/-}$ cell suspensions.

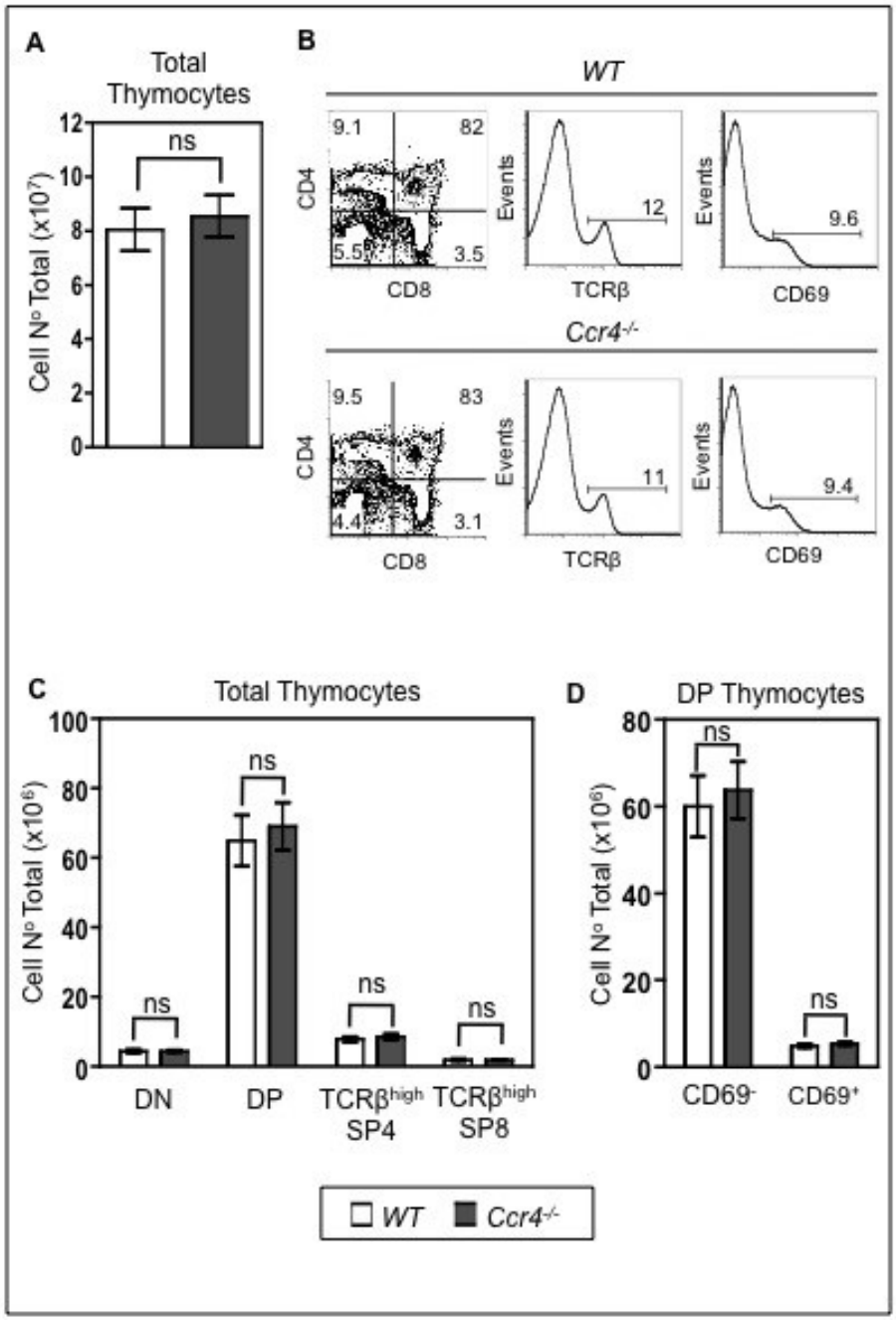
A
Total Thymocytes
ns
Cell Nº Total (x10⁷)
12
10
8
6
4
2
0
B
WT
9.1
82
5.5
3.5
CD4
CD8
Events
12
TCRβ
9.6
CD69
Ccr4-/-
9.5
83
4.4
3.1
11
9.4
C
Total Thymocytes
Cell Nº Total (x10⁶)
100
80
60
40
20
0
ns
DN
DP
TCRβhigh SP4
TCRβhigh SP8
D
DP Thymocytes
CD69-
CD69+
WT
Ccr4-/-

Figure 5. 7 Conventional SP4 and SP8 T Cell Development Is Not Disrupted In CCR4 Deficient Mice

Thymocytes from adult WT (top) or *Ccr4*$^{-/-}$ (bottom) mice were isolated and stained for flow cytometry analysis. The Qa2 and CD69 expression was explored within: (A) TCRβ^{high} SP4 population, or (C) TCRβ^{high} SP8 subset, and represented as contour FACS plots.

The percentages (top) and AN (bottom) of (B) SP4 populations: CD69^{+} Qa2^{-} TCRβ^{high} SP4 (left) and CD69^{-} Qa2^{+} TCRβ^{high} SP4 (right), or (D) SP8 populations: CD69^{+} Qa2^{-} TCRβ^{high} SP8 (left) and CD69^{-} Qa2^{+} TCRβ^{high} SP8 (right), were calculated per mouse and displayed as bar graphs. Each bar graph represents the mean percentage or ANof thymocyte subsets recovered from x6 individual WT (white bars) or *Ccr4*$^{-/-}$ (gray bars) mice. The standard error bars display the SEM, and a student's two tailed unpaired T test was performed on all results, where ns denoted a non-significant difference, as $P > 0.05$.

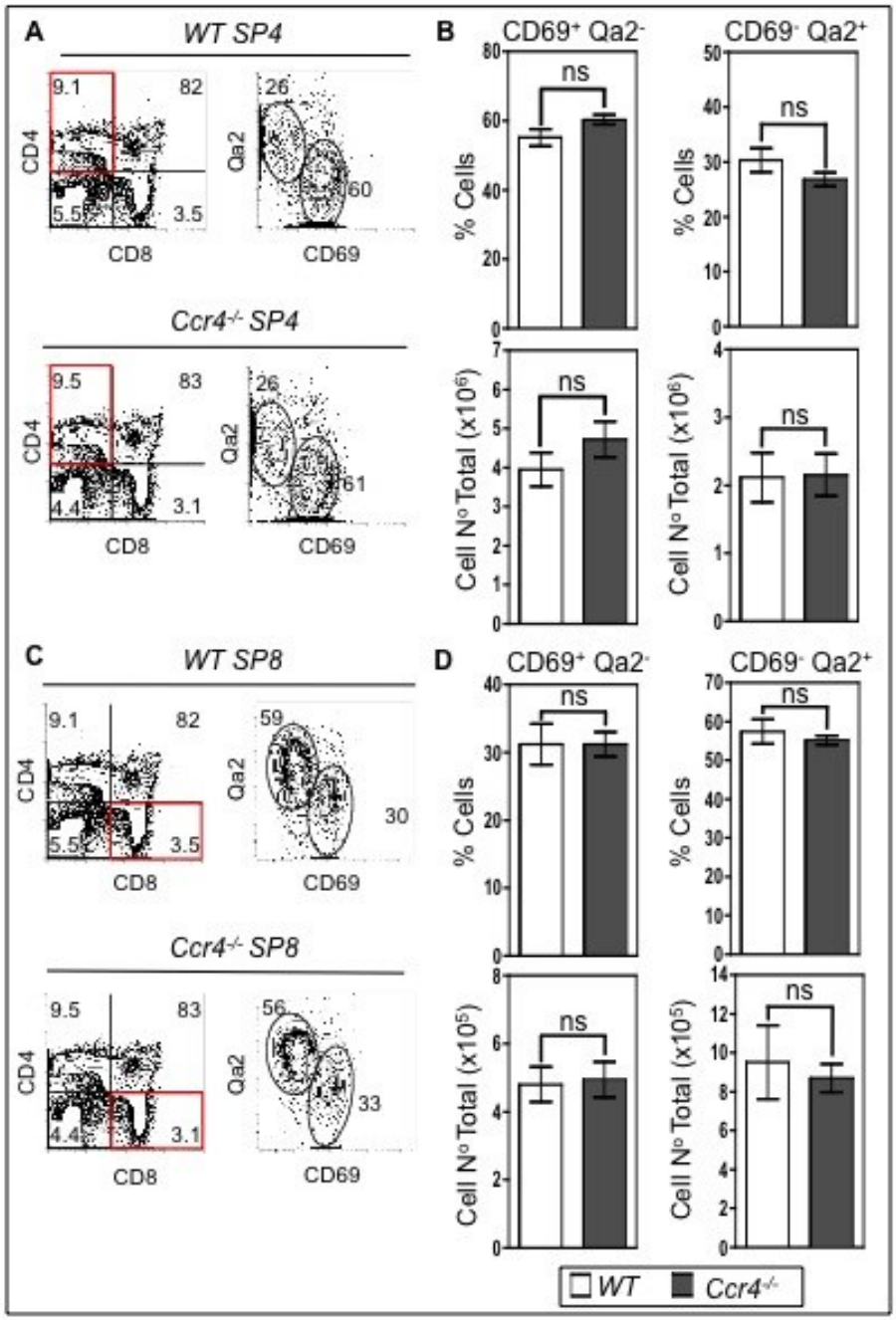
A
WT SP4
9.1
82
5.5
3.5
CD4
CD8
26
60
Qa2
CD69
Ccr4-/- SP4
9.5
83
4.4
3.1
26
61
B
CD69+ Qa2-
CD69- Qa2+
ns
% Cells
Cell Nº Total (x10⁶)
C
WT SP8
9.1
82
5.5
3.5
59
30
Ccr4-/- SP8
9.5
83
4.4
3.1
56
33
D
CD69+ Qa2-
CD69- Qa2+
ns
% Cells
Cell Nº Total (x10⁵)
WT
Ccr4-/-

Figure 5. 8 The Frequency Of Foxp3^{+} CD25^{+} Treg Or CD25^{+} Foxp3^{-} Treg Precursors Is Not Disrupted In CCR4 Deficient Mice

(A) Thymocytes recovered from adult WT (top) or *Ccr4*$^{-/-}$ (bottom) mice were isolated and analyzed for intracellular staining of Foxp3 within the TCRβ^{high} SP4 population. The Foxp3^{-} fraction of TCRβ^{high} SP4 thymocytes was also explored for their surface expression levels of CD25.

(B) The percentages (top) and AN (bottom) of the Foxp3^{+} TCRβ^{high} SP4 Treg subset (left) and Foxp3^{-} CD25^{+} TCRβ^{high} SP4 Treg precursors (right) were calculated from WT (white bars) and *Ccr4*$^{-/-}$ (gray bars) hosts and displayed as mean bar graphs, representing x6 individual mice per condition. The standard error bars indicate the SEM, and a student's two tailed unpaired T test was performed on all results, where ns denoted a non-significant difference, where $P > 0.05$.

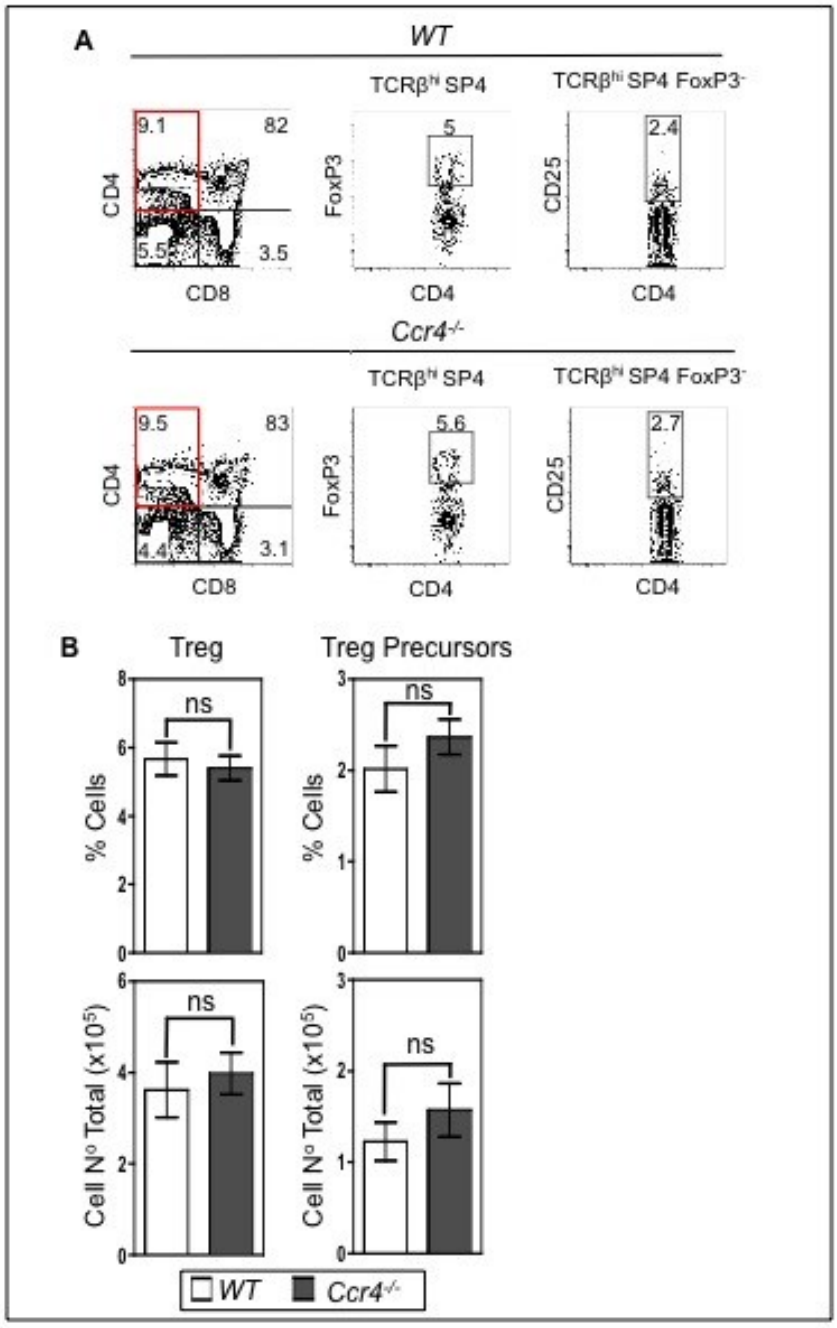
A
WT
TCRβhi SP4
TCRβhi SP4 FoxP3-
9.1
82
5.5
3.5
CD4
CD8
5
FoxP3
CD4
2.4
CD25
CD4
Ccr4-/-
TCRβhi SP4
TCRβhi SP4 FoxP3-
9.5
83
4.4
3.1
CD4
CD8
5.6
FoxP3
CD4
2.7
CD25
CD4
B
Treg
Treg Precursors
% Cells
ns
% Cells
ns
Cell N° Total (x10^5)
ns
Cell N° Total (x10^5)
ns
WT
Ccr4-/-

Figure 5. 9 Normal Accumulation Of SP4 And SP8 Thymocytes Within Medullary Regions In CCR4 Deficient Mice

WT and *Ccr4*$^{-/-}$ adult thymi were frozen for confocal analysis. 7μm whole thymus sections were cut and stained for immunofluorescence confocal analysis.

(A) Tile scans of a series of low resolution images are shown for whole thymus sections from WT (left) and *Ccr4*$^{-/-}$ (right) host, staining for ERTR5 and β5T. Bars represent a scale of 1mm

(B) Higher resolution images of smaller thymic areas for the analysis of CD4 and CD8 staining. The white dashed line denotes the corticomedullary junction, C=cortex and M=medulla. Bars represent a scale of 100 μm

(C) The number of SP4 (left graph) or SP8 (right graph) cells within a 100μm x 100μm square medullary area were counted within x3 regions per section, on x4 serial section images per host. The numbers acquired from x3 WT (white bars) and x3 *Ccr4*$^{-/-}$ (grey bars) hosts are displayed as mean bar graphs. The standard error bars indicate the SEM, and a student's two tailed unpaired T test was performed on all results, where * denoted a significant difference ($P = < 0.05$).

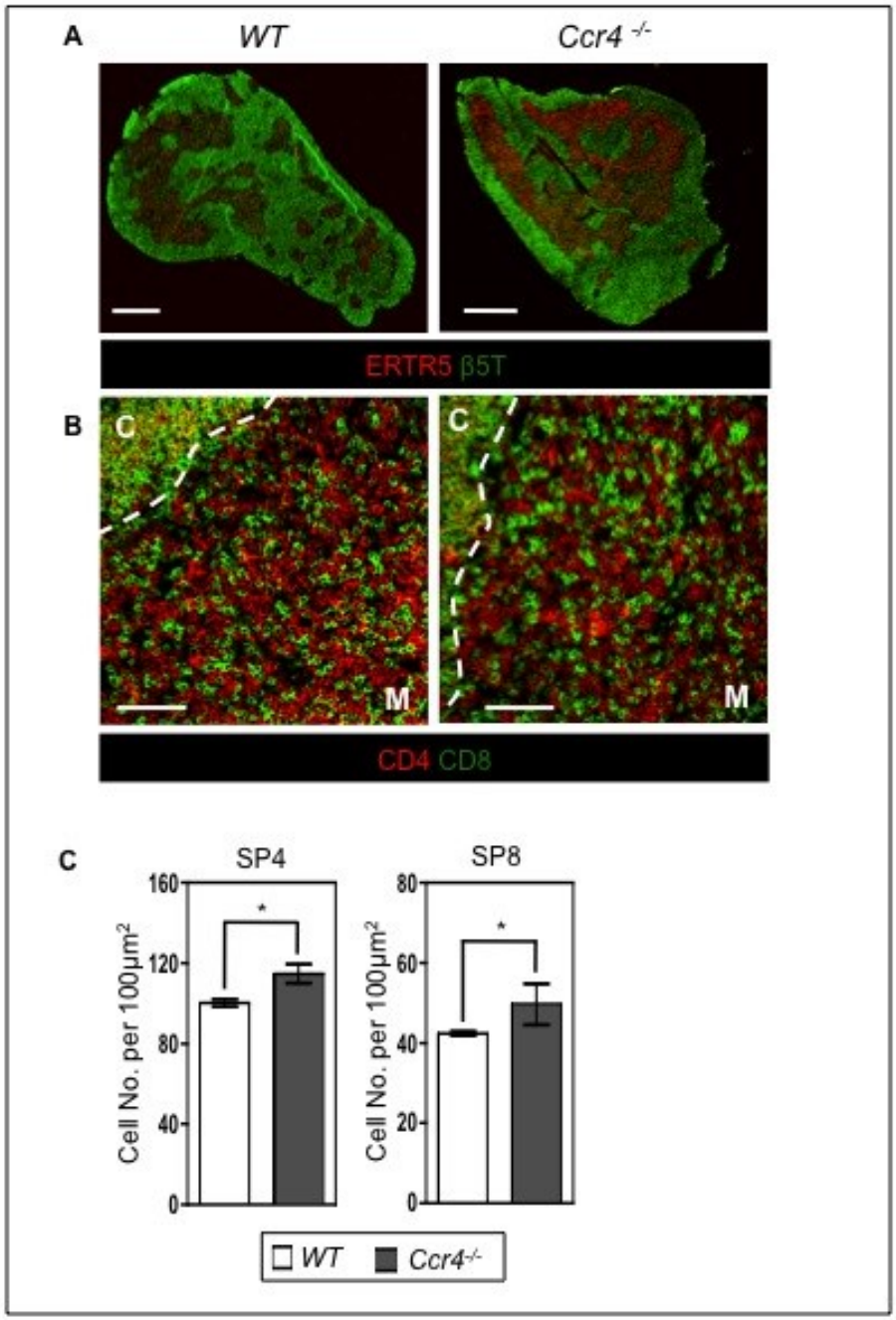
A
WT
Ccr4 -/-
ERTR5 β5T
B
C
C
M
M
CD4 CD8
C
SP4
SP8
160
120
80
40
0
80
60
40
20
0
Cell No. per 100μm²
Cell No. per 100μm²
*
*
WT
Ccr4-/-

To further investigate a potential subtle role for CCR4 in adult intrathymic T cell development, we established mixed bone marrow chimaeras with WT or *Ccr4*$^{-/-}$ bone marrow samples. Lethally irradiated CD45.1^{+} hosts were reconstituted with an intra-venous transfer mixture of BM cells from WT CD45.1^{+} donors and either CD45.2^{+} WT or CD45.2^{+} *Ccr4*$^{-/-}$ donors, at a 1:1 input ratio. Initially hosts received total BM cells from WT or *Ccr4*$^{-/-}$ donors, but on repeat, BM samples were T cell depleted prior to transfer. Results are displayed from both total and T cell depleted BM chimera mice. Chimera hosts were sacrificed 5 weeks post BM reconstitution and thymocyte development and intrathymic position of CD45.1^{+} WT or CD45.2^{+} *Ccr4*$^{-/-}$ donor cellswas explored.

Initial analysis of thymocyte development between the WT and *Ccr4*$^{-/-}$ donors in competitive environments revealed CD45.2^{+} *Ccr4*$^{-/-}$ thymocytes displayed no disruption to their development program compared to their CD45.1^{+} WT counterparts (Figure 5.10-12), including successful generation of the most mature CD69^{-} Qa2^{+} SP4 and SP8 cohorts (Figure 5.11), along with the differentiation of CD25^{+} FoxP3^{-} nTreg precursors and their CD25^{+} FoxP3^{+} nTreg progeny (Figure 5.12). Both T cell depleted and total BM reconstitutions displayed comparable unaffected phenotypical effects on the T cell development program. Due to small sample sizes no statistical analysis was performed and more extensive analysis is needed to draw any firm conclusions from this experimental model. The study of thymocyte localization within this competitive microenvironment also revealed no disruption to the positioning of *Ccr4*$^{-/-}$ SP4 and SP8 cells compared to WT counterparts (Figure 5.13).

Figure 5. 10 *Ccr4*$^{-/-}$ Thymocyte Maturation Within A Competitive Microenvironment With Their WT Counterparts

(A) Lethally irradiated WT CD45.1^{+} hosts were intravenously (IV) injected with a mixture of adult bone marrow cells (total BM or T cell depleted BM) from a WT CD45.1^{+} donor combined with either *Ccr4*$^{-/-}$ CD45.2^{+} or control WT CD45.2^{+} donor cells (littermate controls), at a 1:1 ratio. In this experimental setting *Ccr4*$^{-/-}$ thymocytes develop within a WT thymic microenvironment within competition with WT developing thymocytes. 5 weeks post bone marrow reconstitution mice were sacrificed and the thymus analysed to explore developmental differences between the WT CD45.2^{+} and *Ccr4*$^{-/-}$ CD45.2^{+}donor populations. Thymocytes were analysed for their developmental status by flow cytometry analysis and their intrathymic localization determined via immunofluorescence confocal analysis

(B) Thymocytes were isolated from non-T cell depleted WT bone marrow reconstituted hosts. The CD45.2^{+} WT (top) or CD45.2^{+} *Ccr4*$^{-/-}$ (bottom) donor thymocytes were identified from a histogram and their CD4 versus CD8 surface expression was explored and displayed as a contour plot. The TCRβ expression and CD69 expression levels of total CD45.2^{+} thymocytes was also investigated and displayed as histograms. The numbers depict the percentages of cells within each gate.

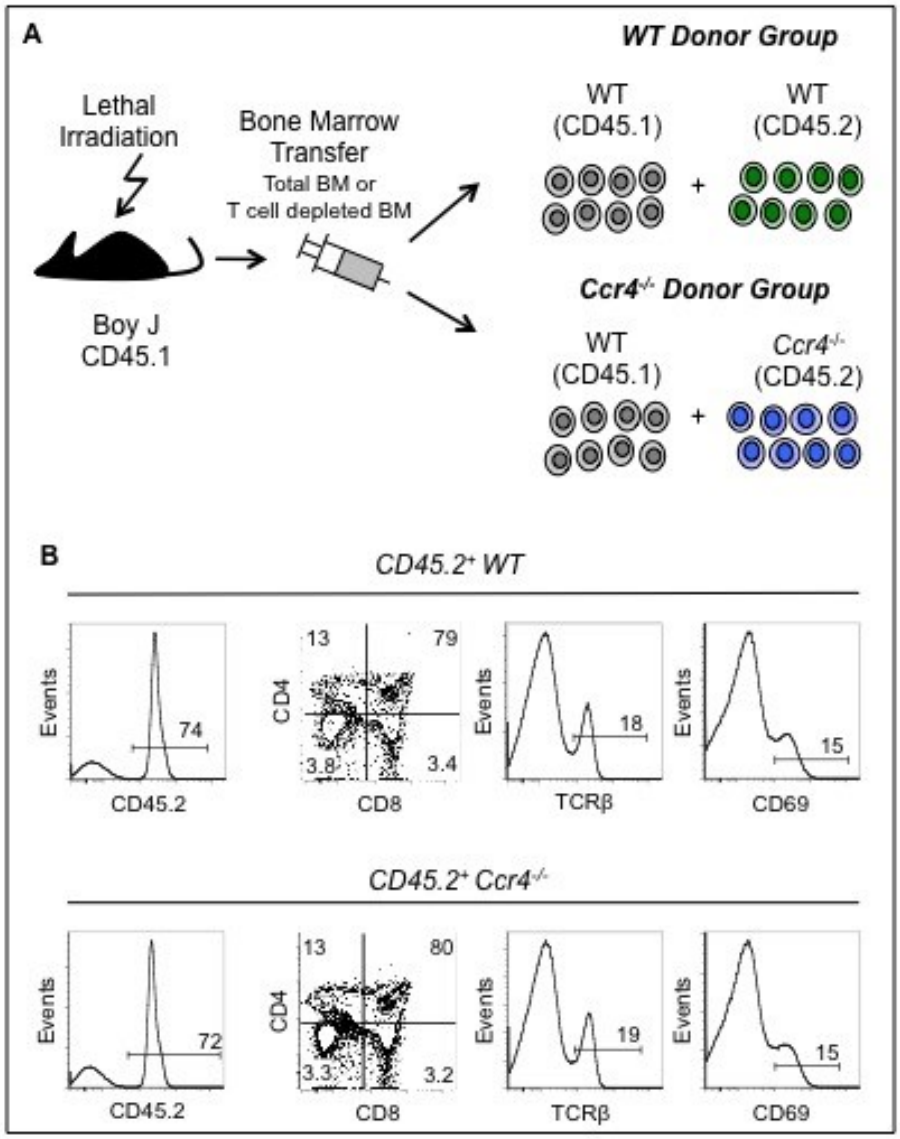
A
WT Donor Group
Lethal Irradiation
Bone Marrow Transfer
Total BM or T cell depleted BM
Boy J CD45.1
WT (CD45.1)
WT (CD45.2)
+
Ccr4-/- Donor Group
WT (CD45.1)
Ccr4-/- (CD45.2)
+
B
CD45.2+ WT
Events
74
CD45.2
CD4
13
79
3.8
3.4
CD8
Events
18
TCRβ
Events
15
CD69
CD45.2+ Ccr4-/-
Events
72
CD45.2
CD4
13
80
3.3
3.2
CD8
Events
19
TCRβ
Events
15
CD69

Figure 5. 11 CCR4 Deficient Thymocytes Do Not Present With Altered Conventional SP4 And SP8 T Cell Development In The Presence Of WT Competition

CD45.2^{+} WT donor thymocytes (left) or CD45.2^{+} *Ccr4*$^{-/-}$ donor thymocytes (right) from non-T cell depleted bone marrow reconstituted WT hosts were identified and their Qa2 and CD69 expression was explored within: (A) TCRβ^{high} CD4^{+} SP subsets or (D) TCRβ^{high} CD8^{+} SP subsets, represented as contour FACS plots.

The percentages of CD45.2^{+} WT (white bars) or CD45.2^{+} *Ccr4*$^{-/-}$ (grey bars) populations:
CD69^{+} Qa2^{-} TCRβ^{high} SP4 (left) and CD69^{-} Qa2^{+} TCRβ^{high} SP4 (right) from (B) total BM reconstitution or (C) T cell depleted BM reconstitution.
CD69^{+} Qa2^{-} TCRβ^{high} SP8 (left) and CD69^{-} Qa2^{+} TCRβ^{high} SP8 (right) from (E) total BM reconstituted hosts or (F) T cell depleted BM reconstituted hosts.

Percentages are displayed as mean bars graphs, representing x3 individual hosts per non-T cell depleted BM condition, and x 2 hosts per T cell depleted BM condition. The standard error bars display the SEM.

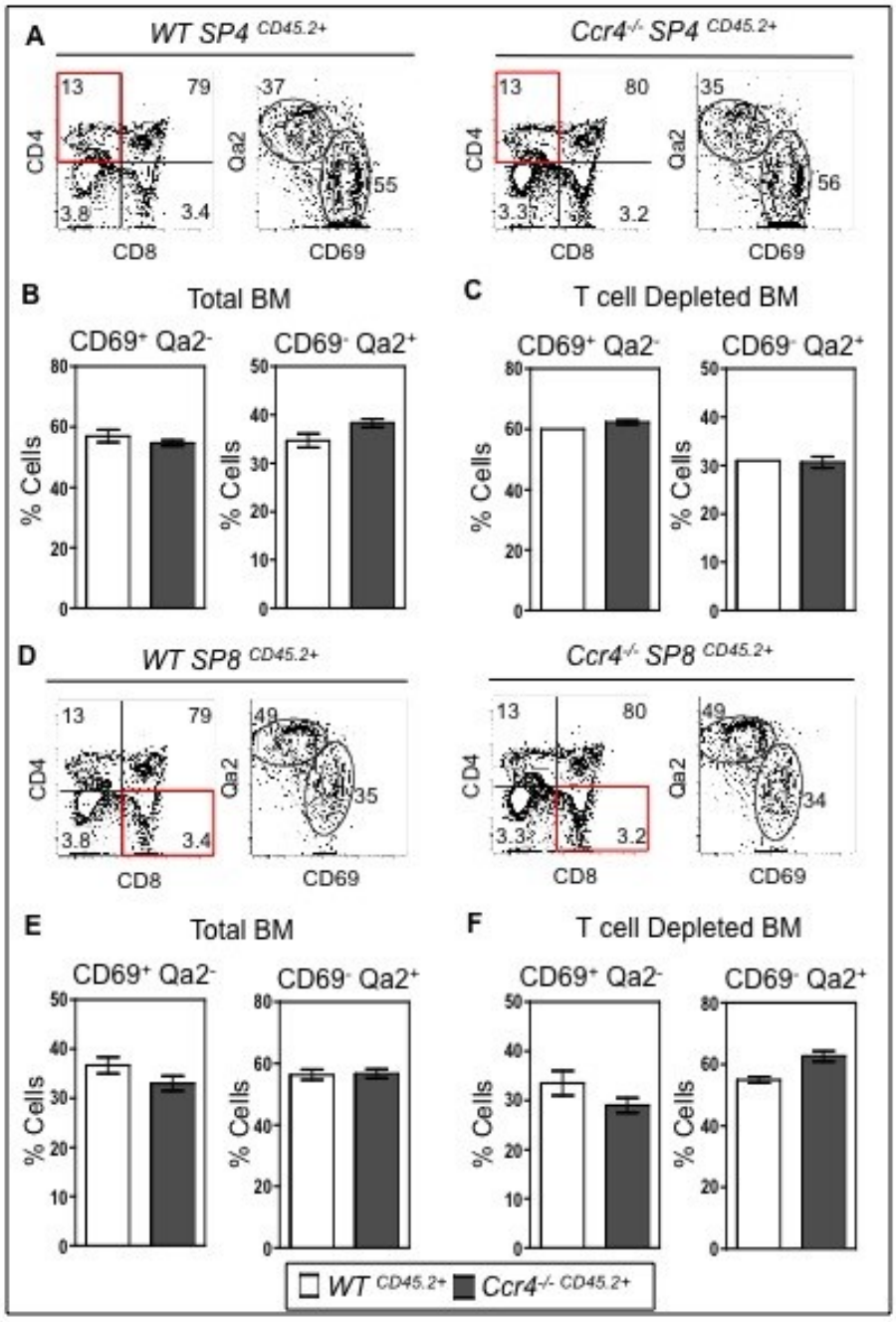
A
WT SP4 CD45.2+
Ccr4-/- SP4 CD45.2+
13
79
3.8
3.4
CD4
CD8
37
55
Qa2
CD69
13
80
3.3
3.2
35
56
B
Total BM
C
T cell Depleted BM
CD69+ Qa2-
CD69- Qa2+
% Cells
D
WT SP8 CD45.2+
Ccr4-/- SP8 CD45.2+
49
35
34
E
Total BM
F
T cell Depleted BM
WT CD45.2+
Ccr4-/- CD45.2+

Figure 5. 12 CCR4 Deficient Thymocytes Do Not Display Reduced Frequencies Of Foxp3^{+} CD25^{+} Treg Or CD25^{+} Foxp3^{-} Treg Precursors In The Presence Of WT Competition

(A) CD45.2^{+} WT donor thymocytes (top) or CD45.2^{+} *Ccr4*$^{-/-}$ donor thymocytes (bottom) from non-T cell depleted bone marrow reconstituted WT hosts were identified by flow cytometry and analyzed for intracellular staining of Foxp3 within the TCRβ^{high} SP4 population. The Foxp3^{-} fraction of TCRβ^{high} SP4 thymocytes was also explored for their surface expression levels of CD25. All data is represented as contour FACS plots.

The percentages of CD45.2^{+} WT (white bars) or CD45.2^{+} *Ccr4*$^{-/-}$ (grey bars) donor cells within the Foxp3^{+} TCRβ^{high} SP4 Treg subset (left) or Foxp3^{-} CD25^{+} TCRβ^{high} SP4 nTreg precursor population (right), recovered from (B) total BM reconstituted hosts or (C) T cell depleted BM reconstituted hosts.

Results are displayed as mean bar graphs, representing x3 individual hosts per non-T cell depleted BM condition, and x 2 hosts per T cell depleted BM condition. The standard error bars display the SEM.

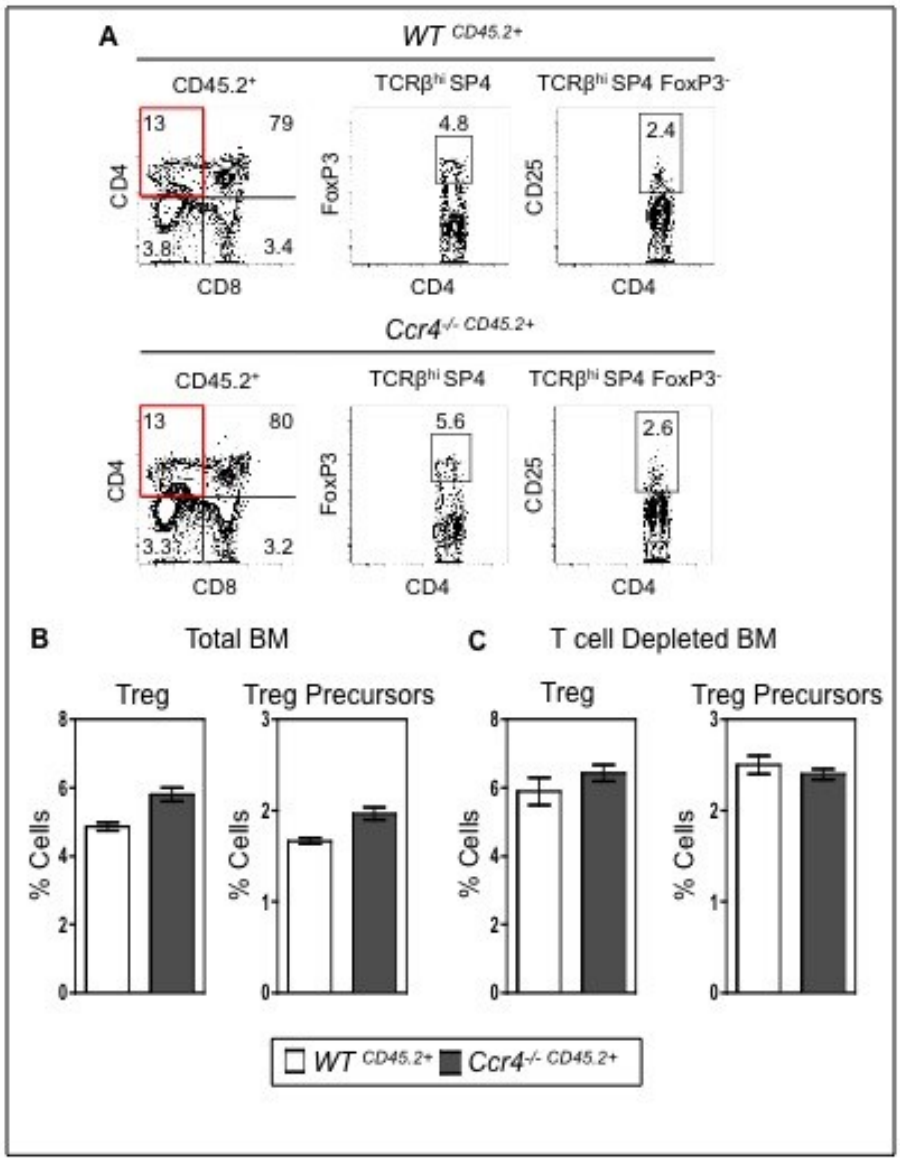
A
WT CD45.2+
CD45.2+
TCRβhi SP4
TCRβhi SP4 FoxP3-
13
79
3.8
3.4
CD4
CD8
4.8
FoxP3
CD4
2.4
CD25
CD4
Ccr4-/- CD45.2+
CD45.2+
TCRβhi SP4
TCRβhi SP4 FoxP3-
13
80
3.3
3.2
CD4
CD8
5.6
FoxP3
CD4
2.6
CD25
CD4
B
Total BM
C
T cell Depleted BM
Treg
Treg Precursors
Treg
Treg Precursors
% Cells
% Cells
% Cells
% Cells
WT CD45.2+
Ccr4-/- CD45.2+

Figure 5. 13 Grossly Normal Intrathymic Accumulation Of CCR4 Deficient Thymocytes in The Presence Of WT Competition

WT host thymi receiving either: CD45.1^{+} WT + CD45.2^{+} WT T cell depleted bone marrow or CD45.1^{+} WT + CD45.2^{+} *Ccr4*$^{-/-}$ T cell depleted bone marrow (see model 5.10) were frozen for confocal analysis. 7μm thymus sections were cut and stained for CD45.1, CD45.2 and the medullary marker ERTR5.

(A) High resolution images of the cortex (right) or medulla (right) from CD45.1^{+} WT + CD45.2^{+} WT hosts (top) or CD45.1^{+} WT + CD45.2^{+} *Ccr4*$^{-/-}$ host (bottom). C=cortex and M=medulla. Bars represent a scale of 100 μm

(B) The number of CD45.2^{+} WT donor thymocytes (white bars) or CD45.2^{+} *Ccr4*$^{-/-}$ donor thymocytes (grey bars) within a 100μm x 100μm area of either cortical (left) or medullary regions (right) were counted within x3 regions per section, on x4 serial section images per host. A total of x3 hosts per condition were analysed and cell counts are displayed as mean bar graphs. The standard error bars indicate the SEM and a student's two tailed unpaired T test was performed on all results, where ns denoted a non-significant difference, ($P > 0.05$) and * denoted a significant difference ($P = < 0.05$).

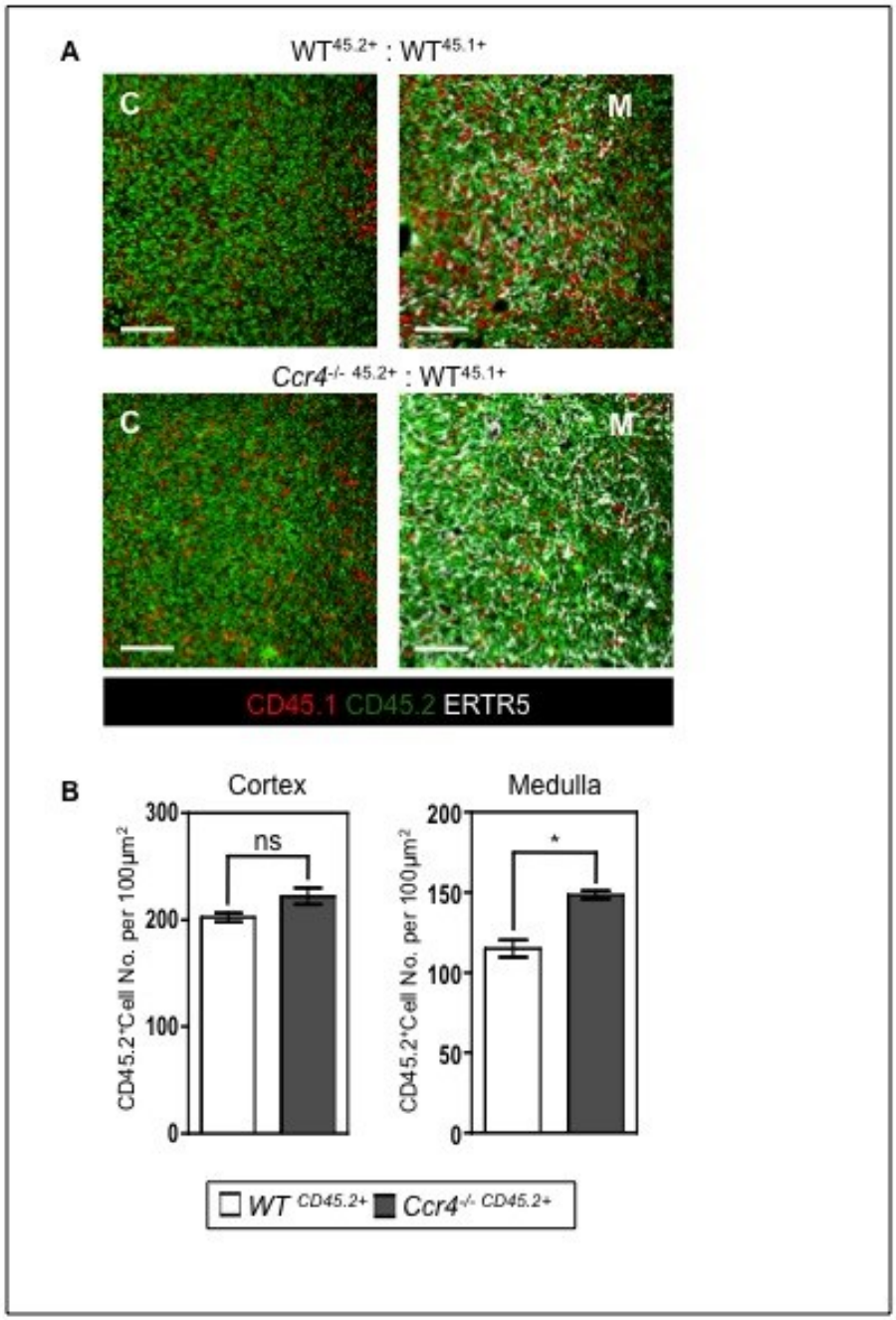
A
WT45.2+ : WT45.1+
C
M
Ccr4-/- 45.2+ : WT45.1+
C
M
CD45.1 CD45.2 ERTR5
B
Cortex
Medulla
ns
*
CD45.2+Cell No. per 100μm2
300
200
100
0
200
150
100
50
0
WT CD45.2+
Ccr4-/- CD45.2+

5.2.3 CCR4 x CCR7 Double Deficient Mice Display Disrupted T Cell Development And Intrathymic Localisation of SP4/SP8 Thymocytes

Although establishing competitive bone marrow chimeras was aimed at eliminating possible compensatory chemokine receptors that may facilitate unperturbed thymocyte development and cortex to medulla migration in *Ccr4*$^{-/-}$ mice, we were interested to explore this further. As both previously published data (Kwan and Killeen, 2004; Ueno et al., 2004) and our own analysis (Figure 5.1 to 5.4) shows CCR7 drives cortex to medulla migration of SP4 and SP8 thymocytes, we speculated that the lack of CCR4 may be partially compensated by the presence of CCR7. We therefore generated *Ccr4*$^{-/-}$ x *Ccr7*$^{-/-}$ double deficient mice and in preliminary experiments explored thymocyte development and intrathymic localization of SP4 and SP8 lineages. Analysis of thymocyte development within *Ccr4*$^{-/-}$ x *Ccr7*$^{-/-}$ double deficient mice revealed striking differences in comparison to their WT counterparts (Figure 5.14), including significantly reduced thymocyte cellularity, with an approximate one-third decline to the total cell count compared to their WT controls (Figure 5.14 A). Despite this, no major disruption of CD4 or CD8 thymocyte subsets was found (Figure 5.14 B and D), although *Ccr4*$^{-/-}$ x *Ccr7*$^{-/-}$ mice perhaps showed an increase in the percentage of the TCRβ^{high} SP4 fraction (Figure 5.14 B and C- top graph).

Analysis of the generation of immature CD69^{+} Qa2^{-} versus mature CD69^{-} Qa2^{+} fractions of convention SP4 cells in *Ccr4*$^{-/-}$ x *Ccr7*$^{-/-}$ mice revealed differences in the proportions of thymocytes at these two maturational stages, compared to the WT controls (Figure 5.15), with *Ccr4*$^{-/-}$ x *Ccr7*$^{-/-}$ mice showing an increase in the percentages of CD69^{+} Qa2^{-} cells and a percentage decrease in CD69^{-} Qa2^{+} SP4 thymocytes (Figure 5.15 B). This preliminarily

Figure 5. 14 Absence of CCR4 And CCR7 Results In Decreased Thymocyte Cell Numbers And An Increase In The Frequency Of The TCRβ^{high} SP4 Cohort

Adult *Ccr4*$^{-/-}$ x *Ccr7*$^{-/-}$ or WT thymocyte cell suspensions were isolated and absolute cell numbers obtained before staining for flow cytometry analysis.

The AN of each distinct population was calculated per mouse from the total thymocte cell count and the percentage of each population acquired via flow cytometry analysis. The AN of each distinct population was displayed as a mean bar graph from WT (white bars) or *Ccr4*$^{-/-}$ x *Ccr7*$^{-/-}$ (grey bars) samples, with data representing x6 independent mice per condition and the error bars denoting the SEM. A student's two tailed unpaired T test was performed on all results, where ns denoted a non-significant difference ($P > 0.05$) and *, ** or *** indicate a significant difference (* = $P < 0.05$, ** = $P < 0.01$ and ***= $P < 0.001$).

(A) The absolute cell count of total WT or *Ccr4*$^{-/-}$ x *Ccr7*$^{-/-}$ thymus samples.
(B) The CD4 versus CD8 surface expression on total thymocytes was explored in WT (top) and *Ccr4*$^{-/-}$ x *Ccr7*$^{-/-}$ (bottom) cell samples and displayed as contour plots. The TCRβ expression and CD69 expression levels of total thymocytes was also investigated and displayed as histograms. The numbers depict the frequency of cells within each gate.
(C) The percentages (top) and AN (bottom) of CD4^{-}CD8^{-} DN, CD4^{+} CD8^{+} DP, TCRβ^{high} CD4^{+}CD8^{-} SP and TCRβ^{high} CD8^{+}CD4^{-} SP thymocyte subsets from WT or *Ccr4*$^{-/-}$ x *Ccr7*$^{-/-}$ samples.
(D) The CD4^{+} CD8^{+} DP population was separated on the basis of their CD69 expression and the percentages (top) or AN (bottom) of CD69^{-} versus CD69^{+} DP displayed from WT or *Ccr4*$^{-/-}$ x *Ccr7*$^{-/-}$cell suspensions.

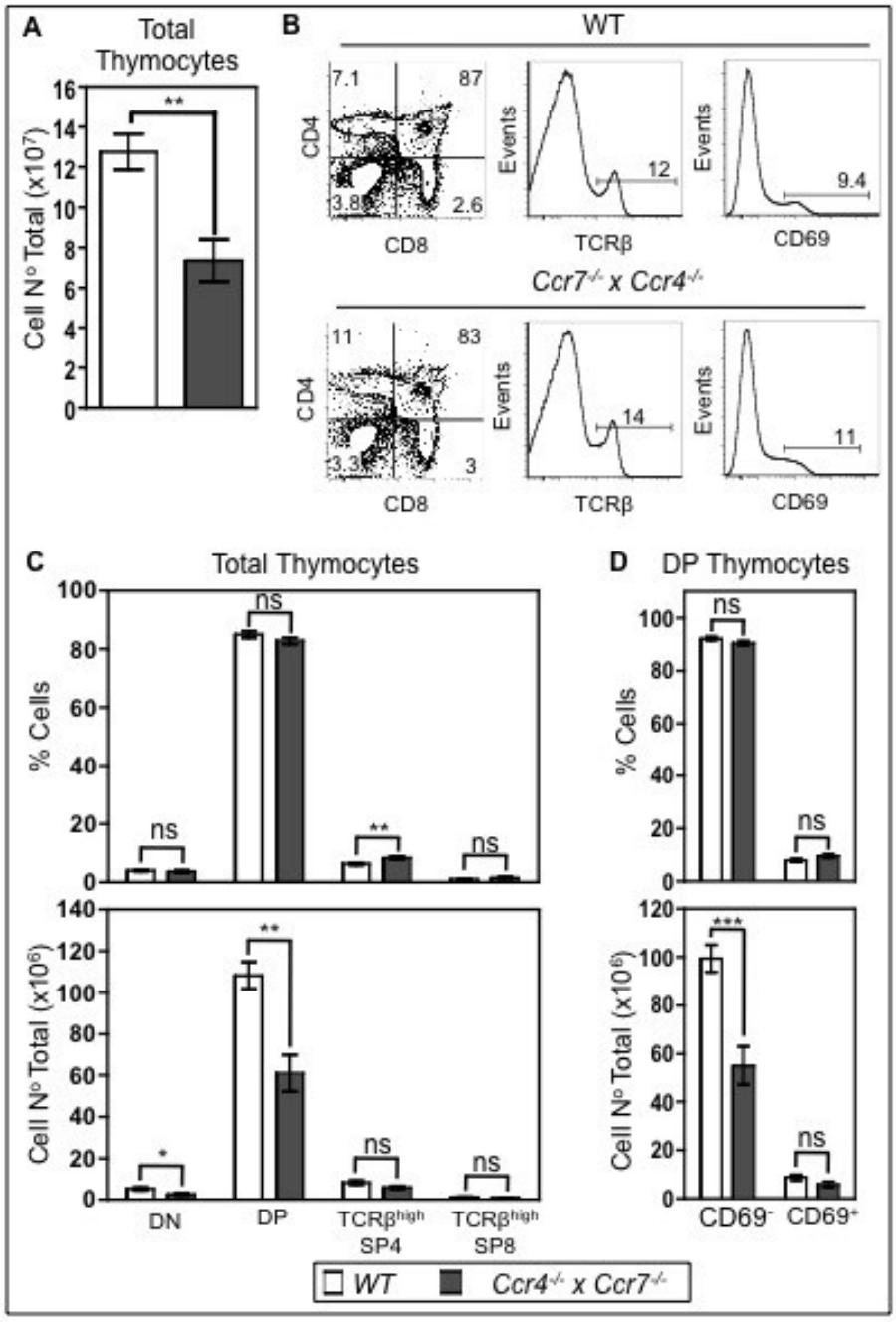
A
Total Thymocytes
Cell Nº Total (x10⁷)
**
B
WT
7.1
87
3.8
2.6
CD4
CD8
Events
12
TCRβ
9.4
CD69
Ccr7-/- x Ccr4-/-
11
83
3.3
3
14
11
C
Total Thymocytes
% Cells
ns
**
Cell Nº Total (x10⁶)
*
DN
DP
TCRβhigh SP4
TCRβhigh SP8
D
DP Thymocytes
***
CD69-
CD69+
WT
Ccr4-/- x Ccr7-/-

Figure 5. 15 Conventional SP4 T Cell Development Is Disrupted In A CCR4 x CCR7 Double Deficient Mice

(A) Thymocytes from adult WT (top) or *Ccr4*$^{-/-}$ x *Ccr7*$^{-/-}$ (bottom) mice were isolated and stained for flow cytometry analysis. The Qa2 and CD69 expression was explored within the TCRβ^{high} SP4 population and represented as contour FACS plots.

(B) The percentages (top) and AN (bottom) of SP4 populations: total TCRβ^{high} SP4 thymocytes (left), CD69^{+} Qa2^{-} TCRβ^{high} SP4 (middle) and CD69^{-} Qa2^{+} TCRβ^{high} SP4 (right), were calculated per mouse and displayed as bar graphs. Each bar graph represents the mean percentages or AN of thymocyte subsets recovered from x6 individual WT (white bars) or *Ccr4*$^{-/-}$ x *Ccr7*$^{-/-}$ (gray bars) mice. The standard error bars denote the SEM, and a student's two tailed unpaired T test was performed on all results, where ns denoted a non-significant difference ($P > 0.05$) and * or ** indicates a significant difference (*= $P < 0.05$ and **= $P < 0.01$).

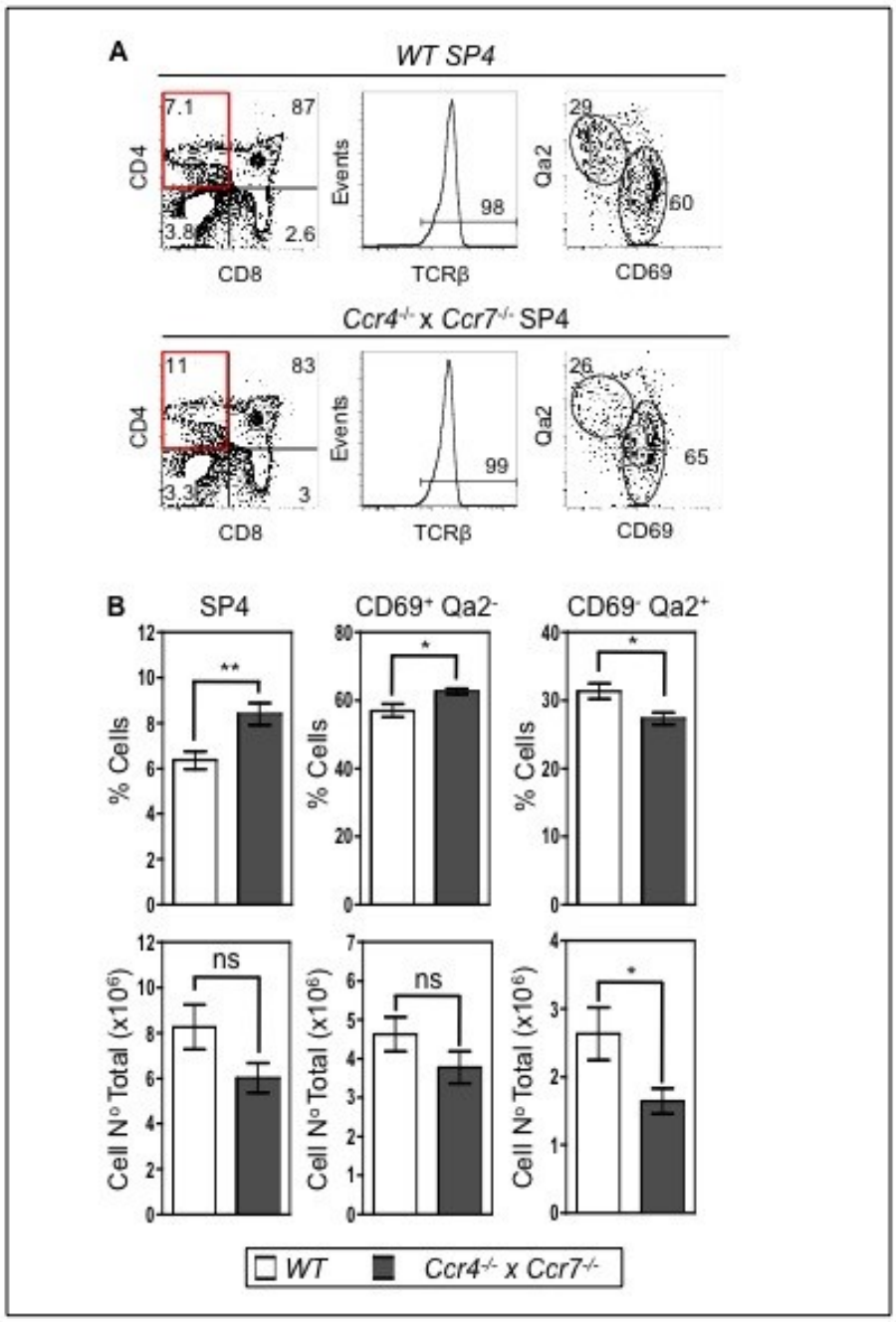
A
WT SP4
7.1
87
3.8
2.6
CD4
CD8
Events
98
TCRβ
Qa2
29
60
CD69
Ccr4-/- x Ccr7-/- SP4
11
83
3.3
3
CD4
CD8
Events
99
TCRβ
Qa2
26
65
CD69
B
SP4
CD69+ Qa2-
CD69- Qa2+
% Cells
Cell Nº Total (x10⁶)
**
*
*
ns
ns
*
WT
Ccr4-/- x Ccr7-/-

analysis of TCRβ^{high} SP4 population, therefore, suggests the absence of both CCR4 and CCR7 disrupts the developmental program of this SP lineage, with the immature versus mature status of this subset skewed toward a CD69^{+} Qa2^{-} phenotype.

Analysis of the equivalent populations within the TCRβ^{high} SP8 thymocyte subset exposed additional variation within *Ccr4*$^{-/-}$ x *Ccr7*$^{-/-}$ mice (Figure 5.16). FACS plots displaying CD69 and Qa2 expression within the *Ccr4*$^{-/-}$ x *Ccr7*$^{-/-}$ TCRβ^{high} SP8 population differed to those obtained from the WT controls (Figure 5.16 A). Overall Qa2 levels appeared higher within the total *Ccr4*$^{-/-}$ x *Ccr7*$^{-/-}$ TCRβ^{high} SP8 population compared to their WT counterparts, with a detectable subset of cells co-expressing very high levels of Qa2 and CD69, not evident within the WT TCRβ^{high} SP8 cohort. The average percentage analysis of the immature versus mature TCRβ^{high} SP8 subsets identified an overall reduction to the percentage of *Ccr4*$^{-/-}$ x *Ccr7*$^{-/-}$ mature CD69^{-} Qa2^{+} TCRβ^{high} SP8 cells, compared to their WT counterparts (Figure 5.16 B). The decline of this mature SP8 fraction was complimentary to the decrease observed in the equivalent population of TCRβ^{high} SP4 thymocytes. In contrast, no alterations were observed to the percentage of immature CD69^{+} Qa2$^{-/intermediate}$ TCRβ^{high} SP8 cells from *Ccr4*$^{-/-}$ x *Ccr7*$^{-/-}$ hosts compared to WT. Collectively, preliminary investigations into SP4 and SP8 thymocyte development within a *Ccr4*$^{-/-}$ x *Ccr7*$^{-/-}$ thymic microenvironment suggest both receptors are essential for successful maturation of both SP conventional lineages.

Analysis of the development of the CD25^{+} FoxP3^{+} nTreg SP4 lineage within the *Ccr4*$^{-/-}$ x *Ccr7*$^{-/-}$ microenvironment also displayed disruptions in the absence of these two receptors. The percentages of *Ccr4*$^{-/-}$ x *Ccr7*$^{-/-}$ CD25^{+} FoxP3^{+} nTreg was significantly increased and the frequency of CD25^{+} FoxP3^{-} nTreg precursors reduced, compared to their WT counterparts

Figure 5. 16 Conventional SP8 T Cell Development Is Disrupted In CCR4 x CCR7 Double Deficient Mice

(A) Thymocytes from adult WT (top) or *Ccr4*$^{-/-}$ x *Ccr7*$^{-/-}$ (bottom) mice were isolated and stained for flow cytometry analysis. The Qa2 and CD69 expression was explored within the TCRβ^{high} SP8 population and represented as contour FACS plots.

(B) The percentages (top) and AN (bottom) of SP8 populations: total TCRβ^{high} SP8 thymocytes (left), CD69^{+} Qa2^{-} TCRβ^{high} SP8 (middle) and CD69^{-} Qa2^{+} TCRβ^{high} SP8 (right), were calculated per mouse and displayed as bar graphs. Each bar graph represents the mean percentages or AN of thymocyte subsets recovered from x6 individual WT (white bars) or *Ccr4*$^{-/-}$ x *Ccr7*$^{-/-}$ (gray bars) mice. The standard error bars denote the SEM, and a student's two tailed unaired T test was performed on all results, where ns denoted a non-significant difference ($P > 0.05$) and * or *** indicate a significant difference (* = $P < 0.05$ and ***= $P < 0.001$).

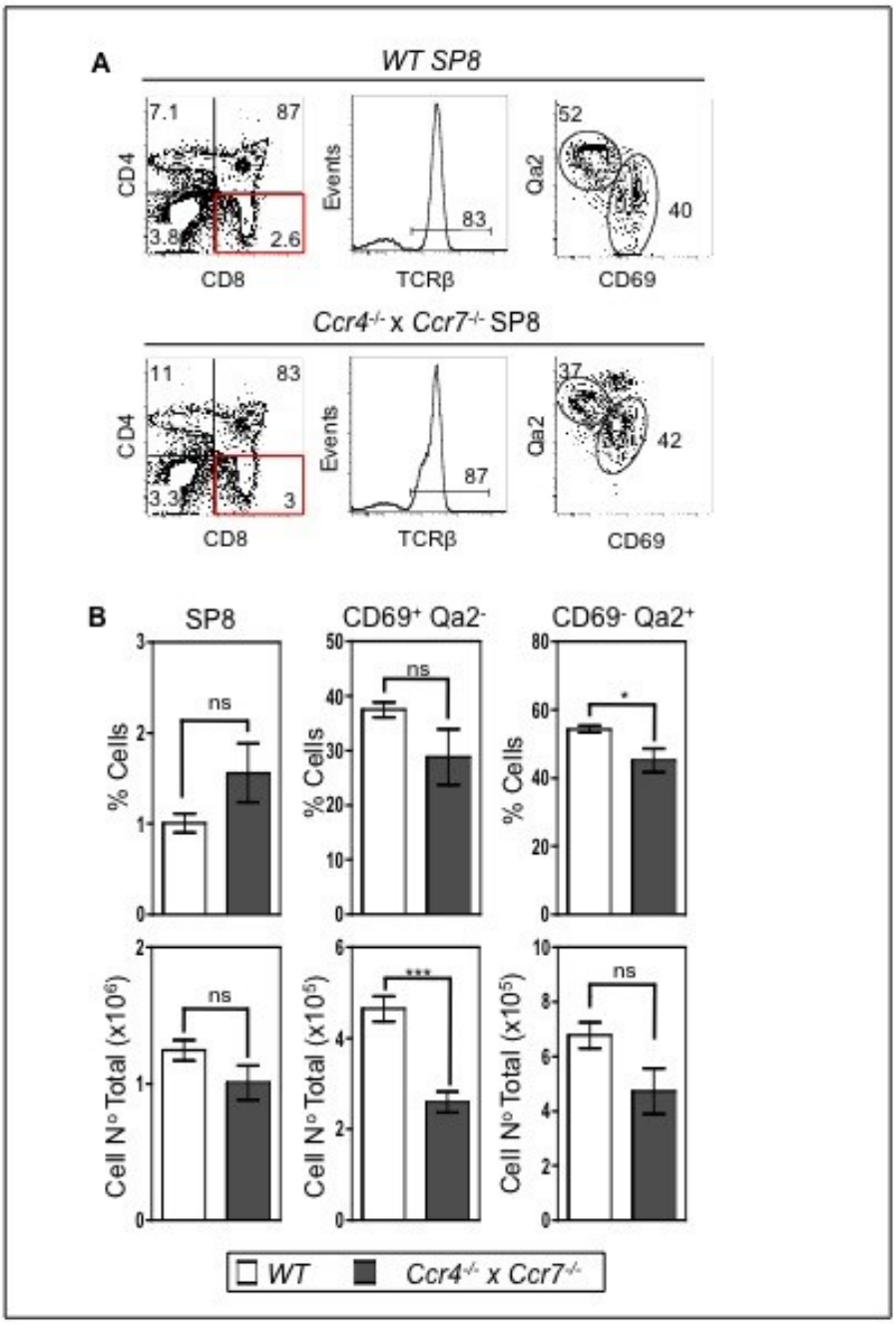
A
WT SP8
7.1
87
3.8
2.6
CD4
CD8
Events
83
TCRβ
52
40
Qa2
CD69
Ccr4-/- x Ccr7-/- SP8
11
83
3.3
3
CD4
CD8
Events
87
TCRβ
37
42
Qa2
CD69
B
SP8
CD69+ Qa2-
CD69- Qa2+
% Cells
ns
ns
*
Cell N° Total (x10^6)
Cell N° Total (x10^5)
Cell N° Total (x10^5)
ns
***
ns
WT
Ccr4-/- x Ccr7-/-

(Figure 5.17 A and B). The percentage increase in FoxP3^{+} nTreg was comparable to the increase observed within *Ccr7*$^{-/-}$ mice (Figure 5.3). In contrast, however, the decreased frequency of CD25^{+} FoxP3^{-} nTreg precursors was a unique characteristic of *Ccr4*$^{-/-}$ x *Ccr7*$^{-/-}$ mice, not shared by *Ccr4*$^{-/-}$ (Figure 5.8) or *Ccr7*$^{-/-}$ (Figure 5.3) strains. This data, therefore, suggests the absence of CCR4 and CCR7 results in the decreased generation of CD25^{+} FoxP3^{-} nTreg precursors, but conflictingly, evokes an increase to their CD25^{+} FoxP3^{+} nTreg progeny.

Exploration of the thymic architecture and intrathymic distribution of SP thymocytes within the adult *Ccr4*$^{-/-}$ x *Ccr7*$^{-/-}$ microenvironment displayed severe disruptions in comparison to their WT counterparts and additionally the *Ccr7*$^{-/-}$ strain (Figure 5.18). In comparison to *Ccr7*$^{-/-}$ thymic structure (Figure 5.4), the *Ccr4*$^{-/-}$ x *Ccr7*$^{-/-}$ thymus grossly appeared to contain smaller medullary structures. From the data displayed we cannot confirm if the medullary volume is significantly less and additional analysis is required. The numbers of SP4 and SP8 thymocytes within these small *Ccr4*$^{-/-}$ x *Ccr7*$^{-/-}$ medullary areas were significantly reduced compared to their WT counterparts (Figure 5.18 C). Quantification revealed a two fold decreased to the numbers of both SP4 and SP8 lineages as a consequence of the absence of both CCR4 and CCR7. The two fold decrease in the SP4 thymocyte population was at a comparable level to the reduction observed within the *Ccr7*$^{-/-}$ adult thymus, however, surprisingly, a greater reduction was observed within the SP8 population of the *Ccr7*$^{-/-}$ microenvironment, in comparison to *Ccr4*$^{-/-}$ x *Ccr7*$^{-/-}$ mice. Therefore, confocal analysis of the *Ccr4*$^{-/-}$ x *Ccr7*$^{-/-}$ thymic microenvironment suggested the absence of both CCR4 and CCR7 increases the severity of the reduced medullary size observed within the *Ccr7*$^{-/-}$ adult strain. The number of SP thymocytes within a given area of the reduced *Ccr4*$^{-/-}$ x *Ccr7*$^{-/-}$ medullary region, however, is not further reduced compared to *Ccr7*$^{-/-}$condition.

Figure 5. 17 CCR7 x CCR4 Double Deficiency Disturbs The Frequencies Of Both Foxp3^{+} CD25^{+} Treg And CD25^{+} Foxp3^{-} Treg Precursors

(A) Thymocytes recovered from adult WT (top) or *Ccr4*$^{-/-}$ x *Ccr7*$^{-/-}$ (bottom) mice were isolated and analysed for intracellular staining of Foxp3 within the TCRβ^{high} SP4 population. The Foxp3^{-} fraction of the TCRβ^{high} SP4 thymocytes were also explored for their surface expression levels of CD25.

(B) The percentages (top) and AN (bottom) of the Foxp3^{+} TCRβ^{high} SP4 Treg subset (left) and Foxp3^{-} CD25^{+} TCRβ^{high} SP4 Treg precursors (right) were calculated from WT (white bars) and *Ccr4*$^{-/-}$ x *Ccr7*$^{-/-}$ (gray bars) hosts and displayed as mean bar graphs, representing x6 individual mice per condition. The standard error bars indicate the SEM, and a student's two tailed unpaired T test was performed on all results, where ns denoted a non-significant difference ($P > 0.05$) and *or *** indicate a significant difference (* = $P < 0.05$ and ***= $P < 0.001$).

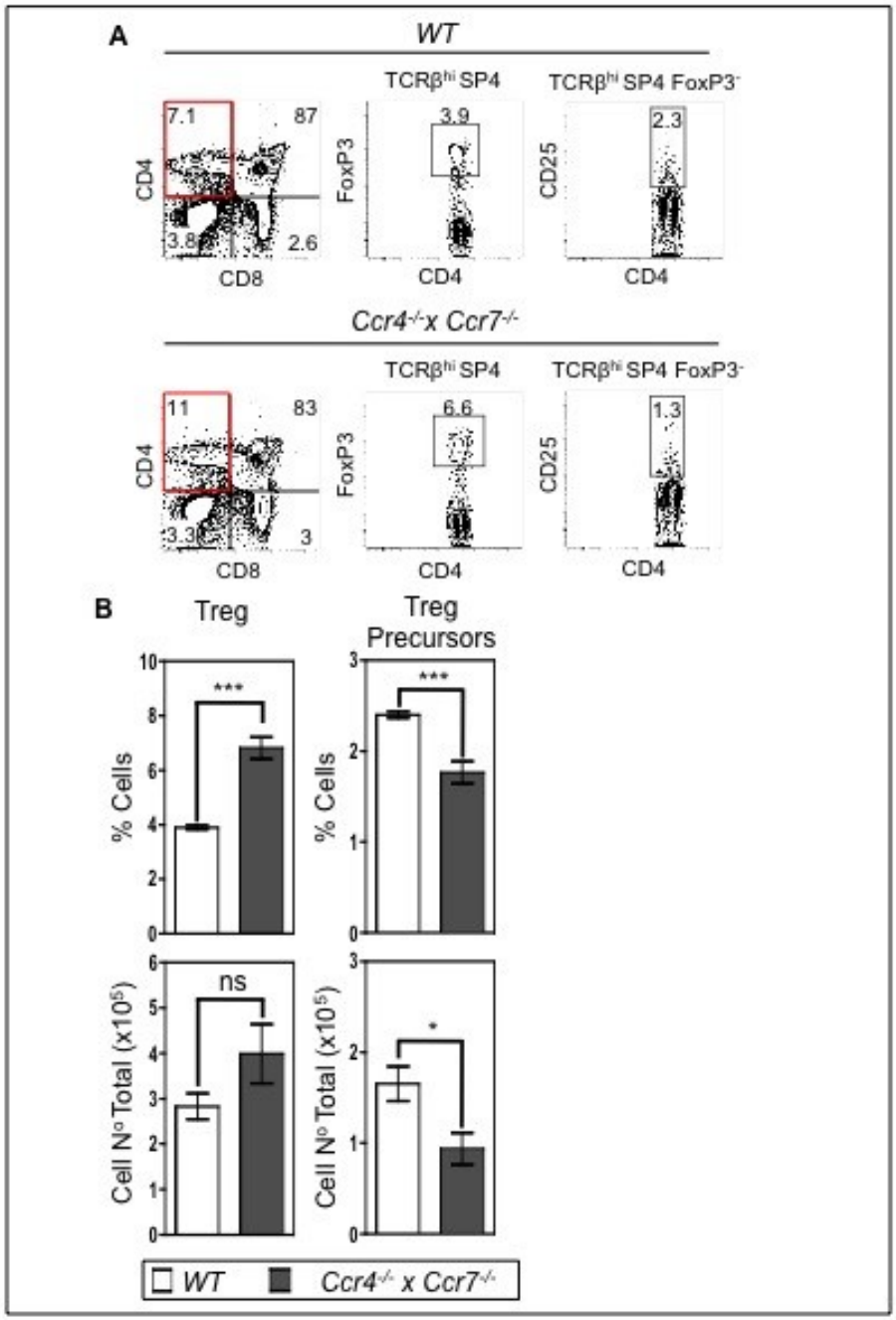
A
WT
TCRβhi SP4
TCRβhi SP4 FoxP3-
7.1
87
3.8
2.6
CD4
CD8
3.9
FoxP3
CD4
2.3
CD25
CD4
Ccr4-/-x Ccr7-/-
TCRβhi SP4
TCRβhi SP4 FoxP3-
11
83
3.3
3
CD4
CD8
6.6
FoxP3
CD4
1.3
CD25
CD4
B
Treg
Treg Precursors
% Cells
***
***
Cell N° Total (x10⁵)
ns
*
WT
Ccr4-/- x Ccr7-/-

Figure 5. 18 Absence of Both CCR4 and CCR7 Results In Reduced Numbers Of SP4 And SP8 Thymocytes Within Medullary Regions

WT and *Ccr4*$^{-/-}$ x *Ccr7*$^{-/-}$ adult thymi were frozen for confocal analysis. 7μm thymus sections were cut and stained for immunofluorescence confocal analysis.

(A) Tile scans of a series of low resolution images are shown for whole thymus sections from WT (left) and *Ccr4*$^{-/-}$ x *Ccr7*$^{-/-}$ (right) hosts, stained for ERTR5 and β5T. Bars represent a scale of 1mm

(B) Higher resolution images of smaller thymic areas stained for CD4 and CD8. The white dashed line denotes the corticomedullary junction, C=cortex and M=medulla. Bars represent a scale of 100 μm

(C) The number of SP4 (left graph) or SP8 (right graph) cells within a 100μm x 100μm medullary area were counted within x3 regions per section, on x4 serial section images per host. The numbers acquired from x3 WT (white bars) and x3 *Ccr4*$^{-/-}$ x *Ccr7*$^{-/-}$ (grey bars) hosts are displayed as mean bar graphs. The standard error bars indicate the SEM and a student's two tailed unpaired T test was performed on all results, where *** and ** denotes a significant difference (** = $P < 0.01$ and ***= $P < 0.001$).

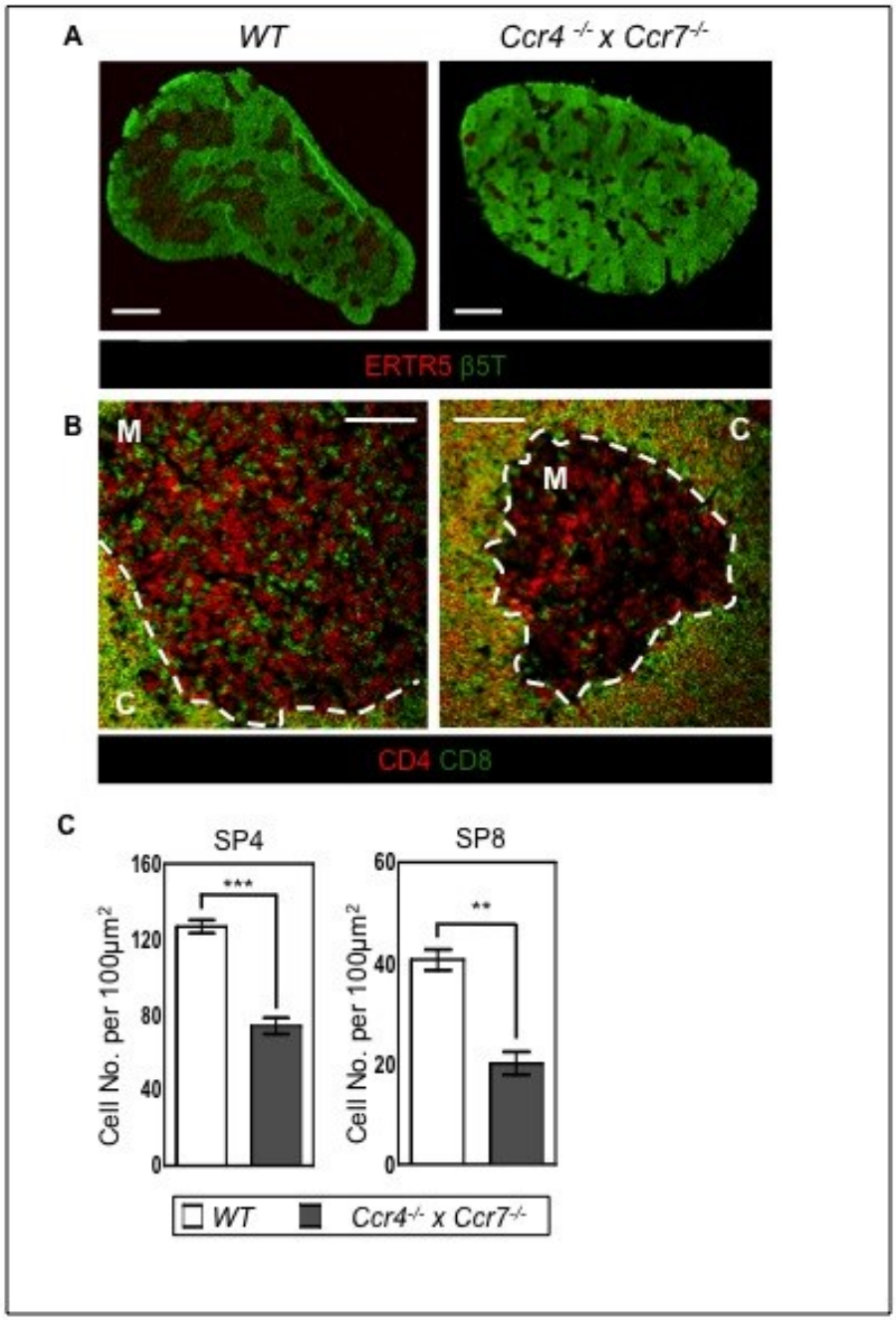
A
WT
Ccr4 -/- x Ccr7-/-
ERTR5 β5T
B
M
C
M
C
CD4 CD8
C
SP4
SP8
Cell No. per 100μm2
160
120
80
40
0
***
60
40
20
0
**
WT
Ccr4-/- x Ccr7-/-

5.3 DISCUSSION

Relocation of positively selected thymocytes to the medulla is essential for tolerance induction and is controlled, at least in part, by CCR7 (Kurobe et al., 2006). The level of involvement of CCR7 however, remains under some dispute (Davalos-Misslitz et al., 2007). As absence of CCR7 does not result in a total absence of SP4 and SP8 cohorts within adult thymic medullary regions, we were interested to explore the role of additional chemokine receptors in cortex to medulla migration of thymocytes, on the initiation of positive selection. From work in Chapter 3, CCR4 was identified as an attractive candidate to be involved in this process. The receptor displayed rapid upregulation upon the initiation of positive selection within a large fraction of $CD69^+$ DP thymocytes and was maintained on the cell surface of SP4 subsets at their early stages in development. In addition, we confirmed CCL17 and CCL21 are highly expressed within medullary areas, predominately by $Sirp\alpha^+$ DC, but also by mature mTEC. However, in both the steady state and within a competitive setting, *Ccr4*$^{-/-}$ thymocytes displayed no disruption to their intrathymic T cell development program. Therefore, if CCR4 is indeed involved in post-selection maturation, its role must be dispensable and compensated for by redundancy within the chemokine receptor system.

We hypothesized that CCR7 may have compensatory effects over the absence of CCR4 and to address this, towards the end of my PhD studies we generated a novel *Ccr4*$^{-/-}$ *x Ccr7*$^{-/-}$ double deficient compound mutant mouse strain. Preliminary analysis of *Ccr4*$^{-/-}$ *x Ccr7*$^{-/-}$ mice suggested perturbed post-positive selection maturation and thymic localization at a greater severity than that observed in *Ccr7*$^{-/-}$ adults. Absence of both CCR4 and CCR7 resulted in reductions to overall thymic cellularity and perturbed differentiation of conventional SP4 and

SP8 development. *Ccr4*$^{-/-}$ x *Ccr7*$^{-/-}$ presented with increased percentages of total TCRβ^{high} SP4, but attenuated development of the most mature CD69^{-} Qa2^{+} fractions within both lineages. In addition, medullary areas of adult *Ccr4*$^{-/-}$ x *Ccr7*$^{-/-}$ mice appeared smaller than those of *Ccr7*$^{-/-}$ mice. Further experiments are required to analyze directly the medullary volume of these mice. Importantly, while reductions were observed in the thymic cellularity of *Ccr4*$^{-/-}$ x *Ccr7*$^{-/-}$ mice, absolute cell numbers obtained from WT mice used as controls for this condition were higher compared to the counts acquired from the controls of the *Ccr4*$^{-/-}$ and *Ccr7*$^{-/-}$ single mutants. This difference could be due to variability in sourcing of C57BL/6 WT mice, due to limitations with availability in our animal facility. Further experiments are required to study the potential impact on T cell development caused by combined absence of CCR4 and CCR7.

As absence of CCR7 has been linked to defective negative selection (Davalos-Misslitz et al., 2007; Kurobe et al., 2006), it would be of interest to address the possible involvement of both CCR4 and CCR7 in the process of negative selection of the T cell repertoire. To address this, additional analysis is essential, along with analysis of any potential breakdown in central tolerance. This could be examined by analyzing the deletion of particular αβTCRs to endogenous mouse mammary tumor viruses, or by crossing our mutant mice onto TCR transgenic backgrounds. Interestingly, within this chapter we demonstrated that the Sirpα^{+} CD8^{-} DC population is the predominate producer of CCR4 ligands CCL17 and CCL21 within the thymic environment. Collectively this could suggest that absence of CCR4 may disrupt SP thymocyte interactions with DC, which manifest as alterations in negative selection.

In addition to conventional SP thymocytes, differentiation of CD25^{+} FoxP3^{-} nTreg precursors and their CD25^{+} FoxP3^{+} nTreg progeny was also examined in *Ccr4*$^{-/-}$ x *Ccr7*$^{-/-}$ adult mice and

a possible reduction in the SP4 $CD25^+$ $FoxP3^-$ nTreg precursor population was observed. However, given that an increase in their $CD25^+$ $FoxP3^+$ nTreg progeny was also detected, these findings clearly identify the need for additional analysis, to include not only analysis of intrathymic development, but also disturbed localization, perhaps hindering thymic exit resulting in thymic accumulation. Regardless of the detailed impact of combined CCR4 and CCR7 deficiency and in contrast to the effects observed following Pertussis Toxin treatment (Ehrlich et al., 2009; Suzuki et al., 1999), double deficient mice still have medullary areas that contain both SP4 and SP8 thymocytes. Hence, cortex to medulla migration must still occur in the combined absence of both CCR4 and CCR7. This implies that other unknown chemokine receptors are facilitating this migratory pathway and may compensate for CCR4 and CCR7 removal. CCR8 is an attractive candidate to be involved at this specific stage in intrathymic development, as it has been identified to display very similar expression patterns to that of CCR4. TCR activation during positive selection results in the upregulation of this receptor and its surface expression is increased further within the immature CD4 SP faction ($CD69^+$ HSA^+ $CD62L^-$). Its expression, like that of CCR4, is limited to SP4 cells, with undetectable levels on CD8 SP thymocytes (Kremer et al., 2001). However, to date no investigations have explored the potential involvement of CCR8 in cortex to medulla migration. CCR9 is an additional receptor that could possibly compensate for the removal of CCR4 and CCR7, based upon its surface expression patterns on DP thymocytes and immature SP4 and SP8 subsets (Chapter 3). Although CCR9 is important for DP cortical retention (Choi et al., 2008), CCL25 is expressed in both the corticex and medulla (Uehara et al., 2002) so it may also be involved in medullary migration. Additional CCR4/CCR9 compound mutants could explore this possibility in more depth.

In conclusion our investigations into the role of CCR4 in cortex to medulla migration and the continued differentiation of positively selected thymocytes support a model in which this receptor is not essential for either T cell development nor appropriate intrathymic thymocyte localization. Further analysis of mice lacking both CCR4 and CCR7 will reveal whether compensatory mechanisms by CCR7, at least partly, explains these observations, or if CCR4 has no involvement in the chemokine receptor- mediated migration of SP thymocytes and their continued maturation.

CHAPTER 6: GENERAL DISCUSSION

6.1 BACKGROUND AND OVERALL AIMS

The differentiation of a diverse and self-tolerant T cell repertoire is dependent on the unique thymic microenvironment and stringent selection processes. Positive selection is a fundamental checkpoint in T cell development and thymocytes that successfully rearrange their TCRα and TCRβ genes are screened for their ability to recognize self-MHC in the cortex. The αβTCR must interact at low avidity with self peptide-MHC complex presented on the cell surface of cTEC and such engagements stimulate the transition from DP to SP thymocytes. At this stage in development, cells commit to either a $CD4^+$ $CD8^-$ or $CD4^-$ $CD8^+$ SP lineage fate and undergo the transition from cortical regions, across the corticomedullary junction, into medullary areas, a migratory pathway facilitated by chemotatic signals (Ehrlich et al., 2009; Suzuki et al., 1999). Those thymocytes that fail to be positively selected undergo death by neglect. Following entry to the medulla, high avidity TCR interactions with peptide-MHC complexes induce death signals and negative selection, contributing to the deletion of self-reactive thymocytes, which is essential for the establishment of central tolerance.

Thymocyte residency within the medulla is indispensible for the establishment of tolerance. Positively selected SP cells are thought to reside within the medulla between 5 to 14 days, although the precise medullary dwell time remains unclear (McCaughtry et al., 2007; Scollay and Godfrey, 1995). During this medullary residency SP thymocytes interact with medullary thymic epithelial cells (mTEC) and DC and any residual thymocytes displaying αβTCRs with potential specificity to self, that have escaped negative selection within the cortex are deleted (Anderson and Takahama, 2012). A proportion of these self reactive thymocytes have an alternative fate and upon high avidity bind of their TCR to self-peptide-MHC complexes

undergo maturing into Foxp3$^+$ nTreg (Moran et al., 2011; Stritesky et al., 2012) This Foxp3$^+$ SP4 nTreg population is vital in the regulation of immune homeostasis and immunological tolerance (Sakaguchi et al., 1995). In addition, while residing within the medulla conventional SP4 and SP8 lineages complete their multistep maturation program of late stage αβT cell development, before their export into the periphery to become naive T cells. Disruptions in either thymocyte homing to the medulla, or normal development of its structure, have been suggested to result in a breakdown of tolerance, which can manifest as autoimmunity (Burkly et al., 1995; Kurobe et al., 2006; Naspetti et al., 1997).

The general aim of this study was to explore the importance of specialized medullary microenvironments in T cell development and selection. The main emphasis of our investigations was to address the following questions:

a) What is the role of the thymic medulla in the post-positive selection maturation processes of conventional and Foxp3$^+$ regulatory SP thymocytes?

b) What are the signals that control cortical-to-medullary transition of developing thymocytes?

6.2 Redefining the Role of the Thymic Medulla in αβT Cell Development

The role of thymic medulla in the establishment of central tolerance is well established. However, the function of the thymic medulla in supporting the late stages of conventional CD4 and CD8 SP development, along with the generation of the specialized non-conventional nTreg lineage, is less well known. Literature suggests mTEC interactions are essential in the

differentiation program of SP4 thymocytes (Li et al., 2007), in addition to the intrathymic generation of $Foxp3^+$ nTreg (Aschenbrenner et al., 2007; Hinterberger et al., 2010). Thus, we explored the effects of mTEC deficiency on development of these diverse thymocyte lineages, post-positive selection.

Amid the exploration of the role of the thymic medulla we established a new classification system to map the phenotypic changes of thymocytes during the process of positive selection. We utilized chemokine receptor surface expression patterns to defined distinct stage of SP4 and SP8 intrathymic T cell development. This approach facilitated the identification of a new cohort of the most immature SP4 thymocytes, based upon their $CCR9^+CCR4^+CCR7^-$ $CD69^+$ phenotype. We predicted this immature fraction of thymocytes is the most recent population to have undergone the positive selection process and we demonstrated at this stage in maturity SP4 cells have yet to commit to the SP4 lineage, maintaining their ability to differentiate into SP8 thymocytes. This chemokine receptor classification system also provides an alternative to commonly used "developmental stage defining markers" such as CD62L HSA and Qa2, with markers of potential functional importance within the intrathymic T cell development process (Chapter 3).

We designed an experimental model to directly explore intrathymic T cell development within an mTEC deficient microenvironment, in the presence of an otherwise normal immune system. Experiments using this mTEC deficient grafting model challenged the suggestion that mTEC provide essential support for SP4 differentiation, but instead implies conventional SP thymocyte development can occur independently of the thymus medulla. Furthermore analysis of extrathymic maturation offered additional confirmation to the notion that mTEC do not provide vital support for SP4 differentiation. In marked contrast, our experiments

support the proposal that the generation of $Foxp3^+$ nTreg is critically dependent upon an intact thymus medulla, as we demonstrated the requirement of mTEC for the differentiation of the $Foxp3^-CD25^+$ nTreg precursor population and their progeny (described in Figure 6.1).

Collectively, the results of Chapter 4 warrant reconsideration of the role of the medullary microenvironment during αβT cell development. These findings demonstrate a disparity in the requirement of the thymic medulla with regards to the $FoxP3^+$ nTreg versus conventional SP lineages, suggesting the principle role of the medulla is in the establishment of tolerance, via both negative selection and nTreg generation, as opposed to an essential site that nurtures later stages of conventional αβT cell development. Such findings raise a complexity of questions into the essential signals that drive both developmental pathways. For example, while differentiation into the most mature stages in conventional SP development can occur independently of mTEC, based upon their $CD69^-$ $Qa2^+$ surface phenotype, the transplantation of mTEC deficient grafts into an athymic host demonstrated that those mature CD4 and CD8 T cells raised in the absence of an intact medulla induce autoimmunity, in the absence of protection by peripheral tolerance. Thus, whilst we suggest conventional SP thymocytes can complete their full differentiation program in the absence of mTEC on the basis of their surface expression patterns of age defining markers, we demonstrate such thymocytes are not likely to be tolerant to self. Moreover, we established that WT hosts provide sufficient peripheral tolerance to control autoreactive T cells raised in an mTEC deficient environment, preventing autoimmunity. Overall, the data indicates an intact medulla may not be fundamental in the generation of a mature conventional CD4 or CD8 T cell pool, although it is essential for the development of a self-tolerant repertoire. In addition, this study calls for a rethink of the length of medullary residency and emigration in regards to differentiation of

Figure 6. 1 A Requirement For mTEC The Generation Of Foxp3$^+$ nTreg But Not Conventional SP Thymocytes

The figure demonstrates a proposed model of the requirement for medullary thymic epithelial cell (mTEC) during SP thymocyte development.

Initially, CD4$^+$CD8$^+$ DP cells that successfully undergo positive selection differentiate into the most immature CCR7$^-$CCR9$^+$CD69$^+$ SP4 thymocyte subset. In the absence of mTEC these newly selected SP4 cells can continue their development into conventional CD69$^-$Qa2$^+$ mature SP4 and SP8 thymocytes. In contrast, differentiation into Foxp3$^+$ CD25$^+$ T-regulatory SP4 cells is blocked in the absence of mTEC, indicating an essential role for these cells to support the development of newly generated SP4 thymocytes into Foxp3$^+$ CD25$^+$ T-regulatory cells.

The surface expression profiles of each thymocyte subset at different maturational stages are highlighted.

Red crosses indicate the absence of a cell type.

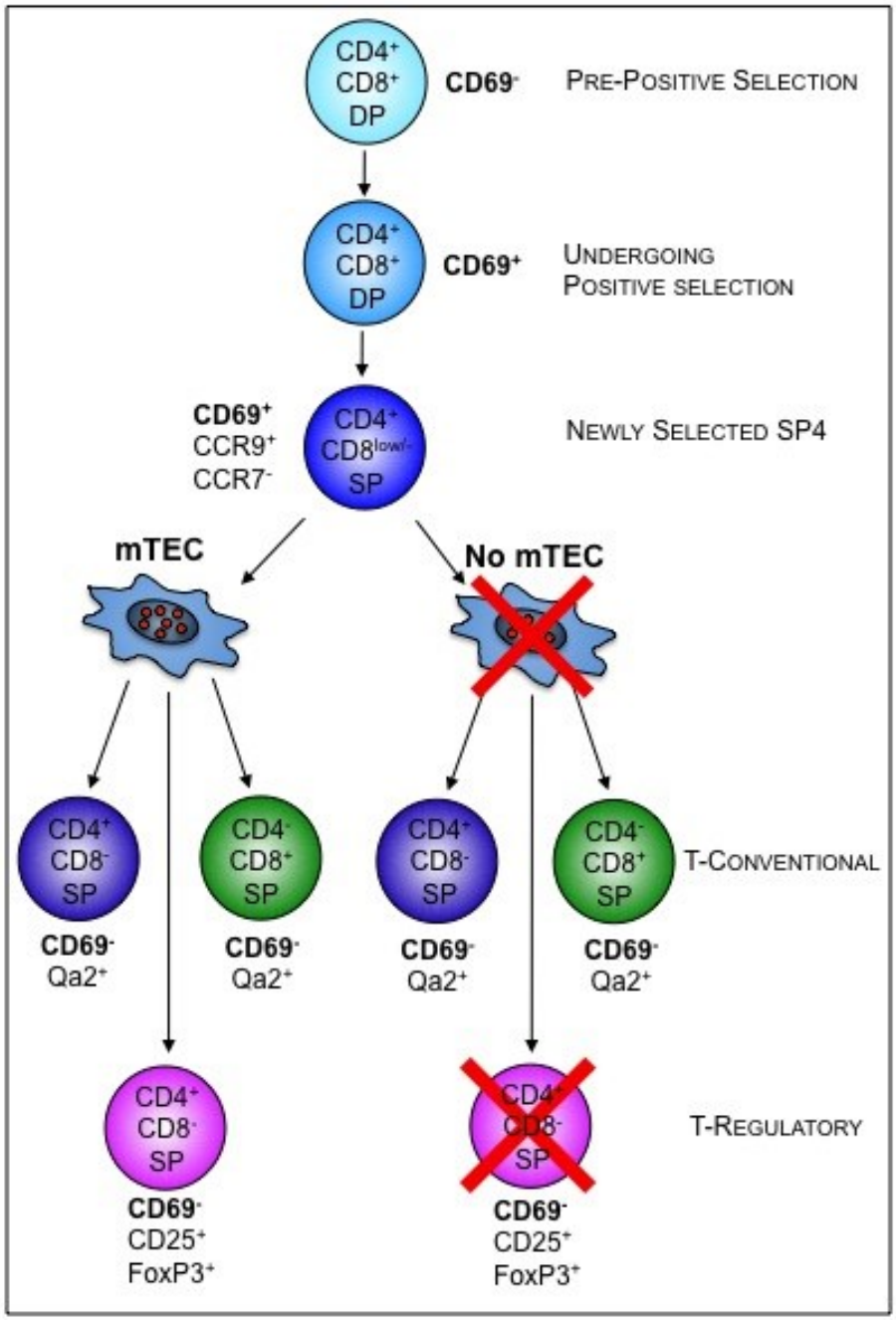
CD4+ CD8+ DP
CD69-
PRE-POSITIVE SELECTION
CD4+ CD8+ DP
CD69+
UNDERGOING POSITIVE SELECTION
CD69+ CCR9+ CCR7-
CD4+ CD8low- SP
NEWLY SELECTED SP4
mTEC
No mTEC
CD4+ CD8- SP
CD69- Qa2+
CD4- CD8+ SP
CD69- Qa2+
CD4+ CD8- SP
CD69- Qa2+
CD4- CD8+ SP
CD69- Qa2+
T-CONVENTIONAL
CD4+ CD8- SP
CD69- CD25+ FoxP3+
CD4+ CD8- SP
CD69- CD25+ FoxP3+
T-REGULATORY

various T cell lineages. The diverse mTEC requirements of conventional versus FoxP3^{+} nTreg lineages may influence their specific medullary dwell time. The exact time thymocytes are believed to reside in the medulla remains under dispute (McCaughtry et al., 2007; Scollay and Godfrey, 1995), however, there are two well-established yet conflicting models of how thymic residency and egress is regulated. The 'conveyor belt' mechanism suggests the oldest thymocytes leave first and all immature T cell share the same maturational phenotype as they exit the thymus as recent thymic emigrants (RTE) (McCaughtry et al., 2007). In contrast the 'lucky dip' model suggests thymocytes can leave the medullary pool randomly at any stage in their maturation program and hence the RTE cell pool represents cells at various stages of their maturity (Egerton et al., 1990; Kelly and Scollay, 1990; Scollay and Godfrey, 1995). The most recent investigations into medulla dwell time using the RAG-2 GFP model suggests conventional SP4 and SP8 lineages emigrate via the conveyor belt method into the periphery 4 to 5 days after medullary entry. These studies propose non-conventional thymocytes have extended medullary dwell times in comparison to conventional lineages. This assumption is based specifically on NKT and nTreg lineages, due to a large proportion of the two populations displaying an intrathymic RAG-2 GFP^{-} phenotype. The decay of GFP expression within these specialized subsets would imply they represent either long term thymic residents or recirculating cells (McCaughtry et al., 2007). It has been demonstrated the most mature NK1.1^{+} fraction of NKT cells undergo longer term retention in the thymus (Berzins et al., 2006), whilst investigations ongoing within our own laboratory suggest the sufficient generation of this distinct mature NK1.1^{+} subsets is dependent on an intact medullary environment (unpublished). In contrast, to date there is no research in to the possible long term residency of nTreg within medullary regions, however the re-entry of Treg back to the

thymus has been reported (Bosco et al., 2006). Further experiments are planned to investigate whether the absence of an intact mTEC compartment alters the medullary dwell time of positively selected αβT cells. As we have revealed the initial development of the nTreg lineage occurs at the intermediate CCR9^{-} CCR7^{+} CD69^{+} SP4 stage of maturation and this processes is dependent upon mTEC signals, this may suggest a need for additional medullary dwell time. The reduced RAG-2 GFP^{-} populations recovered from our mTEC deficient microenvironments grafted into a RAG-2 GFP host supports such a theory, if we make the assumption at least a fraction of the RAG-2 GFP^{-} population represents the nTreg population. Currently while we have been unsuccessful in our attempts to successfully intracellular stain for Foxp3 without disrupting GFP expression and thus, we aim to modify the technique to simultaneously detect the two molecules. This would aid the identification of the RAG-2 GFP^{-} thymic residents, offering confirmation if they are indeed the nTreg population. In addition, we have recently generated new mouse colonies in which RAG-2 GFP mice have been crossed with either LTβR-deficient or Aire-deficient, both of which display medullary abnormalities. These mice should prove to be useful in investigating how altered medullary microenvironments might impact upon thymic medullary dwell time and the frequency of recent thymus emigrants.

The thymic medulla is not exclusively comprised of developing thymocytes and mTEC. This unique specialized microenvironment is comprised of additional cell types including thymic DC (Barclay, 1981; Lei et al., 2011). Intrathymic DC subsets, via antigen presentation, are capable of regulating negative selection (Gallegos and Bevan, 2004), or inducing the generation of nTreg (Proietto et al., 2008b; Spence and Green, 2008; Watanabe et al., 2005a; Wirnsberger et al., 2009). Our investigations into DC subsets within mTEC deficient thymus

grafts demonstrated that in the absence of this epithelial cell population the Sirpα^{+} CD8^{-} cDC cohort, which homes to the thymus from the periphery (Li et al., 2009), was present at normal frequencies. In contrast, in the absence of an intact medullary environment the thymically generated Sirpα^{-} CD8^{+} cDC and the peripherally derived pDC populations were both significantly reduced (Li et al., 2009; Wu and Shortman, 2005). While the importance of mTEC for the other DC subsets is not fully understood, this finding may suggest that the Sirpα^{+} CD8^{-} cDC division may stimulate conventional SP4 and SP8 development, yet its presence must be insufficient to drive the generation of nTreg. Surprisingly, this DC subset specifically has been identified as having superior capacity to generate Foxp3^{+} nTreg (Proietto et al., 2008b), however the additional Sirpα^{-} CD8^{+} cDC and pDC populations have also demonstrated the ability to induce this specific T cell lineage intrathymically (Guerri et al., 2013; Martin-Gayo et al., 2010; Proietto et al., 2008b). Collectively, the involvement of mTEC in nTreg induction identified within our own studies, together with the well-documented role of distinct DC subsets, supports the idea that the generation of this specialized population is unlikely to require the interactions of a dedicated antigen presenting cells type, but rather it is dependent on either or perhaps a collective of these two cohorts (Wirnsberger et al., 2009). We are currently performing *in vitro* RTOC experiments involving defined combinations of distinct DC subsets, together with the presence or absence of mTEC to gain a better understanding of the importance of these cells in conventional and Foxp3^{+} nTreg T cell development. Furthermore it has been suggested that diverse DC subsets induce nTreg population with distinct functions, on the basis of their cytokines production profile (Martin-Gayo et al., 2010). Therefore this experimental approach could also be

utilized to explore the possibility of distinct nTreg subpopulations, on the basis of the APC upon which they were selected.

Overall, more detailed analysis is essential to confirm mTEC are essential for DC mediated nTreg selection and reveal what critical signals this specialized epithelial cell type is providing. The generation of $Foxp3^{-}CD25^{+}$ nTreg precursors is thought to be dependent upon CD28-CD80/CD86 interactions (Hinterberger et al., 2011; Lio et al., 2010; Vang et al., 2010), in addition to TCR-MHC binding (Lio and Hsieh, 2008). Thus, it is possible the absence of the mTEC population results in the failure of TRA production and self-antigen cross-presentation to DC, consequentially leading to their inability to induce the differentiation of this nTreg SP4 lineage. The expression of endogenous self-antigen is considered a distinct function of the $Aire^{+}$ mTEC population (Derbinski et al., 2001). Interestingly, however, Aire protein has also been found in the thymically induced $Sirp\alpha^{-}CD8^{+}$ cDC population, although this population is significantly reduced in the mTEC deficient microenvironment (Heino et al., 2000). It has also been found that thymic homing DC subsets, particularly the pDC cohort, but to a lesser extent the $Sirp\alpha^{+}CD8^{-}$ cDC fraction, have been shown to transport antigens from the periphery for presentation to the developing thymocytes (Hadeiba et al., 2012). The inability of the DC resident within our mTEC deficient environments to induce nTreg generation, would suggest any DC bound antigen, perhaps peripherally derived, present within the grafts must be insufficient at driving the development of this non-conventional SP4 lineage and thus, mTEC derived self-antigen specifically must be crucial. One possible explanation for this is that peripheral derived antigen is not able to induce sufficient TCR affinity and signal strength to drive the differentiation of this specific SP4 subset. In contrast any peripheral antigen presented to developing T cells by DC subsets present within our

mTEC deficient environment may be sufficient to complete conventional SP4 and SP8 development, in addition to the interactions they undergo with the cTEC population. From this data, however, we are unable to confirm if conventional SP4 and SP8 development is TCR mediated via DC interaction, or if indeed DC are even involved, as additional survival signals could be facilitating this continued maturational process.

Thus, we hypothesize the mTEC production of TRA is vital for the development of the $CD25^{+}$ $FoxP3^{-}$ nTreg precursor population and their $CD25^{+}$ $FoxP3^{-}$ nTreg progeny. The synthesis of self-antigen and their direct presentation by mTEC, or cross-presentation by DC, to developing thymocytes facilitates the generation of this specialized regulatory T cell subset via high avidity TCR- self -peptide MHC complex interactions. In additional we speculate homed DC populations within our mTEC deficient microenvironment may present peripheral antigen to developing thymocytes, which may support their continued development to the later stage of conventional αβT cell development, or perhaps provide the correct survival signals in a TCR-peptide MHC independent manner to foster their development (Described in Figure 6.2).

6.3 How Do Positively Selected Thymocytes Enter The Medulla?

An additional aim of this thesis was to explore how thymocytes undergo ordered migration into the specialized medullary thymic microenvironment. Pertussis Toxin treatment results in the complete absence of SP thymocytes entering the thymic medulla (Ehrlich et al., 2009; Suzuki et al., 1999), whilst the absence of CCR7 alone results in small medullary areas that still contain SP4 and SP8 thymocytes (Ueno et al., 2004). Thus, we hypothesized that

Figure 6. 2 Proposed Interactions of Antigen Presenting Cells With Immature SP Thymocytes During CD4 SP Conventional And Foxp3$^+$ nTreg Development

Conventional T cell development (upper panel):

In this model, dendritic cells (DC) can interact with newly generated CCR7$^-$ CCR9$^+$CD69$^+$ SP4 thymocytes, via either T cell receptor (TCR)- MHC cell mediated interactions, or other survival signals, to mediate the continued development of conventional SP4 and SP8 thymocytes that can occur in the absence of mTEC.

Foxp3$^+$ T regulatory development (lower panel):

Here, the direct presentation of self-peptides by Aire$^+$ medullary thymic epithelial cell (mTEC) to newly generated CCR7$^-$CCR9$^+$CD69$^+$ SP4 thymocytes induces the generation of Foxp3$^-$ CD25$^+$ nTreg precursors and their Foxp3$^+$ CD25$^+$ nTreg progeny. This model also suggests that the cross-presentation of self-peptides from Aire$^+$ mTEC to DC facilitates their ability to also drive Foxp3$^+$ CD25$^+$ nTreg differentiation, supporting the idea of a dual requirement for both mTEC and DC in nTreg development.

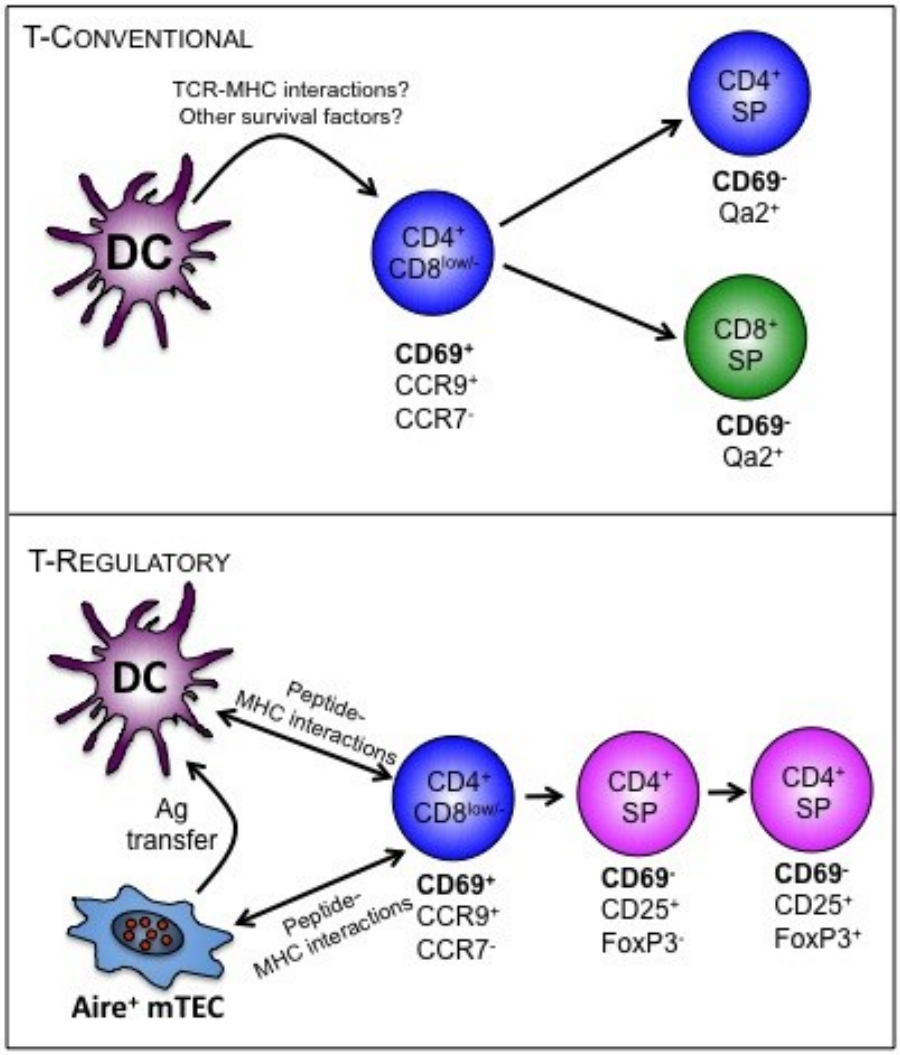
T-CONVENTIONAL
TCR-MHC interactions?
Other survival factors?
DC
CD4+ CD8low/-
CD69+ CCR9+ CCR7-
CD4+ SP
CD69- Qa2+
CD8+ SP
CD69- Qa2+
T-REGULATORY
DC
Peptide-MHC interactions
Ag transfer
Peptide-MHC interactions
Aire+ mTEC
CD4+ CD8low/-
CD69+ CCR9+ CCR7-
CD4+ SP
CD69- CD25+ FoxP3-
CD4+ SP
CD69- CD25+ FoxP3+

additional chemokine receptors are involved in this process. Analysis of the chemokine receptor surface expression patterns of developing thymocytes, along with the gene expression patterns of chemokines within distinct TEC populations, identified CCR4 as a promising additional candidate for intrathymic cortex to medulla migration. Most published data on expression of CCR4 and its ligands in the thymus is limited to either PCR analysis or functional chemokine migration assays (Campbell et al., 1999) and thus, per cell analysis of expression of CCR4 during T cell development remained unexplored. Our own results clearly show CCR4 is expressed on the cell surface of thymocytes undergoing the positive selection process, which are likely to be undertaking corticomedullary relocalization. However, detailed analysis of mice lacking CCR4 expression suggested that this chemokine receptor is not essential for intrathymic positioning of developing thymocytes.

As a consequence of the known redundancy that occurs within the chemokine receptor system it is very difficult to explore the effects of the removal of individual chemokine receptors, as additional receptors may conceal their true involvement. Thus, in an attempt to overcome this problem we generated a novel compound mutant mouse strain with a double deficiency in CCR4 and CCR7, as CCR7 has been identified to be pivotal in cortex to medulla migration (Kwan and Killeen, 2004; Ueno et al., 2004). Initial preliminary analysis of these mice was performed and such experiments suggested that all major SP4 and SP8 thymocyte subsets were present, including $CD4^+$ cells expressing Foxp3, indicating that a normal program of T cell development can occur in the combined absence of these receptors. In addition, confocal analysis of thymus sections showed very small medullary areas containing SP4 and SP8 thymocytes. It is important to note such findings are at their preliminary stage and require further detailed analysis, to confirm if these mice display with further reductions to their

medullary size in comparison to *Ccr7*$^{-/-}$ mice. To obtain a more definitive idea of the effects of the combined absence of CCR4 and CCR7 has on medullary size we hope to explore the architecture of different chemokine receptor deficient thymic microenvironments using advanced imaging techniques, with the aid of collaborations with Dr Magali Irla, at the Center of Immunology in Marseille. Due to limitations of two-dimensional thymic sections, we hope to instead image a series of immunolabelled thymic sections to create a full three-dimensional (3D) organ reconstruction of intact thymus samples, to enable the visualization of the whole tissue. The establishment of this method has already facilitated insight into the organization, development and function of the thymic medulla (Irla et al., 2013) and we hope by utilizing this technique we can explore the alteration to thymic structure in the absence of CCR4, CCR7, or within the compound mutant. Therefore we should be able to directly address the effects of CCR4 deficiency, either exclusively or in conjunction with CCR7, on thymic architecture. We will particularly focus on the medullary volume and the quantification of medullary islet within the different chemokine receptor deficient mouse strains, to offer more clarity to the role of CCR4 in cortex to medulla migration of positively selected SP thymocytes.

If indeed the hints within our preliminary data are correct and the medullary volumes are significantly reduced as a consequence of absence of CCR4 and CCR7, this raises the question as to where the increased percentages of both the total TCRβ^{high} SP4 population and the raised CD25^{+} FoxP3^{+} nTreg subset detected within these mouse strains reside within the thymic microenvironment. A reduction to medullary size and an increase to the two SP4 subsets would suggest the thymocytes must be mislocalised within cortical regions. Thus, more detailed imaging of the thymic microenvironment will be extremely beneficial to offer

more clarity on thymocyte positioning as a consequence of the removal of specific chemokine-receptor mediated migration. One experimental approach could be the use of live cell imaging and two-photon microscopy, which has been used in the past to track the migratory pathway of CCR7 deficient mice (Ehrlich et al., 2009). Such experimental analysis of the migratory pattern of CCR4 deficient and CCR4 x CCR7 double deficient thymocytes may identify any existing subtle alterations to SP intrathymic migration pathways. In experiments involving standard confocal microscopy, the visualization of mislocalized SP thymocytes can be difficult due to the overwhelming numbers of DP residents tightly packed within the cortical regions of a steady state adult mouse. To overcome this problem competitive bone marrow chimeras of WT hosts can be used for more successful identification of the intrathymic localization of SP thymocyte. This technique was adopted in the identification of misloclaised *Ccr7*$^{-/-}$ SP thymocytes within cortical regions (Ueno et al., 2004) and thus the reconstitution of *Ccr4*$^{-/-}$ x *Ccr7*$^{-/-}$ bone marrow in competition with WT cells may aid the detection of the *Ccr4*$^{-/-}$ x *Ccr7*$^{-/-}$ SP positioning. This experimental approach may provide more detailed analysis of the migratory potential of the *Ccr4*$^{-/-}$ x *Ccr7*$^{-/-}$ thymocytes when place under the selective pressures of a competitive environment, although this technique revealed no alterations to the positioning of *Ccr4*$^{-/-}$ thymocytes.

6.4 CONCLUDING REMARKS

In summary, the experiments in this thesis have helped in our understanding of the importance of the thymic medulla in late stage αβT cell development. The observation conventional αβT cell development occurs in the absence of an intact mTEC compartment, while Treg development is mTEC dependent, raising the possibility that the primary role of

the medulla is not to act as a site of general SP thymocyte differentiation, but as a microenvironment specialized for tolerance induction. In addition, our investigations into the role of CCR4 in cortex to medulla migration identified this chemokine receptor is not essential in the cortex to medulla reclocalizaion of positively selected thymocytes, or their subsequent intrathymic developmental program. Therefore, if CCR4 is involved in post-selection maturation, its contribution must be both dispensable and compensated for by redundancy within the chemokine receptor system. Nevertheless, although CCR4 may not have a vital role in intrathymic T cell development, due to its tight window of expression, the receptor acts as a good marker of newly generated SP4 thymocytes. To expose possible redundancy by CCR7, concealing the involvement of CCR4 in cortex to medulla migration, more advance imaging techniques are need to visualize thymocyte migratory pathways and the medulla architecture of *Ccr4*$^{-/-}$ x *Ccr7*$^{-/-}$ steady state microenvironments. Collectively, we aim to confirm if the removal of CCR4 and CCR7 simultaneously increases the severity of the phenotype observed upon CCR7 removal exclusively.

Papers arising from this thesis:

1. **Cowan JE**, Parnell SM, Nakamura K, Caamano JH, Lane PJL, Jenkinson EJ, Jenkinson WE, AndersonG. **The thymic medulla is required for Foxp3^{+} regulatory but not conventional CD4^{+} thymocyte development**. J Exp Med. 2013 April 8 ;210(4):675-81

2. Desanti GE, **Cowan JE**, Baik S, Parnell SM, White AJ, Penninger JM, Lane PJ, Jenkinson EJ, Jenkinson WE, Anderson G. **Developmentally regulated availability of RANKL and CD40 ligand reveals distinct mechanisms of fetal and adult cross-talk in the thymus medulla.** J Immunol. (2012) Dec 15;189(12):5519-26

SECTION 7: REFERENCES

Akiyama, T., S. Maeda, S. Yamane, K. Ogino, M. Kasai, F. Kajiura, M. Matsumoto, and J. Inoue. 2005. Dependence of self-tolerance on TRAF6-directed development of thymic stroma. *Science* 308:248-251.

Akiyama, T., Y. Shimo, H. Yanai, J. Qin, D. Ohshima, Y. Maruyama, Y. Asaumi, J. Kitazawa, H. Takayanagi, J.M. Penninger, M. Matsumoto, T. Nitta, Y. Takahama, and J. Inoue. 2008. The tumor necrosis factor family receptors RANK and CD40 cooperatively establish the thymic medullary microenvironment and self-tolerance. *Immunity* 29:423-437.

Alam, S.M., P.J. Travers, J.L. Wung, W. Nasholds, S. Redpath, S.C. Jameson, and N.R. Gascoigne. 1996. T-cell-receptor affinity and thymocyte positive selection. *Nature* 381:616-620.

Allende, M.L., J.L. Dreier, S. Mandala, and R.L. Proia. 2004. Expression of the sphingosine 1-phosphate receptor, S1P1, on T-cells controls thymic emigration. *The Journal of biological chemistry* 279:15396-15401.

Allison, J.P., and W.L. Havran. 1991. The immunobiology of T cells with invariant gamma delta antigen receptors. *Annu Rev Immunol* 9:679-705.

Alves, N.L., N.D. Huntington, H.R. Rodewald, and J.P. Di Santo. 2009. Thymic epithelial cells: the multi-tasking framework of the T cell "cradle". *Trends in immunology* 30:468-474.

Anderson, G., and E.J. Jenkinson. 2007. Fetal thymus organ culture. *CSH protocols* 2007:pdb prot4808.

Anderson, G., W.E. Jenkinson, T. Jones, S.M. Parnell, F.A. Kinsella, A.J. White, J.E. Pongrac'z, S.W. Rossi, and E.J. Jenkinson. 2006. Establishment and functioning of intrathymic microenvironments. *Immunol Rev* 209:10-27.

Anderson, G., and Y. Takahama. 2012. Thymic epithelial cells: working class heroes for T cell development and repertoire selection. *Trends Immunol* 33:256-263.

Anderson, M.S., E.S. Venanzi, L. Klein, Z. Chen, S.P. Berzins, S.J. Turley, H. von Boehmer, R. Bronson, A. Dierich, C. Benoist, and D. Mathis. 2002. Projection of an immunological self shadow within the thymus by the aire protein. *Science* 298:1395-1401.

Aschenbrenner, K., L.M. D'Cruz, E.H. Vollmann, M. Hinterberger, J. Emmerich, L.K. Swee, A. Rolink, and L. Klein. 2007. Selection of Foxp3+ regulatory T cells specific for self antigen expressed and presented by Aire+ medullary thymic epithelial cells. *Nat Immunol* 8:351-358.

Baik, S., E.J. Jenkinson, P.J. Lane, G. Anderson, and W.E. Jenkinson. 2013. Generation of both cortical and Aire(+) medullary thymic epithelial compartments from CD205(+) progenitors. *European journal of immunology* 43:589-594.

Barclay, A.N. 1981. Different reticular elements in rat lymphoid tissue identified by localization of Ia, Thy-1 and MRC OX 2 antigens. *Immunology* 44:727-736.

Basset, C., J. Holton, R. O'Mahony, and I. Roitt. 2003. Innate immunity and pathogen-host interaction. *Vaccine* 21 Suppl 2:S12-23.

Bautista, J.L., C.W. Lio, S.K. Lathrop, K. Forbush, Y. Liang, J. Luo, A.Y. Rudensky, and C.S. Hsieh. 2009. Intraclonal competition limits the fate determination of regulatory T cells in the thymus. *Nat Immunol* 10:610-617.

Bennett, A.R., A. Farley, N.F. Blair, J. Gordon, L. Sharp, and C.C. Blackburn. 2002. Identification and characterization of thymic epithelial progenitor cells. *Immunity* 16:803-814.

Bensinger, S.J., A. Bandeira, M.S. Jordan, A.J. Caton, and T.M. Laufer. 2001. Major histocompatibility complex class II-positive cortical epithelium mediates the selection of CD4(+)25(+) immunoregulatory T cells. *J Exp Med* 194:427-438.

Berzins, S.P., R.L. Boyd, and J.F. Miller. 1998. The role of the thymus and recent thymic migrants in the maintenance of the adult peripheral lymphocyte pool. *The Journal of experimental medicine* 187:1839-1848.

Berzins, S.P., F.W. McNab, C.M. Jones, M.J. Smyth, and D.I. Godfrey. 2006. Long-term retention of mature NK1.1+ NKT cells in the thymus. *J Immunol* 176:4059-4065.

Bettelli, E., Y. Carrier, W. Gao, T. Korn, T.B. Strom, M. Oukka, H.L. Weiner, and V.K. Kuchroo. 2006. Reciprocal developmental pathways for the generation of pathogenic effector TH17 and regulatory T cells. *Nature* 441:235-238.

Bhandoola, A., H. von Boehmer, H.T. Petrie, and J.C. Zuniga-Pflucker. 2007. Commitment and developmental potential of extrathymic and intrathymic T cell precursors: plenty to choose from. *Immunity* 26:678-689.

Bjorses, P., J. Aaltonen, N. Horelli-Kuitunen, M.L. Yaspo, and L. Peltonen. 1998. Gene defect behind APECED: a new clue to autoimmunity. *Human molecular genetics* 7:1547-1553.

Bleul, C.C., T. Corbeaux, A. Reuter, P. Fisch, J.S. Monting, and T. Boehm. 2006. Formation of a functional thymus initiated by a postnatal epithelial progenitor cell. *Nature* 441:992-996.

Boehm, T. 2012. Evolution of vertebrate immunity. *Current biology : CB* 22:R722-732.
Boehm, T., I. Hess, and J.B. Swann. 2012. Evolution of lymphoid tissues. *Trends Immunol* 33:315-321.
Boehm, T., S. Scheu, K. Pfeffer, and C.C. Bleul. 2003. Thymic medullary epithelial cell differentiation, thymocyte emigration, and the control of autoimmunity require lympho-epithelial cross talk via LTbetaR. *The Journal of experimental medicine* 198:757-769.
Bonneville, M., R.L. O'Brien, and W.K. Born. 2010. Gammadelta T cell effector functions: a blend of innate programming and acquired plasticity. *Nat Rev Immunol* 10:467-478.
Bosco, N., F. Agenes, A.G. Rolink, and R. Ceredig. 2006. Peripheral T cell lymphopenia and concomitant enrichment in naturally arising regulatory T cells: the case of the pre-Talpha gene-deleted mouse. *J Immunol* 177:5014-5023.
Bottomly, K. 1988. A functional dichotomy in CD4+ T lymphocytes. *Immunology today* 9:268-274.
Boursalian, T.E., J. Golob, D.M. Soper, C.J. Cooper, and P.J. Fink. 2004. Continued maturation of thymic emigrants in the periphery. *Nat Immunol* 5:418-425.
Brandle, D., C. Muller, T. Rulicke, H. Hengartner, and H. Pircher. 1992. Engagement of the T-cell receptor during positive selection in the thymus down-regulates RAG-1 expression. *Proceedings of the National Academy of Sciences of the United States of America* 89:9529-9533.
Burchill, M.A., J. Yang, K.B. Vang, J.J. Moon, H.H. Chu, C.W. Lio, A.L. Vegoe, C.S. Hsieh, M.K. Jenkins, and M.A. Farrar. 2008. Linked T cell receptor and cytokine signaling govern the development of the regulatory T cell repertoire. *Immunity* 28:112-121.
Burkly, L., C. Hession, L. Ogata, C. Reilly, L.A. Marconi, D. Olson, R. Tizard, R. Cate, and D. Lo. 1995. Expression of relB is required for the development of thymic medulla and dendritic cells. *Nature* 373:531-536.
Calderon, L., and T. Boehm. 2011. Three chemokine receptors cooperatively regulate homing of hematopoietic progenitors to the embryonic mouse thymus. *Proceedings of the National Academy of Sciences of the United States of America* 108:7517-7522.
Campbell, J.J., J. Pan, and E.C. Butcher. 1999. Cutting edge: developmental switches in chemokine responses during T cell maturation. *J Immunol* 163:2353-2357.
Carding, S.R., and P.J. Egan. 2002. Gammadelta T cells: functional plasticity and heterogeneity. *Nature reviews. Immunology* 2:336-345.
Carlson, C.M., B.T. Endrizzi, J. Wu, X. Ding, M.A. Weinreich, E.R. Walsh, M.A. Wani, J.B. Lingrel, K.A. Hogquist, and S.C. Jameson. 2006. Kruppel-like factor 2 regulates thymocyte and T-cell migration. *Nature* 442:299-302.
Chaplin, D.D. 2006. 1. Overview of the human immune response. *The Journal of allergy and clinical immunology* 117:S430-435.
Chaplin, D.D. 2010. Overview of the immune response. *The Journal of allergy and clinical immunology* 125:S3-23.
Choi, Y.I., J.S. Duke-Cohan, W.B. Ahmed, M.A. Handley, F. Mann, J.A. Epstein, L.K. Clayton, and E.L. Reinherz. 2008. PlexinD1 glycoprotein controls migration of positively selected thymocytes into the medulla. *Immunity* 29:888-898.
Chvatchko, Y., A.J. Hoogewerf, A. Meyer, S. Alouani, P. Juillard, R. Buser, F. Conquet, A.E. Proudfoot, T.N. Wells, and C.A. Power. 2000. A key role for CC chemokine receptor 4 in lipopolysaccharide-induced endotoxic shock. *J Exp Med* 191:1755-1764.
Ciofani, M., and J.C. Zuniga-Pflucker. 2005. Notch promotes survival of pre-T cells at the beta-selection checkpoint by regulating cellular metabolism. *Nat Immunol* 6:881-888.
Curotto de Lafaille, M.A., and J.J. Lafaille. 2009. Natural and adaptive foxp3+ regulatory T cells: more of the same or a division of labor? *Immunity* 30:626-635.
Daniels, M.A., E. Teixeiro, J. Gill, B. Hausmann, D. Roubaty, K. Holmberg, G. Werlen, G.A. Hollander, N.R. Gascoigne, and E. Palmer. 2006. Thymic selection threshold defined by compartmentalization of Ras/MAPK signalling. *Nature* 444:724-729.
Davalos-Misslitz, A.C., T. Worbs, S. Willenzon, G. Bernhardt, and R. Forster. 2007. Impaired responsiveness to T-cell receptor stimulation and defective negative selection of thymocytes in CCR7-deficient mice. *Blood* 110:4351-4359.
Davodeau, F., M. Difilippantonio, E. Roldan, M. Malissen, J.L. Casanova, C. Couedel, J.F. Morcet, M. Merkenschlager, A. Nussenzweig, M. Bonneville, and B. Malissen. 2001. The tight interallelic positional coincidence that distinguishes T-cell receptor Jalpha usage does not result from homologous chromosomal pairing during ValphaJalpha rearrangement. *The EMBO journal* 20:4717-4729.

Delamarre, L., H. Holcombe, and I. Mellman. 2003. Presentation of exogenous antigens on major histocompatibility complex (MHC) class I and MHC class II molecules is differentially regulated during dendritic cell maturation. *J Exp Med* 198:111-122.

Delves, P.J., and I.M. Roitt. 2000a. The immune system. First of two parts. *The New England journal of medicine* 343:37-49.

Delves, P.J., and I.M. Roitt. 2000b. The immune system. Second of two parts. *The New England journal of medicine* 343:108-117.

Dempsey, P.W., S.A. Vaidya, and G. Cheng. 2003. The art of war: Innate and adaptive immune responses. *Cellular and molecular life sciences : CMLS* 60:2604-2621.

Derbinski, J., J. Gabler, B. Brors, S. Tierling, S. Jonnakuty, M. Hergenhahn, L. Peltonen, J. Walter, and B. Kyewski. 2005. Promiscuous gene expression in thymic epithelial cells is regulated at multiple levels. *J Exp Med* 202:33-45.

Derbinski, J., A. Schulte, B. Kyewski, and L. Klein. 2001. Promiscuous gene expression in medullary thymic epithelial cells mirrors the peripheral self. *Nat Immunol* 2:1032-1039.

Desanti, G.E., J.E. Cowan, S. Baik, S.M. Parnell, A.J. White, J.M. Penninger, P.J. Lane, E.J. Jenkinson, W.E. Jenkinson, and G. Anderson. 2012. Developmentally regulated availability of RANKL and CD40 ligand reveals distinct mechanisms of fetal and adult cross-talk in the thymus medulla. *J Immunol* 189:5519-5526.

Dudley, E.C., H.T. Petrie, L.M. Shah, M.J. Owen, and A.C. Hayday. 1994. T cell receptor beta chain gene rearrangement and selection during thymocyte development in adult mice. *Immunity* 1:83-93.

Dunn, R.J., C.J. Luedecker, H.S. Haugen, C.H. Clegg, and A.G. Farr. 1997. Thymic overexpression of CD40 ligand disrupts normal thymic epithelial organization. *The journal of histochemistry and cytochemistry : official journal of the Histochemistry Society* 45:129-141.

Egerton, M., R. Scollay, and K. Shortman. 1990. Kinetics of mature T-cell development in the thymus. *Proc Natl Acad Sci U S A* 87:2579-2582.

Ehrlich, L.I., D.Y. Oh, I.L. Weissman, and R.S. Lewis. 2009. Differential contribution of chemotaxis and substrate restriction to segregation of immature and mature thymocytes. *Immunity* 31:986-998.

Falk, I., G. Nerz, I. Haidl, A. Krotkova, and K. Eichmann. 2001. Immature thymocytes that fail to express TCRbeta and/or TCRgamma delta proteins die by apoptotic cell death in the CD44(-)CD25(-) (DN4) subset. *European journal of immunology* 31:3308-3317.

Fontenot, J.D., M.A. Gavin, and A.Y. Rudensky. 2003. Foxp3 programs the development and function of CD4+CD25+ regulatory T cells. *Nat Immunol* 4:330-336.

Foss, D.L., E. Donskoy, and I. Goldschneider. 2001. The importation of hematogenous precursors by the thymus is a gated phenomenon in normal adult mice. *The Journal of experimental medicine* 193:365-374.

Gabor, M.J., D.I. Godfrey, and R. Scollay. 1997a. Recent thymic emigrants are distinct from most medullary thymocytes. *European journal of immunology* 27:2010-2015.

Gabor, M.J., R. Scollay, and D.I. Godfrey. 1997b. Thymic T cell export is not influenced by the peripheral T cell pool. *European journal of immunology* 27:2986-2993.

Gallegos, A.M., and M.J. Bevan. 2004. Central tolerance to tissue-specific antigens mediated by direct and indirect antigen presentation. *J Exp Med* 200:1039-1049.

Gaspal, F., D. Withers, M. Saini, V. Bekiaris, F.M. McConnell, A. White, M. Khan, H. Yagita, L.S. Walker, G. Anderson, and P.J. Lane. 2011. Abrogation of CD30 and OX40 signals prevents autoimmune disease in FoxP3-deficient mice. *J Exp Med* 208:1579-1584.

Gilfillan, S., A. Dierich, M. Lemeur, C. Benoist, and D. Mathis. 1993. Mice lacking TdT: mature animals with an immature lymphocyte repertoire. *Science* 261:1175-1178.

Gill, J., M. Malin, G.A. Hollander, and R. Boyd. 2002. Generation of a complete thymic microenvironment by MTS24(+) thymic epithelial cells. *Nature immunology* 3:635-642.

Gillard, G.O., J. Dooley, M. Erickson, L. Peltonen, and A.G. Farr. 2007. Aire-dependent alterations in medullary thymic epithelium indicate a role for Aire in thymic epithelial differentiation. *J Immunol* 178:3007-3015.

Godfrey, D.I., J. Kennedy, T. Suda, and A. Zlotnik. 1993. A developmental pathway involving four phenotypically and functionally distinct subsets of CD3-CD4-CD8- triple-negative adult mouse thymocytes defined by CD44 and CD25 expression. *J Immunol* 150:4244-4252.

Gommeaux, J., C. Gregoire, P. Nguessan, M. Richelme, M. Malissen, S. Guerder, B. Malissen, and A. Carrier. 2009. Thymus-specific serine protease regulates positive selection of a subset of CD4+ thymocytes. *European journal of immunology* 39:956-964.

Gray, D., J. Abramson, C. Benoist, and D. Mathis. 2007. Proliferative arrest and rapid turnover of thymic epithelial cells expressing Aire. *The Journal of experimental medicine* 204:2521-2528.
Gray, D.H., F. Kupresanin, S.P. Berzins, M.J. Herold, L.A. O'Reilly, P. Bouillet, and A. Strasser. 2012. The BH3-only proteins Bim and Puma cooperate to impose deletional tolerance of organ-specific antigens. *Immunity* 37:451-462.
Gray, D.H., N. Seach, T. Ueno, M.K. Milton, A. Liston, A.M. Lew, C.C. Goodnow, and R.L. Boyd. 2006. Developmental kinetics, turnover, and stimulatory capacity of thymic epithelial cells. *Blood* 108:3777-3785.
Gray, D.H., T. Ueno, A.P. Chidgey, M. Malin, G.L. Goldberg, Y. Takahama, and R.L. Boyd. 2005. Controlling the thymic microenvironment. *Curr Opin Immunol* 17:137-143.
Griffith, A.V., M. Fallahi, H. Nakase, M. Gosink, B. Young, and H.T. Petrie. 2009. Spatial mapping of thymic stromal microenvironments reveals unique features influencing T lymphoid differentiation. *Immunity* 31:999-1009.
Grueter, B., M. Petter, T. Egawa, K. Laule-Kilian, C.J. Aldrian, A. Wuerch, Y. Ludwig, H. Fukuyama, H. Wardemann, R. Waldschuetz, T. Moroy, I. Taniuchi, V. Steimle, D.R. Littman, and M. Ehlers. 2005. Runx3 regulates integrin alpha E/CD103 and CD4 expression during development of CD4-/CD8+ T cells. *J Immunol* 175:1694-1705.
Guerau-de-Arellano, M., M. Martinic, C. Benoist, and D. Mathis. 2009. Neonatal tolerance revisited: a perinatal window for Aire control of autoimmunity. *The Journal of experimental medicine* 206:1245-1252.
Guerri, L., I. Peguillet, Y. Geraldo, S. Nabti, V. Premel, and O. Lantz. 2013. Analysis of APC types involved in CD4 tolerance and regulatory T cell generation using reaggregated thymic organ cultures. *J Immunol* 190:2102-2110.
Guo, J., A. Hawwari, H. Li, Z. Sun, S.K. Mahanta, D.R. Littman, M.S. Krangel, and Y.W. He. 2002. Regulation of the TCRalpha repertoire by the survival window of CD4(+)CD8(+) thymocytes. *Nat Immunol* 3:469-476.
Hadeiba, H., K. Lahl, A. Edalati, C. Oderup, A. Habtezion, R. Pachynski, L. Nguyen, A. Ghodsi, S. Adler, and E.C. Butcher. 2012. Plasmacytoid dendritic cells transport peripheral antigens to the thymus to promote central tolerance. *Immunity* 36:438-450.
Hale, J.S., and P.J. Fink. 2009. Back to the thymus: peripheral T cells come home. *Immunology and cell biology* 87:58-64.
Halkias, J., H.J. Melichar, K.T. Taylor, J.O. Ross, B. Yen, S.B. Cooper, A. Winoto, and E.A. Robey. 2013. Opposing chemokine gradients control human thymocyte migration in situ. *The Journal of clinical investigation* 123:2131-2142.
Hamazaki, Y., H. Fujita, T. Kobayashi, Y. Choi, H.S. Scott, M. Matsumoto, and N. Minato. 2007. Medullary thymic epithelial cells expressing Aire represent a unique lineage derived from cells expressing claudin. *Nature immunology* 8:304-311.
Hanabuchi, S., T. Ito, W.R. Park, N. Watanabe, J.L. Shaw, E. Roman, K. Arima, Y.H. Wang, K.S. Voo, W. Cao, and Y.J. Liu. 2010. Thymic stromal lymphopoietin-activated plasmacytoid dendritic cells induce the generation of FOXP3+ regulatory T cells in human thymus. *J Immunol* 184:2999-3007.
Hare, K.J., E.J. Jenkinson, and G. Anderson. 1999. CD69 expression discriminates MHC-dependent and -independent stages of thymocyte positive selection. *J Immunol* 162:3978-3983.
Hare, K.J., E.J. Jenkinson, and G. Anderson. 2000. An essential role for the IL-7 receptor during intrathymic expansion of the positively selected neonatal T cell repertoire. *J Immunol* 165:2410-2414.
Hare, K.J., R.W. Wilkinson, E.J. Jenkinson, and G. Anderson. 1998. Identification of a developmentally regulated phase of postselection expansion driven by thymic epithelium. *J Immunol* 160:3666-3672.
Harrington, L.E., R.D. Hatton, P.R. Mangan, H. Turner, T.L. Murphy, K.M. Murphy, and C.T. Weaver. 2005. Interleukin 17-producing CD4+ effector T cells develop via a lineage distinct from the T helper type 1 and 2 lineages. *Nat Immunol* 6:1123-1132.
Harty, J.T., A.R. Tvinnereim, and D.W. White. 2000. CD8+ T cell effector mechanisms in resistance to infection. *Annu Rev Immunol* 18:275-308.
He, X., X. He, V.P. Dave, Y. Zhang, X. Hua, E. Nicolas, W. Xu, B.A. Roe, and D.J. Kappes. 2005. The zinc finger transcription factor Th-POK regulates CD4 versus CD8 T-cell lineage commitment. *Nature* 433:826-833.
He, X., K. Park, and D.J. Kappes. 2010. The role of ThPOK in control of CD4/CD8 lineage commitment. *Annual review of immunology* 28:295-320.

Hedrick, S.M., E.A. Nielsen, J. Kavaler, D.I. Cohen, and M.M. Davis. 1984. Sequence relationships between putative T-cell receptor polypeptides and immunoglobulins. *Nature* 308:153-158.
Heino, M., P. Peterson, N. Sillanpaa, S. Guerin, L. Wu, G. Anderson, H.S. Scott, S.E. Antonarakis, J. Kudoh, N. Shimizu, E.J. Jenkinson, P. Naquet, and K.J. Krohn. 2000. RNA and protein expression of the murine autoimmune regulator gene (Aire) in normal, RelB-deficient and in NOD mouse. *Eur J Immunol* 30:1884-1893.
Hernandez-Hoyos, G., S.J. Sohn, E.V. Rothenberg, and J. Alberola-Ila. 2000. Lck activity controls CD4/CD8 T cell lineage commitment. *Immunity* 12:313-322.
Hernandez-Munain, C., B.P. Sleckman, and M.S. Krangel. 1999. A developmental switch from TCR delta enhancer to TCR alpha enhancer function during thymocyte maturation. *Immunity* 10:723-733.
Hikosaka, Y., T. Nitta, I. Ohigashi, K. Yano, N. Ishimaru, Y. Hayashi, M. Matsumoto, K. Matsuo, J.M. Penninger, H. Takayanagi, Y. Yokota, H. Yamada, Y. Yoshikai, J. Inoue, T. Akiyama, and Y. Takahama. 2008. The cytokine RANKL produced by positively selected thymocytes fosters medullary thymic epithelial cells that express autoimmune regulator. *Immunity* 29:438-450.
Hinterberger, M., M. Aichinger, O. Prazeres da Costa, D. Voehringer, R. Hoffmann, and L. Klein. 2010. Autonomous role of medullary thymic epithelial cells in central CD4(+) T cell tolerance. *Nature immunology* 11:512-519.
Hinterberger, M., G. Wirnsberger, and L. Klein. 2011. B7/CD28 in central tolerance: costimulation promotes maturation of regulatory T cell precursors and prevents their clonal deletion. *Front Immunol* 2:30.
Hubert, F.X., S.A. Kinkel, G.M. Davey, B. Phipson, S.N. Mueller, A. Liston, A.I. Proietto, P.Z. Cannon, S. Forehan, G.K. Smyth, L. Wu, C.C. Goodnow, F.R. Carbone, H.S. Scott, and W.R. Heath. 2011. Aire regulates the transfer of antigen from mTECs to dendritic cells for induction of thymic tolerance. *Blood* 118:2462-2472.
Hughes, E.A., C. Hammond, and P. Cresswell. 1997. Misfolded major histocompatibility complex class I heavy chains are translocated into the cytoplasm and degraded by the proteasome. *Proc Natl Acad Sci U S A* 94:1896-1901.
Ioannidis, V., F. Beermann, H. Clevers, and W. Held. 2001. The beta-catenin--TCF-1 pathway ensures CD4(+)CD8(+) thymocyte survival. *Nat Immunol* 2:691-697.
Irla, M., J. Guenot, G. Sealy, W. Reith, B.A. Imhof, and A. Serge. 2013. Three-dimensional visualization of the mouse thymus organization in health and immunodeficiency. *J Immunol* 190:586-596.
Itoi, M., H. Kawamoto, Y. Katsura, and T. Amagai. 2001. Two distinct steps of immigration of hematopoietic progenitors into the early thymus anlage. *International immunology* 13:1203-1211.
Iwasaki, A., and R. Medzhitov. 2010. Regulation of adaptive immunity by the innate immune system. *Science* 327:291-295.
Janas, M.L., and M. Turner. 2010. Stromal cell-derived factor 1alpha and CXCR4: newly defined requirements for efficient thymic beta-selection. *Trends in immunology* 31:370-376.
Janas, M.L., G. Varano, K. Gudmundsson, M. Noda, T. Nagasawa, and M. Turner. 2010. Thymic development beyond beta-selection requires phosphatidylinositol 3-kinase activation by CXCR4. *The Journal of experimental medicine* 207:247-261.
Janeway, C.A., Jr., and R. Medzhitov. 2002. Innate immune recognition. *Annu Rev Immunol* 20:197-216.
Jenkinson, E.J., and G. Anderson. 1994. Fetal thymic organ cultures. *Curr Opin Immunol* 6:293-297.
Jenkinson, E.J., G. Anderson, and J.J. Owen. 1992. Studies on T cell maturation on defined thymic stromal cell populations in vitro. *J Exp Med* 176:845-853.
Jin, R., W. Wang, J.Y. Yao, Y.B. Zhou, X.P. Qian, J. Zhang, Y. Zhang, and W.F. Chen. 2008. Characterization of the in vivo dynamics of medullary CD4+CD8- thymocyte development. *J Immunol* 180:2256-2263.
Jordan, M.S., A. Boesteanu, A.J. Reed, A.L. Petrone, A.E. Holenbeck, M.A. Lerman, A. Naji, and A.J. Caton. 2001. Thymic selection of CD4+CD25+ regulatory T cells induced by an agonist self-peptide. *Nat Immunol* 2:301-306.
Kelly, K.A., and R. Scollay. 1990. Analysis of recent thymic emigrants with subset- and maturity-related markers. *Int Immunol* 2:419-425.
Kerdiles, Y.M., D.R. Beisner, R. Tinoco, A.S. Dejean, D.H. Castrillon, R.A. DePinho, and S.M. Hedrick. 2009. Foxo1 links homing and survival of naive T cells by regulating L-selectin, CCR7 and interleukin 7 receptor. *Nat Immunol* 10:176-184.
Kimura, A., and T. Kishimoto. 2010. IL-6: regulator of Treg/Th17 balance. *Eur J Immunol* 40:1830-1835.
Kishimoto, H., and J. Sprent. 1997. Negative selection in the thymus includes semimature T cells. *The Journal of experimental medicine* 185:263-271.

Klein, L., B. Roettinger, and B. Kyewski. 2001. Sampling of complementing self-antigen pools by thymic stromal cells maximizes the scope of central T cell tolerance. *European journal of immunology* 31:2476-2486.
Koble, C., and B. Kyewski. 2009. The thymic medulla: a unique microenvironment for intercellular self-antigen transfer. *The Journal of experimental medicine* 206:1505-1513.
Kondo, M. 2010. Lymphoid and myeloid lineage commitment in multipotent hematopoietic progenitors. *Immunol Rev* 238:37-46.
Kremer, L., L. Carramolino, I. Goya, A. Zaballos, J. Gutierrez, M.d.C. Moreno-Ortiz, A.C. Martinez, and G. Marquez. 2001. The transient expression of C-C chemokine receptor 8 in thymus identifies a thymocyte subset committed to become CD4+ single-positive T cells. *J Immunol* 166:218-225.
Kreslavsky, T., M. Gleimer, A.I. Garbe, and H. von Boehmer. 2010. alphabeta versus gammadelta fate choice: counting the T-cell lineages at the branch point. *Immunol Rev* 238:169-181.
Kumar, H., T. Kawai, and S. Akira. 2009. Pathogen recognition in the innate immune response. *The Biochemical journal* 420:1-16.
Kurobe, H., C. Liu, T. Ueno, F. Saito, I. Ohigashi, N. Seach, R. Arakaki, Y. Hayashi, T. Kitagawa, M. Lipp, R.L. Boyd, and Y. Takahama. 2006. CCR7-dependent cortex-to-medulla migration of positively selected thymocytes is essential for establishing central tolerance. *Immunity* 24:165-177.
Kwan, J., and N. Killeen. 2004. CCR7 directs the migration of thymocytes into the thymic medulla. *J Immunol* 172:3999-4007.
Kyewski, B., and L. Klein. 2006. A central role for central tolerance. *Annu Rev Immunol* 24:571-606.
Laan, M., K. Kisand, V. Kont, K. Moll, L. Tserel, H.S. Scott, and P. Peterson. 2009. Autoimmune regulator deficiency results in decreased expression of CCR4 and CCR7 ligands and in delayed migration of CD4+ thymocytes. *J Immunol* 183:7682-7691.
Landsverk, O.J., O. Bakke, and T.F. Gregers. 2009. MHC II and the endocytic pathway: regulation by invariant chain. *Scandinavian journal of immunology* 70:184-193.
Laufer, T.M., J. DeKoning, J.S. Markowitz, D. Lo, and L.H. Glimcher. 1996. Unopposed positive selection and autoreactivity in mice expressing class II MHC only on thymic cortex. *Nature* 383:81-85.
Lei, Y., A.M. Ripen, N. Ishimaru, I. Ohigashi, T. Nagasawa, L.T. Jeker, M.R. Bosl, G.A. Hollander, Y. Hayashi, W. Malefyt Rde, T. Nitta, and Y. Takahama. 2011. Aire-dependent production of XCL1 mediates medullary accumulation of thymic dendritic cells and contributes to regulatory T cell development. *J Exp Med* 208:383-394.
Li, J., Y. Li, J.Y. Yao, R. Jin, M.Z. Zhu, X.P. Qian, J. Zhang, Y.X. Fu, L. Wu, Y. Zhang, and W.F. Chen. 2007. Developmental pathway of CD4+CD8- medullary thymocytes during mouse ontogeny and its defect in Aire-/- mice. *Proc Natl Acad Sci U S A* 104:18175-18180.
Li, J., J. Park, D. Foss, and I. Goldschneider. 2009. Thymus-homing peripheral dendritic cells constitute two of the three major subsets of dendritic cells in the steady-state thymus. *J Exp Med* 206:607-622.
Lieberam, I., and I. Forster. 1999. The murine beta-chemokine TARC is expressed by subsets of dendritic cells and attracts primed CD4+ T cells. *Eur J Immunol* 29:2684-2694.
Lind, E.F., S.E. Prockop, H.E. Porritt, and H.T. Petrie. 2001. Mapping precursor movement through the postnatal thymus reveals specific microenvironments supporting defined stages of early lymphoid development. *J Exp Med* 194:127-134.
Lio, C.W., L.F. Dodson, C.M. Deppong, C.S. Hsieh, and J.M. Green. 2010. CD28 facilitates the generation of Foxp3(-) cytokine responsive regulatory T cell precursors. *J Immunol* 184:6007-6013.
Lio, C.W., and C.S. Hsieh. 2008. A two-step process for thymic regulatory T cell development. *Immunity* 28:100-111.
Lio, C.W., and C.S. Hsieh. 2011. Becoming self-aware: the thymic education of regulatory T cells. *Curr Opin Immunol* 23:213-219.
Liston, A., S. Lesage, J. Wilson, L. Peltonen, and C.C. Goodnow. 2003. Aire regulates negative selection of organ-specific T cells. *Nat Immunol* 4:350-354.
Liston, A., K.M. Nutsch, A.G. Farr, J.M. Lund, J.P. Rasmussen, P.A. Koni, and A.Y. Rudensky. 2008. Differentiation of regulatory Foxp3+ T cells in the thymic cortex. *Proc Natl Acad Sci U S A* 105:11903-11908.
Liu, C., F. Saito, Z. Liu, Y. Lei, S. Uehara, P. Love, M. Lipp, S. Kondo, N. Manley, and Y. Takahama. 2006. Coordination between CCR7- and CCR9-mediated chemokine signals in prevascular fetal thymus colonization. *Blood* 108:2531-2539.

Liu, C.P., F. Crawford, P. Marrack, and J. Kappler. 1998. T cell positive selection by a high density, low affinity ligand. *Proceedings of the National Academy of Sciences of the United States of America* 95:4522-4526.
Liu, X., and R. Bosselut. 2004. Duration of TCR signaling controls CD4-CD8 lineage differentiation in vivo. *Nature immunology* 5:280-288.
Lucas, B., F. Vasseur, and C. Penit. 1994. Production, selection, and maturation of thymocytes with high surface density of TCR. *J Immunol* 153:53-62.
Lundberg, K., W. Heath, F. Kontgen, F.R. Carbone, and K. Shortman. 1995. Intermediate steps in positive selection: differentiation of CD4+8int TCRint thymocytes into CD4-8+TCRhi thymocytes. *The Journal of experimental medicine* 181:1643-1651.
Lynch, H.E., G.L. Goldberg, A. Chidgey, M.R. Van den Brink, R. Boyd, and G.D. Sempowski. 2009. Thymic involution and immune reconstitution. *Trends in immunology* 30:366-373.
Manz, M.G., D. Traver, T. Miyamoto, I.L. Weissman, and K. Akashi. 2001. Dendritic cell potentials of early lymphoid and myeloid progenitors. *Blood* 97:3333-3341.
Martin-Gayo, E., E. Sierra-Filardi, A.L. Corbi, and M.L. Toribio. 2010. Plasmacytoid dendritic cells resident in human thymus drive natural Treg cell development. *Blood* 115:5366-5375.
Martins, V.C., E. Ruggiero, S.M. Schlenner, V. Madan, M. Schmidt, P.J. Fink, C. von Kalle, and H.R. Rodewald. 2012. Thymus-autonomous T cell development in the absence of progenitor import. *The Journal of experimental medicine* 209:1409-1417.
Matechak, E.O., N. Killeen, S.M. Hedrick, and B.J. Fowlkes. 1996. MHC class II-specific T cells can develop in the CD8 lineage when CD4 is absent. *Immunity* 4:337-347.
Matloubian, M., C.G. Lo, G. Cinamon, M.J. Lesneski, Y. Xu, V. Brinkmann, M.L. Allende, R.L. Proia, and J.G. Cyster. 2004. Lymphocyte egress from thymus and peripheral lymphoid organs is dependent on S1P receptor 1. *Nature* 427:355-360.
McCaughtry, T.M., T.A. Baldwin, M.S. Wilken, and K.A. Hogquist. 2008. Clonal deletion of thymocytes can occur in the cortex with no involvement of the medulla. *J Exp Med* 205:2575-2584.
McCaughtry, T.M., M.S. Wilken, and K.A. Hogquist. 2007. Thymic emigration revisited. *J Exp Med* 204:2513-2520.
Medzhitov, R., and C. Janeway, Jr. 2000. Innate immunity. *The New England journal of medicine* 343:338-344.
Medzhitov, R., and C.A. Janeway, Jr. 1997. Innate immunity: impact on the adaptive immune response. *Curr Opin Immunol* 9:4-9.
Medzhitov, R., and C.A. Janeway, Jr. 2002. Decoding the patterns of self and nonself by the innate immune system. *Science* 296:298-300.
Miller, J.F. 1961. Immunological function of the thymus. *Lancet* 2:748-749.
Miller, J.F. 2002. The discovery of thymus function and of thymus-derived lymphocytes. *Immunological reviews* 185:7-14.
Modlin, R.L. 2012. Innate immunity: ignored for decades, but not forgotten. *The Journal of investigative dermatology* 132:882-886.
Mombaerts, P., A.R. Clarke, M.A. Rudnicki, J. Iacomini, S. Itohara, J.J. Lafaille, L. Wang, Y. Ichikawa, R. Jaenisch, M.L. Hooper, and et al. 1992a. Mutations in T-cell antigen receptor genes alpha and beta block thymocyte development at different stages. *Nature* 360:225-231.
Mombaerts, P., J. Iacomini, R.S. Johnson, K. Herrup, S. Tonegawa, and V.E. Papaioannou. 1992b. RAG-1-deficient mice have no mature B and T lymphocytes. *Cell* 68:869-877.
Moran, A.E., K.L. Holzapfel, Y. Xing, N.R. Cunningham, J.S. Maltzman, J. Punt, and K.A. Hogquist. 2011. T cell receptor signal strength in Treg and iNKT cell development demonstrated by a novel fluorescent reporter mouse. *J Exp Med* 208:1279-1289.
Morrison, S.J., A.M. Wandycz, H.D. Hemmati, D.E. Wright, and I.L. Weissman. 1997. Identification of a lineage of multipotent hematopoietic progenitors. *Development* 124:1929-1939.
Mosmann, T.R., and R.L. Coffman. 1989. TH1 and TH2 cells: different patterns of lymphokine secretion lead to different functional properties. *Annual review of immunology* 7:145-173.
Mouri, Y., M. Yano, M. Shinzawa, Y. Shimo, F. Hirota, Y. Nishikawa, T. Nii, H. Kiyonari, T. Abe, H. Uehara, K. Izumi, K. Tamada, L. Chen, J.M. Penninger, J. Inoue, T. Akiyama, and M. Matsumoto. 2011. Lymphotoxin signal promotes thymic organogenesis by eliciting RANK expression in the embryonic thymic stroma. *J Immunol* 186:5047-5057.
Murata, S., K. Sasaki, T. Kishimoto, S. Niwa, H. Hayashi, Y. Takahama, and K. Tanaka. 2007. Regulation of CD8+ T cell development by thymus-specific proteasomes. *Science* 316:1349-1353.

Muroi, S., Y. Naoe, C. Miyamoto, K. Akiyama, T. Ikawa, K. Masuda, H. Kawamoto, and I. Taniuchi. 2008. Cascading suppression of transcriptional silencers by ThPOK seals helper T cell fate. *Nat Immunol* 9:1113-1121.

Naspetti, M., M. Aurrand-Lions, J. DeKoning, M. Malissen, F. Galland, D. Lo, and P. Naquet. 1997. Thymocytes and RelB-dependent medullary epithelial cells provide growth-promoting and organization signals, respectively, to thymic medullary stromal cells. *Eur J Immunol* 27:1392-1397.

Neefjes, J., M.L. Jongsma, P. Paul, and O. Bakke. 2011. Towards a systems understanding of MHC class I and MHC class II antigen presentation. *Nat Rev Immunol* 11:823-836.

Negishi, I., N. Motoyama, K. Nakayama, K. Nakayama, S. Senju, S. Hatakeyama, Q. Zhang, A.C. Chan, and D.Y. Loh. 1995. Essential role for ZAP-70 in both positive and negative selection of thymocytes. *Nature* 376:435-438.

Nikolich-Zugich, J., M.K. Slifka, and I. Messaoudi. 2004. The many important facets of T-cell repertoire diversity. *Nature reviews. Immunology* 4:123-132.

Nitta, T., S. Nitta, Y. Lei, M. Lipp, and Y. Takahama. 2009. CCR7-mediated migration of developing thymocytes to the medulla is essential for negative selection to tissue-restricted antigens. *Proc Natl Acad Sci U S A* 106:17129-17133.

Nopora, K., C.A. Bernhard, C. Ried, A.A. Castello, K.M. Murphy, P. Marconi, U. Koszinowski, and T. Brocker. 2012. MHC class I cross-presentation by dendritic cells counteracts viral immune evasion. *Frontiers in immunology* 3:348.

Owen, J.J., and M.A. Ritter. 1969. Tissue interaction in the development of thymus lymphocytes. *The Journal of experimental medicine* 129:431-442.

Palmer, D.B., J.L. Viney, M.A. Ritter, A.C. Hayday, and M.J. Owen. 1993. Expression of the alpha beta T-cell receptor is necessary for the generation of the thymic medulla. *Developmental immunology* 3:175-179.

Palmer, E. 2003. Negative selection--clearing out the bad apples from the T-cell repertoire. *Nature reviews. Immunology* 3:383-391.

Parkin, J., and B. Cohen. 2001. An overview of the immune system. *Lancet* 357:1777-1789.

Peaudecerf, L., S. Lemos, A. Galgano, G. Krenn, F. Vasseur, J.P. Di Santo, S. Ezine, and B. Rocha. 2012. Thymocytes may persist and differentiate without any input from bone marrow progenitors. *The Journal of experimental medicine* 209:1401-1408.

Penit, C., B. Lucas, and F. Vasseur. 1995. Cell expansion and growth arrest phases during the transition from precursor (CD4-8-) to immature (CD4+8+) thymocytes in normal and genetically modified mice. *J Immunol* 154:5103-5113.

Petrie, H.T. 2003. Cell migration and the control of post-natal T-cell lymphopoiesis in the thymus. *Nature reviews. Immunology* 3:859-866.

Petrie, H.T., P. Hugo, R. Scollay, and K. Shortman. 1990. Lineage relationships and developmental kinetics of immature thymocytes: CD3, CD4, and CD8 acquisition in vivo and in vitro. *The Journal of experimental medicine* 172:1583-1588.

Petrie, H.T., F. Livak, D. Burtrum, and S. Mazel. 1995. T cell receptor gene recombination patterns and mechanisms: cell death, rescue, and T cell production. *The Journal of experimental medicine* 182:121-127.

Petrie, H.T., F. Livak, D.G. Schatz, A. Strasser, I.N. Crispe, and K. Shortman. 1993. Multiple rearrangements in T cell receptor alpha chain genes maximize the production of useful thymocytes. *J Exp Med* 178:615-622.

Petrie, H.T., R. Scollay, and K. Shortman. 1992. Commitment to the T cell receptor-alpha beta or -gamma delta lineages can occur just prior to the onset of CD4 and CD8 expression among immature thymocytes. *European journal of immunology* 22:2185-2188.

Petrie, H.T., and J.C. Zuniga-Pflucker. 2007. Zoned out: functional mapping of stromal signaling microenvironments in the thymus. *Annu Rev Immunol* 25:649-679.

Philpott, K.L., J.L. Viney, G. Kay, S. Rastan, E.M. Gardiner, S. Chae, A.C. Hayday, and M.J. Owen. 1992. Lymphoid development in mice congenitally lacking T cell receptor alpha beta-expressing cells. *Science* 256:1448-1452.

Pongracz, J., K. Hare, B. Harman, G. Anderson, and E.J. Jenkinson. 2003. Thymic epithelial cells provide WNT signals to developing thymocytes. *Eur J Immunol* 33:1949-1956.

Ponta, H., L. Sherman, and P.A. Herrlich. 2003. CD44: from adhesion molecules to signalling regulators. *Nature reviews. Molecular cell biology* 4:33-45.

Porritt, H.E., L.L. Rumfelt, S. Tabrizifard, T.M. Schmitt, J.C. Zuniga-Pflucker, and H.T. Petrie. 2004. Heterogeneity among DN1 prothymocytes reveals multiple progenitors with different capacities to generate T cell and non-T cell lineages. *Immunity* 20:735-745.

Proietto, A.I., M.H. Lahoud, and L. Wu. 2008a. Distinct functional capacities of mouse thymic and splenic dendritic cell populations. *Immunology and cell biology* 86:700-708.

Proietto, A.I., S. van Dommelen, P. Zhou, A. Rizzitelli, A. D'Amico, R.J. Steptoe, S.H. Naik, M.H. Lahoud, Y. Liu, P. Zheng, K. Shortman, and L. Wu. 2008b. Dendritic cells in the thymus contribute to T-regulatory cell induction. *Proc Natl Acad Sci U S A* 105:19869-19874.

Raposo, G., H.M. van Santen, R. Leijendekker, H.J. Geuze, and H.L. Ploegh. 1995. Misfolded major histocompatibility complex class I molecules accumulate in an expanded ER-Golgi intermediate compartment. *The Journal of cell biology* 131:1403-1419.

Roberts, N.A., A.J. White, W.E. Jenkinson, G. Turchinovich, K. Nakamura, D.R. Withers, F.M. McConnell, G.E. Desanti, C. Benezech, S.M. Parnell, A.F. Cunningham, M. Paolino, J.M. Penninger, A.K. Simon, T. Nitta, I. Ohigashi, Y. Takahama, J.H. Caamano, A.C. Hayday, P.J. Lane, E.J. Jenkinson, and G. Anderson. 2012. Rank signaling links the development of invariant gammadelta T cell progenitors and Aire(+) medullary epithelium. *Immunity* 36:427-437.

Robey, E.A., B.J. Fowlkes, J.W. Gordon, D. Kioussis, H. von Boehmer, F. Ramsdell, and R. Axel. 1991. Thymic selection in CD8 transgenic mice supports an instructive model for commitment to a CD4 or CD8 lineage. *Cell* 64:99-107.

Rodewald, H.R. 2008. Thymus organogenesis. *Annu Rev Immunol* 26:355-388.

Rodewald, H.R., S. Paul, C. Haller, H. Bluethmann, and C. Blum. 2001. Thymus medulla consisting of epithelial islets each derived from a single progenitor. *Nature* 414:763-768.

Rossi, F.M., S.Y. Corbel, J.S. Merzaban, D.A. Carlow, K. Gossens, J. Duenas, L. So, L. Yi, and H.J. Ziltener. 2005. Recruitment of adult thymic progenitors is regulated by P-selectin and its ligand PSGL-1. *Nature immunology* 6:626-634.

Rossi, S.W., A.P. Chidgey, S.M. Parnell, W.E. Jenkinson, H.S. Scott, R.L. Boyd, E.J. Jenkinson, and G. Anderson. 2007a. Redefining epithelial progenitor potential in the developing thymus. *European journal of immunology* 37:2411-2418.

Rossi, S.W., W.E. Jenkinson, G. Anderson, and E.J. Jenkinson. 2006. Clonal analysis reveals a common progenitor for thymic cortical and medullary epithelium. *Nature* 441:988-991.

Rossi, S.W., M.Y. Kim, A. Leibbrandt, S.M. Parnell, W.E. Jenkinson, S.H. Glanville, F.M. McConnell, H.S. Scott, J.M. Penninger, E.J. Jenkinson, P.J. Lane, and G. Anderson. 2007b. RANK signals from CD4(+)3(-) inducer cells regulate development of Aire-expressing epithelial cells in the thymic medulla. *J Exp Med* 204:1267-1272.

Rudd, C.E., and H. Schneider. 2003. Unifying concepts in CD28, ICOS and CTLA4 co-receptor signalling. *Nat Rev Immunol* 3:544-556.

Saini, M., C. Sinclair, D. Marshall, M. Tolaini, S. Sakaguchi, and B. Seddon. 2010. Regulation of Zap70 expression during thymocyte development enables temporal separation of CD4 and CD8 repertoire selection at different signaling thresholds. *Science signaling* 3:ra23.

Saint-Ruf, C., K. Ungewiss, M. Groettrup, L. Bruno, H.J. Fehling, and H. von Boehmer. 1994. Analysis and expression of a cloned pre-T cell receptor gene. *Science* 266:1208-1212.

Saito, H., D.M. Kranz, Y. Takagaki, A.C. Hayday, H.N. Eisen, and S. Tonegawa. 1984. Complete primary structure of a heterodimeric T-cell receptor deduced from cDNA sequences. *Nature* 309:757-762.

Sakaguchi, S., N. Sakaguchi, M. Asano, M. Itoh, and M. Toda. 1995. Immunologic self-tolerance maintained by activated T cells expressing IL-2 receptor alpha-chains (CD25). Breakdown of a single mechanism of self-tolerance causes various autoimmune diseases. *J Immunol* 155:1151-1164.

Schlenner, S.M., and H.R. Rodewald. 2010. Early T cell development and the pitfalls of potential. *Trends in immunology* 31:303-310.

Scollay, R., and D.I. Godfrey. 1995. Thymic emigration: conveyor belts or lucky dips? *Immunology today* 16:268-273; discussion 273-264.

Sebzda, E., V.A. Wallace, J. Mayer, R.S. Yeung, T.W. Mak, and P.S. Ohashi. 1994. Positive and negative thymocyte selection induced by different concentrations of a single peptide. *Science* 263:1615-1618.

Shakib, S., G.E. Desanti, W.E. Jenkinson, S.M. Parnell, E.J. Jenkinson, and G. Anderson. 2009. Checkpoints in the development of thymic cortical epithelial cells. *J Immunol* 182:130-137.

Sharpe, A.H., and G.J. Freeman. 2002. The B7-CD28 superfamily. *Nat Rev Immunol* 2:116-126.

Shinkai, Y., S. Koyasu, K. Nakayama, K.M. Murphy, D.Y. Loh, E.L. Reinherz, and F.W. Alt. 1993. Restoration of T cell development in RAG-2-deficient mice by functional TCR transgenes. *Science* 259:822-825.
Shinkai, Y., G. Rathbun, K.P. Lam, E.M. Oltz, V. Stewart, M. Mendelsohn, J. Charron, M. Datta, F. Young, A.M. Stall, and et al. 1992. RAG-2-deficient mice lack mature lymphocytes owing to inability to initiate V(D)J rearrangement. *Cell* 68:855-867.
Shortman, K., M. Egerton, G.J. Spangrude, and R. Scollay. 1990. The generation and fate of thymocytes. *Seminars in immunology* 2:3-12.
Shrimpton, R.E., M. Butler, A.S. Morel, E. Eren, S.S. Hue, and M.A. Ritter. 2009. CD205 (DEC-205): a recognition receptor for apoptotic and necrotic self. *Molecular immunology* 46:1229-1239.
Sinclair, C., M. Saini, I. Schim van der Loeff, S. Sakaguchi, and B. Seddon. 2011. The long-term survival potential of mature T lymphocytes is programmed during development in the thymus. *Science signaling* 4:ra77.
Smith-Garvin, J.E., G.A. Koretzky, and M.S. Jordan. 2009. T cell activation. *Annual review of immunology* 27:591-619.
Spence, P.J., and E.A. Green. 2008. Foxp3+ regulatory T cells promiscuously accept thymic signals critical for their development. *Proceedings of the National Academy of Sciences of the United States of America* 105:973-978.
Starr, T.K., S.C. Jameson, and K.A. Hogquist. 2003. Positive and negative selection of T cells. *Annual review of immunology* 21:139-176.
Stritesky, G.L., S.C. Jameson, and K.A. Hogquist. 2012. Selection of self-reactive T cells in the thymus. *Annu Rev Immunol* 30:95-114.
Stritesky, G.L., Y. Xing, J.R. Erickson, L.A. Kalekar, X. Wang, D.L. Mueller, S.C. Jameson, and K.A. Hogquist. 2013. Murine thymic selection quantified using a unique method to capture deleted T cells. *Proc Natl Acad Sci U S A* 110:4679-4684.
Sun, G., X. Liu, P. Mercado, S.R. Jenkinson, M. Kypriotou, L. Feigenbaum, P. Galera, and R. Bosselut. 2005. The zinc finger protein cKrox directs CD4 lineage differentiation during intrathymic T cell positive selection. *Nature immunology* 6:373-381.
Sun, Z., D. Unutmaz, Y.R. Zou, M.J. Sunshine, A. Pierani, S. Brenner-Morton, R.E. Mebius, and D.R. Littman. 2000. Requirement for RORgamma in thymocyte survival and lymphoid organ development. *Science* 288:2369-2373.
Surh, C.D., B. Ernst, and J. Sprent. 1992. Growth of epithelial cells in the thymic medulla is under the control of mature T cells. *J Exp Med* 176:611-616.
Surh, C.D., and J. Sprent. 1994. T-cell apoptosis detected in situ during positive and negative selection in the thymus. *Nature* 372:100-103.
Suzuki, G., H. Sawa, Y. Kobayashi, Y. Nakata, K. Nakagawa, A. Uzawa, H. Sakiyama, S. Kakinuma, K. Iwabuchi, and K. Nagashima. 1999. Pertussis toxin-sensitive signal controls the trafficking of thymocytes across the corticomedullary junction in the thymus. *J Immunol* 162:5981-5985.
Takahama, Y. 2006. Journey through the thymus: stromal guides for T-cell development and selection. *Nature Reviews Immunology* 6:127-135.
Takahama, Y., E.W. Shores, and A. Singer. 1992. Negative selection of precursor thymocytes before their differentiation into CD4+CD8+ cells. *Science* 258:653-656.
Teng, F., Y. Zhou, R. Jin, Y. Chen, X. Pei, Y. Liu, J. Dong, W. Wang, X. Pang, X. Qian, W.F. Chen, Y. Zhang, and Q. Ge. 2011. The molecular signature underlying the thymic migration and maturation of TCRalphabeta+ CD4+ CD8 thymocytes. *PloS one* 6:e25567.
Tourigny, M.R., S. Mazel, D.B. Burtrum, and H.T. Petrie. 1997. T cell receptor (TCR)-beta gene recombination: dissociation from cell cycle regulation and developmental progression during T cell ontogeny. *The Journal of experimental medicine* 185:1549-1556.
Trampont, P.C., A.C. Tosello-Trampont, Y. Shen, A.K. Duley, A.E. Sutherland, T.P. Bender, D.R. Littman, and K.S. Ravichandran. 2010. CXCR4 acts as a costimulator during thymic beta-selection. *Nat Immunol* 11:162-170.
Trzpis, M., P.M. McLaughlin, L.M. de Leij, and M.C. Harmsen. 2007. Epithelial cell adhesion molecule: more than a carcinoma marker and adhesion molecule. *The American journal of pathology* 171:386-395.
Turvey, S.E., and D.H. Broide. 2010. Innate immunity. *The Journal of allergy and clinical immunology* 125:S24-32.
Uehara, S., K. Song, J.M. Farber, and P.E. Love. 2002. Characterization of CCR9 expression and CCL25/thymus-expressed chemokine responsiveness during T cell development: CD3(high)CD69+

thymocytes and gammadeltaTCR+ thymocytes preferentially respond to CCL25. *J Immunol* 168:134-142.
Ueno, T., K. Hara, M.S. Willis, M.A. Malin, U.E. Hopken, D.H. Gray, K. Matsushima, M. Lipp, T.A. Springer, R.L. Boyd, O. Yoshie, and Y. Takahama. 2002. Role for CCR7 ligands in the emigration of newly generated T lymphocytes from the neonatal thymus. *Immunity* 16:205-218.
Ueno, T., F. Saito, D.H. Gray, S. Kuse, K. Hieshima, H. Nakano, T. Kakiuchi, M. Lipp, R.L. Boyd, and Y. Takahama. 2004. CCR7 signals are essential for cortex-medulla migration of developing thymocytes. *J Exp Med* 200:493-505.
Van Bleek, G.M., and S.G. Nathenson. 1990. Isolation of an endogenously processed immunodominant viral peptide from the class I H-2Kb molecule. *Nature* 348:213-216.
van der Merwe, P.A., and O. Dushek. 2011. Mechanisms for T cell receptor triggering. *Nature reviews. Immunology* 11:47-55.
van Ewijk, W., E.W. Shores, and A. Singer. 1994. Crosstalk in the mouse thymus. *Immunology today* 15:214-217.
Vang, K.B., J. Yang, A.J. Pagan, L.X. Li, J. Wang, J.M. Green, A.A. Beg, and M.A. Farrar. 2010. Cutting edge: CD28 and c-Rel-dependent pathways initiate regulatory T cell development. *J Immunol* 184:4074-4077.
Verbeek, S., D. Izon, F. Hofhuis, E. Robanus-Maandag, H. te Riele, M. van de Wetering, M. Oosterwegel, A. Wilson, H.R. MacDonald, and H. Clevers. 1995. An HMG-box-containing T-cell factor required for thymocyte differentiation. *Nature* 374:70-74.
Vignali, D.A., L.W. Collison, and C.J. Workman. 2008. How regulatory T cells work. *Nat Rev Immunol* 8:523-532.
von Boehmer, H. 1996. CD4/CD8 lineage commitment: back to instruction? *The Journal of experimental medicine* 183:713-715.
von Freeden-Jeffry, U., N. Solvason, M. Howard, and R. Murray. 1997. The earliest T lineage-committed cells depend on IL-7 for Bcl-2 expression and normal cell cycle progression. *Immunity* 7:147-154.
Walunas, T.L., A.I. Sperling, R. Khattri, C.B. Thompson, and J.A. Bluestone. 1996. CD28 expression is not essential for positive and negative selection of thymocytes or peripheral T cell tolerance. *J Immunol* 156:1006-1013.
Watanabe, N., Y.H. Wang, H.K. Lee, T. Ito, W. Cao, and Y.J. Liu. 2005a. Hassall's corpuscles instruct dendritic cells to induce CD4+CD25+ regulatory T cells in human thymus. *Nature* 436:1181-1185.
Watanabe, N., Y.H. Wang, H.K. Lee, T. Ito, Y.H. Wang, W. Cao, and Y.J. Liu. 2005b. Hassall's corpuscles instruct dendritic cells to induce CD4+CD25+ regulatory T cells in human thymus. *Nature* 436:1181-1185.
Weih, F., D. Carrasco, S.K. Durham, D.S. Barton, C.A. Rizzo, R.P. Ryseck, S.A. Lira, and R. Bravo. 1995. Multiorgan inflammation and hematopoietic abnormalities in mice with a targeted disruption of RelB, a member of the NF-kappa B/Rel family. *Cell* 80:331-340.
Weinreich, M.A., and K.A. Hogquist. 2008. Thymic emigration: when and how T cells leave home. *J Immunol* 181:2265-2270.
Wildt, K.F., G. Sun, B. Grueter, M. Fischer, M. Zamisch, M. Ehlers, and R. Bosselut. 2007. The transcription factor Zbtb7b promotes CD4 expression by antagonizing Runx-mediated activation of the CD4 silencer. *J Immunol* 179:4405-4414.
Williams, C.B., D.L. Engle, G.J. Kersh, J. Michael White, and P.M. Allen. 1999. A kinetic threshold between negative and positive selection based on the longevity of the T cell receptor-ligand complex. *The Journal of experimental medicine* 189:1531-1544.
Wirnsberger, G., M. Hinterberger, and L. Klein. 2011. Regulatory T-cell differentiation versus clonal deletion of autoreactive thymocytes. *Immunol Cell Biol* 89:45-53.
Wirnsberger, G., F. Mair, and L. Klein. 2009. Regulatory T cell differentiation of thymocytes does not require a dedicated antigen-presenting cell but is under T cell-intrinsic developmental control. *Proc Natl Acad Sci U S A* 106:10278-10283.
Wong, P., and E.G. Pamer. 2003. CD8 T cell responses to infectious pathogens. *Annu Rev Immunol* 21:29-70.
Wu, L., A. D'Amico, K.D. Winkel, M. Suter, D. Lo, and K. Shortman. 1998. RelB is essential for the development of myeloid-related CD8alpha- dendritic cells but not of lymphoid-related CD8alpha+ dendritic cells. *Immunity* 9:839-847.
Wu, L., and K. Shortman. 2005. Heterogeneity of thymic dendritic cells. *Seminars in immunology* 17:304-312.
Xing, Y., and K.A. Hogquist. 2012. T-cell tolerance: central and peripheral. *Cold Spring Harbor perspectives in biology* 4:

Xiong, N., and D.H. Raulet. 2007. Development and selection of gammadelta T cells. *Immunological reviews* 215:15-31.
Xiong, Y., and R. Bosselut. 2012. CD4-CD8 differentiation in the thymus: connecting circuits and building memories. *Current opinion in immunology* 24:139-145.
Yamashita, I., T. Nagata, T. Tada, and T. Nakayama. 1993. CD69 cell surface expression identifies developing thymocytes which audition for T cell antigen receptor-mediated positive selection. *Int Immunol* 5:1139-1150.
Yano, M., N. Kuroda, H. Han, M. Meguro-Horike, Y. Nishikawa, H. Kiyonari, K. Maemura, Y. Yanagawa, K. Obata, S. Takahashi, T. Ikawa, R. Satoh, H. Kawamoto, Y. Mouri, and M. Matsumoto. 2008. Aire controls the differentiation program of thymic epithelial cells in the medulla for the establishment of self-tolerance. *The Journal of experimental medicine* 205:2827-2838.
Yasutomo, K., C. Doyle, L. Miele, C. Fuchs, and R.N. Germain. 2000. The duration of antigen receptor signalling determines CD4+ versus CD8+ T-cell lineage fate. *Nature* 404:506-510.
Yin, X., E. Ladi, S.W. Chan, O. Li, N. Killeen, D.J. Kappes, and E.A. Robey. 2007. CCR7 expression in developing thymocytes is linked to the CD4 versus CD8 lineage decision. *J Immunol* 179:7358-7364.
Yokosuka, T., and T. Saito. 2009. Dynamic regulation of T-cell costimulation through TCR-CD28 microclusters. *Immunol Rev* 229:27-40.
Yu, W., H. Nagaoka, M. Jankovic, Z. Misulovin, H. Suh, A. Rolink, F. Melchers, E. Meffre, and M.C. Nussenzweig. 1999. Continued RAG expression in late stages of B cell development and no apparent re-induction after immunization. *Nature* 400:682-687.
Yui, M.A., N. Feng, and E.V. Rothenberg. 2010. Fine-scale staging of T cell lineage commitment in adult mouse thymus. *J Immunol* 185:284-293.
Zachariah, M.A., and J.G. Cyster. 2010. Neural crest-derived pericytes promote egress of mature thymocytes at the corticomedullary junction. *Science* 328:1129-1135.
Zhang, X., H. Wang, E. Claudio, K. Brown, and U. Siebenlist. 2007. A role for the IkappaB family member Bcl-3 in the control of central immunologic tolerance. *Immunity* 27:438-452.
Zhou, L., M.M. Chong, and D.R. Littman. 2009. Plasticity of CD4+ T cell lineage differentiation. *Immunity* 30:646-655.
Zlotoff, D.A., A. Sambandam, T.D. Logan, J.J. Bell, B.A. Schwarz, and A. Bhandoola. 2010. CCR7 and CCR9 together recruit hematopoietic progenitors to the adult thymus. *Blood* 115:1897-1905.
Zuniga-Pflucker, J.C., and M.J. Lenardo. 1996. Regulation of thymocyte development from immature progenitors. *Current opinion in immunology* 8:215-224.